



The
University
Of
Sheffield.

**Cultural and Socio-economic Interaction Reflected by Glass Beads in
Early Iron Age Taiwan**

By:

Kuan-Wen Wang

A thesis submitted in partial fulfilment of the requirements for the degree of
Doctor of Philosophy

The University of Sheffield
Faculty of Arts and Humanities
Department of Archaeology

August 2016

Acknowledgements

It is a long journey. First of all, I would like to express my greatest and sincerest gratitude to my supervisor, Professor Caroline Jackson. At many times that I encountered difficulties in the research, you are always encouraging, supportive and guiding me with patience. Thank you for your contributions of times and ideas for discussing my research and editing this thesis. You are not simply a supervisor, but also a great mentor and friend throughout my PhD life, and surely in the days ahead. I also thank Professor Maureen Carroll for your advice and help in my PhD research.

I would also like to thank my parents for your moral support and encouragement since I decided to change my career to archaeology. Special thanks are also given to Dr Scarlett Chiu (邱斯嘉), Dr Yoshiyuki Iizuka (飯塚義之) and Professor Nyan-Hwa Tai (戴念華). Without your supports, it is not possible that I keep on the path. Thank you for your constructive suggestions, academically and emotionally.

I am especially grateful to Professor Kwang-Tzoo Chen (陳光祖), Professor Kuang-Ti Li (李匡悌), Professor Cheng-Hwa Tsang (臧振華), Mr. Shui-Jing Chiu (邱水金) and Mr. Kun-Hsiu Lee (李坤修). Thank you for providing the precious research materials and for your patience in answering my queries and questions since the beginning. I also thank the excavation team and staff in the Yilan County Cultural Affairs Bureau, in particular Jun-Yao Lai (賴俊堯), the excavation teams of the Tainan Science Park project and the staffs in the National Prehistory Museum, in particular Jun-Nan Chen (陳俊男), for all of your assistance in the field sessions. My thanks also go to Dr Yi-Kong Hsieh (謝易恭) and Professor Chu-Fang Wang (王竹方) for

your technical supports in the LA-ICP-MS analysis at National Tsing Hua University, and again to Dr Yoshiyuki Iizuka (飯塚義之) for your generous support in the SEM-EDS and EPMA analysis at the Institute of Earth Sciences, Academia Sinica. I also thank Dr Shu-Fen Lin for your help in using the instruments at the lab of the Institute of History and Philology, Academia Sinica.

I greatly appreciate Dr Laure Dussubieux for the discussion of analysed data and sharing of unpublished results. You are always helpful and willing to answer my questions. I would also like to acknowledge Dr Hsiao-Chun Hung (洪曉純), Dr Chin-Yun Chao (趙金勇) and Dr Chih-Hua Chiang (江芝華). Thank you for your advice and sharing your ideas and papers in discussing the archaeological context of my research.

In my field session, I particularly indebted to Yu-Hsiang Wang (王宇祥). You are always supportive of the sample preparation, instrument operation and discussion of the analytical results. Thank you for keeping me company in the out-of-hours periods for doing SEM analysis. I am also grateful to Evin Tsai, my dear housemate and colleague, for the discussion of ideas at Sheffield, and Hui-Ho Hsieh (謝惠合) for the consultation of sample preparation and instrumental operation at the Institute of Earth Sciences, Academia Sinica. Thanks are also given to Gareth Perry and other colleagues at the Department of Archaeology, in particular the group of Cultural Materials. It is great to meet you at Sheffield and be part of the lovely group.

I would like to express my gratitude to Professor Thilo Rehren and Professor Marcos Martín-Torres for building my background of archaeological science during studying my Masters degree at UCL, and for helping me get the scholarship and travel funding in my PhD research. I am glad to have you as my teachers in my career life.

Thanks are also given to the Ministry Education of Taiwan government and the Chiang Ching-Kuo Foundation for providing the scholarships in my PhD research. I also thank the Association for the History of Glass, the Society for Archaeological Sciences and the Learned Society Fund in the University of Sheffield for providing the travel funding to carry out analyses in Taiwan and attend conferences.

Lastly, my dearest grandfathers, I know it is always your expectation that I get this doctorate degree. Here I am in the last mile of the way. May you rest in peace.

Abstract

The archaeological record witnesses the presence of glass beads in early Iron Age Taiwan and the potential evidence of glass beadmaking on the southeastern coast. Previous research has proposed that the appearance of glass beads in Taiwan is in association with the South China Sea exchange network, and this particular material culture replaced the indigenous nephrite in local societies in Taiwan. Therefore, this research studies glass beads from 7 Iron Age sites (Kiwulan, Jiuxianglan, Guishan, Daoye, Wujiancuo, Shisanhang and Xiliao) in Taiwan in an attempt to understand the provenance and hence exchange, consumption and production of glass beads in the 1st millennium AD in Taiwan and the interaction shown by these specific goods with the South China Sea network. Beads from around the island, from Kiwulan, Jiuxianglan, Guishan, Daoye and Wujiancuo are analysed data in this research, and this is supplemented with data from Shisanhang and Xiliao from published reports. The evidence of glass beadmaking from Jiuxianglan is also investigated. The material covers a wide geographic region including northern, northeastern, southeastern, southern and southwestern Taiwan, and spans the 1st millennium AD. To elucidate the research questions, the methodology chosen combines the typological study, compositional analysis (to trace elemental level), microstructural investigation and archaeological context of glass beads from each site.

This research proposes regional and chronological patterns in terms of the typology and chemical composition of glass beads in early Iron Age Taiwan, which suggests primarily a Southeast Asian source of early Iron Age glass beads in Taiwan and later a transition to a Chinese origin during the turn of the 2nd millennium AD. The results also indicate the presence of a regional exchange network within Taiwan, particularly within northern and northeastern Taiwan, which may be related to the socio-political interaction between societies. It is also

found that the mortuary contexts of glass beads from different sites shows different degrees of social differentiation between the broad eastern and southwestern Taiwan. In addition, this research reveals a paradox between the glass beads and glass waste from Jiuxianglan, which does not suggest the local production of finished beads at this site. The findings also do not indicate the exchange of glass beads made at Jiuxianglan to other contemporary sites in Taiwan. In addition, the production of m-Na-Al glass and v-Na-Ca glass and their movement within the broad South China Sea network suggests the possibility of shared knowledge but less standardised process of m-Na-Al glass production of the beads found in Taiwan, and a different tradition of glass colouring between m-Na-Al glass and v-Na-Ca glasses which may be related to different provenances.

Contents

ACKNOWLEDGEMENTS	I
ABSTRACT.....	IV
CONTENTS.....	VI
LIST OF TABLES.....	XII
LIST OF FIGURES	XV
PART I: SETTING THE BACKGROUND.....	1
1. INTRODUCTION.....	2
1.1. Overview.....	3
1.2. Aims and objectives.....	5
1.3. Research questions.....	6
1.4. Structure of the thesis.....	7
2. SELECTED SITES.....	9
2.1. Introduction.....	9
2.2. Kiwulan, northeastern Taiwan (7 th -12 th century AD).....	10
2.2.1. Glass beads from the Lower Cultural Layer in Kiwulan	11
2.3. Shisanhang, northern Taiwan (2 nd -15 th century AD).....	12
2.3.1. Glass beads from Shisanhang	13
2.4. Jiuxianglan, southeastern Taiwan (300 BC-AD 770)	14
2.4.1. Glass beads from Jiuxianglan	15
2.5. Guishan, southern Taiwan (late 1 st millennium AD).....	16
2.5.1. Glass beads from Guishan	18
2.6. Daoye, southwestern Taiwan (2 nd -6 th century AD).....	18
2.6.1. Glass beads from Daoye	19
2.7. Wujiancuo, southeastern Taiwan (5 th -8 th century AD).....	19
2.7.1. Glass beads from Wujiancuo	21
2.8. Xiliao, southwestern Taiwan (6 th -14 th century AD).....	21
2.8.1. Glass beads from Xiliao.....	22

2.9.	Summary	22
3.	THE EARLY IRON AGE IN TAIWAN	24
3.1.	Introduction.....	24
3.2.	The production and consumption of nephrite in the late Neolithic Age ..	26
3.3.	The early Iron Age in Taiwan	30
3.3.1.	Regional cultures, exchange activities and exotic influences	30
3.3.1.1.	Northern Taiwan	30
3.3.1.2.	Eastern Taiwan.....	31
3.3.1.3.	Southern Taiwan	33
3.3.1.4.	Southwestern Taiwan	34
3.3.1.5.	Middle-western Taiwan.....	36
3.3.1.6.	Central mountainous regions	36
3.3.1.7.	The offshore islands	37
3.3.2.	Glass beads in early Iron Age Taiwan.....	37
3.3.2.1.	The introduction of glass beads	37
3.3.2.2.	Glass bead production in southeastern Taiwan?	39
3.4.	Summary	40
4.	PRODUCTION AND CONSUMPTION OF GLASS BEADS AROUND THE SOUTH CHINA SEA	43
4.1.	Introduction.....	43
4.2.	The nature of glass	43
4.3.	The raw materials.....	44
4.4.	Glassmaking and glassworking.....	46
4.5.	Glass beadmaking	50
4.5.1.	The Indo-Pacific drawn method.....	50
4.5.2.	The Chinese wound method.....	51
4.5.3.	Other methods.....	52
4.6.	Social and cultural practices reflected by glass beads	53
4.7.	Summary	55
5.	PREVIOUS CHEMICAL STUDIES OF PREHISTORIC GLASS BEADS IN TAIWAN AND AROUND THE SOUTH CHINA SEA.....	58
5.1.	Introduction.....	58
5.2.	Southeast Asia.....	58
5.2.1.	m-Na-Al glass	60

5.2.2.	Potash glass	61
5.2.3.	v-Na-Ca glass (soda plant ash glass)	63
5.3.	Southern China.....	64
5.3.1.	High lead glass	64
5.3.2.	Potash glass	65
5.4.	Taiwan.....	65
5.5.	Summary	67

PART II: METHODOLOGY, RESULTS, DISCUSSION AND CONCLUSION 73

6. METHODOLOGY74

6.1.	Introduction.....	74
6.2.	The sample selection.....	74
6.3.	The typological study.....	77
6.3.1.	Length and diameter	78
6.3.2.	Shape.....	79
6.3.3.	Colour	79
6.3.4.	Diaphaneity	79
6.3.5.	End roundness.....	80
6.3.6.	Manufacturing technique	80
6.4.	The chemical and microstructural analysis.....	81
6.4.1.	Sample preparation	81
6.4.2.	SEM-EDS	82
6.4.3.	EPMA	84
6.4.4.	LA-ICP-MS.....	87
6.4.5.	Comparison between EPMA and LA-ICP-MS data	88
6.5.	The integration of typological and compositional data with context.....	88
6.6.	Summary	90

7. RESULTS: TYPOLOGY AND OPTICAL MICROSCOPY100

7.1.	Introduction.....	100
7.2.	Kiwulan, northeastern Taiwan (7 th -12 th century AD).....	102
7.3.	Shisanhang, northern Taiwan (2 nd -15 th century AD).....	106
7.4.	Comparison of glass beads from Kiwulan and Shisanhang.....	110
7.5.	Jiuxianglan, southeastern Taiwan (300 BC-AD700)	112
7.6.	Guishan, southern Taiwan (late 1 st millennium AD).....	116
7.7.	Comparison of glass beads from Jiuxianglan and Guishan	120
7.8.	Daoye, southwestern Taiwan (2 nd -6 th century AD).....	121

7.9.	Wujiancuo, southwestern Taiwan (5 th -8 th century AD).....	124
7.10.	Xiliao, southwestern Taiwan (6 th -14 th century AD).....	127
7.11.	Comparison of beads from Daoye, Wujiancuo and Xiliao	129
7.12.	Summary	130

8. RESULTS: CHEMICAL COMPOSITION – PART I: OVERVIEW AND M-NA-AL GLASS.....133

8.1.	Introduction.....	133
8.2.	An overview of the chemical groups	133
8.3.	M-Na-Al glass.....	137
8.3.1.	Chemical composition related to the glass melt	137
8.3.1.1.	The sub-groups.....	137
8.3.1.2.	The MgO-FeO and MgO-CaO correlation	140
8.3.1.3.	The Fe, Ti, Sc, V and Nb relationship.....	142
8.3.1.4.	The Zr-Hf relationship	145
8.3.1.5.	The Ba-Sr relationship	145
8.3.1.6.	The rare earth elements.....	149
8.3.2.	Microstructure and colourant.....	149
8.3.2.1.	The glass matrix	149
8.3.2.2.	The red glass	153
8.3.2.3.	The orange glass	158
8.3.2.4.	The blue glass	167
8.3.2.5.	The yellow glass	169
8.3.2.6.	The green glass	173
8.3.2.7.	The aqua glass.....	179

9. RESULTS: CHEMICAL COMPOSITION – PART II: V-NA-CA GLASS, OTHER GLASS COMPOSITION AND SUMMARY.....180

9.1.	Introduction.....	180
9.2.	v-Na-Ca glass.....	180
9.2.1.	Chemical composition related to the base glass	180
9.2.1.1.	The Al ₂ O ₃ , Zr and Ce relationship.....	183
9.2.1.2.	The FeO, Ti and V relationship.....	184
9.2.1.3.	The MnO contents.....	185
9.2.2.	Microstructure and chemistry of the colourants	186
9.2.2.1.	The red glass	187
9.2.2.2.	The yellow glass	188
9.2.2.3.	The light blue and dark blue glass	193

9.2.2.4.	The glass with an orange surface and blue body (KWL-LL02 type)	196
9.2.2.5.	The green glass	203
9.2.2.6.	The aqua glass.....	203
9.3.	Other chemical groups	203
9.3.1.	Potash glass.....	203
9.3.2.	Soda-lime-silica glass (SLS glass).....	205
9.3.3.	Lead silicate glass	206
9.4.	Summary.....	206
10.	RESULTS: THE DISTRIBUTION OF BEADS BY CONTEXT	213
10.1.	Introduction.....	213
10.2.	Kiwulan, northeastern Taiwan (7 th -12 th century AD).....	213
10.3.	Shisanhang, northern Taiwan (2 nd -15 th century AD).....	218
10.4.	Jiuxianglan, southeastern Taiwan (300 BC-AD 770)	220
10.5.	Guishan, southern Taiwan (late 1 st millennium AD).....	224
10.6.	Daoye, southwestern Taiwan (2 nd -6 th century AD)	225
10.7.	Wujiancuo, southwestern Taiwan (5 th -8 th century AD).....	227
10.8.	Xiliao, southwestern Taiwan (6 th -14 th century AD).....	229
10.9.	Summary.....	231
11.	DISCUSSION: THE EXCHANGE, CONSUMPTION AND PRODUCTION OF GLASS BEADS IN TAIWAN AND BETWEEN TAIWAN AND THE SOUTH CHINA SEA REGION.....	234
11.1.	Introduction.....	234
11.2.	The exchange activities through time and by region	234
11.2.1.	The chronological distribution.....	234
11.2.2.	The regional distribution.....	237
11.2.3.	Bead types and compositions over time and space.....	238
11.2.3.1.	The cross-regional bead exchange network in Iron Age Taiwan.....	238
11.2.3.2.	Glass bead exchange in northern and eastern coastal Taiwan	239
11.2.3.3.	Glass bead exchange in southwestern Taiwan	241
11.2.3.4.	A prestige good exchange network?	242
11.3.	Social differentiation reflected by the distribution of glass beads within different contexts	244
11.3.1.	Social differentiation in northern and eastern Taiwan	244
11.3.2.	Social differentiation in southwestern Taiwan.....	246
11.3.3.	The analogy to aborigines in Taiwan	247
11.4.	Glass bead production in Taiwan and around the South China Sea.....	248

11.4.1.	Glass bead production at Jiuxianglan	248
11.4.2.	The production of m-Na-Al 1 glass around the South China Sea.....	250
11.4.3.	The production and recycling of v-Na-Ca glass around the South China Sea region?.....	251
11.4.4.	Linking the red and orange glass colouring to base chemical groups ...	252
12.	CONCLUSIONS AND FUTURE PROSPECTS.....	254
	BIBLIOGRAPHY	257
	APPENDIX 1: FULL SAMPLE LIST OF EACH SITE.	281
	APPENDIX 2: CHEMICAL COMPOSITION OF ANALYSED SAMPLES.	319

List of Tables

<i>Table 3.1: General chronology of Taiwan, Southeast Asia and southern China.</i>	26
<i>Table 5.1: A summary of glass composition in Southeast Asia based on major and minor elements (Dussubieux and Gratuze 2010).</i>	59
<i>Table 5.2: A summary of chemical composition of glass artefacts in prehistoric Taiwan.</i>	69
<i>Table 6.1: A summary of sample selection for chemical analysis in the study sites. ...</i>	92
<i>Table 6.2: The precision and accuracy of SEM-EDS in this research. (wt%)</i>	93
<i>Table 6.3: The precision and accuracy of EPMA in this research. (wt%)</i>	94
<i>Table 6.4: A list of the slope and R² of LA-ICP-MS calibration curves of each element.</i>	95
<i>Table 6.5: The precision and accuracy of LA-ICP-MS (Corning A, B, C, D and NIST621). (wt%)</i>	95
<i>Table 6.6: The precision and accuracy of LA-ICP-MS (NIST610 and 612).</i>	97
<i>Table 7.1: The 12 typological groups of glass beads from the Lower Cultural Layer in Kiwulan (Chen et al. 2008e: 26-28).</i>	102
<i>Table 7.2: The 18 types of glass beads from Shisanhang (Integrated from Tsang and Liu (2001: 91-106).)</i>	107
<i>Table 7.3: A summary of comparing bead typology between Kiwulan and Shisanhang.</i>	111
<i>Table 7.4: The groups and manufacturing methods of selected samples from Jiuxianglan (JXL).</i>	113
<i>Table 7.5: The groups and manufacturing methods of all Iron Age beads from Guishan (GS).</i>	117
<i>Table 7.6: A summary of comparing bead typology between Guishan and Jiuxianglan.</i>	121
<i>Table 7.7: The groups and manufacturing methods of all beads from Daoye (DY)...</i>	123
<i>Table 7.8: The groups and manufacturing methods of all Iron Age beads from Wujiancuo (WJC).</i>	125
<i>Table 7.9: A summary of comparing bead typology between Daoye, Wujiancuo and Xiliao.</i>	130
<i>Table 8.1: The average base composition of each chemical group at Kiwulan, Shisanhang, Jiuxianglan, Guishan, Daoye, Wujiancuo and Xiliao.</i>	135
<i>Table 8.2: Average base composition of the five sub-groups of m-Na-Al glass (Dussubieux et al. 2010).</i>	138
<i>Table 8.3: The composition of Cu, Cu₂S and Cu₂S/Cu₂O in Figure 8.14(d). (wt% by</i>	

EPMA).....	155
Table 8.4: The average, maximum and minimum value of PbO (%), SnO ₂ (%), Co (ppm), Ni (ppm), Zn (ppm), As (ppm) and Sb (ppm) in m-Na-Al glass coloured by Cu-based colourants.	158
Table 8.5: The chemical composition of the particles labelled 1 to 10 in Figure 8.16 (b)-(e). (wt%).....	162
Table 9.1: The characteristic chemical composition of Southeast Asian v-Na-Ca glass sub-groups reported in Dussubieux (2014).	181
Table 9.2: The average, maximum and minimum value of PbO (%), SnO ₂ (%), Co (ppm), Ni (ppm), Zn (ppm), As (ppm) and Sb (ppm) in v-Na-Ca glass coloured by Cu-based colourant.	188
Table 9.3: SEM-EDS analysis on different sections of KWL001. (wt%).....	198
Table 9.4: SEM-EDS analysis on different sections of KWL002. (wt%).....	201
Table 10.1: Grave goods found from the burials in the Lower Cultural Layer in Kiwulan. (Adapted from Chen et al. (2008b) and Chen et al. (2008c).)	214
Table 10.2: The typological groups of glass bead in each burial and in the non-burial context of P187(H204), P038, P250, P256, P258 and P260.	216
Table 10.3: The location where the glass beads were unearthed from Xiliao (Liu 2011b).	230
Table A1. 1: A list of selected samples from Kiwulan.	281
Table A1. 2: A list of selected samples from Jiuxianglan.	288
Table A1.3: A list of full samples from Guishan.	293
Table A1.4: A list of full samples from Daoye.	300
Table A1.5: A list of full samples from Wujiancuo in Niaosong period.	307
Table A1.6: A list of analysed Shisanhang samples from Tsang and Liu (2001).	311
Table A1.7: A list of analysed Xiliao samples from Chen and Cheng (2011).	314
Table A1.8: A full list of Xiliao samples in Niaosong period. Data collected from Liu (2011d).	315
Table A2.1: Chemical composition of samples from Kiwulan (major and minor elements analysed by EPMA, except for samples labelled with ‘*’, which are analysed by LA-ICP-MS.)	319
Table A2.2: Chemical composition of samples from Kiwulan (minor and trace elements analysed by LA-ICP-MS.)	321
Table A2.3: Chemical composition of samples from Jiuxianglan (major and minor elements analysed by EPMA, except for samples labelled with ‘*’, which are analysed by LA-ICP-MS.)	325
Table A2.4: Chemical composition of samples from Jiuxianglan (minor and trace elements analysed by LA-ICP-MS.)	327

<i>Table A2.5: Chemical composition of samples from Guishan (major and minor elements analysed by EPMA, except for samples labelled with ‘*’, which are analysed by LA-ICP-MS.)</i>	333
<i>Table A2.6: Chemical composition of samples from Guishan (minor and trace elements analysed by LA-ICP-MS.)</i>	337
<i>Table A2.7: Chemical composition of samples from Daoye (major and minor elements analysed by EPMA.)</i>	345
<i>Table A2.8: Chemical composition of samples from Wujiancuo (major and minor elements analysed by EPMA.)</i>	345

List of Figures

<i>Figure 1.1: Map showing the location of Taiwan, Southeast Asia and China.</i>	<i>2</i>
<i>Figure 2.1: The location and chronology of selected sites.</i>	<i>9</i>
<i>Figure 2.2: Evidence of glass beadmaking at Jiuxianglan. (a) glass rods (the length of red glass rod is ~1.5 cm), (b) a mandrel encircled with glass bead (length ~1 cm), (c) fused glass and (d) glass beads attached together. ((a), (b) and (c): courtesy of Mr. Kun-Hsiu Lee.).....</i>	<i>15</i>
<i>Figure 3.1: Map showing sites in Taiwan mentioned in this chapter and the Iron Age cultures in coastal regions. This figure only shows the prehistoric cultures relevant to the study sites in this research, and the artefact symbols do not show typological differences. (The geographic distribution of each culture is based on Liu (2011f:46).).....</i>	<i>27</i>
<i>Figure 6.1: A schematic drawing of the measured variables and recorded shapes.</i>	<i>78</i>
<i>Figure 6.2: A schematic drawing showing the different orientations of fabric lines and bubbles in drawn-made and wound-made bead respectively.</i>	<i>80</i>
<i>Figure 6.3: The LA-ICP-MS calibration curves of Na, Mg, Al, Ca, Cu and Pb.</i>	<i>86</i>
<i>Figure 6.4: The comparison between EPMA and LA-ICP-MS data of Corning Glass A, B, C and D. (The linear equation shows $y=x$.)</i>	<i>89</i>
<i>Figure 6.5: A summary of different aspects of the methodology.</i>	<i>91</i>
<i>Figure 7.1: The colour distribution of glass beads from Kiwulan, Shisanhang, Jiuxianglan, Daoye, Wujiancuo, Guishan and Xiliao. Please note that the data from Kiwulan is not the full number of beads from the Lower Cultural Layer. All the data from Shisanhang are from Tsang and Liu (2001), and all the data from Xiliao are from Liu (2011e).</i>	<i>101</i>
<i>Figure 7.2: The size of selected samples from the Lower Cultural Layer at Kiwulan.</i>	<i>104</i>
<i>Figure 7.3: Optical microscopic observation reveals three manufacturing methods for Kiwulan beads.</i>	<i>105</i>
<i>Figure 7.4: Optical microscopic observation on LL02 beads reveals (a) the use of the dipped or wound method, (b) the loose bonding between the clay body and the glass surface, and (c) and (d) the red interlayer between the orange glass surface and the glass body. ((a) and (b): KWL017; (c) and (d): KWL001.).....</i>	<i>106</i>
<i>Figure 7.5: The size of glass beads from Jiuxianglan.</i>	<i>114</i>
<i>Figure 7.6: Optical microscopic observation reveals the manufacturing methods for Jiuxianglan beads.....</i>	<i>114</i>
<i>Figure 7.7: The analysed glass waste from Jiuxianglan.</i>	<i>115</i>
<i>Figure 7.8: The size of all Iron Age glass beads from Guishan.</i>	<i>119</i>

<i>Figure 7.9: Optical microscopic observation reveals the manufacturing methods for Guishan beads.</i>	120
<i>Figure 7.10: The size of all glass beads from Daoye.</i>	122
<i>Figure 7.11: Optical microscopic observation reveals the parallel fabric lines and the quartz remains (arrow) in beads from Daoye.</i>	122
<i>Figure 7.12: The size of all Iron Age glass beads from Wujiancuo.</i>	124
<i>Figure 7.13: Optical microscopic observation showing the manufacturing methods for Wujiancuo beads.</i>	126
<i>Figure 7.14: The size of glass beads from Xiliao. (Data collected from Chen and Cheng (2011).)</i>	128
<i>Figure 7.15: The proportion of bead shapes from each site.</i>	131
<i>Figure 8.1: Al₂O₃-(MgO+K₂O) bi-plot showing the chemical groups of beads from Kiwulan, Shisanhang, Jiuxianglan, Guishan, Wujiancuo, Daoye and Xiliao (base compositions).</i>	136
<i>Figure 8.2: The distributions of colours in each chemical group for all the sites studied.</i>	136
<i>Figure 8.3: The Ba-U bi-plot of m-Na-Al glass.</i>	138
<i>Figure 8.4: The MgO-FeO bi-plot of m-Na-Al glass by colour.</i>	140
<i>Figure 8.5: The MgO-CaO bi-plot of m-Na-Al glass by colour.</i>	141
<i>Figure 8.6: The bi-plots of (a) Ti-FeO, (b) Sc-FeO, (c) V-FeO and (d) Ti-Nb of m-Na-Al glass.</i>	142
<i>Figure 8.7: The Ba-Sr bi-plots of m-Na-Al glass.</i>	144
<i>Figure 8.8: The CaO-Ba and CaO-Sr bi-plots of yellow m-Na-Al glass.</i>	146
<i>Figure 8.9: Some examples of the chondrite normalisation of the rare earth elemental pattern in the red, orange, yellow, green and blue glass. (Chondrite value using McDonough and Sun (1995).)</i>	148
<i>Figure 8.10: An example of mineral relics in the m-Na-Al glass (JXL12).</i>	150
<i>Figure 8.11: A plot of m-Na-Al glasses in the Na₂O-Al₂O₃-SiO₂ phase diagram. The oxides from the base composition are further reduced into three components (SiO₂, Al₂O₃* and Na₂O*) – the FeO, MgO and CaO are transmuted to Al₂O₃ (labelled Al₂O₃*), using a transmuting factor of 0.71, 1.26 and 0.91, respectively (Rehren 2016, pers. comm.). The K₂O is incorporated into Na₂O (labelled Na₂O*) transmuted by the factor of 0.66. The base phase diagram is from Levin and McMurdie (1959: 27).</i>	151
<i>Figure 8.12: A series of feldspar relics identified in the m-Na-Al glass. ((a): GS005; (b): WJC15; (c): JXL25; (d): JXL09; (e): GS052.)</i>	152
<i>Figure 8.13: The remains of accessory minerals identified in the m-Na-Al glass. ((a): DY39; (b): JXL04; (c): GS103.)</i>	153

Figure 8.14: (a) An overview of the red glass; (b), (c), (d), (e), (f) and (g) the copper sulphide, copper oxide and metallic copper particles identified in the red glass. The chemical composition of inclusions shown in (d) is provided in Table 8.3. ((a): JXL35; (b): JXL10; (c): DY47; (d): GS004;(e): JXL34; (f): JXL02; (g): JXL10.)	154
Figure 8.15: The PbO-SnO ₂ bi-plot of orange glass from Kiwulan and Jiuxianglan.	159
Figure 8.16: Inclusions or crystals identified in the orange glass. (a) the cross-section of JXL25; (b) the bronze-related prill; (c) and (d) the oxidised Cu/Sn in the prill; (e) the CuO prill, which is the bright round particle to the left of the bronze-related prill in (a); (f) acicular tin oxide; (g) nodular tin oxide; (h) Cu ₂ O crystal. (The composition of particles labelled from 1 to 10 is shown in Table 8.5. ((a)-(f): JXL25; (g)-(h): JXL27.)	160
Figure 8.17: The cross-section of orange glass (JXL24). (a) the reddish streaks in the orange glass can be observed under optical microscope; (b) the BSE image shows the cluster of large copper oxide particles in the reddish streak (middle) and the absence of fine copper particles in comparison to the orange area (top and bottom).	162
Figure 8.18: (a) and (b): the metallic copper crystals identified in KWL003; (c) the copper oxide identified in KWL004.	163
Figure 8.19: The inclusion of copper oxide and tin oxide seen in KWL005, showing possibly the decomposition of bronze.	164
Figure 8.20: The Sb-Ag bi-plot of orange glass from Kiwulan and Jiuxianglan.....	165
Figure 8.21: The cluster of copper oxide and tin oxide seen in JXL28, showing possibly the decomposition of bronze.	168
Figure 8.22: The inclusions of barite in JXL17.	168
Figure 8.23: The inclusions and crystals in the yellow glass from Jiuxianglan. (a) the non-homogenous matrix and the cluster of lead tin oxide (1), nepheline (2) and sodalite (3) (JXL05); (b) the typical aggregate of lead tin oxide and nepheline crystals seen in Jiuxianglan samples (JXL15); (c) the cluster of sodalite crystal in the yellow glass from Jiuxianglan (JXL12); (d) the yellow glass from Daoye, showing the homogeneous matrix and the crystal of lead tin oxide (DY14).....	170
Figure 8.24: Inclusions and crystals in GS028 and GS029. (a): the bone ash remains in GS028; (b) and (c): the bone ash remains in GS029; (d): the nodular lead tin oxide (bright crystal) and sodalite (dark crystal) in GS029; (e): the acicular lead tin oxide (bright crystal) and sodalite (dark crystal within the acicular lead tin oxide) in GS028.....	172
Figure 8.25: The microstructure of green glass from Jiuxianglan. (a) The heterogeneous	

<i>glass matrix dispersed with lead tin oxide (bright crystals) and nepheline (dark crystals); (b) iron oxide inclusions; (c) and (d) tin oxide crystals. ((a) and (d): JXL14; (b): JXL13; (d): JXL23.)</i>	174
Figure 8.26: <i>The inclusion of barite found in JXL09 (1: sodium aluminosilicate; 2-4: glassy matrix; 5-6: barite.)</i>	175
Figure 8.27: <i>The microstructure of green glass from Guishan. (a) the lead tin oxide (bright crystal) dispersed throughout the glass matrix in absence of sodalite (GS001); (b) the inclusion of copper oxide in GS001; (c) the cluster of lead tin oxide (bright crystal) and sodalite (dark crystal) in the glass matrix (GS103); (d) the tin-rich inclusion in GS103.</i>	177
Figure 8.28: <i>The microstructure of green glass from Daoye. (a) The lead tin oxide without nepheline in DY14; (b) the lead tin oxide (bright crystal) and nepheline (dark crystal) in DY33; (c) the tin remains in TY42-1. (The table shows the atomic% of inclusions in (c).)</i>	178
Figure 8.29: <i>The relatively homogeneous matrix in the aqua glass from Jiuxianglan (JXL41). The bright inclusion is zircon.</i>	179
Figure 9.1: <i>The bi-plots of (a) Al₂O₃-CaO, (b) MgO-K₂O, (c) CaO-Na₂O and (d) Zr-Ti in v-Na-Ca glass. The black symbols show the average value of the v-Na-Ca 1, v-Na-Ca 2 and v-Na-Ca 3 sub-groups.</i>	182
Figure 9.2: <i>The bi-plots of Al₂O₃-Ce and Zr-Ce in the v-Na-Ca glass. The symbol colours of Kiwulan samples present the colour of sample in each typological group. JXL46 has relatively high Ce content (42.5 ppm) and is not shown here</i>	183
Figure 9.3: <i>The bi-plot of FeO-Ti and FeO-V in the v-Na-Ca glass. (a) and (c) by site, (b) and (d) by colour.</i>	184
Figure 9.4: <i>The bi-plots of FeO-MnO in the v-Na-Ca glass: (a) by site; (b) by colour; (c) yellow glass only; (d) yellow glass by chemical group.</i>	186
Figure 9.5: <i>The Cu₂S particle in the red v-Na-Ca glass waste from Jiuxianglan (JXL47).</i>	187
Figure 9.6: <i>The non-homogeneous matrix of yellow v-Na-Ca glass (KWL011). The white crystals are lead tin oxide.</i>	189
Figure 9.7: <i>The crystals related to the yellow colourant in the v-Na-Ca glass. (a) the lead tin oxide (1) and tin oxide crystals (2) (KWL014); (b) The Pb(Sn,Si)O₃ (1) and Pb₂SnO₄ (2) crystals (KWL009).</i>	189
Figure 9.8: <i>The PbO-SnO₂ bi-plot of the yellow v-Na-Ca and m-Na-Al glass.</i>	190
Figure 9.9: <i>The bi-plots showing (a) MnO-Sb, (b) SnO₂-Sb, (c) PbO-Sb, (d) As-Sb, (e) Ni-Sb and (f) Zn-Sb of the yellow v-Na-Ca and m-Na-Al glass.</i>	192
Figure 9.10: <i>The CuO-Co bi-plot of blue and dark blue v-Na-Ca glass.</i>	193
Figure 9.11: <i>The Co-Zn and PbO-Zn bi-plots of blue and dark blue v-Na-Ca glass.</i>	194

<i>Figure 9.12: The SEM-EDS line analysis of KWL001, showing the distribution of Mg, Al, Cu and Pb.</i>	<i>197</i>
<i>Figure 9.13: The microstructure of KWL001. (a) The upper bright grey layer is the orange surface, while the lower dark grey area is the blue body; (b) a closer look at the interface has shown the aggregates of copper oxide between the red and blue glass; (c) some areas show the loose adherence between surface and body.</i>	<i>198</i>
<i>Figure 9.14: The SEM-EDS line analysis of KWL002, showing the distribution of Mg, Al, Cu and Pb.</i>	<i>200</i>
<i>Figure 9.15: The microstructure of KWL002. (a) The lower bright grey layer and dark grey layer are the orange surface with different concentrations of PbO, while the upper area is the body with the mixture of glass and 'sand' materials; (b) minerals such as albite and aluminosilicate rich in Fe, Mg and Na are distributed over the glass body; (c) the area far from the orange surface shows a relatively loose structure, with a frequent presence of silica or silicate (not shown).</i>	<i>201</i>
<i>Figure 9.16: (a) The yellowish outer area and greenish inner area in JXL38; (b) the BSE image shows compositional differences in the two areas.</i>	<i>204</i>
<i>Figure 9.17: (a) The microstructure of the greenish area and the composition of the matrix; (b) the microstructure of the yellowish area and the composition of the matrix</i>	<i>205</i>
<i>Figure 9.18: The distribution of chemical groups at Shisanhang, Kiwulan, Jiuxianglan, Guishan, Wujiancuo, Daoye and Xiliao.</i>	<i>210</i>
<i>Figure 10.1: The distribution of glass beads from the Lower Cultural Layer at Kiwulan. (Black dot labelled with M: burials with grave goods which contain glass beads; grey dots labelled with M: burials with grave goods but no glass beads; black dots labelled with P: non-burial context with glass beads.) (Background map redrawn from Chen et al. (2008a: 18).).....</i>	<i>215</i>
<i>Figure 10.2: The distribution of glass beads from Shisanhang. The labels A, B, C, D, E and H indicate the excavated sections. The number within the brackets is the quantity of beads. (Background image redrawn from Tsang and Liu (2001).) ..</i>	<i>219</i>
<i>Figure 10.3: Map of Jiuxinaglan, showing the coastal area where the potential pyrotechnological activities are suggested and where the beads sampled in this research were found. (Background map: courtesy of Mr. Kun-Hsiu Lee.).....</i>	<i>220</i>
<i>Figure 10.4: The distribution and quantity of glass bead in each trench. The location of trenches where glass beads were unearthed (red area) and the potential region of pyrotechnological activities (black symbol as potential furnace and orange symbol as burned clay) are shown in the upper right of the figure, and the number in the brackets represents the quantity of bead fragments.</i>	<i>221</i>

Figure 10.5: The distribution and quantity of glass waste in each trench. The location of trenches where glass waste was unearthed (red area) and the potential region of pyrotechnological activities (black symbol as potential furnace and orange symbol as burned clay) are shown in the upper right of the figure.....222

Figure 10.6: The quantity and colour of glass beads in the three burials from Guishan.225

Figure 10.7: The distribution of glass beads at Daoye (Yellow square: excavated trench. Orange circle: midden. Blue symbol: burial. R: red bead. Y: yellow bead. G: green bead. B: blue bead.) (Background map: courtesy of Professor Kuang-Ti Li and Professor Cheng-Hwa Tsang.)226

Figure 10.8: The distribution of glass beads from Wujiancuo. (R: red bead; G: green bead; B: blue bead.) (Background map: courtesy of Professor Kuang-Ti Li and Professor Cheng-Hwa Tsang)228

Figure 11.1: The chronological distribution of glass compositions from Shisanhang, Kiwulan, Jiuxianglan, Guishan, Wujiancuo, Daoye and Xiliao.236

Part I: Setting the background

Chapter 1: Introduction

Chapter 2: Selected sites

Chapter 3: The early Iron Age in Taiwan

Chapter 4: Production and consumption of glass beads around the South China Sea

Chapter 5: Previous chemical studies of prehistoric glass beads in Taiwan and around the
South China Sea

1. Introduction

This research examines the cultural, social and economic interaction within Taiwan and between Taiwan and the South China Sea region, through glass beads in the early Iron Age period of the 1st millennium AD. This introductory chapter provides a basic background to the research, stating the purpose of the research and the particular research questions which will be investigated. The final section outlines the structure of this thesis to show how these questions are explored and how the findings are used.

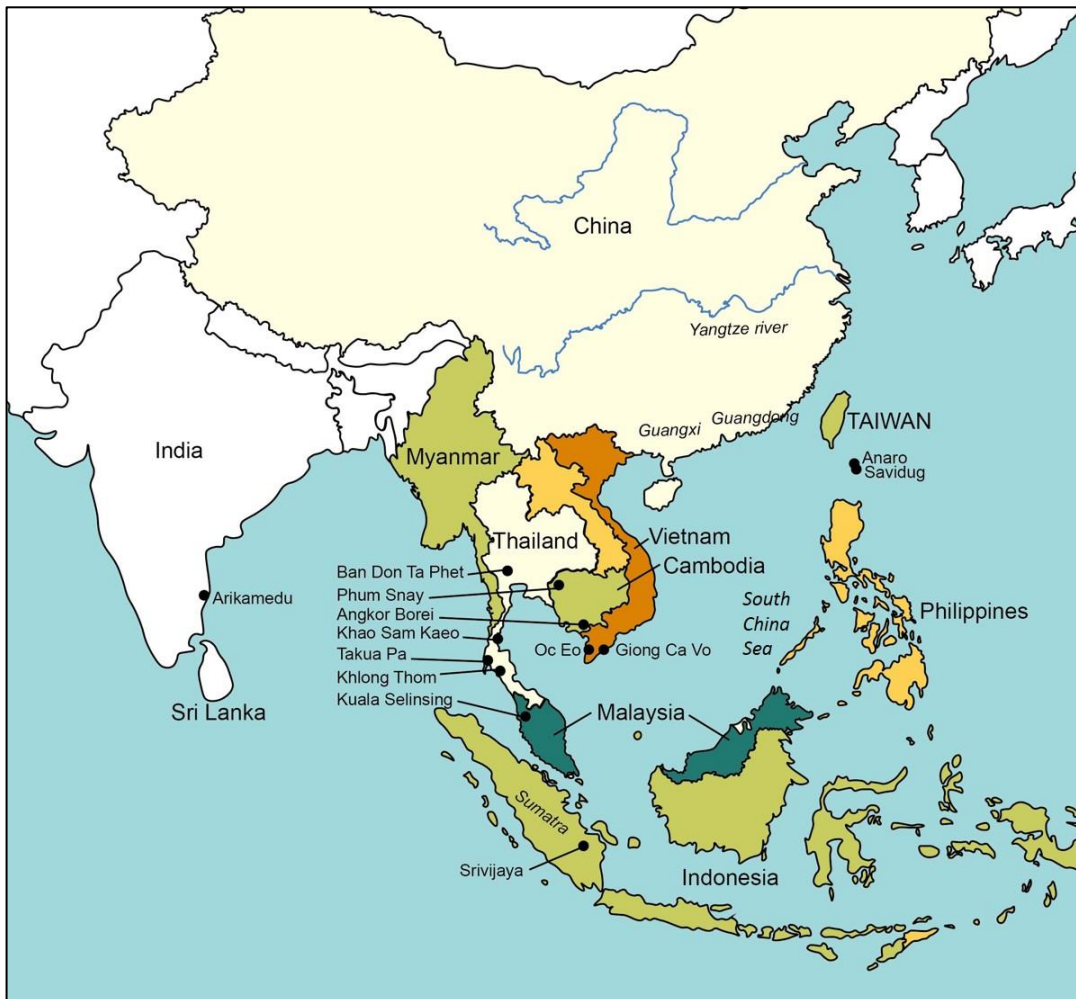


Figure 1.1: Map showing the location of Taiwan, Southeast Asia and China.

1.1. Overview

Taiwan is an island, which allows extensive maritime trade routes to be developed. It is well connected to Southeast Asia and China by accessible and busy seafaring routes (Figure 1.1). The coastal ocean currents, particularly alongside the east coast of Taiwan are one important factor connecting inland exchange with long-distance exchange from eastern Taiwan through the South China Sea. This exchange pattern developed early, evidenced by the circulation of nephrite from the Neolithic period between eastern Taiwan and the South China Sea region (Hung and Bellwood 2010; Liu 2010), and was fully developed by the early Iron Age in Taiwan (the mid-1st millennium BC to the 1st millennium AD). It should be noted that there is no clear division of different stages of the Iron Age in Taiwan archaeology, although a recent paper has tentatively suggested three periods based on the study of imported objects – the Early Stage (400 BC-AD 200), the Middle Stage (AD 200-800) and the Late Stage (AD 800-the 16th /17th century AD) (Hung and Chao *in press*). In this thesis, the ‘early Iron Age’ refers to the broad period of the 1st millennium AD, as it is in this period that intensive interaction is seen between Taiwan and Southeast Asia rather than between Taiwan and the Chinese Han people.

It has long been thought that Iron Age glass beads in Taiwan are exotic and prestige objects, brought to the island through exchange activities with people from Southeast Asia. Prestige goods are excellent indicators of long distance contact, as they are more likely to be exchanged than more utilitarian artefacts; for this reason, this research uses glass beads as a case study to explore exchange networks through the early Iron Age. Prior to the Iron Age, the inhabitants of prehistoric Taiwan commonly used nephrite as a raw material for the manufacture of either prestige items or daily tools. The nephrite is thought to have been indigenous to the island and was exported from Taiwan via the South China Sea from as

early as the Neolithic period, from around 2000 BC and up to AD 100 (Hung *et al.* 2007). However, from the 1st century AD onwards the use of nephrite on the island declined, being gradually replaced by increasing numbers of ‘exotic’ glass beads (as decorative items) found in archaeological contexts in Taiwan. Such replacement is seen first to occur in coastal areas rather than in the more mountainous regions (Liu 2005). This has led archaeologists to suggest that the beads were brought into Taiwan, hence they are termed ‘exotic’, and that the exchange route for glass beads was based on the networks established for nephrite from the Neolithic Age (Hung and Bellwood 2010).

Several early Iron Age sites in Taiwan have glass beads. These beads are monochrome and small, resembling the glass beads found from contemporary sites in Southeast Asia. However, the chronological appearance of beads in the archaeological record in Taiwan and the relative abundance of both beads and nephrite at different sites differs by region. Glass beads are generally more abundant in eastern sites than in western sites; small numbers of beads are found in southern regions and few glass beads are reported in any contexts in middle-western Taiwan during the early part of this period. Furthermore, in the late Neolithic period nephrite is found infrequently in the south, it is relatively rare in the middle-west but is abundant in the north and east (Liu 2003). By the Iron Age nephrite continues to be found in large quantities in eastern sites (but has a different function to that of the late Neolithic period), while in the north nephrite artefacts cease to be found (Liu 2003). This highlights the differences in material culture between regions, and may suggest potential connections between the use and exchange of nephrite and glass beads. There is also evidence for localised glass bead production in eastern Taiwan (Lee 2005a; Lee 2005b). This evidence implies an early development of glass beadmaking in the area.

These phenomena, concerning glass beads in different regions in early Iron Age Taiwan,

have elicited questions and prompted assumptions as to the origins of the production of glass beads, the role(s) of glass beads in local societies and the types of economic activities between Taiwan and the South China Sea network, yet many of these topics lack in-depth investigation and thus at this moment the picture remains unclear.

1.2. Aims and objectives

The main purpose of this research is to conduct a systematic study of glass beads in early Iron Age Taiwan. First to test some assumptions made by Taiwan archaeologists relating to the production and exchange of beads in the Iron Age, and second to explore cultural, social and economic practices which may be demonstrated through the study of these Iron Age glass beads, by stylistic and compositional analysis.

To study the evidence for bead production found at Jiuxianglan, the composition of the glass waste and the beads found at the site and at other sites in Taiwan will be compared, as will the styles of beads at Jiuxianglan and at other contemporary sites. This analysis will show the likely selection of raw materials for glass bead production or indicate the exchange mechanisms at the proposed production site, Jiuxianglan. Further consideration of the manufacturing evidence through comparative stylistic studies may also help to understand the technological methods of bead production at Jiuxianglan. It is hoped that this information will help to shed light on the development of beadmaking technology at this site and the exchange of the products to other sites in Taiwan.

The other sites examined in this thesis do not show evidence for production but have considerable evidence of bead consumption; for these sites the research will explore the movement and exchange of glass beads. This focuses on two aspects: the economic activities

associated with intra-, inter- or cross-regional exchange, and the use of glass beads within local societies.

Overall, this study will integrate the stylistic and compositional data obtained by the analysis of the beads with the archaeological context in which they were found in order to study (1) the potential provenance of glass beads in Iron Age Taiwan, (2) the temporal and/or spatial differentiation of glass assemblages at different sites which may be associated with different exchange networks, (3) the use of glass beads at different sites which may suggest cultural differences between different social groups and (4) the nature of the technology of glass production around the South China Sea region.

1.3. Research questions

Several research questions are pertinent to answer these broad aims.

1. Archaeologists assume that glass beads were brought into Taiwan through the network of nephrite exchange originally established in the Neolithic period (3500-500 BC) (Hung and Bellwood 2010; Chao and Wang 2012). Therefore, to what extent do the glass beads in Taiwan in the Iron Age reflect the overseas economic activities between Taiwan and the South China Sea region and is it similar to that of the nephrite exchange?
2. Glass beads are found earlier in eastern Taiwan than in western Taiwan (Liu 2005). So, can any regional and chronological differentiation in the exchange/presence of glass beads at different sites be seen and is there any evidence of a local exchange network of glass beads in Iron Age Taiwan?

3. Archaeologists regard Iron Age glass beads as prestige goods (Liu 2005) and the exchange and acquisition of prestige goods are often associated with social differentiation (Junker 1999: 305-311; Bellina 2014). Therefore, to what extent does the consumption of Iron Age glass beads in Taiwan reflect the social and cultural practices in different societies and can this be observed through differences in bead styles, contexts or compositions?

4. There is evidence of beadmaking at Jiuxianglan in southeastern Taiwan (Lee 2005a; Lee 2005b). Are the contemporary glass beads from Jiuxianglan made at this site, and are the glass beads made at Jiuxianglan found in other regions in Taiwan? Also, does the beadmaking method seen in the beads thought to be made at Jiuxianglan suggests an affinity or link to glass beadmaking practices seen around the South China Sea region?

1.4. Structure of the thesis

This thesis is divided into 2 parts and 12 chapters.

Part 1, 'Setting the background' gives an overview of the aims of the thesis (Chapter 1). Chapter 2 presents the archaeological contexts and beads from different sites analysed in this thesis in order to provide a background to the research area, material and potential differences between sites. Chapter 3 discusses the background of the early Iron Age in Taiwan, addressing the transition from late Neolithic Age to early Iron Age and the development of different cultures in each region and their interaction. The interaction of cultures in Taiwan with contemporary Southeast Asia is also provided in this chapter in an attempt to place Taiwan in the context of the South China Sea region. Chapter 4 addresses the production and consumption of glass beads around the contemporary South China Sea

region, discussing the raw materials used in glass production, the methods of glass beadmaking and the use of glass beads. Chapter 5 focuses on the previous chemical studies of glass from around the South China Sea region, addressing different types of chemical groups, linking these to different types of raw materials and assessing their origins in order to compare the compositions of the beads from Taiwan in this thesis.

Part 2 contains the methodology, results, discussion and conclusions of this research. Chapter 6 provides the methodology of this research, discussing the sampling strategies, the methods of stylistic analysis and compositional analysis and their integration with the archaeological context. The results are divided into 4 chapters based on the different methods used to illustrate the similarities and differences of the beads between regions and through time. Chapter 7 discusses the bead typology and optical microscopy which can elucidate technological characteristics of the beads. The results of the chemical analysis are split into two chapters because of the complexity of the datasets. Chapter 8 presents an overview of the chemical groups found and discusses the m-Na-Al glass, while Chapter 9 discusses the v-Na-Ca glass, the other minor chemical groups and provides a summary of the chemical compositions found. Chapter 10 discusses the spatial distribution of glass beads within each site and integrates the typological and chemical data with these distributions to explore consumption patterns of the beads within each site. Chapter 11 explores the research questions. It highlights differences and similarities between regions, looks at trade and exchange links in more detail, analyses the beads within their social context and examines glass production in the broad South China Sea region. The conclusions to the thesis and future prospects are given in Chapter 12.

2. Selected sites

2.1. Introduction

Five Iron Age sites, Kiwulan, Jiuxianglan, Daoye, Wujiancuo and Guishan were selected for analysis in this research. These sites cover a wide geographic region from northeastern, eastern, southern and southwestern Taiwan as well as a broad chronological sequence from the 3rd century BC to the 12th century AD. In addition, the published data of glass beads from Shisanhang and Xiliao sites were added to the database and re-interpreted in this research, and therefore these two sites also included in the study. A discussion of each site is provided in this chapter to gain a more complete understanding of the different contexts of the beads analysed in the study. The geographic locations of the study sites can be seen in Figure 2.1.

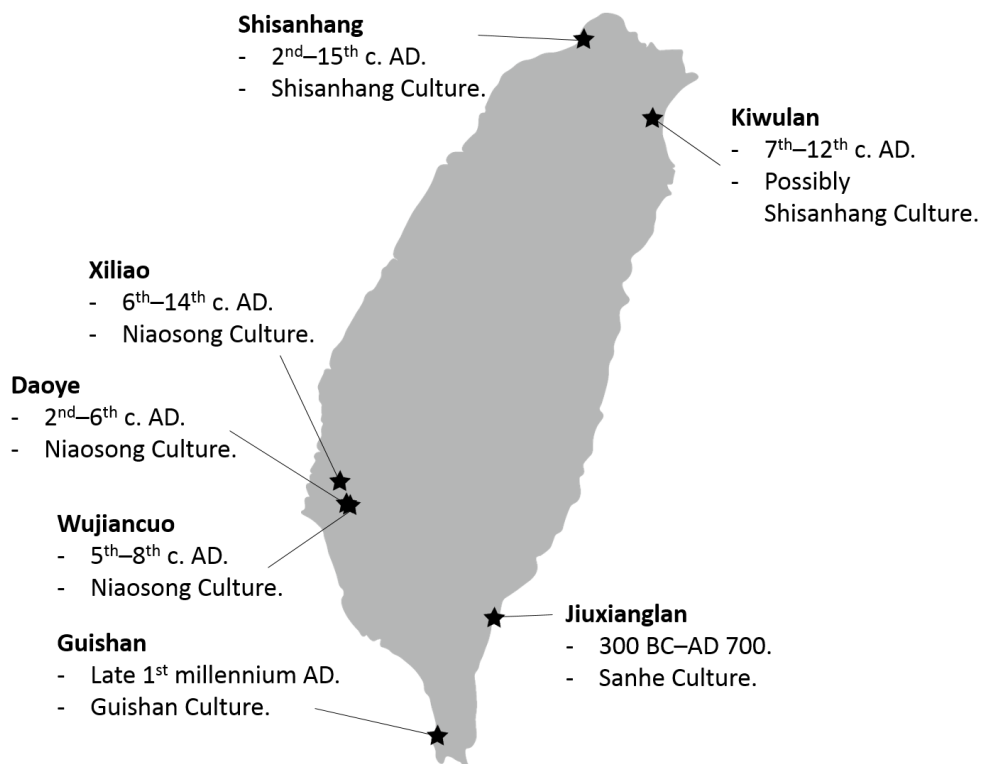


Figure 2.1: The location and chronology of selected sites.

2.2. Kiwulan, northeastern Taiwan (7th-12th century AD)

Kiwulan is located in the north part of the Lanyang Plain in northeastern Taiwan. Most areas of the Kiwulan site are now submerged under the Dezikou Stream. The salvage excavations in the early 2000s revealed two discontinuous cultural stratigraphies. The earlier Iron Age stratigraphy (Lower Cultural Layer) was dated to be around 7th to 12th century AD, and the later stratigraphy (Upper Cultural Layer) was from around the 14th century AD to the early modern period (Chen *et al.* 2008a: 38-39). Research has attributed the non-occupation period between these two layers to the unstable climate (Lin *et al.* 2012). The cultural affinities between the two stratigraphic units remains controversial. Chen (2006) suggests that the two stratigraphies present the same cultural group based on the similarities of artefact styles (in particular pottery), while Chiu (2004) holds the opposite point of view, as the mortuary practices show dramatic differences between the two layers (in particular the body arrangement and the building of burial chambers). This research focuses on the Lower Cultural Layer period during 7th to 12th century AD as this is where the early Iron Age beads were recovered.

The Lower Cultural Layer has both habitation and mortuary contexts. A total of 35 burials were unearthed near the habitation area, and a concentrated distribution of the burials was found (Chen *et al.* 2008b: 30). Only 11 burials were found with grave goods, which include glass beads, agate beads, pottery and a few metal artefacts. Due to the poor condition of the human remains, the age, gender and body arrangement were hard to determine (Chiu 2004; Chen *et al.* 2008b: 28). Stones, and occasionally wood, were used as building materials for both living spaces and burial chambers (Chen *et al.* 2008b: 27-28; 2008e: 60-61).

The principal type of the pottery in the Lower Cultural Layer is the geometrically impressed

jar, and research has indicated that most of the pottery was produced by the paddle and anvil method using local raw materials (Chen *et al.* 2008d: 234-236; Wu 2012). This particular type of pottery is not only used as utilitarian pottery but also found in the mortuary context. Additionally, a small amount of pottery is possibly of non-local styles, fabrics and tempers, with a possible origin in northern or eastern coastal Taiwan (Chen *et al.* 2008d: 12).

2.2.1. Glass beads from the Lower Cultural Layer in Kiwulan

A total of 10789 glass beads were found at Kiwulan, and 1134 beads were excavated from the Lower Cultural Layer (Cheng 2007: 37-39; Chen *et al.* 2008e: 17-30). Most of the beads in the Lower Cultural Layer were found in the habitation contexts or middens (1033 in comparison to 101 from the mortuary context). This is contrary to the Upper Cultural Layer, where the majority of beads were from mortuary contexts (6474 items) rather than habitation or middens (643 items).

Glass beads from the Lower Cultural Layer have been previously grouped into 12 types (see Chapter 7.2) (Cheng 2007: 39; Chen *et al.* 2008e: 26-28), and 12 beads were analysed by SEM-EDS in a Masters dissertation (Cheng 2007: 40). It was reported in the dissertation that glass beads from the Lower Cultural Layer were enriched in Na₂O (soda) and CaO (lime), using soda as flux, but there was no mention of the types or sources of soda flux (Cheng 2007: 44). Further investigation here of this dataset indicates that these glass beads fall into two major groups: m-Na-Al glass and v-Na-Ca glass (see Chapter 5). Further analysis of beads in this research increases this database of chemical compositions of glass beads from the Lower Cultural Layer, and also includes trace elemental data.

2.3. Shisanhang, northern Taiwan (2nd-15th century AD)

Shisanhang is located on the south bank of the Dansui River, and is nowadays the location of the Waste Water Treatment Plant. The salvage excavation was carried out in 1990 and 1991, and revealed a large and long-term settlement (Tsang and Liu 2001). The C-14 data has suggested an Iron Age chronology from 2nd-15th century AD, with the major occupation between the 5th and the 10th century AD. The archaeological remains of the Iron Age have led to the nomenclature of Shisanhang Culture (see Chapter 3.3.1), although there was also evidence suggesting interactions with the Han people in the later period of the Iron Age. The presence of postholes, middens, fireplaces, kilns, an iron smelting furnace and a water well have shown the use of space of the residents at Shisanhang.

Red pottery with a geometrically stamped decoration is the predominant pottery type at Shisanhang, and jars are the most common type of vessel forms (Tsang and Liu 2001: 49-54). The excavators suggested that this type of pottery was locally made at Shisanhang. Non-local pottery was also unearthed, this was reported to have blackish surface, and was probably imported from middle-western or eastern coastal Taiwan (Tsang and Liu 2001: 56, 61-66).

Bronze artefacts, iron artefacts, iron slags and an iron smelting furnace were found at Shisanhang. Among the 238 bronze artefacts, Chinese and Japanese coins were found. The presence of Chinese coins of the Tang Dynasty (AD 618-901) and Song Dynasty (AD 960-1279) and also Japanese coins (contemporary to the Tang Dynasty) may indicate the exchange of goods between Shisanhang, China and Japan (Tsang and Liu 2001: 79). It was suggested that these coins were not used as currency for economic activities but were used instead as decorative objects or grave goods in Shisanhang society, suggesting they had a

more symbolic meaning. Most of the iron artefacts were heavily corroded, although a total of 344 items were identified. The iron artefacts from Shisanhang were mostly daily tools or weapons (Tsang and Liu 2001: 83). Previous research on the iron smelting evidence at Shisanhang has suggested the local innovation of using iron-rich sand from the nearby beach for iron smelting (Chen 2000: 242-245).

Ornaments made of nephrite, clay, shell, animal bones, glass, agate, gold and silver were found. A particularly small number of nephrite objects (n=3) were unearthed, while a large quantity of beads made of glass (n~35000) and agate (n~1000) were reported (Tsang and Liu 2001: 91-110). Most of these ornaments were found from the burials.

Among the 284 burials at Shisanhang, most were sideways flexed burials facing toward the southwest, and only a few burials were extended supine or extended prone (Tsang and Liu 2001: 34-39). It was reported that the distribution of the burials was outside the habitation area. Single and multiple burials were both unearthed, with pottery as the predominant grave good, but no specific detail about the context of the pottery types has been published. In some cases, bronze coins, beads and other ornaments were placed inside the mortuary pottery.

2.3.1. Glass beads from Shisanhang

Around 35000 glass beads, 78 glass bracelets and 97 glass earrings were found at Shisanhang, but the detailed context is unclear. The glass beads have been grouped into 18 types based on their colours and shapes (Tsang and Liu 2001: 91-106). Chemical composition of some glass beads, bracelets and earrings was also reported but not interpreted (Tsang and Liu 2001: 91-106, 110-113). This thesis will use and interpret the published data

from the report.

2.4. Jiuxianglan, southeastern Taiwan (300 BC-AD 770)

Jiuxianglan is located on the south bank of the estuary of the Taimali Stream in southeastern Taiwan. The C-14 data has shown an occupation period between 300 BC-AD 770 (Lee 2005b: 168; 2010: 30-31; 2015: 182-183).

Examination of the pottery assemblages from Jiuxianglan (Sanhe Culture) also reveals cultural affinities or interaction of people from this site with those from contemporary southern Taiwan. Lee (2005b: 69-74) has suggested that some of the decorated pottery may reveal a development from the earlier style of Sanhe Culture to the later motif of 'Guishan type'. Pottery of the Guishan type is often found in southern Taiwan, and therefore its presence at Jiuxianglan has led to the discussion of the relationship between the Sanhe Culture in southeastern Taiwan and the Guishan Culture in southern Taiwan (see Chapter 3.3.1). However, recent petrographic analysis on the decorated pottery of Guishan type at Jiuxianglan has shown that the raw materials may in fact be locally procured in southeastern Taiwan (Yang *et al.* 2012), suggesting some interaction was taking place between southeastern and southern Taiwan. This provides an impetus in this thesis to investigate whether the interaction between the two regions can also be observed through glass beads.

A total of 26 burials have been excavated at Jiuxianglan, and 25 were slate slab burials (Lee 2010). The presence of slate slab coffins, together with the multiple burials and the potsherds covering over the face of individuals at Jiuxianglan suggests a possible relationship to the Neolithic Beinan Culture. Nineteen burials were found with grave goods, including glass beads, pottery and a few agate beads, shell beads, nephrite beads and metal artefacts (Lee

2010: 180-181). It was reported that most of the pottery found in mortuary contexts are smaller vessels in comparison to the utilitarian pottery found on settlement sites, and the typology and decoration is similar to the Guishan type pottery (Lee 2010: 182-183).

2.4.1. Glass beads from Jiuxianglan

One of the striking finds at Jiuxianglan was the evidence of pyrotechnology relating to glass beadmaking and metal casting (Lee 2005b; 2007). This includes small fragments of glass rods, a mandrel encircled with a glass bead, fused glass and glass beads attached together (Figure 2.2). Sandstone casting moulds and metal slags were found as evidence for metal production (more details in Chapter 3.3.2).

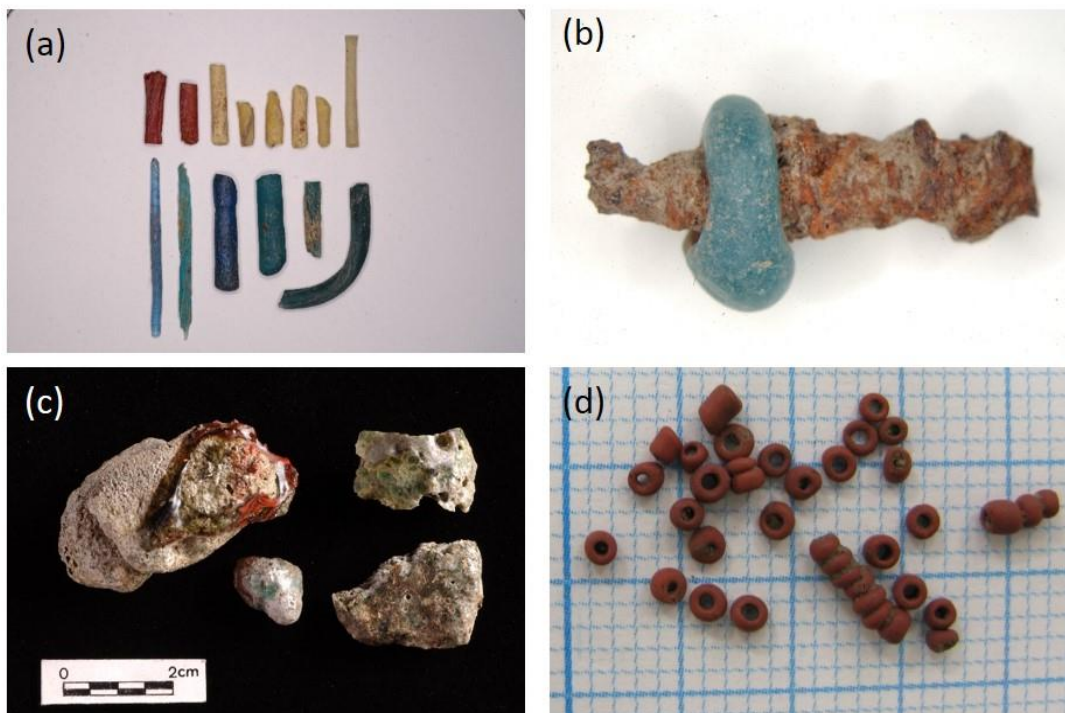


Figure 2.2: Evidence of glass beadmaking at Jiuxianglan. (a) glass rods (the length of red glass rod is ~1.5 cm), (b) a mandrel encircled with glass bead (length ~1 cm), (c) fused glass and (d) glass beads attached together. ((a), (b) and (c): courtesy of Mr. Kun-Hsiu Lee.)

Thousands of glass beads (intact beads or fragments), glass waste and glass bracelets were unearthed from Jiuxianglan (Lee 2005a; 2005b; 2007), but there is no detailed investigation of their distribution at the site. Except for two polychrome beads, all of the glass beads are monochrome, including red, orange, yellow, green, blue and black. No detailed stylistic or chemical analyses have been done on the glass from Jiuxianglan. This thesis will study their style and chemical composition in order to understand the relationship between the glass waste and the beads at the site, the relationship of the glass at this site to assemblages at other sites and regions, and hence the production and distribution of glass beads in Taiwan.

2.5. Guishan, southern Taiwan (late 1st millennium AD)

Guishan is located on a small hill composed of a coral reef in the southernmost region in Taiwan. The name ‘Guishan’ actually means ‘Turtle Mountain’ in Chinese, which describes the shape of the hill where the site is located.

The first trial excavation at Guishan was conducted in 1985, when small quantities of iron artefacts, pottery, lithic tools, animal bones and shellfish were unearthed (Li *et al.* 1985). More survey and excavations have been carried out in 1987, 1990-1992, 1993 and 1994 (Huang *et al.* 1987; Sung *et al.* 1992; Li 1993; 1994) and have revealed Neolithic and Iron Age deposits. The Neolithic period represents the 3rd Eluanbi Prehistoric Cultural Phase (or Fengbitou Culture, ca. 1500 BC) and the 4th Eluanbi Prehistoric Cultural Phase (ca. 500 BC), while the Iron Age period shows the Guishan Culture (ca. 5th-10th century AD) (Li 1993: 18-19). The large area of reef, however, has made a detailed excavation difficult. This research focuses on the archaeological finds from the Iron Age layers.

The C-14 data from shell and skeleton samples revealed the Iron Age of the site is around

the 5th to the 8th century AD (Huang *et al.* 1987; Li 1995), although a recent publication indicated that the C-14 dating from the seashell must be calibrated and a new chronology of around the 7th to the 10th century AD was suggested (Yang *et al.* 2012).

Most of the potsherds unearthed at Guishan were red and plain. A large proportion of potsherds were unearthed from Locus A, a different area to the burials where glass beads were found. However, the dispersed deposit over the coral reef has made it difficult to study the context of most areas. One distinct find was the presence of decorated potsherds with a complicated motif, which is unique in contemporary Taiwan. The motif includes, for example, human figures, geometric shapes and punched dots, and research has suggested that the human figure motif may be associated with the Paiwan aborigines in southern and southeastern Taiwan (Li 2003). Alternatively, the petrographic analysis has shown that this pottery may originate from southeastern Taiwan (Li 2003; Yang *et al.* 2012). The typical Guishan decorated pottery is frequently found in the broad eastern Taiwan (e.g. at Jiuxianglan in southeastern Taiwan and Huagangshan in eastern Taiwan), and therefore may indicate the potential interaction between the Guishan site and broad eastern areas of Taiwan (see Chapter 3.3.1).

Three burials were found at Guishan during the excavation in 1994. Multiple burials of two, three or four bodies were identified in the three burials (Li 2014, *pers. comm.*). Stone slab coffins were built upon the coral reef, and extended supine and prone burials were both identified (Li 1994). Grave goods including glass beads, greyish pottery, iron artefacts and ornaments made of bronze, perforated animal teeth and human teeth were unearthed (Li 1994: 15). Research has suggested that the grave goods of perforated human teeth might be regarded as prestige goods representing the social status of the owner (Li 2001).

2.5.1. Glass beads from Guishan

A total of 123 glass beads were found from three burials. All of them are monochrome beads, and detailed stylistic and chemical analyses of these beads will be carried out in this research.

2.6. Daoye, southwestern Taiwan (2nd-6th century AD)

Daoye is one of the sites found in the salvage excavations of Tainan Science Park since 1995. This site is located in the vast alluvial plain in southwestern Taiwan. However, during the early Iron Age, the western side of the site was very close to the coast (Li *et al.* 2008). The C-14 data has shown the major occupation was during the 2nd to the 6th century AD, which is the early period of the Niasong Culture in the Iron Age (see Chapter 3.3.1) (Tsang and Li 2010). Dispersed finds of an early modern period are also reported in the south area of the site. The focus here is on the Iron Age deposits.

Middens, burials and fireplaces were found at Daoye, located near an ancient river course which passed through the north side of the site. Large quantities of potsherds, seeds and animal bones were unearthed from the middens as well as from the ancient river courses.

Both the middens and burials were thought to be part of the household compound, but there seems to be a slightly separated space between the middens and burials (Tsang and Li 2010). Burials are usually located around the middens, and thus the excavators indicate that the deceased may have been buried inside the house.

A total of 47 Iron Age burials were found from Daoye (Tsang and Li 2010). The mortuary practice reveals most bodies were extended supine and oriented towards the north. Many of

the burials have shown a cluster of individuals from two to six. One distinct characteristic of the mortuary practice at Daoye was that a pot, mostly red plain pottery, was usually put at the north side of the head of the deceased, and fragmented potsherds were paved under the body. Thirty-eight burials were found with grave goods, including pottery, glass beads, glass bracelets, clay bracelets and metal artefacts, but the total amount in each burial is generally less than 10 items.

A large percentage of the pottery/potsherds found in mortuary or settlement contexts was red pottery (94.7% by weight) (Tsang and Li 2010). Most were plain pottery jars in the shape of a long oval body. No distinct difference was observed between the mortuary jars and the commodity jars from settlement contexts. The typical clay-made bird-head figurine of the Niaosong Culture was found at the site, confirming that it was occupied by the Niaosong Culture (see Chapter 3.3.1).

2.6.1. Glass beads from Daoye

A total of 62 glass beads were unearthed from Daoye. All of them are monochrome, and the preliminary observations show these are similar styles to Indo-Pacific beads. The beads were found from middens or burials, but the detailed distribution of the finds is not available. These beads have not been analysed previously.

2.7. Wujiancuo, southeastern Taiwan (5th-8th century AD)

Wujiancuo is another site excavated in the salvage excavations of Tainan Science Park. It lies around 1 kilometre to the southeast of Daoye. This site has three stratigraphic contexts representing three different cultural periods: the late Neolithic Dahu Culture, the Iron Age

Niaosong Culture and the early modern Siraya period. This section focuses on the Iron Age Niaosong Culture. According to the C-14 data, the Iron Age occupation here is around 5th-8th century AD, which is the middle period of the Niaosong Culture (Tsang *et al.* 2009: 97-98).

Middens and burials were both identified at Wujiancuo. In most cases, the midden clusters and burial clusters were quite close to each other. It was reported that most of the middens were distributed towards the northwest or northeast, and therefore it has led to the preliminary suggestion of the planned human use of space at this site (Tsang *et al.* 2009: 16).

In terms of the burials, 85 Iron Age burials were found at Wujiancuo and extended supine bodies facing towards north was the principal mortuary practice (Tsang *et al.* 2009: 23-25). The tradition of paving potsherds under the body at Daoye was not seen at Wujiancuo, suggesting slightly different mortuary practices despite the close location of the sites. In several burials, one or two pots were placed near the head of the deceased. Tsang *et al.* (2009: 16-17) also suggest that burial mounds instead of graves were used at Wujiancuo, as the bottom of the burials were usually at the same altitude as the settlements.

Fifty-two burials were found with grave goods, most with small quantities. Pottery and clay bracelets were the most common grave goods, and glass beads, iron artefacts and bone artefacts were occasionally found.

Red plain pottery, principally jars, was the most frequent type of pottery found at Wujiancuo. Pottery with string holes and short foot rings, which are characteristic of pottery of the middle stage of the Niaosong Culture, was popular at Wujiancuo. The typical bird-head figurines of the Niaosong Culture were also found at this site. Thus whilst the cultural group

identified here is the same as that at Daoye, there are some similar and different cultural traits between the evidence found at Wujiancuo and Daoye.

2.7.1. Glass beads from Wujiancuo

A total of 39 glass beads were found in Iron Age contexts (5th-8th century AD) at Wujiancuo. All the beads are monochrome, and most of them resemble the Indo-Pacific beads. These glass beads were found from middens or burials, but the exact distribution and context is unclear. These beads have not been studied previously.

2.8. Xiliao, southwestern Taiwan (6th-14th century AD)

The Xiliao site is located on the north bank of Cengwen Stream in southwestern Taiwan. The salvage excavation from 2006 to 2010 has revealed an occupation as early as the 17th century BC (Liu 2011b: 119-130). After a period of non-occupation during 13th-8th century BC, the site was then reoccupied by the late Neolithic Dahu Culture (the 8th century BC-the 6th century AD) and the Iron Age Niaosong Culture (the 6th-14th century AD). Middens, fireplaces and a water well were found surrounding the habitation area (Liu 2011a).

The Niaosong Culture at Xiliao is from the same period as the middle and late stage of the Niaosong Culture at the Tainan Science Park area (that is, Wujiancuo site; Chapter 3.3.1.4). Red pottery became the most common type in the Naiosong period at Xiliao, and a large quantity of bird-head figurines were unearthed (Liu 2011c: 466-467, 893-900).

The mortuary practice has shown extended supine burials of individuals facing towards the north. In the late Neolithic period at Xiliao, the tradition of paving potsherds under the

deceased (extended supine) as well as placing a pot in the north side of the burial has been reported (Liu 2011b: 175-191). This is similar to the mortuary practice seen at the Iron Age Daoye site (section 2.6). In the Niaosong period at Xiliao, 13 extended supine burials were found without potsherds paving under the body, and a mortuary pot was usually placed to the north side of the head; this is similar to the mortuary practices seen at Wujiancuo. This transition of mortuary practice seen at Xiliao, from the late Neolithic period to the Iron Age Niaosong period, echoes those seen at the Iron Age sites of Daoye and Wujiancuo in Tainan Science Park. This research focuses on the Iron Age Niaosong period at Xiliao.

2.8.1. Glass beads from Xiliao

A total of 62 glass beads were found at Xiliao from the Niaosong period; the most common were blue beads (Liu 2011d: 1189-1190). An analytical report was provided in the excavation report, including XRF analysis on 12 beads from the Niaosong period (Chen and Cheng 2011), but no interpretation was given. This research re-examines and interprets the published data from the excavation report, comparing them with the analysed data from Daoye and Wujiancuo in order to increase the database of beads studied from southwestern Taiwan.

2.9. Summary

This chapter has provided an overview of the study sites in the research. Glass beads from five sites, Kiwulan, Jiuxianglan, Daoye, Wujiancuo and Guishan will be analysed, and published data from Shisanhang and Xiliao will be interpreted and integrated in this research. These sites cover a wide geographic area including northern (Shisanhang), northeastern (Kiwulan), southeastern (Jiuxianglan), southwestern (Daoye, Wujiancuo and Xiliao) and the

southernmost (Guishan) Taiwan (Figure 2.1). The site with the earliest chronology is Jiuxianglan (300 BC-AD 700). Shisanhang covers a wide chronology from the 2nd to the 15th century AD. Daoye, Wujiancuo and Xiliao are of 2nd-6th century AD, 5th-8th century AD and 6th-14th century AD, respectively. The date of Guishan is around late 1st millennium AD, although a chronology of 5th-8th century AD and 7th-10th century AD were both suggested. At Kiwulan, two discontinuous cultural layers were identified, and this study focuses on the Lower Cultural Layer dated to 7th-12th century AD. Glass beads from Guishan, Daoye, Wujiancuo and Xiliao are predominantly found from mortuary contexts, while at Kiwulan and Jiuxianglan they are mostly from non-burial contexts. The context of the Shisanhang beads remains less clear.

Almost all of the glass beads from the seven sites are monochrome beads, and a wide variety of colours, including red, orange, yellow, green, blue and dark blue, were found. The preliminary investigation, however, has indicated potential differences between the sites in terms of the quantities, colours and the contexts that these beads were found (Chapter 3.3.2). The archaeological evidence also suggests the possibility of glass beadmaking at Jiuxianglan in southeastern Taiwan. This study therefore examines the style and chemical composition of glass beads from the seven sites, and beadmaking glass waste from Jiuxianglan, in order to study the regional and chronological differences of 1st millennium AD beads in Iron Age Taiwan. This data will be used to explore different social and cultural practices at different sites and regions and to place these in the wider context of economic activities within Taiwan and between Taiwan and the South China Sea region.

3. The early Iron Age in Taiwan

3.1. Introduction

Taiwan is located off the southeast coast of continental Asia (Figure 1.1). The geographic location of Taiwan allows easy contact with Southeast Asia and China, with which it has developed extensive exchange routes and allowed the movement of goods and people in both directions since prehistory. Overseas immigrants from southeast coastal China settled in Taiwan as early as the 4th millennium BC, in the early Neolithic period. Later on, through the Neolithic period, archaeological evidence witnesses the regional developments of different cultures in Taiwan. During the middle and late Neolithic period, extensive interaction between Taiwan and Southeast Asia can be seen through the exchange of indigenous nephrite materials, for example, within the South China Sea network (Hung and Bellwood 2010).

The start of the Iron Age in Southeast Asia is as early as around 500 BC in mainland Southeast Asia (Higham 2004), while in Taiwan the earliest evidence of the Iron Age dates back to around 300 BC in eastern coastal Taiwan (Lee 2005b; 2015). During this period in the South China Sea, the Iron Age ‘Sa Huynh-Kalanay interaction sphere’ (500 BC-AD 100) was identified by Solheim based on similar styles of pottery assemblages and jar burial practices in central Vietnam (the Sa Huynh Culture) and the central Philippines (the Kalanay Culture) (Solheim 1964; 2006). With more research in recent decades, it is now acknowledged that this interaction network in the South China Sea, developed since the Neolithic period, covers complex intra- and inter-regional interactions from the Neolithic Age onwards (Solheim 2006; Hung *et al.* 2007; Bulbeck 2008; Dussubieux and Gratuze

2010; Murillo-Barroso *et al.* 2010; Glover and Bellina 2011; Hung *et al.* 2013; Bellina 2014).

During the Iron Age, the material culture in Taiwan shows a distinct transition, possibly in association with the exchange activities in the South China Sea network. The archaeological evidence shows the introduction of iron artefacts and, in some sites, bronze and gold. Another remarkable difference is the presence of large quantities of glass beads which mirrors the decline of nephrite at several Iron Age sites in Taiwan. These glass beads are thought to replace Neolithic nephrite artefacts as decorative items (Liu 2005). It is suggested that the presence of metal artefacts and glass beads, and the knowledge of how to produce them, were introduced through the South China Sea network which was initially built upon the exchange of nephrite in the Neolithic period (Hung and Bellwood 2010; Chao and Wang 2012).

This chapter begins with a discussion of the production and consumption of nephrite in the Neolithic period in Taiwan, as the exchange network of nephrite may be strongly related to the introduction of new materials to Iron Age Taiwan. The Iron Age in Taiwan covers a particular long period from the 3rd century BC to the 15th century AD. As this research focuses on the 1st millennium AD, the ‘early’ Iron Age discussed here is generally within the 1st millennium AD. The general chronology of Taiwan, Southeast Asia and southern China is provided in Table 3.1, and the location of the sites around the South China Sea and within Taiwan mentioned in this chapter is shown in Figure 1.1 and Figure 3.1, respectively.

Table 3.1: General chronology of Taiwan, Southeast Asia and southern China.

	Taiwan	Mainland SEA	Island SEA	Southern China
AD 1500				
AD 1000	Iron Age	Historic Period	Metal Age*	Song Dynasty (AD 960-1279)
				Tang Dynasty (AD 618-901)
AD 500				
AD 1		Iron Age		Han Dynasty (202 BC-AD 220)
500 BC	Late Neolithic Age	Bronze Age	Neolithic Age	Bronze Age**
1000 BC				
1500 BC	Middle Neolithic Age	Neolithic Age	Neolithic Age	Neolithic Age
2000 BC				
2500 BC	Early Neolithic Age	Neolithic Age	Neolithic Age	Neolithic Age
3000 BC				
3500 BC				

*: Western Indonesia witnesses the emergence of early Kingdom in the late period, but most of the regions in island Southeast Asia still remain in the Metal Age.

** : In the Central Plain area in China, this period belongs to Warring States (476-221 BC), Spring and Autumn (770-476 BC), Zhou Dynasty (ca. 11th century BC - 771 BC) and Shang Dynasty (ca. 17th century BC - 11th century BC).

3.2. The production and consumption of nephrite in the late Neolithic Age

The use of nephrite, green jade, in prehistoric Taiwan can be traced back to the early Neolithic Age (3500-2500 BC), as daily tools made of nephrite, such as axes, adzes and chisels, have been sporadically unearthed in early contexts (Liu 2003). Later in the middle Neolithic Age (2500-1500 BC), nephrite was found in both funerary or settlement contexts, in the forms of decorative items such as beads, earrings and bracelets (Tsang 1992; Li 1999: 34-37; Lee and Yeh 2001: 70; Liu 2003). The late Neolithic Age (1500 BC to late 1st millennium BC) witnesses a flourishing of nephrite consumption and production, and this is

particularly seen in northern and eastern Taiwan, where substantial amounts of nephrite objects are often excavated (Lien 1998; Yeh 2001; Liu 2003).

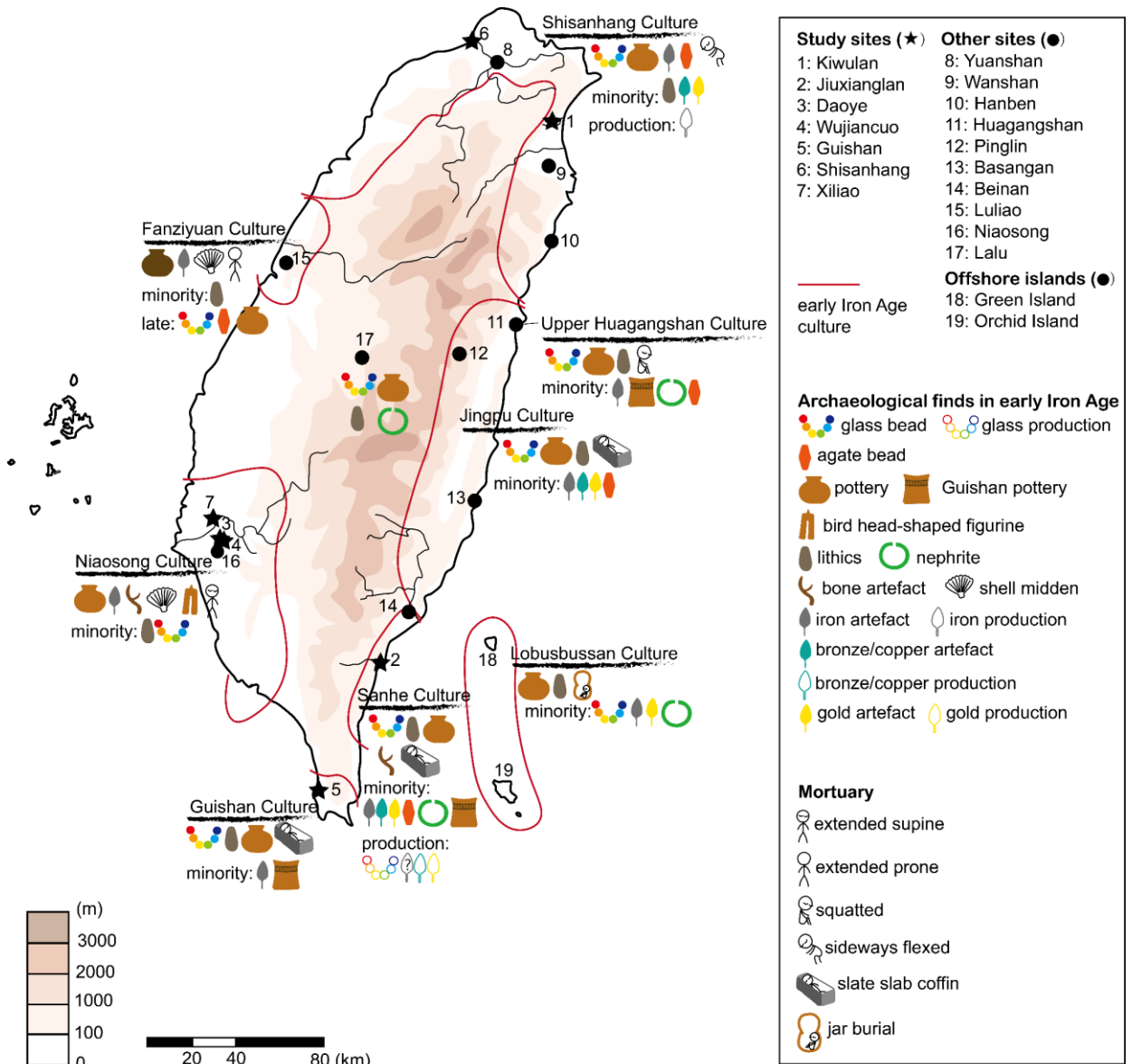


Figure 3.1: Map showing sites in Taiwan mentioned in this chapter and the Iron Age cultures in coastal regions. This figure only shows the prehistoric cultures relevant to the study sites in this research, and the artefact symbols do not show typological differences. (The geographic distribution of each culture is based on Liu (2011f:46).)

Nephrite mineral deposits have been identified in the Fengtian area, near the Pinglin site, in eastern Taiwan (Tan *et al.* 1997; Iizuka and Hung 2005). It is believed that from the middle Neolithic Age, Pinglin was a principal centre of nephrite production, as large amounts of nephrite debitage, semi-finished products and potential production tools have been found (Liu 2003; 2006b). Recent excavations at the Zhongguang site, near Pinglin, indicate the possibility of multiple production centres (Liu and Chung 2014; Kuo 2015). In the late Neolithic Age, it is suggested that most sites showing nephrite artefact production belong to the Huagangshan Culture, which occupied the upper Coastal Mountain Range in eastern Taiwan (Liu 2003; 2013a). Although some scholars suggest that the Beinan Culture in southeastern coastal Taiwan also produced nephrite artefacts (e.g. Lien 1998), Liu (2003) however suggests that the people from Beinan, where large quantities of nephrite artefacts have been unearthed, were consumers instead of producers.

During this late Neolithic period, the consumption of nephrite artefacts appears to show regional patterns, and it is hypothesised that nephrite objects found in western Taiwan were imported from eastern Taiwan through the central mountainous area (Liu 2013b). Compared to the abundance of nephrite in northern and eastern Taiwan, smaller quantities of nephrite artefacts are found in western Taiwan. These differences are also highlighted by different traditions of pottery in western and eastern Taiwan in this period. The late Neolithic period in western Taiwan is known for the use of black pottery, while in contemporary northern and eastern Taiwan red pottery is predominantly found. This may indicate a regional differentiation based on the production and consumption of nephrite and pottery.

In the northern and eastern regions, the typology of nephrite items also shows differences. This can be seen particularly in nephrite earrings *Jue* (玦). Earrings excavated from sites in northern and northeastern Taiwan, such as Yuanshan, Wanshan and Huagangshan, possess a

round cross-section, while those excavated from the southeastern region, in particular Beinan, show rectangular cross-sections (Liu 2013b).

Neolithic Taiwan was also an important centre for exporting nephrite objects or raw materials to the South China Sea region. Research has shown the spread of nephrite from Taiwan to the South China Sea region occurred in two stages: the first stage around 2000-500 BC with the finished objects being exported to mainly the Philippines, and the second stage around 500 BC- AD 100 which witnessed the export of raw materials, as pre-processed blanks, to a wider region including the Philippines, central and southern Vietnam, southern Cambodia, peninsular Thailand and east Malaysia across the South China Sea (Hung *et al.* 2007; Hung and Bellwood 2010). The exported nephrite blanks were processed into ornaments at local workshops in Southeast Asia. Nephrite blanks with similar shapes and manufacturing debritages were found at the Pinglin site in eastern Taiwan as well as Anaro (the Philippines), Giong Ca Vo (Vietnam) and Khao Sam Kaeo (Thailand) in Southeast Asia (Hung 2012; Hung and Iizuka *in press*). During the second stage, the most common types of ornament in Southeast Asia are the *lingling-o* (three pointed circumferential earrings) and the double-headed animal pendants. These two types of nephrite artefact are regarded as typical in the Sa Huynh-Kalanay Culture in contemporary South China Sea region. However, a large number of these two artefacts was not seen in Taiwan, although a rather small quantity of *lingling-o* and double-headed animal pendants was found in southeastern Taiwan and the offshore islands (Lee 2005b; 2007; Hung and Bellwood 2010).

The decline of nephrite production and consumption in Taiwan can be traced back to around the turn of the 1st century AD. In this period, archaeological evidence witnesses the presence of metal artefacts, glass beads and agate beads, although at different times through the Iron Age. It is the decline in nephrite associated with the introduction of new materials that has

led to the suggestion that the nephrite objects were replaced by iron artefacts, as daily tools, and glass and agate beads, as decorative items, although tools made of nephrite are still unearthed in eastern Taiwan dating to this period (Liu 2005).

3.3. The early Iron Age in Taiwan

As early as from the late 1st millennium BC, Taiwan witnessed the transition to the Iron Age. This transition shows a greater impact of exotic materials on local material culture. The presence of glass beads, and probably metal artefacts, in several Iron Age cultures is recognised as exotica, which may suggest population migration or exchange activities with foreign cultures. The emergence of chiefdoms and alliances in some regions is also tentatively suggested (Liu 2011f: 227). This indicates more complex relationships and interactions between regions in Iron Age Taiwan and overseas countries in comparison to the late Neolithic period. The distribution of the known regional cultures around coastal areas is provided in Figure 3.1.

3.3.1. Regional cultures, exchange activities and exotic influences

3.3.1.1. Northern Taiwan

The Shisanhang Culture (ca. 2nd-15th century AD) in northern and northeastern Taiwan (Figure 3.1) is known for the use of geometrically stamped pottery, which may indicate its development from the Neolithic Botanic Garden Culture. Geometrically stamped red pottery and sideways flexed burial is representative of this culture. The evidence of iron smelting found at the Shisanhang site suggests the Shisanhang Culture may be the only group in prehistoric Taiwan that knew the technique of iron smelting. The origin of the knowledge

of smelting remains unclear, although independent innovation is suggested (Chen 2000). Archaeological evidence, such as copper coins dating to between the Tang and Song Dynasties (Table 3.1), suggests interaction between the Shisanhang Culture and Han people of China (Tsang 2001; Tsang and Liu 2001). On the other hand, the presence of glass beads, agate beads, bronze coins and gold artefacts from sites such as Shisanhang, Hanben (ongoing excavation) and Chongde indicate the involvement of exchange activities between not only China but also with other cultures from around the South China Sea (Gushi 2015; Liu 2007; Liu 2014; Tsang 2001).

It should be noted that an exchange network based on mainly iron and greyish black pottery in northern and eastern coastal Taiwan has been proposed, which corresponds to the area of Shisanhang, Jingpu, Sanhe and Lobusbussan Cultures (Liu 2010; 2011f: 262) (details of other cultures see below). The origin of iron artefacts in this network is thought to derive from the Shisanhang site in northern Taiwan due to the evidence of iron production at this site. The Shisanhang people are thought to be intensively involved in local and regional exchange activities in northern and eastern coastal Taiwan (Tsang 2001; Tsang and Liu 2001).

3.3.1.2. Eastern Taiwan

In eastern Taiwan, the Jingpu Culture (ca. 5th-15th century AD) is the principal phase found in the upper Coastal Mountain Range (Figure 3.1), but there is a lack of archaeological research and clear chronological dating. Plain red pottery is used in the Jingpu Culture, and the typology of some pottery resembles the utilitarian vessels and the sacrificial pottery vessels, *dewas* for example, used by current Ami aborigines (Chen 1968: 113; Huang and Liu 1980; Liu and Yen 2000: 153-155). Glass beads, agate beads and gold artefacts are often found in the Jingpu Culture (Tsang 1995; Lee and Yeh 2001: 137-138), but the presence of

large quantities of glass and agate beads seem to appear rather late in comparison to other early Iron Age cultures in northern and eastern Taiwan.

Recent excavations at the Huagangshan site in the upper Coastal Mountain Range, however, has revealed possibly a different Iron Age culture, named the Upper Huagangshan Culture (ca. 1st-4th century AD) (Chao *et al.* 2013) (Figure 3.1). The excavators suggest that this may have been occupied by new immigrants, for the pottery styles and burial practice are different from the Neolithic Huagangshan Culture (Liu and Chao 2010; Chao *et al.* 2013). In the newly identified Upper Huagangshan Culture squatted sitting burials were found, while in the Neolithic Huagangshan Culture jar burials dominated (Yeh 2001; Liu and Chao 2010). In the Upper Huagangshan Culture, grave goods such as glass beads, nephrite earrings and footed blackish or reddish pottery with long necks were unearthed, which are different from those of the Neolithic Huagangshan Culture where most of the grave goods consist of nephrite artefacts. The importance of the Upper Huagangshan Culture to this research, is that it reveals the early presence of glass beads in the upper Coastal Mountain Range and also probably shows the transition of nephrite consumption and production between the late Neolithic Age and early Iron Age. Although a few nephrite earrings and some production waste were found in the Iron Age layers, the excavators suggest that these new immigrants did not possess the knowledge of nephrite production, which the Neolithic peoples did (Chao *et al.* 2013).

In southeastern Taiwan, the Sanhe Culture (ca. the 3rd century BC-the 6th century AD) is found (Figure 3.1). Although iron artefacts are found in this culture, lithic tools predominate. Slate slab coffins, a burial practice which may be inherited from the Neolithic Beinan Culture, are used in Sanhe Culture (Liu *et al.* 1994; Lee 2010: 171-180). Together, it has been suggested that the presence of nephrite ornaments and some red pottery showing

Beinan characteristics, indicate that the Sanhe people may be descendants of the Neolithic Beinan Culture (Lee and Yeh 2001: 120; Kuo 2008; Liu 2011f: 248-251). However, the funerary pottery from the Jiuxianglan site (Sanhe Culture) shows a diverse typology in comparison to those of the earlier Neolithic culture. Most of the funerary pottery is smaller than that used as functional vessels, and these are decorated with mainly punched-dotted geometric and circle-stamped motifs (Lee 2010: 182-183). The shape and motifs of some funerary pottery also shows a similarity to those found in the Guishan Culture in southern Taiwan (see section 3.3.1.3) (Lee 2010: 182-183). This may indicate some potential interaction or cultural affinities to other cultures in southern Taiwan. Also, excavations at the Jiuxianglan site reveals the presence of sandstone moulds used for casting and it has been suggested that the style of these sandstone casting moulds is similar to the moulds found in Southeast Asia (Hung and Bellwood 2010; Hund and Chao *in press*), although recent investigation has shown that the sandstone used to produce the mould is procured locally in southern Taiwan (Yang *et al.* 2012). Substantial amounts of glass beads are often found at the Sanhe Culture sites. The presence of the Southeast Asian style sandstone moulds and the significant numbers of glass bead suggest interaction with contemporary Southeast Asia.

3.3.1.3. Southern Taiwan

The Guishan Culture (ca. 5th-10th century AD) is found in southern Taiwan (Figure 3.1). Although most pottery is plain ware, this culture is well-known for the elaborately decorated vessels using a combination of impressed human figure motifs and geometric patterns, which are unique compared to other contemporary cultures in Taiwan (Li *et al.* 1985; Li 1993; 2003). The motifs on the decorated pottery are believed to be related to current Paiwan aborigines in southern Taiwan. The human figure motif on Guishan pottery, for example, is

one of the typical decorative elements found on Paiwan artefacts (Li 2003). Guishan style pottery is also found in the Upper Huagangshan Culture and Sanhe Culture along the eastern Taiwan. Petrographic analysis, however, suggests that the decorated Guishan pottery may have been produced in southeastern Taiwan instead of locally manufactured in southern Taiwan (Li 2003; Yang *et al.* 2012).

There is the issue of the relationship between the Guishan Culture and the Sanhe Culture. Similar to the material culture of the Sanhe Culture, the majority of artefacts from the Guishan culture are made of stone instead of metal, and slate slab coffins were also used (Li *et al.* 1985; Liu 2011f: 252). At the Sanhe Culture site of Jiuxianglan, the handles on some pots are made in the shape of a Hundred-pace Viper, these handles are also sometimes found on 'Guishan type' pottery. The Hundred-pace Viper decorative element is also associated with the current Paiwan aborigine people, who regard the Hundred-pace Viper as their ancestor (Lee 2006; Kuo 2008). Therefore, some archaeologists believe that, based on the stylistic similarities and chronological sequence of the Guishan Culture and Sanhe Culture, the Guishan Culture may be the late stage of, or have developed from, the Sanhe Culture. Both the cultures also show relationships to the Paiwan aborigines (Lee 2006; Kuo 2008).

3.3.1.4. Southwestern Taiwan

In southwestern Taiwan, the Niasong Culture (ca. 2nd-15th century AD) occupies a vast plain area (Figure 3.1). In contrast to contemporary eastern and southern Taiwan, few lithic tools were excavated in this Iron Age culture. It is thought to be more likely that iron tools were used for the production of bone implements of high quality, as abundant numbers of delicate bone artefacts, with manufacturing traces of sharp tools, were found (Tsang and Li 2013: 246-248, 255-259). However, the source of these large quantities of iron artefacts

found remains unclear, as no archaeological evidence related to iron production was identified in southwestern Taiwan.

In most Niaosong Culture sites, bird-head shaped figurines made of clay were frequently found (Liu 2011c: 905-909; Tsang and Li 2013: 237). Their function is unknown. Analogy with similar artefacts associated with the Siraya aborigines suggests they may have a religious purpose (Liu 1986) or they may function as a musical instrument (Tsang and Li 2010). The presence of pottery steamers and clay stand bars, which may be used to support cooking vessels, also suggest a unique development in dietary habits in southwestern Taiwan in the Iron Age (Liu 2011c: 504, 919-927; Tsang and Li 2013: 242-243).

The Niaosong Culture has been divided into three stages: the Anzi Stage (2nd-6th century AD), the Niaosong Stage (6th-10th century AD) and the Kanxi Stage (10th-15th century AD). The Anzi and Niaosong Stages are the focus of this research. Slight differences of pottery and burial practice can be seen in the two stages. In the later Niaosong Stage, pottery with ‘button holes’ and short foot rings emerged. The mortuary practice shows extended supine burials in both stages, but the tradition of paving potsherds under the body of the deceased seen in the Anzi Stage is not seen in the Niaosong Stage.

The Iron Age Niaosong Culture in southwestern Taiwan shows some differences and similarities, in terms of the pottery artefacts, to that of the Neolithic culture in this region. The tradition of using blackish pottery in the Neolithic Age in this area seems to disappear in Iron Age. Instead, red plain pottery predominates, and the size of pottery vessels decreases. However, the typology and motifs of some Iron Age red pottery is similar to the Neolithic black pottery, which has led to the suggestion that the Iron Age Niaosong Culture may be locally developed with some ‘exotic influences’ reflected by the presence of iron artefacts,

glass beads and agate beads (Liu 2011b: 126; 2011c: 565-566, 782-788).

3.3.1.5. Middle-western Taiwan

The Fanziyuan Culture (ca. 1st-16th century AD) is found in middle-western Taiwan (Figure 3.1). The early stage (1st-12th century AD) shows the use of black pottery, while in the late stage (12th-16th century AD) red pottery became more abundant (Liu 1999: 93-98). Prone burials and shell middens are the distinct characteristics of Fanziyuan Culture.

The quantity of glass beads unearthed in Fanziyuan Culture sites differs in the two chronological stages. In the early stage, which is the focus of this research, the presence of glass beads in any context is rarely reported, while in the late stage thousands of glass beads were unearthed particularly at the Luliao site (Liu 1999; Ho and Liu 2005; Liu and Ho 2005). However, the typology of most glass beads found at Luliao probably suggests different origins of glass beads in early 2nd millennium AD in Taiwan to those found in early sites, as they do not resemble those found in the 1st millennium AD in Taiwan (see Chapter 7 and Chapter 11).

3.3.1.6. Central mountainous regions

In the mountainous areas, several cultural phases were found, such as the Daqiuyuan Culture (ca. 1st-10th century AD) (Sung 1980: 92; Liu 1999), the Yingiana Upper Layer Culture (ca. the 10th century BC-the 18th century AD) (Tsang and Chang 1996; Hung and Ho 2007) and the Beiyeh Culture (ca. the 2nd century BC-the 16th century AD) (Liu 2011f: 246). Although chronologically parallel to the Iron Age in the coastal areas, only a few iron artefacts were found in the mountainous regions. The transition from the Neolithic Age to the Iron Age is

less distinct in the mountainous areas in comparison to the coastal areas. Archaeological evidence has shown that lithic tools were the main finds, and red pottery was extensively used. The interaction with the coastal areas, however, can be seen based on artefacts showing non-local features, such as glass beads, agate beads and grey blackish potsherds (Liu 2006a; Hung and Ho 2007). In addition, the excavation at the Lalu site (ca. 4th-10th century AD), which is of the Daqiuyuan Culture, has revealed a large amount of nephrite waste and artefacts, indicating that nephrite production continued in the mountainous areas in Iron Age Taiwan (Liu 2001).

3.3.1.7. The offshore islands

In addition to the main island, the Green and Orchid Islands off the southeast coast of Taiwan are of the Lobusbussan Culture (Figure 3.1). Archaeological records relating to the Lobusbussan Culture are limited, but it was reported that metal artefacts and glass beads were found (de Beauclair 1972; Tsang 1995; Chen 2008). The archaeological assemblages from the Green Island are similar to those from the contemporary Jiuxianglan site in southeastern Taiwan (Chen 2008). However, the double jar burial practice seen in the Orchid Island and the typology of most pottery and lithic artefacts in the Lobusbussan Culture are not found on the main island, but are similar to those of the northern Philippines (de Beauclair 1972; Stamps 1980; Chen 2008).

3.3.2. Glass beads in early Iron Age Taiwan

3.3.2.1. The introduction of glass beads

Glass beads appear first in early Iron Age contexts in Taiwan, possibly replacing nephrite.

The first occurrences have been seen around the turn of the the 1st century AD, in particular in eastern Taiwan (e.g. Beinan site (Lee 2002), Jiuxianglan site (Lee 2005a) and Huagangshan site (Liu and Chao 2010)).

Glass beads in the early Iron Age in Taiwan are mostly monochrome and plain, without further decoration. These beads resemble the so-called 'Indo-Pacific glass bead' in contemporary Southeast Asia, which is drawn, monochrome and usually several millimetres in diameter (Francis 2002: 19-26). Glass beads of red, orange, yellow, green and blue colours are found in early Iron Age contexts in Taiwan, but there seems to be regional differentiation in terms of the quantities found.

In general, the numbers of glass beads unearthed in early Iron Age contexts (ca. the 1st millennium AD) are larger in northern and eastern Taiwan than in western Taiwan. For instance, hundreds of glass beads were reported from Shisanhang (northern Taiwan) (Tsang and Liu 2001: 91-106), Kiwulan (northeastern Taiwan) (Chen *et al.* 2008e: 17-33), Huagangshan (eastern Taiwan) (Liu and Chao 2010), Basangan (eastern Taiwan) (Yeh 1993), Jiuxianglan (southeastern Taiwan) (Lee 2005a; 2005b; 2007; 2010) and Guishan (southern Taiwan) (see Chapter 7 for Guishan beads). In contemporary southwestern Taiwan, less than a hundred glass beads were unearthed at Daoye (Nanke Archaeological Team 2005), Wujiancuo (Nanke Archaeological Team 2005), Xiliao (Chen and Cheng 2011) and Niaosong (Huang 1982). In middle-western Taiwan, few glass beads were found in this period. This difference probably indicates different exchange activities in different regions although because of the differences in site sizes and periods of occupation, other factors cannot wholly be discounted from influencing this feature. However, the general trend suggests exchange activities are foremost in influencing this pattern (see Chapter 11).

It is suggested that the import of glass beads in early Iron Age Taiwan was based on the maritime network established in the Neolithic Age (Liu 2005; Hung and Bellwood 2010; Chao and Wang 2012; Hung *et al.* 2013). Previous reviews of chemical analyses on some prehistoric glass beads in Taiwan also contributes to this point of view (Wang and Jackson 2014), and the similar typology in terms of the size and colour of glass beads (in general!) in Southeast Asia probably has been used to support this suggestion as well. However, there is a lack of detailed investigation of the shape, colour distribution and chemical characteristics of glass beads from different regions in Taiwan, which has hindered a comprehensive discussion of the similarity or otherwise (and hence potential origin) of glass beads within Taiwan and between Taiwan and the South China Sea network. This thesis will rectify this omission.

3.3.2.2. Glass bead production in southeastern Taiwan?

In the early 2000s, the excavation at Jiuxianglan revealed evidence for glass beadmaking in southeastern Taiwan, including glass rods, small glass chunks, fused glasses and a mandrel encircled with a glass bead (Figure 2.2). Together with the presence of burned clay, animal bones, iron slags and charcoals in the nearby areas, the excavator suggested that the location where this glass waste was unearthed may be a midden (Lee 2005a; 2010). In a later report, although the exact physical structure relating to glass beadmaking is not identified, the excavator pointed out that the gravel structures near the midden may be related to metal or glass production (Lee 2010: 29). Based on these archaeological finds, archaeologists believe that Jiuxianglan may be a production centre for glass beads.

3.4. Summary

This chapter has discussed the background of the early Iron Age in Taiwan, noting the transition from the late Neolithic period to the early Iron Age and the role of Taiwan in the South China Sea network in different periods. The summary of archaeological finds from each of the sites mentioned in this chapter can be seen in Figure 3.1. The beginning of the Iron Age in Taiwan is earlier, in the late 1st millennium BC in the eastern coastal region, and later, in the early 1st millennium AD in the western coastal area. In early Iron Age, different cultural phases are identified, based on the pottery traditions and mortuary practices, in different geographic regions. Northern and northeastern Taiwan is occupied by the Shisanhang Culture. Eastern Taiwan reveals the presence of the Jingpu Culture and a recently identified Upper Huagangshan Culture. In the southeastern part of the island, the Sanhe Culture is present, and in the southernmost region the Guishan Culture is found. The southwestern plain area was occupied by the Niaosong Culture. In the middle-western Taiwan the Fanziyuan Culture is found.

Archaeological evidence has suggested the local development of most Iron Age cultures, as artefacts showing Neolithic characteristics were sometimes unearthed, in particular pottery types, which continued to some extent in the later Iron Age and were distinct regionally. This can be seen in the Shisanhang Culture in northern Taiwan, the Sanhe Culture in eastern Taiwan and the Niaosong Culture in southwestern Taiwan. In the Sanhe Culture, the use of slate slab coffins also supports the relationship with and continuations from the local Neolithic culture.

The archaeological record also suggests an interaction between different sites/regions within Taiwan. This regional interaction appears to have continued from the Neolithic period. In

the Neolithic period, the prevalence of indigenously produced nephrite artefacts is significant in northern and eastern Taiwan, and the procurement of nephrite raw materials is identified from the eastern region. Nephrite artefacts found in western Taiwan are thought to be non-local objects acquired from eastern areas. This eastern-western differentiation is also seen in the distribution of glass beads in the early Iron Age, when eastern and northern Taiwan have larger quantities of glass beads than in western Taiwan. The presence of particular types of pottery, for instance the Guishan decorated wares in southeastern and southern Taiwan, possibly also indicates interaction along the eastern coastal regions.

However, exotic influences are often found in archaeological sites of Iron Age date. In the Upper Huagangshan Culture, the distinct differences in material culture and burial practices in comparison to the Neolithic culture leads to the suggestion that this culture was formed by new immigrants settling in coastal eastern Taiwan. In addition, at most Iron Age sites, these exotic influences are probably reflected by the presence of glass beads, agate beads and metal artefacts. The Shisanhang Culture in northern Taiwan might have known how to smelt iron, but the origin of this smelting knowledge is unknown. In the Sanhe Culture (southeastern Taiwan), there seems to be glass production and iron smelting at Jiuxianglan site. However, the technological origin of glass production and the exact archaeological remains of iron smelting are not clear. Interestingly, although the evidence of iron smelting is found in northern and eastern Taiwan, generally the quantity of iron artefacts is not as abundant as that found in the Niasong Culture in southwestern Taiwan where no evidence of iron production was unearthed.

The introduction of exotic objects is thought to derive from the South China Sea network, which was established in the Neolithic period. Specifically, late Neolithic Taiwan was a principal contributor of the raw nephrite material to the South China Sea network, while in

the early Iron Age Taiwan became a recipient of glass beads, agate beads, carnelian beads and possibly metal artefacts from around the South China Sea. Although the exact origins of these artefacts remain unknown, this transition can be seen clearly through the similarities of archaeological assemblages in this period in Taiwan, in particular throughout the eastern coastal region. Overall, it is obvious that, through the archaeological evidence, the interaction and exchange activities within Taiwan and between Taiwan and the South China Sea network are diverse and complicated during this period, and therefore it is the purpose of this research to further understand the nature of these interactions through the study of the tiny glass beads.

4. Production and consumption of glass beads around the South China Sea

4.1. Introduction

This chapter provides the background of the production and consumption of glass beads in different regions around the South China Sea. Our current understanding of glass production in Southeast Asia and southern China suggests they are more or less intertwined with each other, and therefore this chapter aims to provide a more comprehensive background for the regional and chronological variations of glass production in the two regions in the South China Sea network. The raw materials and different stages of glass production are introduced as it is necessary to understand these in order to discuss the different compositions identified. This will be followed by a discussion of the manufacturing of glass beads, which is socially and culturally embedded in the region. Although the study of glass beads around the South China Sea is in its early stages, this research uses an archaeological and ethnographic point of view to appreciate the role of glass beads and their relationship with people in past societies.

4.2. The nature of glass

Most archaeological glass is silicate glass, which means the glass is principally composed of SiO₂ (silica). In this case SiO₂ is the glass *network former*, the most essential component in silicate glass. The melting point of pure silica is so high (1700°C) that other materials are added in order to facilitate the melting. For instance, alkalis (soda (Na₂O) or potash (K₂O)) can be added as a *flux* to reduce the melting temperature. Lime (CaO) or magnesia (MgO)

can be used as *stabiliser* to increase the stability and durability of glass. Soda, potash, lime and magnesia are known as glass *network modifiers*.

Colourants, *opacifiers* and *decolourants* are also important components in glass and are a valuable interpretive tool in archaeological glasses. In most archaeological glass, colourants are the 3d transitional metals in the chemical periodic table. For instance, cobalt oxide (CoO) contributes to the production of a dark blue colour, and iron oxide generates turquoise blue (ferrous reduced state, Fe²⁺) or brownish yellow colour (ferric oxidised state, Fe³⁺). An opacifier is added to produce opaque glass, usually by the production of crystals within the glass matrix. Tin-based (e.g. SnO₂) and antimony-based (e.g. Ca₂Sb₂O₇) compounds are the two predominant agents found in white opaque glass in antiquity (Turner and Rooksby 1959). The addition of a decolourant helps produce colourless glass, as most raw glasses are slightly coloured due to the presence of iron in the raw materials. The decolouring of glass is by introducing compounds containing antimony oxide (Sb₂O₃) and manganese oxide (MnO₂) which oxidise the iron and remove some of the blue colour produced by iron, themselves adding weak colours to the glass hue. The role of the antimony ion as an opacifier or decolourant in glass depends on whether the antimony is dissolved or present as a crystalline substance in the glass. Similarly, MnO₂ (Mn⁴⁺) is associated with the colourless effect in glass, while in other valency states such as Mn³⁺ a purple colour is obtained.

4.3. The raw materials

The silica for glass production was obtained from sources such as silica sand or quartz pebbles. Alkalis, as flux, can be derived from minerals or plant ashes. In Late Bronze Age Egypt (ca. 1500-1000 BC) soda plant ash was used as the flux in glass production (Brill 1970). During the Roman period, mineral soda flux was predominantly used, with the raw

material obtained by the addition of a relatively pure soda-containing mineral evaporate to the glass, commonly referred to as *natron* and thought to have been procured from Wadi Natrun in northwestern Egypt (Shortland *et al.* 2006). The tradition of soda plant ash flux appeared again in glass production in the Near East and Middle East in the Sasanian (3rd-7th century AD) and Islamic periods (ca. 8th-13th century AD) (Freestone and Gorin-Rosen 1999; Brill 2001; Mirti *et al.* 2008; Mirti *et al.* 2009), where halophytic plants growing in a saline environment (e.g. coastal region and desert) might have been the plants used. Meanwhile in Medieval Europe, potash flux obtained from forest plant ash was favoured for glass production; this had a distinct high content of lime (Jackson and Smedley 2004). Generally, mineral alkali flux possesses a lower magnesia concentration (typically <1%) than plant ash flux. Therefore, in some literature mineral alkali glass is referred to as Low Magnesia Glass (LMG), while plant ash glass is designated as High Magnesia Glass (HMG) (Henderson 1985). In the South China Sea region, the soda plant ash glass is also called v-Na-Ca glass (v for vegetal) (Lankton and Dussubieux 2006).

In the South China Sea network, soda and potash flux have both been identified in glass composition (Brill *et al.* 1995; Dussubieux and Gratuze 2010). Mineral *soda* glass is a predominant compositional type around the South China Sea, and is widely found in Southeast Asia (Dussubieux *et al.* 2010). It differs from the Roman natron glass for its higher concentration of alumina, which is thought to be contributed from less-refined sand, and therefore is designated as m-Na-Al glass (mineral soda alumina glass) (Dussubieux *et al.* 2010). The origin of m-Na-Al glass in Southeast Asia is currently thought to be South Asia. In South Asia, minerals such as *reh*, an efflorescence from soils, composed of sodium carbonate, sodium chloride and sodium sulphate, has been suggested as one possible source of soda flux (Brill 1987).

As for mineral *potash* glass, this type of glass is abundant in Southeast Asia and southern China. The potash flux may come from mineral substances high in potassium such as saltpetre (KNO_3) (Zhao 1991; Gan 2007; Dussubieux and Gratuze 2010). Gan (2007) further pointed out that the environment and climate in *Guangxi* and *Guangdong* in southern China is favourable for the formation of saltpetre, while in Southeast Asia the potential source of saltpetre is unclear. Zhao (1991) attributes the use of saltpetre as flux in China to the early use of saltpetre in medicine as early as the Western Han period, which probably provided the required knowledge of saltpetre processing for glass production.

In addition to soda and potash glasses, glass with a high concentration of lead (Pb) is a predominant type in southern China, and most high lead glass around the South China Sea probably originated in China. Prior to the Six Dynasties (220-589 AD) (Table 3.1), high lead glass in China often contains substantial amounts of barium. The addition of lead or barium (Ba) helps reduce the melting temperature of glass, and barium also acts as an opacifier in barium lead silicate glass. Brill *et al.* (1991a) found that Chinese glass (possibly 4th-1st century BC) containing lead and barium, shows Pb-isotopes at a low ratio with a tight cluster, and therefore may indicate the local procurement of raw materials in China. Research has suggested there are ores containing lead (galena, PbS) and barium (barite, BaSO_4) along the Yangtze River Valley (Zhao 1991). However, Brill *et al.* (1991b) argue that lead and barium may not be introduced from a single source, as no linear relationship is observed between lead and barium in barium lead silicate glass (see Chapter 5.3.1).

4.4. Glassmaking and glassworking

Glass production is not always a single stage mixing and melting of raw materials. It can be a two stage process: glassmaking as the primary stage and glassworking as the secondary

stage (Freestone *et al.* 2002; Rehren 2014). In general, glassmaking includes the process from the pre-treatment of raw materials, the melting of raw materials (or pre-heated frit) to raw glass and in some cases the colouring when colouring takes place during initial glass manufacture (e.g. Jackson and Nicholson 1998; Gorin-Rosen 2000; Rehren and Pusch 2005; Lankton *et al.* 2006). The end product of glassmaking could be broken glass chunks from larger blocks, rods or formed ingots which are used later for producing glass artefacts either in the same place as production or exchanged/traded to other workshops for reworking. Glassworking is the stage where the craftspeople produce glass artefacts (vessels, beads, bracelets etc.) from glass chunks, ingots or rods (e.g. Price 2005; Lankton *et al.* 2008a; Paynter 2008). These two stages may take place in different locations.

The identification of glassmaking relies on the recovery of relevant glass remains, tools and installations, such as the crucible (if used, but also may be present in secondary working), the furnace and the semi-finished glass attached to the crucible or furnace (Gorin-Rosen 2000; Rehren and Pusch 2005). In most cases, it is hard to suggest unambiguously the occurrence of glassmaking at a specific archaeological site due to the lack of evidence (Jackson 2005a). This problem is also encountered when studying glass production around the South China Sea in antiquity. Although there are assumptions of local development in some regions, these are mainly based on the interpretation of relevant glass waste or through chemical analyses, inferring local use of raw materials instead of the finds of physical installations.

Peter Francis (2002: 28-37) has suggested several glass production sites in Southeast Asia, such as Oc Eo (Vietnam), Khlong Thom (Thailand) and Kuala Selinsing (Malaysia) in early 1st millennium AD and Srivijaya (Indonesia) and Takua Pa (Thailand) in late 1st millennium AD (Figure 1.1). The evidence related to glass production at these sites is in the form of

mostly glass chunks, remelted glass, glass tubes and bead lumps, and therefore does not strongly point to glassmaking (although does not categorically rule it out). In the past decade, more systematic studies on glass from Khao Sam Kaeo and Khlong Thom in Thailand have been conducted, but little evidence from these sites can be directly linked to glassmaking. It was suggested that a particular type of mineral soda glass at Khao Sam Kaeo may be a local product in Thailand (Dussubieux *et al.* 2010), but later analysis seems to indicate the similarity, and potentially the origin, of this composition to glass from northern India (Lankton and Dussubieux 2013: 431). In Khlong Thom, the possibility of glassmaking was proposed based on the presence of large fused glass chunks (Lankton and Dussubieux 2013), but there is still a lack of convincing physical evidence (Dussubieux 2014, *pers. comm.*). Alternatively, evidence of glassmaking was suggested at Giong Ca Vo in Vietnam, for ‘fritty waste and three pits in the ground that contained sand suitable for glass production’ were identified (Nguyen 2001; Nguyen Thi Kim Dung 1995 *pers. comm.*, cited in Francis 2002), but there is no further report or analysis at present. In all, glassmaking in Southeast Asia still remains ambiguous. Most evidence of glass production appears to be associated with glassworking, principally beadmaking (see below).

Alternatively, in southern China, glassmaking is thought to have emerged in the Yangtze River Valley from around the 5th century BC, although a few glazed beads pre-date this period. It is believed that the earliest production of barium lead silicate glass and potash (or potassium silicate) glass emerged along the Yangtze River Valley in the Warring States period (476-221 BC), and then spread southward and southwestward, among which *Guangdong* and *Guangxi* are thought to be important regions for producing potash glass (Gan 2007). In addition to barium lead silicate glass and potash glass, the later lead silicate and potassium lead silicate glasses in southern China are also believed to be local products, as the Pb-isotope analysis reveals the high lead glass from China as a distinct group (Brill *et*

al. 1991a). Despite the lack of evidence of physical installations, the early presence of glass containing high concentrations of lead, potassium or barium in China is often consistent with the potential sources of local raw materials, and generally the chemical composition also shows distinct Chinese characteristics (Chapter 5). Therefore, the evolutionary scenario of glassmaking in southern China is clearer than that in Southeast Asia.

Apart from glassmaking, evidence of glassworking can also be identified in China. Most of the early glass artefacts in China are glass beads, glass disc *bi* or spool-like glass pendants (beadmaking is discussed in section 4.5). It is suggested that mould pressing, which may be influenced by processes used in bronze production, was used to produce glass artefacts, such as *bi*, from the Warring States period (An 2000: 28; Hou 2005: 98). Early glass artefacts made by mould pressing often show Chinese characteristics in both styles and chemical compositions. In the Six Dynasties (AD 220-589), the presence of the glassblowing technique can probably be attributed to imported knowledge from the western world through Central Asia (An 2005: 123-125), and mould pressing and the wound method were also used in glassworking. Similarly, blown vessels were made locally in China and these were of typical Chinese styles and chemical compositions. However, despite the development of blowing techniques in China, many glass vessels are still believed to be exotic objects from the west, for the style and chemical composition do not suggest a Chinese origin (An 2000: 75-90). From the Six Dynasties onwards, no distinct technical change was observed in glassworking, and it is not until around the Yuan Dynasty (AD 1271-1368) that the historic records witness the emergence of glass workshops empowered by the royal court.

4.5. Glass beadmaking

4.5.1. The Indo-Pacific drawn method

The methods of glass beadmaking around the South China Sea may suggest regional and chronological differences. In Southeast Asia, it is believed that the drawn beadmaking method was introduced from South Asia by late 1st millennium BC, and this particular bead is called the *Indo-Pacific Monochrome Drawn Glass Bead* (Francis 1991; 2002). The broad geographic distribution of Indo-Pacific beads covers Southeast Asia, South Asia, East Asia and South Africa during the mid-1st millennium BC to the 1st millennium AD (Francis 2002).

The Indo-Pacific drawn method probably originated in Arikamedu (250 BC-AD 200), on the southeast coast of India (Francis 1990). Later on, this method might have spread to Sri Lanka, Thailand, Malaysia and Vietnam in early 1st millennium AD and later to Sumatra in Indonesia (Francis 1991).

Our understanding of Indo-Pacific drawn beadmaking is generally based on the ethnographic studies from Papanaidupet in northern India (Francis 1990; 1991). At the beginning of the process, glass chunks are placed on the trough of the furnace for melting. A craftsman on the other side of the furnace uses an iron rod called a *lada* to pick up the molten glass, he then rolls it on a plate to form the glass cone. After forming the cone, another rod called a *cheatlek* is inserted from the wide side of the cone, piercing the tip. Then the glass cone, hung by *lada* and pierced by *cheatlek*, is put back to the furnace, and another craftsman at the opposite side of the furnace pulls a glass tube, of around 5m in length, from the glass cone. These glass tubes are then cut into small glass beads, and in many cases these cut beads are mixed with ash to avoid them sticking together, and then

they are slightly re-heated, to get a blunt edge.

Glass beads made by the drawn method are usually several millimeters in length and the edge may be sharp or rounded off, depending on whether the beads were re-heated. Unintentional fabric lines or bubbles parallel to the perforation axis can often be observed on the surface of the bead.

4.5.2. The Chinese wound method

The replacement of Chinese wound beads for Indo-Pacific drawn beads in the South China Sea network from the 12th century AD onwards has been suggested (Francis 2002: 76-78). However, exactly when the wound technique developed and where the wound beads were made in China remain less clear in terms of archaeological and historic evidence, although the early presence of wound beadmaking was thought to be around the Warring States period (An 2000: 18-19; Hou 2005: 99).

The Chinese wound method is probably less labour intensive than the Indo-Pacific drawn method. Basically, the beads were made by heating a glass rod encircling the tip of a metal mandrel. Therefore, glass beads made by the wound method often show fabric lines or bubbles perpendicular to, or encircling, the perforation axis, and are probably more irregular than drawn beads. The wound beads, popular in the South China Sea, are generally smaller than drawn beads.

4.5.3. Other methods

In addition to the drawn and wound methods, the cold-working method of lapidary beadmaking has been identified at Khao Sam Kaeo (early 4th-2nd century BC) in Thailand (Bellina and Silapanth 2006; Lankton and Dussubieux 2013). Glass beads made by this method were knapped and polished in order to get the faceted shapes. Similar glass beads were also unearthed at another Iron Age site, Ban Don Ta Phet, in Thailand (Bellina and Glover 2011). The lapidary glass beadmaking at Khao Sam Kaeo is thought to be associated with the stone-working technique at the same site, as the two methods both involve the use of knapping and polishing (Bellina 2003; Bellina 2014). Research has suggested an Indian origin for the stone-working technique at Khao Sam Kaeo (Bellina 2014). Therefore, the use of lapidary techniques for beadmaking may have been influenced by bead production in India.

On the other hand in east Java in the mid-1st millennium AD, the production of millefiori glass 'Jatim' beads, using the mosaic method has been reported (Lankton *et al.* 2008a). The Jatim bead usually possesses a monochrome yellow glass core covered with polychrome glasses on the surface. Research has indicated that these glass beads were locally made in east Java, as the chemical composition shows the unique pattern of mixing two common glass compositions, and these are found around the South China Sea (Lankton *et al.* 2008a). The exact origin of the technique in east Java is unclear, although the possibility of an Egyptian origin is suggested (Lankton *et al.* 2008a: 355).

The differences of beadmaking methods between regions and periods therefore may inform the stylistic analysis of glass beads from around the South China Sea network. It is with the understanding of the manufacturing methods and context of glass beads that the typological

analysis may illuminate the potential origins and so highlight production locations, consumption and exchange of glass beads in and between different regions and through periods.

4.6. Social and cultural practices reflected by glass beads

Apart from manufacturing methods, another interesting and important aspect of glass beads found in various contexts is the cultural and socio-political practices reflected by the consumption of glass beads in local societies, which is often associated with social relations and the construction of value in a society.

In recent decades, archaeological research in *mainland* Southeast Asia has started to discuss beads, including glass and siliceous stone beads, as ‘status markers’ and the related cultural adaption and socio-political practice relating to elite status or alliance. Recent research on glass and siliceous beads in Southeast Asia has suggested the transition and/or expansion of the exchange network from the earlier South China Sea-oriented network to the later South Asian network, which also led to the adoption of South Asian culture in mainland Southeast Asia (Bellina 2003; Bellina 2014; Carter 2015). Bellina has also suggested that craftspeople in South Asia produced bead ornaments particularly with a Southeast Asian style for exporting, and in Southeast Asia there are also beads with ‘South Asian-inspired’ styles found from local workshops (Bellina 2003; Bellina 2014). Therefore, the unique style and the role of beads here, regardless of whether or not they are locally or non-locally made, is considered as symbolic and prestige objects for local elites in mainland Southeast Asia in order to validate their control over the exchange activities and build intra- and inter-regional alliances (Bellina and Silapanth 2006; Bellina 2014; Carter 2015). Also they propose the settling of local or foreign specialised craftspeople in mainland Southeast Asia, under the

sponsorship of local elites who control labour and control the production and distribution of beads (Bellina 2003; Bellina 2014). Here, beads are regarded as a means to legitimise the elites' political status as well as maintain the social stability of the local hierarchy.

The study of the social and cultural value of beads in prehistoric *island* Southeast Asia is limited to comparison with mainland Southeast Asia. However, the abundance of ethnographic research allows good parallels to assess the use of glass beads in daily life in different societies. The *Orang Ulu* (the remote or upriver people) in central Borneo provide a good case study. Among these communities in Borneo, beads can be used as prestige markers, displaying and legitimising the social status of the owner (Janowski 1998; Munan 2005: 70). In some communities, particular types of bead are thought to have special powers. Shamans can use the beads to protect and strengthen their soul while healing patients or as a means of communicating with the spirits and to also protect their patients' souls or comfort the spirits (Francis 2002: 186; Munan 2005: 41-48). In mortuary practices, beads may be buried with the deceased for the journey to the underworld (Munan 2005: 61, 64-65). Heirloom beads, which have been passed down over many generations, are an important tradition in Borneo, and the inheritance of heirloom beads often reflects a higher social status (Janowski 1998; Francis 2002:185-186; Munan 2005: 74-75). The development of heirloom inheritance in Borneo, however, is suggested to be no earlier than the 13th century AD (Francis 2002: 186). The tradition of inheriting heirloom beads and their association with social status and cultural practice are also seen nowadays in aboriginal populations in Taiwan, the Philippines and the Lesser Sundas in eastern Indonesia (Francis 2002: 183-184, 186-187; Hsu 2005; Umass 2005).

In Taiwan, the use of glass beads is seen in several aboriginal groups. Most research, however, has focused on the polychrome heirloom beads used by Paiwan aborigines in

southern Taiwan. Early studies have shown the value of different forms of heirloom beads in the Paiwan group, as well as the relationship between the decorative patterns and social status (Hsu 2005; Umass 2005). For example, *mulimulidan* is the most valuable bead, and is the status marker of the chieftain (Hsu 2005: 78, 114). Only aristocrats own glass beads; in this way they are therefore regarded as a manifestation of aristocratic status and power. Many Paiwan people store their valuable glass beads in ancient pottery, where the spirits of their ancestors live. Other glass beads commonly worn in daily life are left in a basket, called *chalakulu*, or under the slab in the house; the *chalakulu* or the slab often have holes so that the beads can breathe (Hsu 2005: 84). Despite the lack of a comprehensive study of glass beads in different aboriginal groups in Taiwan, recent research by Hu (2012) proposed possible regional variations in the use of glass beads in aboriginal groups. Through the preliminary comparison of the colours and decorative patterns of glass beads from varied geographic regions in Taiwan, she suggests that there may be ‘internal cultural values and selections’ between different societies, although there is no further discussion of what this may mean (Hu 2012).

4.7. Summary

This chapter has assessed the regional and chronological variation of glass production around the South China Sea and has shown that glass production in Southeast Asia and southern China has different traditions in terms of the raw materials and glassworking methods. Glassmaking in southern China is believed to have emerged from regions around the Yangtze River, and high lead glass and some potash glass are believed to be local products in southern China. The potential locations of lead ores and saltpetre used for glass production are suggested to derive from southern China. Mould pressing and the blown technique are both used in glassworking in China; mould pressing is thought to be a local

development and the blown technique is probably a western import. In contrast, in Southeast Asia, m-Na-Al glass and potash glass are the most common glass types. However, the uncertainty of whether glass was locally produced in this region means that it is impossible to suggest where the raw materials for glass production may have come from. Evidence associated with glassmaking is rather ambiguous and most of the archaeological findings suggest only secondary production of glass beads.

The methods of making glass beads also shows differences between Southeast Asia and southern China. In the South China Sea network, the wound method characterises glass beads made in China particularly from the 12th century AD onwards, while drawn beads were Southeast Asian or South Asian products and were popular before the 12th century AD. The lapidary method for bead production is a unique method identified in Thailand. The origin of both the drawn and lapidary methods in Southeast Asia are associated with South Asian influence. Mosaic beadmaking is used in the production of the polychrome Jatim beads in east Java, and a western origin is suggested for the emergence of the mosaic method.

It is noteworthy that, based on current studies, it is likely that most glass was imported from other regions to the production centres in Southeast Asia, and then reworked into glass beads. In southern China, although the typology and composition generally are thought to be local, some glasses, such as those of potash composition, may have come from Southeast Asia. Therefore, information acquired from chemical compositions is important for the further understanding of glass artefacts and glass production and exchange around the South China Sea. A review of the chemical composition of glass in Southeast Asia and southern China is provided in the next chapter.

Research on mainland Southeast Asia has suggested the use of beads as prestige goods for

the legitimisation of status, and this practice is also seen through ethnographic records in island Southeast Asia and Taiwan. The examination of studies from prehistoric mainland Southeast Asia further indicates the 'adoption' of and 'inspiration' from exotic cultures through the study of beads. Ethnographic research on island Southeast Asia and of Taiwan aborigines on the other hand reflects the social relations and value of glass beads in different present day societies. These studies reveal the way that local elites or aristocrats validate their status and manifest their wealth through exotic prestige goods such as glass beads. Furthermore, they also provide archaeologists with one perspective which shows the use of glass beads in different societies.

5. Previous chemical studies of prehistoric glass beads in Taiwan and around the South China Sea

5.1. Introduction

In the last decade many compositional studies on glass beads around the South China Sea have been published. This chapter reviews these chemical studies of glass beads from approximately 500 BC to AD 1000, starting with the research in Southeast Asia in section 5.2 and southern China in section 5.3 in order to provide an overview with which to place the compositions of the beads analysed in this study. A summary of published compositional analyses of Taiwanese glass beads is provided in section 5.4. Figure 1.1 shows the map of sites mentioned in this chapter.

5.2. Southeast Asia

The compositions of glass beads found in Southeast Asia from 500 BC to AD 1000 are diverse (Dussubieux and Gratuze 2010; Dussubieux and Lankton 2006; 2013). Previous research in the 1990s by Basa *et al.* (1991), Brill (1995), Brill *et al.* (1995) and Glover and Henderson (1995) identified some glass compositions which are typical of Southeast Asia and South Asia based upon major and minor elements. Two most frequent types, alumina soda glass and potash glass, were found, and it is suggested that mineral alkali sources were used in both types of glass (Brill 1995). Later research by Dussubieux (2001), Dussubieux and Lankton (2006; 2013), Dussubieux *et al.* (2010), Dussubieux and Gratuze (2010) and Carter (2013) analysed the compositions at major, minor and trace elemental levels of glass from Southeast Asia and South Asia, which allowed further grouping within these

compositions. These studies shed light on the potential to differentiate specific chemical groups from different geographic regions using trace elements, although the research is still in an early stage. A summary of the different types of glass compositions, in terms of major and minor elements, adapted from Dussubieux and Gratuze (2010) is provided in Table 5.1. The sub-groups, the potential evidence of raw materials and the spatial distribution of different types of glass composition are further discussed below.

Table 5.1: A summary of glass composition in Southeast Asia based on major and minor elements (Dussubieux and Gratuze 2010).

		Flux				
		Soda			Potash	Mixed alkali flux
		mineral source	Additional K ₂ O and MgO flux	plant ash source		
Sand	Alumina rich	m-Na-Al 1 & 3 Al ₂ O ₃ ~ 10%; CaO ~ 3% MgO < 1.5%; K ₂ O < 1.5%				
	Slightly alumina and lime rich	m-Na-Ca-Al Al ₂ O ₃ ~ CaO ~ 5%; MgO < 1% and K ₂ O < 1.5%; UO ₂ ~ 20ppm	Arika glass Al ₂ O ₃ ~ CaO ~ 5%; MgO and K ₂ O are variable with K ₂ O ~ 2 x MgO			
	Lime rich			v-Na-Ca Al ₂ O ₃ ~ 3%; MgO > 1% and K ₂ O > 1.5% and MgO > K ₂ O; CaO ~ 8%		
	With variable lime and alumina				Potash glass SiO ₂ > 70%; Na ₂ O, MgO < 3%	

5.2.1. m-Na-Al glass

M-Na-Al (mineral soda alumina) glass was firstly identified by Brill (1987) in South Asia. Later research indicated it had a wide distribution within Southeast Asia, East Asia and South Africa from the 1st millennium BC onwards (Brill 1995; Dussubieux 2001; Dussubieux *et al.* 2010; Robertshaw *et al.* 2010). This type of glass is typically a silicate glass which is rich in Na₂O (soda, more than 10%) and Al₂O₃ (alumina, 5-15%) and low in MgO (magnesia, less than 1.5%). The CaO (lime) concentration, however, can be varied from less than 1% to around 5%. The characteristic low magnesia concentration has led to the suggestion that mineral soda flux was used in glass production (Brill 1987) (Chapter 4.3).

Dussubieux *et al.* (2010) reported 5 sub-groups of m-Na-Al glass based upon varying degrees of the minor elements Ca (calcium) and Mg (magnesium), and of the trace elements U (uranium), Ba (barium), Sr (strontium), Zr (zirconium) and Cs (caesium). These sub-groups cover a wide geographical and chronological range in South Asia, Southeast Asia, east Africa and Turkey from the 4th century BC to the 14th century AD (Dussubieux *et al.* 2010). Two of these types, m-Na-Al 1 and m-Na-Al 3, were found in Southeast Asia in the early period. The major and minor element compositions do not show distinct differences between the two groups, however, the trace elements display different patterns. The m-Na-Al 1 is low in U (11±10 ppm) and high in Ba (931±432 ppm), Sr (373±91 ppm) and Zr (561±420 ppm), while in m-Na-Al 3 the concentration of U is high (98±87 ppm) and the contents of Ba (353±43 ppm), Sr (132±70 ppm) and Zr (193±27 ppm) are low. The m-Na-Al 1 was found to be earlier in southern India and Sri Lanka (the 4th century BC-the 5th century AD) and later in Southeast Asia (the 3rd century BC-the 10th century AD), with the possible primary production in proximity to Sri Lanka (Dussubieux 2001: 121-124; Dussubieux *et al.* 2010). Conversely, the m-Na-Al 3 composition is mostly found in

Thailand, southern Vietnam and Cambodia in Southeast Asia (Dussubieux *et al.* 2010). This latter type was first thought to be a local product of Southeast Asia, possibly manufactured somewhere in the upper Thai-Malay peninsula, but later publications indicate its similarity to glasses from northern India where it probably originates (Lankton *et al.* 2008b; Dussubieux and Gratuze 2010; Lankton and Dussubieux 2013: 431).

5.2.2. Potash glass

Potash glass is also a common chemical group in Southeast Asia. Lankton and Dussubieux (2013, and see Figure 5.7.3 in the cited article) imply that there seems to be a transition from the dominance of potash glass to that of m-Na-Al glass in Southeast Asia during the turn of the 1st century AD, but the actual picture is still ambiguous. The distribution of potash glass covers a wide geographical range throughout Southeast Asia, South Asia, China, Japan and Korea (Lankton and Dussubieux 2006). This type of glass generally has a K₂O concentration higher than 15% and Na₂O and MgO concentrations lower than 1.5%. A mineral potash source such as saltpetre (KNO₃) may have been used as the flux (Dussubieux and Gratuze 2010). The production and provenance of potash glass remains even more unclear and controversial than that of mineral soda glass, although it is suggested that at least 3 sub-groups, possibly associated with different production regions, can be distinguished: (1) m-K-Ca, low Al₂O₃ and high CaO (Al₂O₃ around or below 1%), (2) m-K-Al, high Al₂O₃ and low CaO (CaO around or below 1%) and (3) m-K-Ca-Al, moderate Al₂O₃ and moderate CaO (CaO and Al₂O₃ in 1-4%) (Lankton and Dussubieux 2006; Dussubieux and Gratuze 2010).

All the three sub-groups can be found in Southeast Asia, but there is a geographical difference in their findspots. The high CaO potash glass (m-K-Ca, sub-group 1) was identified particularly at Ban Don Ta Phet, an Iron Age site in central Thailand (Glover and

Henderson 1995). The m-K-Ca glass seems to be rare in South Asia and East Asia. Glover and Henderson (1995) suggest that this may be a local product in Southeast Asia or southern China. Glass artefacts within this group are also identified in Vietnam. It is also suggested that there may be primary production in southern Vietnam based on the archaeological findings of glassmaking in the area with this composition (Lankton and Dussubieux 2006). Potash glass with high Al₂O₃ (m-K-Al, sub-group 2) is wider spread and found in Thailand (Lankton *et al.* 2008b), northern Vietnam (Lankton and Dussubieux 2006), southeastern Cambodia (Carter 2010) and southern China (Fu and Gan 2006; Gan 2007; Xiong and Li 2011: 79-96). This composition is not identified at Ban Don Ta Phet. The manufacturing evidence (more likely glassworking) was found at Khao Sam Kaeo in Thailand (Lankton and Dussubieux 2013). Lankton and Dussubieux (2006) suggest that primary production is likely to be somewhere in the northern regions of mainland Southeast Asia and southern China due to its predominant distribution in northern Southeast Asia and East Asia. The moderate CaO and moderate Al₂O₃ glass (m-K-Ca-Al, sub-group 3) is more abundant in South Asia than in Southeast Asia and southern China. The site Arikamedu in southern India is thought to be one of the production centres of m-K-Ca-Al glass based on the large numbers of m-K-Ca-Al glass artefacts and the relevant waste found there, and some amount of m-K-Ca-Al glass in Southeast Asia may be imported from southern India (Lankton and Dussubieux 2006). M-K-Ca-Al glass is distributed over Southeast Asia, mostly in Vietnam (Lankton *et al.* 2008b; Lankton and Dussubieux 2013). Recently, the glass debris found at Khao Sam Kaeo suggests the presence of glassworking using m-K-Ca-Al glass in Southeast Asia, and the possible contact between Khao Sam Saeo and some Sa-Huynh culture sites in southern Vietnam is proposed due to the compositional similarities of glass artefacts (Lankton *et al.* 2008b).

5.2.3. v-Na-Ca glass (soda plant ash glass)

V-Na-Ca (vegetal soda lime) glass, also known as soda plant ash glass, contains more MgO and CaO than mineral soda glass, and is also found in Southeast Asia. Dussubieux and Gratuze (2010) noticed that artefacts composed of v-Na-Ca glass in early 1st millennium AD were all glass beads, and after this period there were both glass beads and vessels being made of soda plant ash glass. Glass artefacts in the later period are thought to be imported from Western Asia, identified by their distinct typology and chemical composition which suggests features typical of glass in Western Asia, probably the Sasanian territories (Lankton and Dussubieux 2006; Dussubieux and Gratuze 2010). The provenance of early glass beads of this composition, however, remains unclear. These early v-Na-Ca glasses were found in Sri Lanka in South Asia and in Cambodia, Thailand and Vietnam in Southeast Asia; contact between Southeast Asia and Western Asia in such an early period was thought to be less likely, and therefore there is less possibility that they are of a Western Asian origin (Dussubieux and Gratuze 2010).

A large number of v-Na-Ca glass artefacts were found in Sumatra and peninsular Malaysia after late 1st millennium AD (Brill 1999: 376-387; Lankton and Dussubieux 2006; Dussubieux 2009; Dussubieux 2014; Dussubieux and Allen 2014). Three tentative sub-groups have been recently reported by Dussubieux (2014) and Dussubieux and Allen (2014) – the v-Na-Ca 1 has the lowest Al₂O₃ (ca. 1.4%), the highest CaO (ca. 7.2%) and fairly high Ti (ca. 1068ppm) and Zr (ca. 287ppm), the v-Na-Ca 2 has the highest Na₂O (ca. 17.6%), the highest MgO (ca. 3.5%) and lower CaO (ca. 4.5%), and v-Na-Ca 3 has the lowest Na₂O (ca. 14.6%), moderate Al₂O₃ (ca. 2.2%), moderate CaO (ca. 6.3%) and relatively low Ti (ca. 405ppm) and Zr (ca. 53ppm). It is also suggested that glasses are CaO-rich from 9th to 10th century AD, and then Al₂O₃-rich from 12th to 13th century AD (Dussubieux and Allen 2014).

Both the CaO-rich and Al₂O₃-rich v-Na-Ca glass are tentatively thought to be imported from the Near East and the Middle East, but firm patterns and provenance remain to be elucidated (Dussubieux 2014, *pers. comm.*).

5.3. Southern China

Early glass in southern China predates the Warring States (476-221 BC) and Western Han periods (206 BC-AD 9) (Huang 2005; Gan 2007) (Table 3.1). Among the early glass found in the Warring States and the Han Dynasty, barium lead silicate glass and potash glass are the two most common chemical compositions (Shi *et al.* 1986; Brill *et al.* 1991b; Brill 1995; Li *et al.* 2003). Later, lead silicate glass and potassium lead silicate glass dominated in China (Brill *et al.* 1991b; Gan 2007).

5.3.1. High lead glass

In barium lead silicate glass, high concentrations of PbO (lead oxide) and BaO (barium oxide) can be identified, with BaO generally at more than 9% and PbO more than 20%. The PbO/BaO ratio varies greatly in lead barium silicate glass (reported 0.68-4.87 in Brill *et al.* (1991b) but 2-2.5 in Gan (2005)). The varied ratio led to the suggestion that PbO and BaO were not introduced as a single source (Brill *et al.* 1991b). The Six Dynasties (AD 220-589) witnessed the decline of barium lead silicate glass, and it is thought that barium was replaced by increased lead to produce high lead silicate glass after this period (Gan 2007).

Some authors have suggested that lead silicate glass (PbO 35-75%) and potassium lead silicate glass (K₂O 7-15% and PbO 35-50%) dominated during the period from the Six Dynasties to Northern Song Dynasty (AD 220-1127), and a few lead silicate glass (without

barium) actually date back to the Warring States Period (Brill *et al.* 1991b; Gan 2007). A small amount of lead silicate glass and potassium lead silicate glass in southern China has been recovered (Huang 2003; Li *et al.* 2003), yet the precise amount and distribution remain unclear due to the lack of access to published information.

5.3.2. Potash glass

Most of the potash glasses found in southern China are m-K-Al glass or m-K-Ca-Al glass, like those from Southeast Asia and South Asia (e.g. Shi *et al.* 1986; Huang 1988; Xiong and Li 2011: 152-153). Xiong and Li (2011: 86-96) suggested that some m-K-Al glasses in southern China have high Rb/Sr (rubidium/strontium) ratio (around 10-30) at trace elemental level, while in most m-K-Ca-Al glass the Rb/Sr ratio is usually lower than 3 or 4. In addition to these two types, Li *et al.* (2003) and Fu and Gan (2006) reported a slightly different group in China, mainly found in the Warring States period and the Han Dynasty, which possesses a higher lime content (~10%) than the typical m-K-Ca glass in Southeast Asia (CaO usually less than 7%). Brill *et al.* (1991b) analysed a few potash lime silicate glasses, dated to between 7th-14th century AD in China, and suggested that lime could be added as a stabiliser in potash glass. In addition, another possibly different potash glass found in China was noted by Dussubieux and Gratuze (2010) which had both high Al₂O₃ and CaO concentrations.

5.4. Taiwan

The earliest published compositional studies of glass beads in Taiwan were conducted by Japanese and Taiwanese anthropologists in the mid-20th century (Sato 1988[1944]; Chen 1966). These studies were conducted on glass beads used as heirlooms by aborigines in

Taiwan, rather than on archaeological samples. The results revealed a lead silicate glass, and these authors suggested, using ethnographic records from Borneo in island Southeast Asia, that the beads had a Southeast Asian origin, concluding that they did not show the typical composition of glass beads found in China and South Asia. Chen (1966) further suggested that the glass beads were introduced with the migration of Paiwan aborigines from Southeast Asia to Taiwan in early 1st millennium AD, who have the tradition of using polychrome glass beads as heirlooms.

Research in later decades has questioned these early assumptions, especially because of the chemical similarities of beads found in Taiwan to glass of the 1st millennium AD in Southeast Asia and of the difficulty in inferring a relationship between these heirloom beads and excavated archaeological beads. Specifically, the lead silicate glasses are now known to be an uncommon type in contemporary Southeast Asia. Also, most of the Paiwan heirloom glass beads are polychrome beads which are rarely found in prehistoric Taiwan and may not necessarily show a direct relationship, in terms of chemical composition and provenance, to the abundant monochrome, and smaller, glass beads in early Iron Age in Taiwan.

It is only in the last decade that there have been any scientific analyses on archaeological glass beads from Taiwan. These analyses were conducted using XRF, SEM-EDS or electron microprobe analysis. Table 5.2 shows a summary of previous compositional research on glass beads from Shisanhang, Kiwulan and Xiliao in Iron Age Taiwan. It can be seen that m-Na-Al glass and v-Na-Ca glass are the two most common types found in Taiwan, and glasses rich in lead and potash are rather uncommon and only found at Shisanhang. This might suggest that more glass beads originated from the South China Sea network instead of having a Chinese origin (although these reflect beads from three sites only). The result of these investigations will provide an initial basis for the research conducted in this thesis.

This published data will be further discussed and compared to the compositional results obtained from the study sites in this research (Chapters 8 and 9).

5.5. Summary

The increasing number of scientific studies of glass from around Taiwan, Southeast Asia and southern China in recent decades provides a basis to further investigate the compositional types produced in each area and to examine the interaction between different regions inside and outside Taiwan based on the production, consumption and trade/exchange of glass beads. Glass artefacts in Southeast Asia and southern China generally show regional features in terms of chemical composition and typology, and by using these variables together, different groups can be determined. Taiwan has been little studied within this geographical area, and this research aims to examine how the shapes and compositions of beads from Taiwan fit within this broad geographical 'compositional' area, and what interactions may have taken place.

M-Na-Al (mineral soda alumina) glass is associated with Southeast Asia and South Asia. Further identification of five sub-groups within this m-Na-Al glass shows that only some types are found in Southeast Asia at specific periods (although recent research seems to suggest a potential relationship to northern India), whilst others appear to originate from India or Sri Lanka. Similarly, three chemical groups of potash glass have been found, which may be associated with different production regions. While secure production locations have yet to be determined, these three potash groups have characteristic geographical distributions. A v-Na-Ca (vegetal soda lime or soda plant ash) glass is also found, which may have been produced in the Near or Middle East and traded to Southeast Asia.

In China, other compositional groups are present. Whilst potash compositions are common, many glasses are barium lead silicate, and in later periods lead silicate glasses and potassium lead silicate glasses are present. They may be products of China. The potash glasses in China use a mineral alkali and some are very similar to those found in northern mainland Southeast Asia, but others appear to be specific to China and are believed to have been manufactured in southern China.

These different compositional groups in Southeast Asia, China and beyond allow the beads from Taiwan to be placed within the larger context of production and distribution networks in the area. Previous research on the beads found in the 1st millennium AD in Taiwan shows that there appears to be more similarities with the compositions seen, and potentially originating, in contemporary Southeast Asia than those of China. This is evidenced by the predominance of m-Na-Al glass and v-Na-Ca glass, both of which are more abundant in Southeast Asia. There is the possibility of multiple sources of imported glass beads to Taiwan. However, at present, there is a lack of sufficient published comparable chemical data and detailed contextual information for glass in eastern Taiwan, southeastern China and island Southeast Asia to securely reconstruct the consumption and production of glass beads in Taiwan, mapping any changing prehistoric exchange patterns between these regions and the island, and within Taiwan itself. Therefore, this research aims to significantly extend this database of glass beads in Iron Age Taiwan in the 1st millennium AD and allow this island material culture to be placed within the wider exchange network.

Table 5.2: A summary of chemical composition of glass artefacts in prehistoric Taiwan.

Site	Artefact (n) ^{1,2}	Base composition	Remarks	Analytical technique	Reference
Shisanhang, northern Taiwan. (2 nd -5 th c. AD)	Bead (21): opaque red, orange, yellow or light blue.	m-Na-Al: SiO ₂ 60-70%, Al ₂ O ₃ 7-14%, Na ₂ O 12-20%, MgO < 1.5%, CaO > 4% and FeO < 3%.	1. Different degrees of copper oxide: 1.5-12.1%. 2. A few samples contain ~1.5% PbO.	Electron microprobe.	Tsang and Liu 2001.
	Bead (24): (a) opaque red, orange, yellow or blue, (b) translucent blue, (c) translucent or transparent greenish blue. Bracelet (3): translucent green, blue or yellow. Earring (6): translucent green, yellow, blue or white.	v-Na-Ca (plant ash): SiO ₂ 65-70%, Na ₂ O 15-18%, MgO > 3%, Al ₂ O ₃ < 3%, CaO 4-7% and FeO < 1.5%.	1. The content of copper oxide is less than 0.5% on average. 2. Some orange and yellow beads contain more than 10% of PbO.		

Site	Artefact (n) ^{1,2}	Base composition	Remarks	Analytical technique	Reference
	Bead (1): translucent or transparent greyish blue.	Mineral soda lime silica: SiO ₂ 71.4%, Na ₂ O 15.4%, CaO 8.2%, MgO 0.6%, FeO 1.8% and Al ₂ O ₃ 2.1%.	1. CuO 0.2%.		
	Bead (1): transparent greenish blue.	Potash: SiO ₂ 67.1%, K ₂ O 18.8%, Na ₂ O 2.7%, Al ₂ O ₃ 1.6%, MgO 1.1%, CaO 8.0% and FeO 0.8%.	1. CuO 0.8%. 2. Low un-normalised total (~90%) in raw data.		
	Bead (1): unknown.	Lead silicate: SiO ₂ 44.8%, PbO 34.3%, Na ₂ O 9.2%, CaO 4.0%, K ₂ O 1.9%, MgO 2.7%, Al ₂ O ₃ 2.1% and FeO 1.0%.	1. This bead has a blue body and orange surface (analysed area not noted). 2. CuO 1.3%.		
	Bracelet (2): translucent green, blue or yellow.	Potassium-lead-silicate: SiO ₂ 37-42%, K ₂ O 9-14%, PbO ~45%, Na ₂ O ~0.5%, MgO ~0.15%, CaO ~1%, Al ₂ O ₃ < 1% and FeO ~0.6%.	1. CuO 1.0-1.5%.		

Site	Artefact (n) ^{1,2}	Base composition	Remarks	Analytical technique	Reference
Kiwulan, northeastern Taiwan. (7 th -12 th c. AD) ³	Bead (5): opaque orange.	m-Na-Al: SiO ₂ 63-70%, Al ₂ O ₃ 11-15%, Na ₂ O 10-16%, K ₂ O ~2%, MgO < 1%, CaO 3.5-4% and FeO<1.5%.	1. One sample contains 3.3% FeO.	SEM-EDS.	Cheng 2007.
	Bead (8): (a) opaque red or yellow, (b) translucent blue or yellow.	v-Na-Ca (plant ash): SiO ₂ 57-70%, Na ₂ O 10-16%, MgO > 3%, Al ₂ O ₃ < 3% and CaO 5-9%.	1. PbO of 10-18% in yellow beads.		
Xiliao, southwestern Taiwan. (6 th -14 th c. AD)	Bead (2): translucent greenish blue.	m-Na-Al: SiO ₂ 67-70%, Na ₂ O 13-15%, Al ₂ O ₃ ~9%, K ₂ O ~2%, CaO ~4%, FeO ~1.5% and MgO below detection limit.		XRF (non-destructive surface analysis), SEM-EDS.	Chen and Cheng 2011.
	Bead (10): translucent blue Bracelet (1): translucent greenish blue.	v-Na-Ca (plant ash): SiO ₂ 67-70%, Na ₂ O 12-15%, K ₂ O 2-4%, MgO 4-6%, Al ₂ O ₃ <3%, CaO 4-7% and FeO <1.5%.	1. One sample has 4.5% of Al ₂ O ₃ .		

1: n refers to the number of artefact analysed. All of the beads are monochrome.

2: For Shihsanhang artefacts, the colour and diaphaneity of specific sample are not shown in the original data. The descriptions of these attributes here are obtained from the bead classification sections in the reference, and therefore the colour and the chemical composition may not be one-to-one relationship in this table.

3: This table only uses the data from the Lower Cultural Layer (the Iron Age layer) at Kiwulan.

Part II: Methodology, results, discussion and conclusion

Chapter 6: Methodology

Chapter 7: Results: typology and optical microscopy

Chapter 8: Results: chemical composition – part I: overview and m-Na-Al glass

Chapter 9: Results: chemical composition – part II: v-Na-Ca glass, other glass composition and
summary

Chapter 10: Results: the distribution of beads by context

Chapter 11: Discussion: the exchange, consumption and production of glass beads in Taiwan
and between Taiwan and the South China Sea region

Chapter 12: Conclusions and future prospects

6. Methodology

6.1. Introduction

In this research, all samples were analysed using a combined typological, compositional and contextual approach to understand intra- and inter-site differences. The sampling strategy for each site is discussed, followed by the methodology of typological assessment of the beads. After the analyses of typology and chemical composition were carried out. This research uses SEM-EDS (scanning electron microprobe equipped with energy dispersive spectrometer), EPMA (electron probe microanalysis) and LA-ICP-MS (laser ablation - inductively coupled plasma - mass spectrometry) to understand different levels of chemical composition from major to trace elements and examine the glass microstructures. This chapter addresses the operational parameters and the accuracy and precision of each instrument, and finally addresses the way of integrating the data of typological, compositional and contextual data in this research.

6.2. The sample selection

For Kiwulan, Jiuxianglan, Daoye, Wujiancuo and Guishan, the sampling strategies slightly differ, depending on the context of glass assemblages, and the duration of each field session. For Shisanhang and Xiliao, all the data used in this research are published data. Table 6.1 shows the summary of sample selection in each site.

Kiwulan

Previous research has provided typological groupings and a few semi-quantitative chemical compositions of major and minor elements at Kiwulan (Cheng 2007; Chen *et al.* 2008e: 17-30).

This research increases the sample numbers and adds trace elements to the chemical database. Fifty-five glass beads from 12 reported typological groups (LL01-LL12 types – see Chapter 7.2) in the Lower Cultural Layer were selected, including 12 samples analysed in previous research. In Kiwulan, a large number of glass beads was unearthed from the burial M043 and the pit P187(H204). Eighteen samples were selected from M043, 28 from P187, 1 sample from burial M038 and the 8 samples from pits P038 (1 sample), P250 (1 sample), P256 (4 samples), P258 (1 sample) and P260 (1 sample) respectively. The purpose is to understand the differences and/or similarities of bead typology and chemical composition from different contexts.

Jiuxianglan

All the beads and waste from the first excavation season at Jiuxianglan have been studied and recorded for the analysis of the regional distribution. However, due to the large quantity (thousands of glass beads) of glass beads at this site and the limited field session on site, it was not possible to perform an in-depth study of the glass. Therefore, 49 samples including beads and waste were selected for further analysis. Twenty-two glass beads were selected from pit T3P35, where a tentative chronology is proposed based on the styles of pottery handles and the potential furnace structure is in proximity. The purpose is to test any temporal transition of glass typology or chemical composition based on the samples from a single and dated pit. In order to increase the sample amount, fourteen other beads were selected from the pits T3P37 (1 sample), T3P38 (1 sample), T3P39 (1 sample), the burial B2 (3 samples) and surface collections (8 samples). Glass waste samples included 3 samples each from T2P39 and T3P38, and 5 samples from T3P39 in an attempt to investigate the relationship between glass beads and waste.

Guishan

All the 123 glass beads from Guishan were recorded and measured in order to understand the typological differences. All glass beads from Guishan were excavated from 3 burials, and 64 samples were selected for chemical analysis: 36 beads were from Burial 1 (Locus D), another 36 beads were from Burial 2 (Locus D) and 2 beads were from Burial 3 (Locus D). The selected samples cover different colour groups from the three burials in order to understand the similarities and differences of chemical composition between colours and burials.

Daoye

From Daoye, all 62 glass beads found are recorded for typological assessment and to estimate their regional distribution. Twenty-nine samples were selected for further chemical analysis, including 12 samples from burials and 17 samples from middens from the excavation regions A2, B2, B3, C2, C3, C4 and D6 (see Chapter 10 for the distribution region). Here, the selected samples include different colour groups, excavated areas and contexts in an attempt to investigate the similarities and differences between bead colours and the regions/contexts where the beads were found.

Wujiancuo

Similar criteria were applied at Wujiancuo, where all of the 39 glass beads from the Niaosong period were measured for typological analysis and their spatial distribution. Twenty-one samples were selected from the excavation regions KVI, KVII, KVIII, KVIV, TS1 and 1 was from an unknown region (see Chapter 10 for the distribution region). The precise context, however, was difficult to identify from the record of the bead assemblage. Tracing back to the

initial excavation report showed 8 samples were from burials, while for the other 14 samples the precise context remains less clear. The sampling strategies at Wujiancuo is similar to that at Daoye. The selected samples were from different colour groups and excavated regions for further analysis of the differences between bead colours and excavated regions.

Shisanhang and Xiliao

From Shisanhang and Xiliao, no new samples were analysed in this research, all of the data was collected from the published excavation reports. The analysis of typology and colour was based on published excavation reports – Shisanhang from Tsang and Liu (2001) and Xiliao from Liu (2011b; 2011c; 2011d; 2011e). The chemical composition of 49 samples from Shisanhang published in Tsang and Liu (2001) and 12 samples from Xiliao published in Chen and Cheng (2011) were re-interpreted.

6.3. The typological study

Several systematic description and classification systems of glass beads have been established in different research fields, and have covered beads from different geographic regions and time periods around the world (e.g. Beck 1928; van der Sleen 1967; Kidd and Kidd 1970; Lugay 1974; Santiago 1992; Guido 1978; Guido 1999; DeCorse *et al.* 2003). The nature of the monochrome glass beads in this research (see images in Chapter 7), the simplicity of bead appearance and the lack of design patterns demonstrate the difficulty of systematically establishing a typological scheme and as such a temporal and regional pattern simply through the geometric shapes of glass beads. Nor does it point to the requirement to build a complex classification chart, as most of the superficial differentiation on the beads may be unintentionally left during manufacturing rather than deliberately produced.

This research therefore provides a concise and simple typological scheme of glass beads from each site, exploring and using the possible manufacturing methods and the typological differences and similarities between sites and regions. Information of the shape, colour, length, diameter, diaphaneity and end roundness was recorded. The primary characteristics used to define different types at each site were colour and manufacturing method. Other characteristics were then used to refine the groups. Optical microscopic observation was used in order to investigate the manufacturing method of each bead. Figure 6.1 shows the schematic drawing of the variables and recorded shapes measured.

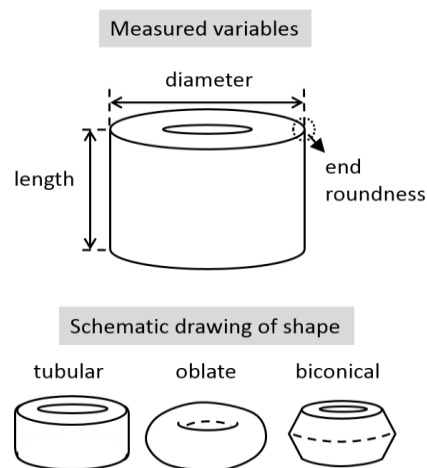


Figure 6.1: A schematic drawing of the measured variables and recorded shapes.

6.3.1. Length and diameter

Length was measured as the distance of the perforation axis. Diameter was measured as the longest distance between the two sides of the transversal surface. For fragmented samples, the maximum diameter was measured wherever possible.

6.3.2. Shape

Three shapes have been identified: tubular, oblate and biconical. Sub-groups of 'short' and 'long' were further recorded in tubular beads. It should be noted that, because of the irregular shapes of the beads, the ability to distinguish short tubular beads and oblate beads may not be as explicit as suggested in Figure 6.1. The purpose of shape classification is to simply provide a generalisation of bead appearance at each site.

6.3.3. Colour

Although the use of standard colour chart such as Munsell colour chart was suggested in some classification systems, a more general encompassing determination of colours was adopted in this research. The colours are described as red, orange, yellow, green, blue and dark blue. Small differences in hues within each colour are not considered particularly important for grouping as these may arise from slight differences within a single glass melt, or due to thickness or opacity of the bead.

6.3.4. Diaphaneity

Opaque, translucent and transparent glasses were recorded. Light does not penetrate an opaque bead. Translucent beads allow the light to pass through without clear perception of object behind, while transparent beads enable the light to be fully transmitted, showing a distinct image on the other side.

6.3.5. End roundness

End roundness refers to the roundness of the edge between the lateral surface and the transversal surface of a bead, and was recorded as ‘round’ and ‘tapered’ in this research. Various degrees of end roundness may result from cutting beads from the tube, grinding or reheating in order to round off the edge. This attribute may not necessarily provide clear evidence of bead manufacturing practices, but shows specific finishing practices.

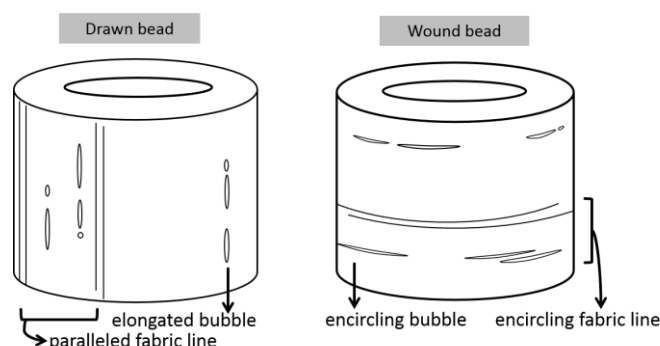


Figure 6.2: A schematic drawing showing the different orientations of fabric lines and bubbles in drawn-made and wound-made bead respectively.

6.3.6. Manufacturing technique

The manufacturing techniques, ‘drawn’ and ‘wound’, were identified through the orientation of the ‘fabric lines’ and bubbles under stereotyped microscope. The fabric lines are the line traces which result from the pulling of molten glass tubes or coiling of glass rods, left on the surface of the bead after cooling. Figure 6.2 shows the different orientations of fabric lines and bubbles in drawn beads and wound beads, respectively. In drawn beads, the fabric lines and elongated bubbles are parallel to the perforation axis, while in wound beads the fabric lines and bubbles encircle the perforation axis. In addition to the two methods, a percentage of glass beads display unclear evidence and therefore the technique of manufacture is ‘unidentifiable’.

6.4. The chemical and microstructural analysis

Three methods were used for the chemical and microstructural analysis: SEM-EDS for the semi-quantitative and microstructural analysis, EPMA for the quantitative analysis of major and minor elements, and LA-ICP-MS for the trace elemental analysis. In this research, small fragments were cut from some samples for destructive analysis in SEM-EDS and EPMA. In order to increase the database of chemical analysis, some more samples were selected to do invasive but non-destructive analysis for full element analysis by LA-ICP-MS. The process of laser ablation takes away a few micrograms of the sample (therefore invasive), leaving a tiny crater which is invisible to the eye on the sample. No further cutting, grinding and polishing are required for the sample preparation of LA-ICP-MS analysis, which avoids huge damage on the sample (therefore non-destructive). The total sample numbers by each technique are provided in Table 6.1. Major and minor elements may help identify different chemical groups relating to the use and combination of raw materials. The trace elemental analysis may provide ‘geological fingerprints’ associated with the procurement of raw materials.

In this research, SEM-EDS and EPMA analyses were undertaken in collaboration with Dr Yoshiyuki Iizuka in the EPMA Lab in the Institute of Earth Sciences, Academia Sinica, Taiwan. LA-ICP-MS is a collaboration with Dr Yi-Kong Hsieh in the Department of Biomedical Engineering and Environmental Sciences, National Tsing Hua University, Taiwan. The sample preparation, the analytical parameters and the accuracy and precision of each method are described below.

6.4.1. Sample preparation

The samples selected for destructive analysis were cut from bead fragments in order to get a

fresh cross-section. These were then mounted in epoxy (Struers EpoFix Kit), and vacuum degassed in order to get rid of the small bubbles. The epoxy blocks were ground and polished with diamond solution down to 1 μ m and then cleaned to prevent contamination and degradation from moisture, then carbon coated to increase the conductivity of the sample surface.

For LA-ICP-MS, the whole samples were embedded into a foam plate before the analysis, so that the surface of each sample is in the same height, and therefore the volume of the ablated area can be controlled. Samples embedded in the foam can be removed without any visual damage after the analysis. As for the epoxy-mounted samples, these blocks were also used in LA-ICP-MS analysis, but the coated carbon layer was removed prior to the analysis.

6.4.2. SEM-EDS

Chemical analysis

SEM-EDS was used here as a pre-procedure for EPMA as it provides a very rapid but semi-quantitative level of chemical analysis. Preliminary results of chemical elements determined through SEM-EDS were used to determine the elements to be used for fully quantitative analysis by EPMA.

The operational parameters of SEM-EDS (JEOL FE-SEM: JSM-7100F, with Oxford EDS, Institute of Earth Sciences, Academia Sinica) are: the accelerating voltage of 15 kV, the probe current of 0.1 nA and the working distance of 10 mm. The stability of beam current is routinely checked with a probe current detector.

At least 3 analyses on the matrix were carried out in one sample. The areas close to the bead

surface were avoided, as the weathering or corrosion on the glass surface from the post-depositional processes may result in the leaching of important elements, such as alkalis, from the glass.

The precision (the repeatability of measured composition) and accuracy (the conformity of the measured composition to the true composition) were monitored by analysing Corning Glass Standards A, B, C and D, and the results are provided in Table 6.2. The precision is evaluated by the standard deviation (SD) and relative standard deviation (RSD). The relative standard deviation in major elements is lower than 5%, and in minor elements the values vary. In terms of the accuracy, the absolute accuracy error (δ absolute) varies from -2.2 to 2.8 for all detectable elements. The relative accuracy error (δ relative) of major elements is between -9.1% and 10.8%, and of minor elements between -24.1% and 67.5%. The minor elements often show a higher relative accuracy error due to their low concentrations. Together with the absolute accuracy error, the range is considered acceptable in SEM-EDS in this research. It is noted that the detection of SiO₂ and Al₂O₃ is always slightly lower, and for CuO the measured value is slightly higher. Any future discussion of SiO₂, Al₂O₃ and in particular CuO using SEM-EDS data is treated with caution.

Microstructural analysis

SEM-EDS was also used to observe and compositionally analyse crystals or mineral remains in the glass beads. With the backscattered electron image (BSE) under SEM, compositional differences can be observed. Mineral relics or crystals dispersed in the glass matrix were identified, and then compositional analysis was carried out in order to get a semi-quantitative composition.

The microstructural analysis in this research allows the evaluation of possible raw materials and the interaction between raw materials. Applicable phase diagrams are used in an attempt to understand these reactions. However, the interpretation should be made very carefully because the interaction between chemical components may be affected by not only the production condition but also the local chemistry, the chemical kinetics and thermodynamics.

6.4.3. EPMA

Quantitative compositional analysis was carried out by EPMA (JEOL JXA-8500F) equipped with WDS (wavelength dispersive spectrometer), managed by Dr Yoshiyuki Iizuka at the Institute of Earth Sciences, Academia Sinica, Taiwan. Sixteen elements were analysed, namely Si (silicon), Al (aluminium), Na (sodium), K (potassium), Mg (magnesium), Ca (calcium), Fe (iron), Pb (lead), Ba (barium), Ti (titanium), Mn (manganese), Co (cobalt), Cu (copper), Sn (tin), Cl (chlorine) and S (sulfur). The analytical parameters were, accelerating voltage of 12kV, beam current of 6nA and the beam diameter of 5 μ m. A defocused beam was used in this research in order to avoid the migration of alkalis in the glass in the bombarded area due to the beam current damage. Linear transverse EPMA analysis was used. Analytical spots were selected across the glass matrix, and voids and mineral remains in the sample were avoided. Data collected close to the bead surface were also ruled out in order to avoid areas of weathering or corrosion. The analysis of mineral remains was also carried out wherever necessary, with the analytical parameter of 12kV accelerating voltage, 6nA beam current and focused beam.

Corning Glass Standard A, B, C and D were used to monitor the precision and accuracy. The result is shown in Table 6.3. For the major elements, the relative standard deviation is lower than 4%. For elements with the concentration lower than 5%, the relative standard deviation is lower than 20%. The absolute accuracy error is in the range of -1.63 and 0.38. The relative

accuracy error of major elements varies from -5.3% to 3.0%, and the measured value of SiO₂ and K₂O is always slightly lower than that reported in the Corning standards (but here was not corrected). As for minor elements, the relative accuracy is between -60.4% and 58.7%, excluding MnO in Corning C and SnO₂ in Corning D. The high (58.7%) and low ends (-60.4%) of the relative accuracy is observed in SO₃ and Cl, and it can be seen from Table 6.3 that SO₃ and Cl generally show less agreement to the recommended value of the standards. This is probably due to the estimation of the incomplete retention from the original ingredients (Brill 1972), and similar issue is also reported in Vicenzi *et al.* (2002). The concentration of SnO₂ could not be detected in Corning D glass, which is possibly due to the detection limit. It is noticed that the detection of MnO in Corning C shows a large relative accuracy error of -96.8% compared to the value reported in Vicenzi *et al.* (2002). There has been issue on the reported value of MnO in Corning C glass. The relevant discussion can be found in Wagner *et al.* (2012), and is not addressed further here.

The analysed data of PbO and BaO in Corning A, B and D show slightly lower values in the minor elemental level compared to the Brill (1999: 544) data. Further comparison to the data reported in Brill (1972) and Wagner *et al.* (2012) has shown that it is within an acceptable range. Specifically, in Corning A, this research reports PbO of 0.08%, and the value of 0.05% and 0.0725% is reported in Brill (1972) and Wagner *et al.* (2012) respectively. In Corning B, PbO is measured as 0.55% and BaO as 0.09%, which do not show significant discrepancies to Brill (1972) (PbO 0.5% and BaO 0.1%) and Wagner *et al.* (2012) (PbO 0.532% and BaO 0.077%). In Corning D, PbO is 0.23% and BaO 0.33% in this research, which is consistent with the value reported in Brill (1972) (PbO 0.25% and BaO 0.33%) and Wagner *et al.* (2012) (0.241% and 0.291%).

Although generally the value of CoO is within acceptable range in the EPMA data (although

higher relative accuracy error is seen in Corning B), the CoO data analysed by LA-ICP-MS is reported here and used for discussing compositional pattern in Chapters 8 and 9. This is because in most cases CoO is within minor to trace elemental level, and LA-ICP-MS provides better resolution in this case.

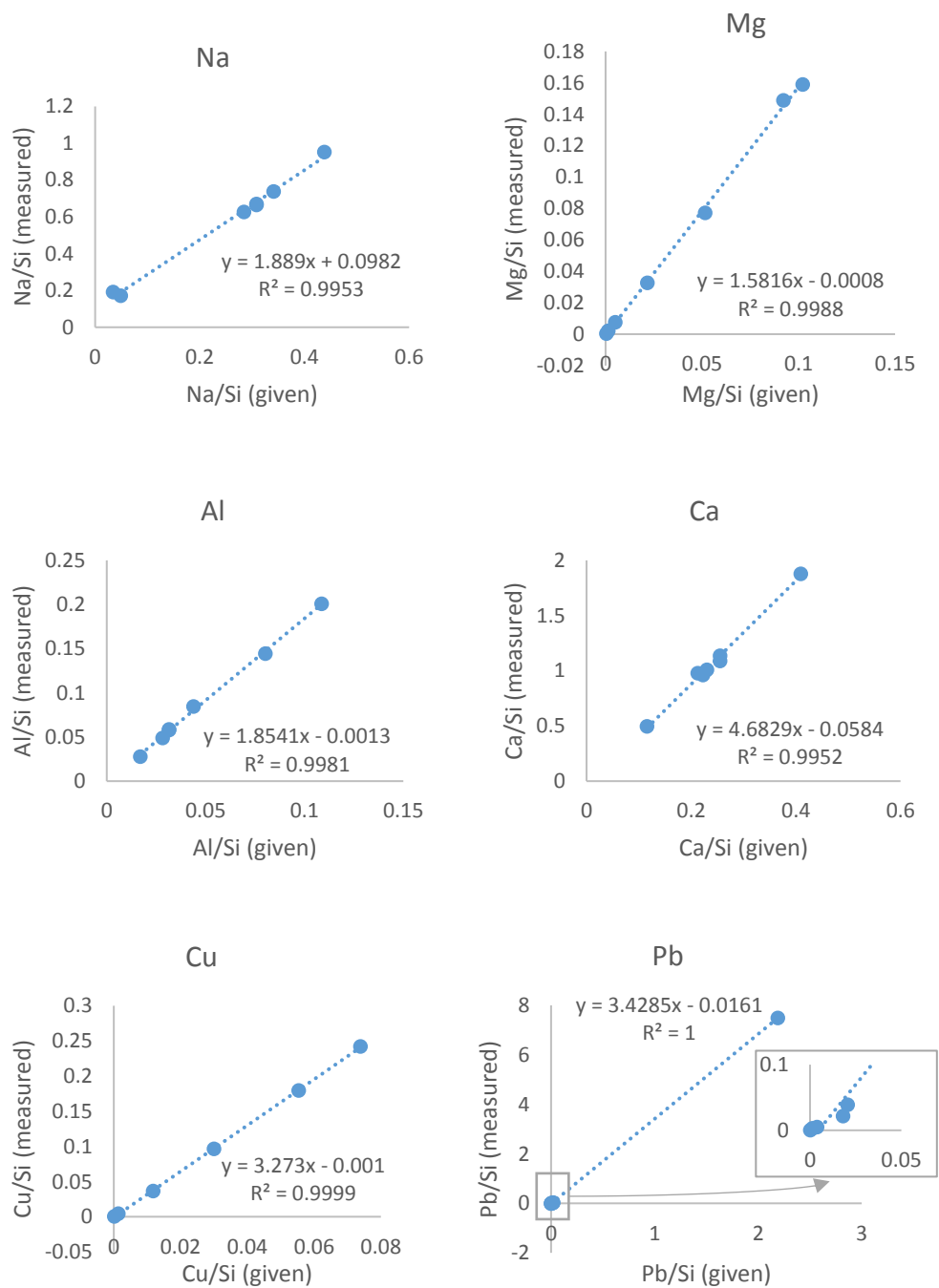


Figure 6.3: The LA-ICP-MS calibration curves of Na, Mg, Al, Ca, Cu and Pb.

6.4.4. LA-ICP-MS

The LA-ICP-MS analysis was carried out with Dr Yi-Kong Hsieh at the Department of Biomedical Engineering and Environmental Sciences, National Tsing Hua University, Taiwan, using an ICP-MS spectrometer (Agilent 7500a, USA) in conjunction with a New Wave UP213 laser ablation system, combined with an Nd:YAG laser at wavelength of 213nm. The analytical protocol follows Dussubieux (2009). Single spot analysis was used with a beam diameter of 55 μ m, a laser energy at around 0.2mJ, the pulse frequency of 15Hz and the pre-ablation time of 20s. In each sample, 4 points were analysed. For samples containing two distinct colours (such as KWL001), each colour was analysed separately.

The calculation of elemental concentration uses the method proposed by Gratuze (1999), and ^{29}Si was used as internal standard. Corning A, B, C, D and NIST610, 612, 621 were used to determine the calibration curve, and this was routinely checked for the precision and accuracy in each analytical session. For elemental concentrations not provided in the original certified value, the data from Pearce *et al.* (1997) were used. The limit of detection was calculated as three times the standard deviation of the measured blanks. Figure 6.3 shows the calibration curve of Na, Mg, Al, Ca, Cu and Pb, where a good linear correlation can be seen from the value of R^2 showing 0.99. The full list of R^2 and slope of each calibration curve is provided in Table 6.4.

The precision and accuracy are shown in Table 6.5 and Table 6.6. Generally, the relative standard deviation for most of the elements analysed is lower than 5%. The absolute accuracy error for major elements is between 1.76 and -1.25, with the relative accuracy error varies from 8% to -15%. The relative accuracy error for minor elements is generally between 17% and -66%, while for the trace element it is between 33% and -30%. Similar to the result of EPMA,

larger discrepancies of relative accuracy error are seen in PbO and BaO in Corning A, B and D. This is considered as acceptable and the relevant discussion can be found in section 6.4.3. The relative accuracy error of Sb₂O₅ is particularly high in Corning C, which may be due to the overestimation of the recommended value in Brill (1999: 544). A relatively low value of Sb₂O₅ is reported in Dussubieux (2009) (0.00014%) and Wagner *et al.* (2012) (0.0001%), and in this research the Sb₂O₅ is measured as 0.0006% in Corning C. The poor relative accuracy error of K₂O in NIST610 and NIST612 is due to the high detection limit of K₂O in ICP-MS. Also, the detection of P₂O₅ in NIST610 and 612 is always higher than the reported value, and generally the poorer accuracy of P₂O₅ was found in several analytical sessions. Therefore, the reported concentration of P₂O₅ in this research is regarded as semi-quantitative only.

6.4.5. Comparison between EPMA and LA-ICP-MS data

Some samples were analysed by both EPMA and LA-ICP-MS. Figure 6.4 shows the comparison of EPMA and LA-ICP-MS data of Corning glass standards A, B, C and D. Generally, there is good consistency in the major elements and most minor elements. The concentration of Na₂O in Corning C and Corning D are frequently lower in LA-ICP-MS. For PbO with the concentration less than 0.5%, it is always reported lower in LA-ICP-MS. Therefore, the reported data of Na₂O (within minor elemental level) and PbO in the minor elemental level may be underestimated in LA-ICP-MS data in this research.

6.5. The integration of typological and compositional data with context

The data collected on typology and chemical composition were integrated with the contextual information provided for each site in order to gain a holistic picture. The spatial and temporal distribution of bead samples were recorded and quantified wherever possible. Furthermore, all

of the analytical data were compared to the glass beads around the South China Sea in an attempt to understand the similarities and differences between Taiwan and the South China Sea network.

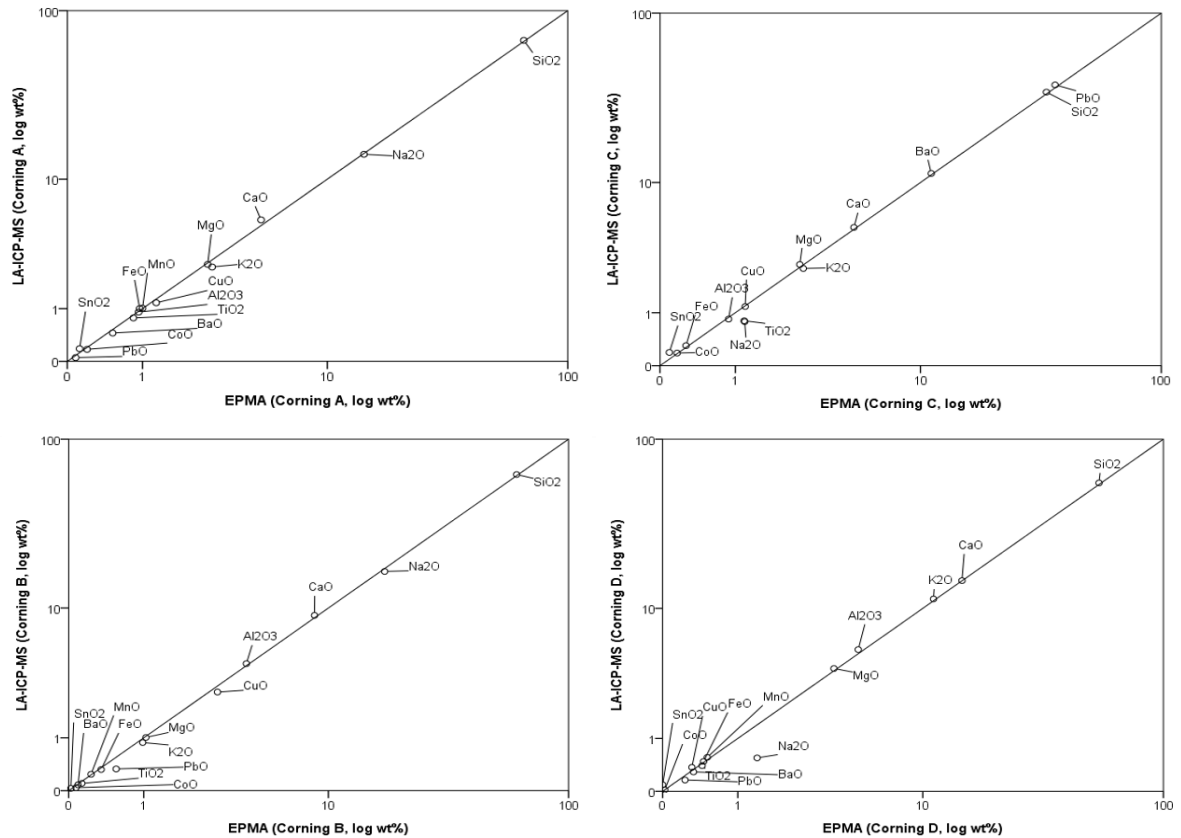


Figure 6.4: The comparison between EPMA and LA-ICP-MS data of Corning Glass A, B, C and D. (The linear equation shows $y=x$.)

For the evidence that was recorded as glass beadmaking at Jiuxianglan, the archaeological contexts where the glass waste was found and their distribution on site were investigated to identify the development and the scale of beadmaking.

For glass beads unearthed from burials, the number and arrangement of glass beads within the burial were recorded. Other grave goods were also used for comparison, as the variations in grave goods between burials may reflect any social differentiation within and between site(s).

This information was linked to the typology and chemical composition of glass beads in order to understand the differences between different sites or regions.

The other method that was used to gain a greater understanding of bead use and status is analogy using ethnographic or ethnohistoric records of glass beads in Taiwan. These records may not explicitly mirror the consumption of glass beads in the past societies, but may serve as good references for any potential archaeological interpretation. There have been recorded traditions of using glass beads as heirlooms in Taiwan (e.g. the Paiwan aborigines (Hsu 2005)) and Southeast Asia (e.g. Kalinga in Luzon (Francis 2002) and the Kelabit in Sarawak (Janowski 1998)), although most of the heirloom beads in current aboriginal societies in Taiwan are polychrome glass beads that differ from the prehistoric glass beads. No ethnographic fieldwork had been carried out in this research but previous ethnographic and ethnohistoric studies were used from Taiwan to understand the possible interpretive pathways rather than the definitive ones.

6.6. Summary

This chapter discusses the methodology used in this research, stating the purpose, the criteria and in some cases the limitations of each method. Figure 6.5 shows a summary of the methodology. The combination of typology, chemical composition and context are the three major methodologies used in this research in order to assess the archaeological patterns, answering the research questions addressed in Chapter 1.

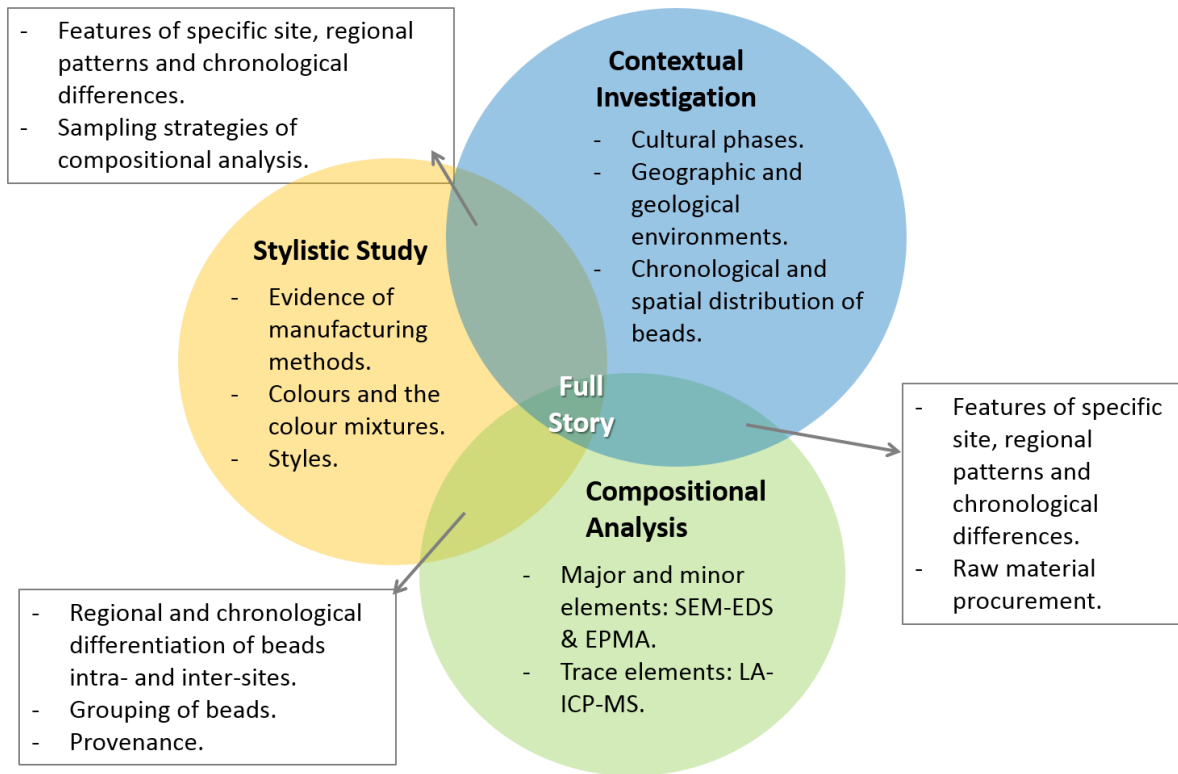


Figure 6.5: A summary of different aspects of the methodology.

Table 6.1: A summary of sample selection for chemical analysis in the study sites.

Site	Period	Sample selection	Sample amount	Destructive analysis (SEM-EDS, EPMA)	Non-destructive analysis (LA-ICP-MS)
Kiwulan	7 th -12 th century AD	1. All are glass beads. 2. Location (sample amount): M043 (18); M038 (1); P187 (28); P256 (4); P038 (1); P250 (1); P258 (1); P260 (1).	55	26	29
Jiuxianglan	300 BC-AD 770	1. Thirty-eight Glass beads and 11 glass waste. 2. Location (sample amount): - Glass bead: T3P35 (22); T3P37 (1); T3P38 (3); T3P39 (1); burial B2 (3); surface (8). - Glass waste: T2P39 (3); T3P38 (3); T3P39 (5).	49	49	0
Daoye	2 nd -6 th century AD	1. All are glass beads. 2. Location (amount): A2 (3 from midden); B2 (5 from burials); B3 (2 from midden); C2 (3 from burials); C3 (1 from midden and 1 from burial); C4 (1 from midden); D6 (10 from midden and 3 from burials).	29	8	21
Wujiancuo	5 th -8 th century AD	1. All are glass beads. 2. Location (amount): KVI (5 from unknown context); KVII (3 from unknown context); KVIII (6 from burials); KVIV (1 from unknown context); TS1 (2 from burials, 4 from unknown context); unknown (1 from unknown context).	22	4	18
Guishan	late 1 st millennium AD	1. All are glass beads. 2. Location (amount): Burial 1 (36); Burial 2 (26); Burial 3 (2).	64	12	52
Shisanhang	2 nd -15 th century AD	All from published excavation reports (Liu and Tsang 2001).	49	n/a	n/a
Xiliao	6 th -14 th century AD	All from published excavation reports (Chen and Cheng 2011).	12	n/a	n/a

Table 6.2: The precision and accuracy of SEM-EDS in this research. (wt%)

	SiO ₂	Al ₂ O ₃	Na ₂ O	K ₂ O	MgO	CaO	FeO	PbO	BaO	CuO	CoO	MnO	TiO ₂	ZnO	Sb ₂ O ₅	SnO ₂	P ₂ O ₅	Total	
Corning A (n=5)																			
Measured average	65.0	0.9	14.2	3.2	2.5	5.2	1.0	nd	nd	2.0	nd	0.9	1.0	nd	1.7	nd	nd	97.4	
SD	0.5	0.1	0.3	0.1	0.1	0.2	0.2			0.3		0.2	0.2		0.3			1.3	
RSD (%)	0.7	15.6	1.8	3.4	4.0	3.7	15.8			13.3		17.6	21.6		18.0			1.4	
Given (Brill 1999)	66.6	1.0	14.3	2.9	2.7	5.0	1.1	0.1	0.6	1.2	0.2	1.0	0.8	0.0	1.8	0.2	0.1	99.4	
δ absolute	-1.6	-0.1	-0.1	0.3	-0.2	0.1	-0.1			0.8		-0.1	0.2		0.0				
δ relative (%)	-2.3	-14.0	-0.7	10.8	-6.0	3.0	-11.9			67.5		-10.0	21.5		-0.6				
Corning B (n=5)																			
Measured average	60.4	4.0	17.2	1.1	0.9	8.5	nd	nd	nd	4.0	nd	nd	nd	nd	nd	nd	0.9	97.0	
SD	0.5	0.2	0.1	0.1	0.1	0.1				0.4							0.1	0.8	
RSD (%)	0.8	4.9	0.6	13.8	9.6	1.4				9.8							10.9	0.8	
Given (Brill 1999)	61.6	4.4	17.0	1.0	1.0	8.6	0.3	0.6	0.1	2.7	0.0	0.3	0.1	0.2	0.5	0.0	0.8	99.1	
δ absolute	-1.1	-0.3	0.2	0.1	-0.1	-0.1				1.3							0.0		
δ relative (%)	-1.8	-7.3	1.1	6.4	-11.5	-0.8				50.5							5.9		
Corning C (n=5)																			
Measured average	32.7	0.7	1.2	3.1	2.6	5.0	nd	36.7	14.2	1.6	nd	nd	nd	nd	nd	nd	nd	97.7	
SD	0.4	0.1	0.1	0.3	0.1	0.2		0.7	0.5	0.4								0.9	
RSD (%)	1.2	20.3	9.3	10.2	3.5	4.5		1.8	3.8	24.5								1.0	
Given (Brill 1999)	34.9	0.9	1.1	2.8	2.8	5.1	0.3	36.7	11.4	1.1	0.2	0.8*	0.8	0.1	0.0	0.2	0.1	99.3	
δ absolute	-2.2	-0.2	0.1	0.2	-0.2	0.0		0.0	2.8	0.5									
δ relative (%)	-6.3	-24.1	10.3	7.7	-7.2	-1.0		-0.1	24.9	43.4									
Corning D (n=5)																			
Measured average	53.2	4.8	1.3	12.2	3.9	14.3	nd	nd	nd	nd	nd	nd	nd	nd	nd	nd	4.2	94.0	
SD	0.8	0.2	0.1	0.1	0.1	0.4											0.2	0.9	
RSD (%)	1.4	3.4	6.7	1.1	2.3	2.7											5.1	1.0	
Given (Brill 1999)	55.2	5.3	1.2	11.3	3.9	14.8	0.5	0.5	0.5	0.4	0.0	0.6	0.4	0.1	1.0	0.1	3.9	99.7	
δ absolute	-2.0	-0.5	0.1	0.9	-0.1	-0.5											0.3		
δ relative (%)	-3.7	-9.1	11.7	8.3	-2.0	-3.4											7.4		

* MnO data from Vicenzi *et al.* 2002.

Table 6.3: The precision and accuracy of EPMA in this research. (wt%)

	SiO ₂	Al ₂ O ₃	Na ₂ O	K ₂ O	MgO	CaO	FeO	PbO	BaO	CuO	CoO	MnO	TiO ₂	SnO ₂	Cl	SO ₃	Total
Corning A (n=24)																	
Measured average	66.34	0.93	14.42	2.80	2.65	4.97	0.95	0.08	0.52	1.27	0.20	1.00	0.84	0.12	0.10	0.16	97.33
SD	0.54	0.05	0.44	0.07	0.09	0.15	0.12	0.07	0.09	0.21	0.09	0.12	0.10	0.09	0.01	0.03	0.80
RSD (%)	0.82	4.89	3.07	2.61	3.43	2.97	12.59	80.95	17.13	16.36	44.27	11.60	11.37	70.87	14.35	16.86	0.82
Given (Brill 1999)	66.56	1.00	14.30	2.87	2.66	5.03	1.09	0.12	0.56	1.17	0.17	1.00	0.79	0.19	0.10	0.10	97.71
δ absolute	-0.22	-0.07	0.12	-0.07	-0.01	-0.06	-0.14	-0.04	-0.04	0.10	0.03	0.00	0.05	-0.07	0.00	0.06	
δ relative (%)	-0.33	-7.32	0.83	-2.31	-0.49	-1.26	-12.85	-31.01	-7.94	8.27	14.78	-0.40	5.94	-35.23	-3.77	58.70	
Corning B (n=24)																	
Measured average	61.52	4.16	17.50	0.98	1.04	8.68	0.35	0.55	0.09	2.95	0.07	0.23	0.13	0.02	0.18	0.64	99.09
SD	0.35	0.10	0.49	0.04	0.06	0.19	0.08	0.08	0.09	0.25	0.07	0.08	0.06	0.03	0.02	0.04	0.59
RSD (%)	0.57	2.38	2.78	4.57	5.72	2.14	21.84	13.85	99.96	8.61	96.96	34.62	45.78	158.67	8.37	6.75	0.60
Given (Brill 1999)	61.55	4.36	17.00	1.00	1.03	8.56	0.34	0.61	0.12	2.66	0.05	0.25	0.09	0.46	0.20	0.50	98.78
δ absolute	-0.03	-0.20	0.50	-0.02	0.01	0.12	0.01	-0.06	-0.03	0.29	0.03	-0.02	0.04	0.04	-0.02	0.14	
δ relative (%)	-0.05	-4.54	2.97	-1.67	0.63	1.39	2.30	-10.10	-25.38	11.07	61.98	-8.72	40.74	8.70	-9.64	27.07	
Corning C (n=24)																	
Measured average	34.08	0.88	1.18	2.74	2.62	4.96	0.27	36.99	11.15	1.19	0.17	0.03	1.17	0.09	0.09	0.10	97.68
SD	0.35	0.05	0.08	0.05	0.08	0.15	0.10	0.51	0.26	0.27	0.12	0.04	0.10	0.11	0.02	0.03	1.06
RSD (%)	1.03	5.40	6.84	1.92	3.16	3.02	35.14	1.39	2.29	22.48	70.08	160.45	8.77	122.57	21.41	34.37	1.09
Given (Brill 1999)	34.87	0.87	1.07	2.84	2.76	5.07	0.34	36.70	11.40	1.13	0.18	0.82	0.79	0.19	0.10	0.10	99.23
δ absolute	-0.79	0.01	0.11	-0.10	-0.14	-0.11	-0.07	0.29	-0.25	0.06	-0.01	-0.79	0.38	-0.10	-0.01	0.00	
δ relative (%)	-2.27	1.05	10.47	-3.55	-5.25	-2.27	-20.34	0.78	-2.20	5.14	-3.88	-96.85	48.10	-52.47	-14.87	-4.91	
Corning D (n=24)																	
Measured average	54.83	5.07	1.39	11.14	3.85	14.79	0.46	0.23	0.33	0.31	0.02	0.51	0.44	nd	0.16	0.23	93.76
SD	0.29	0.12	0.07	0.14	0.08	0.33	0.10	0.07	0.08	0.19	0.04	0.10	0.07		0.02	0.04	0.59
RSD (%)	0.53	2.31	4.88	1.23	1.98	2.22	22.40	31.14	25.85	59.93	169.48	18.63	15.41		10.67	15.53	0.63
Given (Brill 1999)	55.24	5.30	1.20	11.30	3.94	14.80	0.52	0.48	0.51	0.38	0.02	0.55	0.38	0.10	0.40	0.30	95.42
δ absolute	-0.41	-0.23	0.19	-0.16	-0.09	-0.01	-0.06	-0.25	-0.18	-0.07	0.00	-0.04	0.06		-0.24	-0.07	
δ relative (%)	-0.74	-4.37	15.71	-1.42	-2.22	-0.06	-11.51	-53.00	-35.79	-18.33	-1.78	-6.38	16.51		-60.54	-24.60	

* MnO data from Vicenzi *et al.* 2002.

Table 6.4: A list of the slope and R^2 of LA-ICP-MS calibration curves of each element.

	Na	Mg	Al	P	K	Ca	Sc	Ti	V	Mn	Fe	Co	Ni	Cu	Zn	As	Rb	Sr	Y	Zr	Nb	Ag
isotope	23	24	27	31	39	43	45	47	51	55	57	59	60	63	66	75	85	88	89	90	93	107
slope	1.889	1.5816	1.8541	0.1446	3.7715	4.6829	5.0283	4.3106	5.1801	4.3535	4.0749	3.856	3.208	3.273	1.6779	0.676	5.5726	5.9771	6.6234	6.5815	7.8348	3.651
R^2	0.9953	0.9988	0.9981	0.9997	0.9976	0.9952	0.9997	0.999	0.9975	0.9998	0.998	0.9993	0.9974	0.9999	0.999	0.9999	0.9953	0.9999	0.9991	0.9985	0.9994	0.9972
	Sn	Sb	Cs	Ba	La	Ce	Pr	Nd	Sm	Eu	Gd	Tb	Dy	Ho	Er	Tm	Yb	Lu	Hf	Pb	Th	U
isotope	118	121	133	137	139	140	141	146	147	153	157	159	163	165	166	169	172	175	178	208	232	238
slope	5.9968	3.3735	4.427	5.1505	4.6131	5.3884	5.5857	4.8094	4.5646	4.5437	4.8082	4.5546	4.3465	4.1898	4.1041	4.0541	3.5209	3.7187	3.7931	3.4285	1.948	1.8621
R^2	0.9967	0.9975	1	0.9999	0.9999	1	1	1	1	0.9994	0.9999	1	0.9999	1	1	1	1	0.9999	0.9999	1	1	1

Table 6.5: The precision and accuracy of LA-ICP-MS (Corning A, B, C, D and NIST621). (wt%)

	SiO ₂	Al ₂ O ₃	Na ₂ O	K ₂ O	CaO	MgO	FeO	MnO	CuO	PbO	BaO	Sb ₂ O ₅	P ₂ O ₅	TiO ₂	V ₂ O ₅	CoO	NiO	ZnO	Rb ₂ O	SrO	ZrO ₂	Ag ₂ O	SnO ₂	
Corning A (n=4)																								
Measured	67.33	0.91	14.25	2.46	5.43	2.58	1.00	1.01	1.16	0.05	0.45	1.91	0.14	0.77	0.01	0.17	0.02	0.04	0.01	0.10	0.00	0.00	0.18	
SD	0.37	0.01	0.17	0.01	0.24	0.03	0.04	0.01	0.02	0.00	0.01	0.02	0.00	0.01	0.00	0.00	0.00	0.00	0.00	0.00	0.00	0.00	0.00	0.00
RSD (%)	0.55	1.40	1.21	0.24	4.39	1.11	3.92	1.29	1.38	1.67	1.99	1.10	2.90	0.94	2.73	1.32	3.67	4.11	2.42	1.28	0.93	0.68	1.68	
Given (Brill 1999)	66.56	1.00	14.30	2.87	5.03	2.66	0.98	1.00	1.17	0.12	0.56	1.75	0.13	0.79	0.01	0.17	0.02	0.04	0.01	0.10	0.01	0.00	0.19	
δ absolute	0.77	-0.09	-0.05	-0.41	0.40	-0.08	0.02	0.01	-0.01	-0.07	-0.11	0.16	0.01	-0.02	0.00	0.00	0.00	0.00	0.00	0.00	0.00	0.00	-0.01	
δ relative (%)	1.15	-8.55	-0.36	-14.42	7.96	-3.03	2.21	0.66	-1.21	-61.64	-19.18	9.12	4.51	-2.80	1.72	-2.92	24.72	-0.64	-0.77	-1.82	-3.00	-6.99	-7.75	

	SiO ₂	Al ₂ O ₃	Na ₂ O	K ₂ O	CaO	MgO	FeO	MnO	CuO	PbO	BaO	Sb ₂ O ₅	P ₂ O ₅	TiO ₂	V ₂ O ₅	CoO	NiO	ZnO	Rb ₂ O	SrO	ZrO ₂	Ag ₂ O	SnO ₂	
Corning B (n=4)																								
Measured	62.48	4.30	16.79	0.88	8.99	1.01	0.32	0.24	2.65	0.33	0.08	0.51	0.82	0.10	0.03	0.04	0.10	0.19	0.00	0.02	0.02	0.01	0.03	
SD	0.36	0.08	0.11	0.02	0.21	0.01	0.01	0.00	0.02	0.01	0.00	0.00	0.03	0.00	0.00	0.00	0.00	0.00	0.00	0.00	0.00	0.00	0.00	0.00
RSD (%)	0.57	1.80	0.68	1.71	2.34	1.19	4.70	1.78	0.58	1.94	3.93	0.75	3.04	4.03	1.40	0.87	2.40	1.22	8.34	3.55	3.89	1.21	4.71	
Given (Brill 1999)	61.55	4.36	17.00	1.00	8.56	1.03	0.31	0.25	2.66	0.61	0.12	0.46	0.82	0.09	0.03	0.05	0.10	0.19	0.00	0.02	0.03	0.01	0.04	
δ absolute	0.93	-0.06	-0.21	-0.12	0.43	-0.02	0.01	-0.01	-0.01	-0.28	-0.04	0.05	0.00	0.02	0.00	0.00	0.00	0.00	0.00	0.00	0.00	0.00	-0.01	
δ relative (%)	1.52	-1.35	-1.22	-12.25	5.04	-1.70	1.92	-3.03	-0.51	-46.49	-37.03	11.43	0.54	17.15	7.57	-8.38	3.48	0.89	32.77	-12.38	-8.17	-17.80	-36.24	
Corning C (n=4)																								
Measured	34.93	0.84	0.78	2.57	5.11	2.76	0.30		1.17	38.46	11.38	0.00	0.12	0.80	0.01	0.18	0.02	0.05	0.01	0.29	0.00	0.00	0.19	
SD	0.08	0.01	0.01	0.02	0.17	0.02	0.01		0.00	0.25	0.04	0.00	0.01	0.01	0.00	0.00	0.00	0.00	0.00	0.00	0.00	0.00	0.00	
RSD (%)	0.24	1.06	1.60	0.84	3.42	0.83	1.80		0.21	0.65	0.37	29.03	11.26	0.97	1.95	0.66	1.15	2.57	1.65	0.48	1.28	4.98	0.69	
Given (Brill 1999)	34.87	0.87	1.07	2.84	5.07	2.76	0.31		1.13	36.70	11.40	0.03	0.14	0.79	0.01	0.18	0.02	0.05	0.01	0.29	0.01	0.00	0.19	
δ absolute	0.06	-0.03	-0.29	-0.27	0.04	0.00	-0.01		0.04	1.76	-0.02	-0.03	-0.02	0.01	0.00	0.00	0.00	0.00	0.00	0.00	0.00	0.00	0.00	
δ relative (%)	0.17	-3.12	-27.41	-9.46	0.81	0.07	-2.94		3.91	4.79	-0.17	-98.09	-17.79	1.27	14.69	-0.18	11.74	2.16	0.57	-0.17	-3.00	-1.56	0.51	
Corning D (n=4)																								
Measured	55.94	5.41	0.55	11.44	14.83	4.00	0.48	0.56	0.37	0.16	0.29	1.13	4.00	0.40	0.02	0.02	0.05	0.09	0.01	0.06	0.01	0.00	0.09	
SD	0.14	0.03	0.06	0.12	0.30	0.04	0.02	0.00	0.00	0.00	0.00	0.01	0.04	0.01	0.00	0.00	0.00	0.00	0.00	0.00	0.00	0.00	0.00	
RSD (%)	0.25	0.50	10.99	1.02	2.00	1.12	4.14	0.37	0.78	0.90	1.10	0.99	1.04	1.42	0.77	1.69	2.15	3.86	5.07	1.64	1.61	3.15	1.21	
Given (Brill 1999)	55.24	5.30	1.20	11.30	14.80	3.94	0.47	0.55	0.38	0.48	0.51	0.97	3.93	0.38	0.02	0.02	0.05	0.10	0.01	0.06	0.01	0.01	0.10	
δ absolute	0.70	0.11	-0.65	0.14	0.03	0.06	0.01	0.01	-0.01	-0.32	-0.22	0.16	0.07	0.02	0.00	0.00	0.00	-0.01	0.00	0.00	0.00	0.00	-0.01	
δ relative (%)	1.27	2.03	-54.32	1.27	0.22	1.58	2.37	2.17	-3.89	-65.90	-43.06	16.94	1.74	6.16	13.48	-21.49	5.06	-7.44	7.31	-0.92	-8.34	-29.86	-8.26	

	SiO ₂	Al ₂ O ₃	Na ₂ O	K ₂ O	CaO	MgO	FeO	MnO	CuO	PbO	BaO	Sb ₂ O ₅	P ₂ O ₅	TiO ₂	V ₂ O ₅	CoO	NiO	ZnO	Rb ₂ O	SrO	ZrO ₂	Ag ₂ O	SnO ₂	
NIST621 (n=4)																								
Measured	72.13	2.99	11.45	1.63	11.27	0.27	0.04				0.10			0.02					0.00					
SD	0.27	0.01	0.10	0.01	0.19	0.00	0.02				0.00			0.00					0.00					
RSD (%)	0.38	0.46	0.85	0.88	1.66	1.74	38.79				2.14			12.28					16.08					
Given (Brill 1999)	71.10	2.80	12.70	2.00	10.70	0.30	0.04				0.12			0.01					0.01					
δ absolute	1.03	0.19	-1.25	-0.37	0.57	-0.03	0.01				-0.02			0.00					-0.01					
δ relative (%)	1.45	6.76	-9.81	-18.67	5.29	-11.35	18.11				-17.59			21.07					-79.40					

* MnO data from Vicenzi *et al.* 2002.

Table 6.6: The precision and accuracy of LA-ICP-MS (NIST610 and 612).

	SiO ₂ (%)	Al ₂ O ₃ (%)	Na ₂ O(%)	K ₂ O(%)	CaO(%)	MgO(%)	FeO(%)	MnO(ppm)	CuO(ppm)	PbO(ppm)	BaO(ppm)	Sb ₂ O ₅ (ppm)	P ₂ O ₅ (ppm)	Sc ₂ O ₃ (ppm)	TiO ₂ (ppm)
NIST610 (n=4)															
Measured	70.99	2.01	12.59	0.11	11.97	0.08	0.07	592.8	519.2	308.9	462.9	654.3	1536.8	655.4	765.3
SD	0.31	0.01	0.06	0.00	0.35	0.00	0.01	7.9	29.0	6.8	13.4	15.9	107.5	7.7	29.7
RSD (%)	0.43	0.50	0.49	2.08	2.95	1.83	18.94	1.3	5.6	2.2	2.9	2.4	7.0	1.2	3.9
Given	72.00	2.00	14.00	0.06	12.00	0.08	0.06	590.0	556.0	441.0	506.0	552.0	785.0	663.0	729.0
δ absolute	-1.01	0.01	-1.41	0.05	-0.03	0.00	0.01	2.8	-36.8	-132.1	-43.1	102.3	751.8	-7.6	36.3
δ relative (%)	-1.41	0.33	-10.11	75.71	-0.21	3.47	13.25	0.5	-6.6	-30.0	-8.5	18.5	95.8	-1.1	5.0

NIST 612 (n=4)															
Measured	72.47	2.11	12.81	0.05	12.29	0.01		47.7	38.9	49.8	46.3	85.3	646.2	62.3	78.5
SD	0.23	0.01	0.09	0.00	0.18	0.00		1.0	3.5	45.2	3.8	14.0	57.5	3.4	11.8
RSD (%)	0.31	0.46	0.67	5.64	1.43	7.22		2.0	8.9	90.8	8.3	16.5	8.9	5.5	15.0
Given	72.00	2.00	14.00	0.01	12.00	0.01	0.01	49.0	47.0	43.0	43.0	46.0	126.0	65.0	84.0
δ absolute	0.47	0.11	-1.19	0.04	0.29	0.00		-1.3	-8.1	6.8	3.3	39.3	520.2	-2.7	-5.5
δ relative (%)	0.65	5.27	-8.52	444.79	2.42	-0.91		-2.7	-17.3	15.7	7.7	85.5	412.9	-4.1	-6.5
	V ₂ O ₅ (ppm)	CoO(ppm)	NiO(ppm)	ZnO(ppm)	As ₂ O ₃ (ppm)	Rb ₂ O(ppm)	SrO(ppm)	Y ₂ O ₃ (ppm)	ZrO ₂ (ppm)	Nb ₂ O ₅ (ppm)	Ag ₂ O(ppm)	SnO ₂ (ppm)	Cs ₂ O(ppm)	La ₂ O ₃ (ppm)	Ce ₂ O ₃ (ppm)
NIST610 (n=4)															
Measured	745.4	504.4	596.5	479.9	454.9	461.4	571.0	553.9	580.4	526.5	296.9	558.7	449.7	590.3	534.5
SD	7.5	5.6	7.6	10.3	31.2	2.7	7.0	5.7	6.8	7.9	5.1	17.7	10.4	6.6	8.1
RSD (%)	1.0	1.1	1.3	2.1	6.9	0.6	1.2	1.0	1.2	1.5	1.7	3.2	2.3	1.1	1.5
Given	754.0	496.0	584.0	539.0	449.0	466.0	610.0	559.0	588.0	535.0	288.0	497.0	455.0	597.0	542.0
δ absolute	-8.6	8.4	12.5	-59.1	5.9	-4.6	-39.0	-5.1	-7.6	-8.5	8.9	61.7	-5.3	-6.7	-7.5
δ relative (%)	-1.1	1.7	2.1	-11.0	1.3	-1.0	-6.4	-0.9	-1.3	-1.6	3.1	12.4	-1.2	-1.1	-1.4
NIST 612 (n=4)															
Measured	63.9	41.3	48.3	36.2	65.0	35.2	87.5	45.3	47.8	43.6	29.2	51.5	50.7	49.7	45.8
SD	2.2	1.0	3.5	3.5	5.9	1.7	2.0	0.9	2.1	1.0	1.9	3.7	3.4	1.6	1.4
RSD (%)	3.5	2.5	7.3	9.7	9.1	4.9	2.3	2.1	4.5	2.4	6.4	7.1	6.6	3.3	3.2
Given	72.0	45.0	49.0	45.0	49.0	34.0	93.0	49.0	51.0	55.0	24.0	43.0	49.0	43.0	45.0
δ absolute	-8.1	-3.7	-0.7	-8.8	16.0	1.2	-5.5	-3.7	-3.2	-11.4	5.2	8.5	1.7	6.7	0.8
δ relative (%)	-11.3	-8.3	-1.4	-19.7	32.7	3.4	-6.0	-7.6	-6.3	-20.7	21.6	19.7	3.5	15.5	1.8

	Pr ₂ O ₃ (ppm)	Nd ₂ O ₃ (ppm)	Sm ₂ O ₃ (ppm)	Eu ₂ O ₃ (ppm)	Gd ₂ O ₃ (ppm)	Tb ₂ O ₃ (ppm)	Dy ₂ O ₃ (ppm)	Ho ₂ O ₃ (ppm)	Er ₂ O ₃ (ppm)	Tm ₂ O ₃ (ppm)	Yb ₂ O ₃ (ppm)	Lu ₂ O ₃ (ppm)	HfO ₂ (ppm)	ThO ₂ (ppm)	UO ₂ (ppm)
NIST610 (n=4)															
Measured	499.0	524.0	554.6	553.2	497.0	503.4	474.5	503.4	495.8	485.6	524.1	482.9	489.8	513.8	516.1
SD	7.5	19.7	7.9	5.8	18.7	1.3	17.5	2.9	14.6	14.2	5.5	6.4	11.8	4.8	6.4
RSD (%)	1.5	3.8	1.4	1.0	3.8	0.3	3.7	0.6	2.9	2.9	1.1	1.3	2.4	0.9	1.2
Given	506.0	531.0	562.0	555.0	504.0	510.5	482.3	510.5	503.3	492.7	532.0	490.1	494.2	520.2	523.5
δ absolute	-7.0	-7.0	-7.4	-1.8	-7.0	-7.1	-7.8	-7.1	-7.4	-7.1	-7.9	-7.2	-4.4	-6.5	-7.5
δ relative (%)	-1.4	-1.3	-1.3	-0.3	-1.4	-1.4	-1.6	-1.4	-1.5	-1.4	-1.5	-1.5	-0.9	-1.2	-1.4
NIST 612 (n=4)															
Measured	40.5	43.8	46.0	44.3	43.0	42.7	36.2	43.9	41.0	40.0	44.7	41.2	43.3	44.0	39.4
SD	1.1	4.9	5.2	1.7	4.6	1.3	2.7	1.2	2.1	1.7	5.2	0.8	4.0	2.8	2.1
RSD (%)	2.7	11.2	11.3	3.8	10.6	3.1	7.5	2.6	5.0	4.3	11.7	2.1	9.2	6.4	5.2
Given	43.0	44.0	45.0	41.0	44.0	41.6	41.4	43.4	43.4	41.4	46.9	42.8	40.4	43.0	42.4
δ absolute	-2.5	-0.2	1.0	3.3	-1.0	1.1	-5.1	0.5	-2.5	-1.3	-2.2	-1.6	2.9	1.0	-3.0
δ relative (%)	-5.9	-0.4	2.2	8.1	-2.3	2.6	-12.4	1.3	-5.7	-3.2	-4.7	-3.7	7.1	2.2	-7.0

* MnO data from Vicenzi *et al.* 2002.

7. Results: typology and optical microscopy

7.1. Introduction

This chapter discusses the results of the typological study of glass beads from the five sites, Kiwulan, Jiuxianglan, Daoye, Wujiancuo and Guishan. In addition, the published data from Shisanhang (Tsang and Liu 2001) and Xiliao (Liu 2011e) will also be used as comparative data. Due to the lack of decoration on the monochrome glass beads in this research, the typological grouping is mostly based on the colours and the manufacturing methods at each site, and so will be discussed on a case by case basis. It should be mentioned that the purpose of typological study in this research is not to set a universal scheme of bead typology in these monochrome beads, but to identify the differences between sites/regions and provide a base for the discussion of chemical composition and distribution by context in the following chapters. The proportion of bead colours at each site is shown in Figure 7.1, while the detailed lists of variables measured are provided in Appendix 1.

For each site where a typological scheme has been developed in this research, the group is prefixed by the site name (e.g. JXL=Jiuxianglan; GS=Guishan; DY=Daoye; WJC=Wujiancuo) and then colour (e.g. R = red, O = orange; Y = yellow; G = green; B = blue; DB = dark blue), followed by the proposed manufacturing method (e.g. 1 = drawn, 2 = other methods including wound).

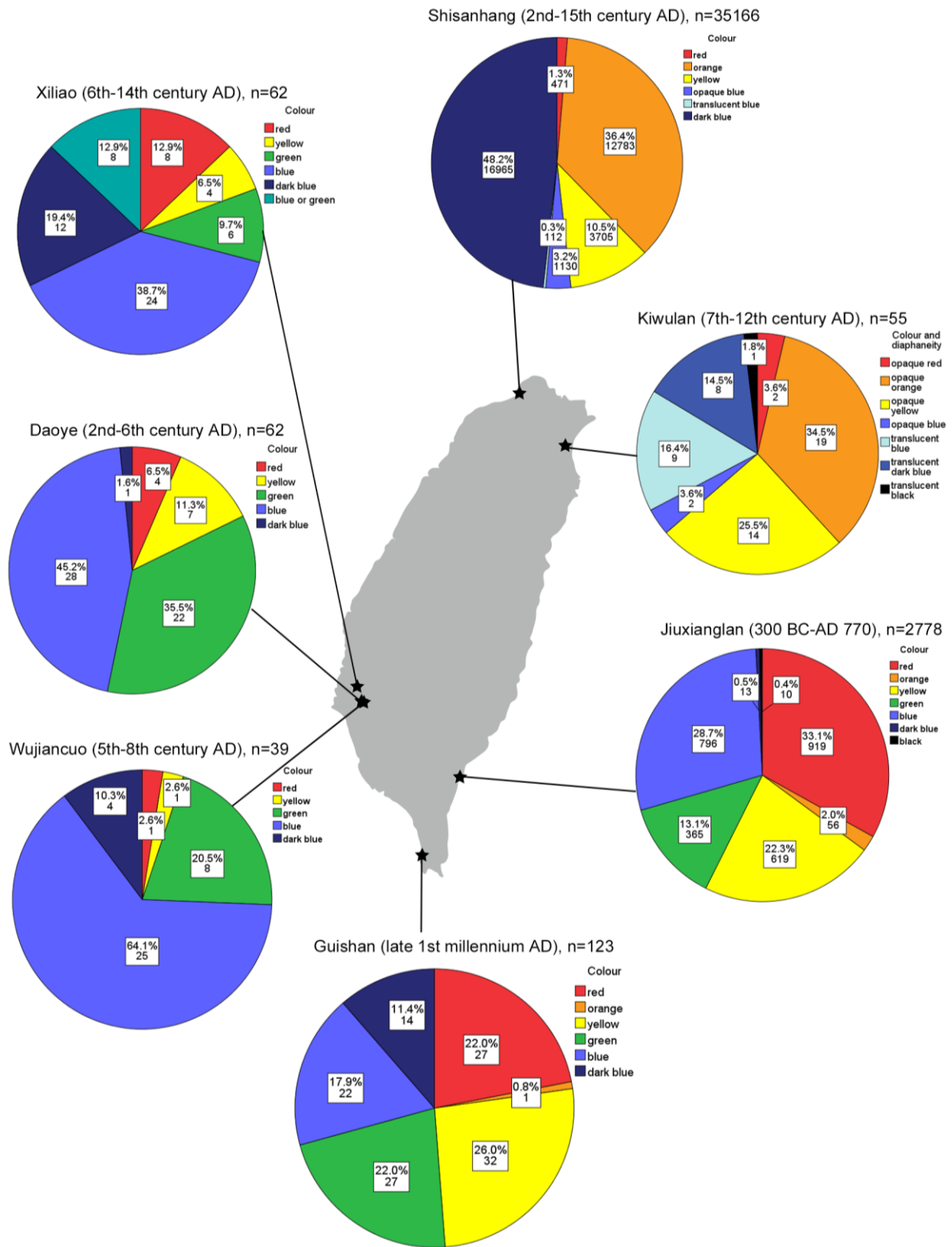
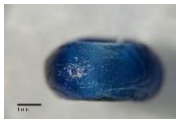


Figure 7.1: The colour distribution of glass beads from Kiwulan, Shisanhang, Jiuxianglan, Daoye, Wujiancuo, Guishan and Xiliao. Please note that the data from Kiwulan is not the full number of beads from the Lower Cultural Layer. All the data from Shisanhang are from Tsang and Liu (2001), and all the data from Xiliao are from Liu (2011e).

7.2. Kiwulan, northeastern Taiwan (7th-12th century AD)

Glass beads from the Lower Cultural Layer had been divided into 12 groups, based on the colour, shape and size, in previous research and so the typological classification given in the publication is replicated here (Table 7.1) (Cheng 2007; Chen *et al.* 2008e: 26-28). This research follows the 12 groups in Table 7.1. The analysis and discussion of typological variables of the Kiwulan beads are based on the 55 selected samples, and use the details of manufacturing method identified for each of these beads in this research.

Table 7.1: The 12 typological groups of glass beads from the Lower Cultural Layer in Kiwulan¹(Chen et al. 2008e: 26-28).

Type (n ²)	Diaphaneity/ Colour	Shape	Manufacturing method	Context	Image
LL01 (166)	Opaque/ orange.	Short tubular.	Drawn.	Burial, non-burial.	
LL02 (22)	Opaque/ orange.	Long tubular.	Dipped or wound.	Burial, non-burial.	
LL03 (456)	Opaque/ orange.	Short tubular or oblate.	Drawn.	Burial, non-burial.	
LL04 (212)	Translucent/ blue.	Long tubular.	Drawn.	Burial, non-burial.	
LL05 (259)	Opaque/ yellow.	Oblate.	Wound.	Burial, non-burial.	
LL06 (46)	Translucent/ dark blue.	Oblate.	Wound.	Non-burial.	

Type (n ²)	Diaphaneity/ Colour	Shape	Manufacturing method	Context	Image
LL07 (4)	Opaque/red.	Short tubular.	Drawn.	Burial, non-burial.	
LL08 (5)	Translucent/ blue.	Long tubular.	Drawn.	Non-burial.	
LL09 (☆)	Opaque/blue.	Oblate.	Drawn.	Burial.	
LL10 (2)	Opaque/ yellow.	Short tubular or oblate.	Drawn.	Burial, non-burial.	
LL11 (☆)	Translucent/ blue.	Oblate.	Wound.	Burial.	
LL12 (☆)	Opaque/blue.	Long tubular.	Drawn.	Burial.	

1: typological groups based on Chen *et al.* (2008f: 26-28).

2: n = quantity provided in Chen *et al.* (2008f: 26-28) (excludes samples from mortuary contexts).

☆: only found in burials; no quantitative data.

Figure 7.1 shows the colour distribution of selected samples from Kiwulan. Together with Table 7.1, it can be seen that, in the Lower Cultural Layer at Kiwulan, the majority of beads are orange, yellow and blue beads. In the LL04 type, most beads are translucent light blue, but a closer examination indicates different degrees of hue between light blue, dark blue and black, which probably resulted from the concentration of colorants introduced into the glass melts. The shapes of these beads include long tubular, short tubular and oblate. Glass beads of LL02, LL04, LL08 and LL12 types are a long tubular shape, while those of the other types are oblate or short

tubular. Except for LL02 and LL08 types, most beads have a length between 1-4 mm and a diameter between 2-5 mm (Figure 7.2). The size of beads in LL01 type, however, shows a larger differentiation in comparison to other types, which can be seen clearly in Figure 7.2. LL02, LL04, LL08, LL10 and LL12 types seem to be less well reported around the South China Sea (if their shape and size are taken into consideration), but a few similar types can be found at the Shisanhang site in northern Taiwan (see section 7.4).

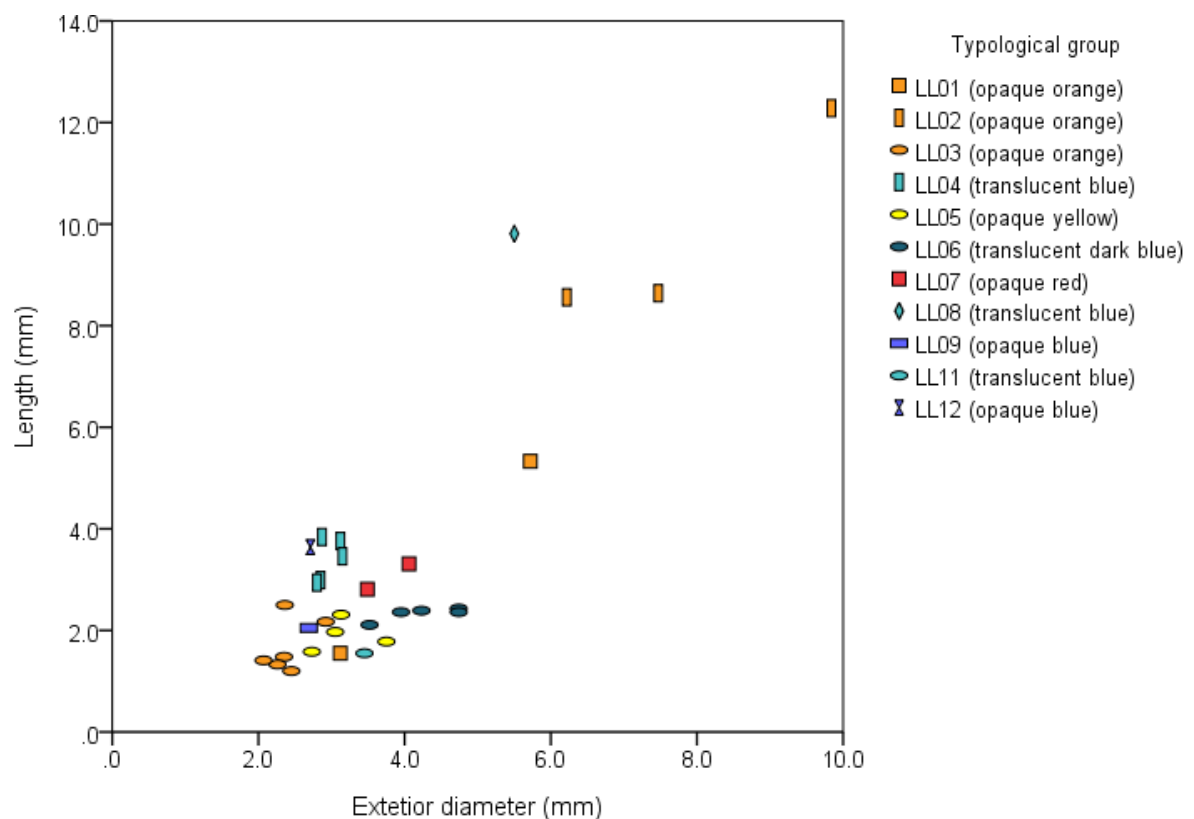


Figure 7.2: The size of selected samples from the Lower Cultural Layer at Kiwulan.

Optical microscopic observation has revealed 2 types of manufacturing methods for the beads at this site: drawn and wound. Most samples in LL01, LL03, LL04, LL07, LL08, LL09, LL10 and LL12 types are found to have fabric lines and bubbles parallel to the perforation axis, which may indicate the use of the drawn method (Figure 7.3). Most LL05, LL06 and LL11 types show encircling fabric lines, and therefore this may suggest they were produced using the wound method. However, the observation on a fragmented sample KWL023, which was grouped into

LL04 in previous research, reveals evidence of production using the wound method, which is in contrast to the other samples of the LL04 type (drawn). The colour of KWL023 is dark blue, which is also different from the light blue colour of other beads of the LL04 type (Table 7.1). This result suggests that KWL023 may not be of LL04 type as previously grouped.

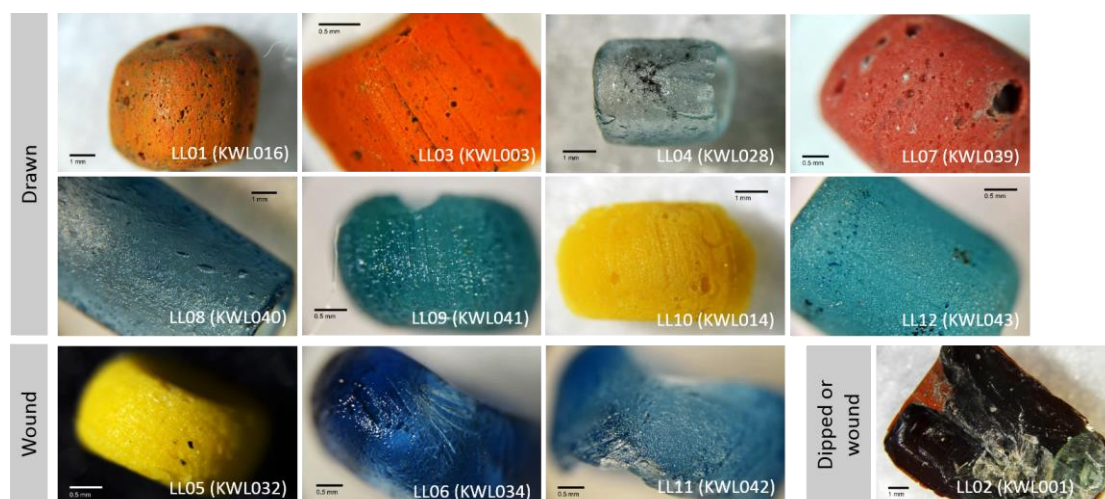


Figure 7.3: Optical microscopic observation reveals three manufacturing methods for Kiwulan beads.

In addition to the typical drawn and wound method, LL02 group is an interesting type which shows the covering of a glass surface on a clay- or glass-made core. Glass beads of this type are also reported from Shisanhang (section 7.3). The optical examination has shown that the inner surface of the perforation hole is not covered with a glass layer (Figure 7.4 (a)), and therefore it is possible that the glass on the outer surface was dipped or wound on the core body. For LL02 types with a clay body, generally the glass layer is not well bonded to the core, as can be seen in Figure 7.4 (b). The loose bonding between the glass surface and the clay body can also be regarded as supportive evidence of the dipped or wound method (Pollard 2015, *pers. comm.*). It is possible that the underlying core body was immersed or wound with re-melted glass rather than covered and re-fired with the glaze ashes. Therefore, the lack of interaction between the glass layer and the underlying body as well as the dissimilarities of material

properties between the glass and clay have resulted in a loose bonding between the two parts. Within the LL02 type, KWL001 is the only sample examined with a glass core, and stronger bonding between the surface and body can be observed. A closer examination of KWL001 further reveals a red inter-layer between the orange surface and inner glass body (Figure 7.4 (c) and (d)).

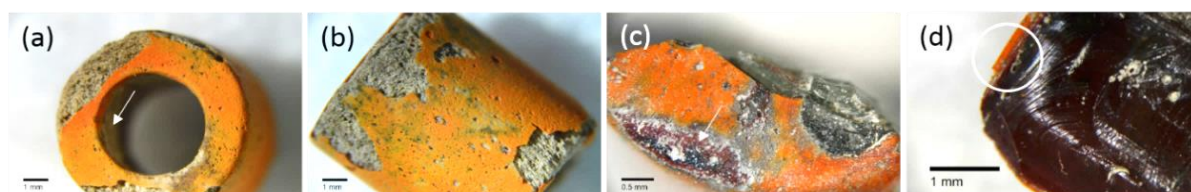


Figure 7.4: Optical microscopic observation on LL02 beads reveals (a) the use of the dipped or wound method, (b) the loose bonding between the clay body and the glass surface, and (c) and (d) the red interlayer between the orange glass surface and the glass body. ((a) and (b): KWL017; (c) and (d): KWL001.)

7.3. Shisanhang, northern Taiwan (2nd-15th century AD)

The distribution of bead colours at Shisanhang can be seen in Figure 7.1. Orange (36.1%, n = 12682) and dark blue (48.2%, n = 16965) are the two dominant colours, with smaller numbers of yellow (10.8%, n=3806), opaque blue (3.2%, n = 1130), red (1.3%, n = 471) and translucent blue (0.3%, n = 112). It is noteworthy that the total quantity of glass beads unearthed from Shisanhang is significantly more than other Iron Age sites in Taiwan, and more diverse types of beads were found.

The classification of the beads presented below is taken from the publication by Tsang and Liu (2001: 91-106), no further examination of the beads was possible here. Glass beads from Shisanhang had been previously classified into 16 types based on shape, size and colour (Tsang

and Liu 2001: 91-106). Table 7.2 shows the integrated bead typologies from Tsang and Liu (2001: 91-106). The colours of some types are re-evaluated here based on the colour plates and the chemical data provided in the published report. The shapes of the Shisanhang beads are short tubular, long tubular and oblate. Table 7.2 shows that the size of most beads from Shisanhang have a length and diameter larger than 5 mm, which is generally larger than the beads from other sites in this research.

Type 8 is a unique group from Shisanhang. Although not mentioned in the original report (Tsang and Liu 2001: 101), the colour plate and the chemical data provided seem to suggest a dark blue or black core inside the Type 8 beads. If it is the case, Type 8 is probably a similar type to the orange-red beads with a dark blue core from Southeast Asia and South Asia (see Photo III-1 in Dussubieux (2001)).

Table 7.2: The 18 types of glass beads from Shisanhang (Integrated from Tsang and Liu (2001: 91-106)).

Type	Shape	Colour	Length (mm)	Diameter (mm)	Sample number	Image ¹
Type 1						
Type 1-1 (10234 beads, 108 fragments)	Oblate.	Dark blue.	2.5-3.0	1.0-2.0	B020, B032, B033, B037, B043, B046,	Image removed due to copyright.
Type 1-2 (360 beads, 4 fragments)	Oblate.	Dark blue.	6.3-6.8	5.0-5.5	B047, B048, B049, B052, B062, B063,	Image removed due to copyright.
Type 1-3 (5442 beads)	Long tubular.	Dark blue.	7.0-10.0	5.0-7.0	B064.	Image removed due to copyright.

Type	Shape	Colour	Length (mm)	Diameter (mm)	Sample number	Image ¹
Type 2 (105 beads, 7 fragments)	Short tubular.	Blue.	7.0	5.0	B024.	Image removed due to copyright.
Type 3						
Type 3-1 (7295 beads)	Tubular.	Orange or red.	3.0-7.0	5.0-7.0	B002, B003, B004, B012, B040.	Image removed due to copyright.
Type 3-2 (1585 beads, 45 fragments)	Long tubular.	Orange.	4.0-5.0	3.0-4.0		Image removed due to copyright.
Type 3-3 (8 beads)	Long tubular.	Orange.	10.0-18.0	10.0		Image removed due to copyright.
Type 4 (6 beads)	Short tubular.	Orange.	5.5	6.0	B017, B019.	Image removed due to copyright.
Type 5 (9 beads)	Long tubular.	Orange (clay body).	8.0	7.0		Image removed due to copyright.
Type 6 (35 beads 7 fragments)	Long tubular.	Orange or red (blue glass body).	8.0	7.0	B029.	Image removed due to copyright.
Type 7 (761 beads 360 fragments)	Short tubular or long	Orange (clay body).	5.0-12.0	6.0-8.0		Image removed due to copyright.

Type	Shape	Colour	Length (mm)	Diameter (mm)	Sample number	Image ¹
	tubular.					
Type 8 (15 beads 24 fragments)	Short tubular.	Orange.	3.0-4.0	3.0-4.0	B005, B006, B008.	Image removed due to copyright.
Type 9 (2864 beads 159 fragments)	Oblate.	Yellow.	2.0-3.0	3.0-4.0	B018, B035.	Image removed due to copyright.
Type 10 (712 beads 105 fragments)	Oblate.	Dark blue*.	n/a	n/a	B057.	Image removed due to copyright.
Type 11 (765 beads 2 fragments)	Long tubular.	Blue.	5.0-8.0	4.0-5.0	B042, B054, B061	Image removed due to copyright.
Type 12 (2528 beads 4 beads)	Short tubular.	Orange*.	3.0-3.5	5.0-6.0	B045, B060.	Image removed due to copyright.
Type 13 (98 beads 3 fragments)	Short tubular.	Yellow*.	6.0-7.0	9.0-10.0	B001, B038.	Image removed due to copyright.
Type 14 (682 beads)	Short tubular.	Yellow.	5.0-6.0	5.0-6.0	B007, B013, B036.	Image removed due to copyright.

Type	Shape	Colour	Length (mm)	Diameter (mm)	Sample number	Image ¹
Type 15 (189 beads)	Short tubular or oblate.	Blue.	<4.0	<4.0	B021, B026, B027, B055.	Image removed due to copyright.
Type 16 (174 beads)	Short tubular.	Blue*.	3.0	4.0	B014.	Image removed due to copyright.
Type 17 (113 beads 4 fragments)	Oblate.	Red.	2.0-3.0	2.0-3.0	B011, B059.	Image removed due to copyright.
Type 18 (353 beads 1 fragment)	Oblate.	Red*.	2.0-3.0	3.0-4.0	B015, B028.	Image removed due to copyright.

1: All images are acquired from Tsang and Liu (2001).

*: Re-evaluation of colour description based on the colour plate and chemical composition in Tsang and Liu (2001).

7.4. Comparison of glass beads from Kiwulan and Shisanhang

Both Kiwulan and Shisanhang are located in the geographic range of Shisanhang Culture (Figure 3.1). A closer comparison between glass beads reveals some similar types at Shisanhang (northern Taiwan) and Kiwulan (northeastern Taiwan), and the summary is provided in Table 7.3. For example, the Type 5, Type 6 and Type 7 from Shisanhang are similar to the LL02 type from Kiwulan. It is reported that glass beads of Type 5 and Type 7 at Shisanhang have a clay-made body covered with orange glass, while glass beads of Type 6 have blue glass body covered

with an orange or red glass surface. Together with the size (length of 8 mm and diameter of 7 mm) and shape (long tubular), the three types from Shisanhang show a close similarity to the LL02 type from Kiwulan (section 7.2). The other example is the yellow glass beads of Type 9 (oblate, length of 2-3 mm and diameter of 3-4 mm) from Shisanhang, which are similar to the LL05 type from Kiwulan. These types of glass beads are only found at Kiwulan and Shisanhang in this study.

Type 1-1 may be another similar style found at both Shisanhang and Kiwulan (LL06), as they are both oblate, dark blue beads. However, a closer investigation indicates that the size of Type 1-1 (length of 2.5-3 mm and diameter of 1-2 mm) at Shisanhang is generally smaller than LL06 (length of 2-2.5 mm and diameter of 3.5-4.5 mm) at Kiwulan, and therefore does not suggest the same group.

Despite the similarities of some bead styles between Shisanhang and Kiwulan, there are several other types of glass bead from Shisanhang which are not found at Kiwulan and other contemporary sites in Taiwan. The dark blue beads of Type 1-3 and the opaque blue beads of Type 11, Type 15 and Type 16 are only found at Shisanhang in this research, and they are also not often reported from Southeast Asia (Dussubieux 2014, *pers. comm.*).

Table 7.3: A summary of comparing bead typology between Kiwulan and Shisanhang.

Similar types
1. Kiwulan LL02 and Shisanhang Type 5/6/7. Only observed at Kiwulan and Shisanhang.
2. Kiwulan LL05 and Shisanhang Type 9.
Unique types not found in other sites
Kiwulan: LL02, LL04, LL08, LL10 and LL12.
Shisanhang: Type 1-3, Type 5/6/7, Type 11, Type 15 and Type 16.

7.5. Jiuxianglan, southeastern Taiwan (300 BC-AD 700)

Glass beads

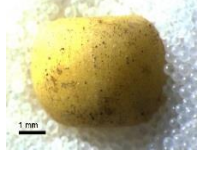
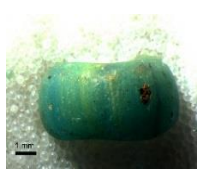
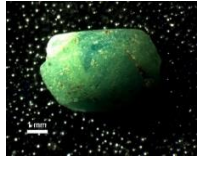
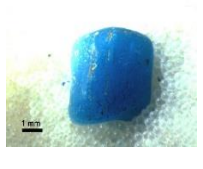
The colour distribution of all glass beads unearthed from Jiuxianglan in the 1st excavation session is shown in Figure 7.1. Red (33.1%, n = 919), blue (28.7%, n = 796), yellow (22.3%, n = 619) and green (13.1%, n = 365) are the most abundant colours found at Jiuxianglan, while the number of orange (2.0%, n = 56), dark blue (0.5%, n = 13) and black (0.4%, n = 10) beads are quite small. The dominant shapes are short tubular or oblate, but no distinct correlations between shapes and colours can be observed.

Based on the 36 selected samples in this research, it can be seen that these beads have similar lengths between 2-5.5 mm and diameters between 2.5-8 mm (Figure 7.5). No obvious size differences have been observed between colour groups, and their size and shape generally match the typical Indo-Pacific glass beads from around the South China Sea region.

Six groups have been recorded based on their colours and manufacturing methods (Table 7.4). The optical microscopic investigation has revealed that, in the 6 groups, 33 out of the 36 beads are likely to be drawn. Figure 7.6 shows some bead samples with evidence of the drawn method where the parallel fabric lines, elongated bubbles and voids can be seen clearly on the surface. One green bead (JXL26) is probably wound, and therefore this sample is separated from other green beads as a single group (JXL-G2). In fact, it is hard to determine the manufacturing method simply through the exterior surface of JXL26, but further examination on the perforation side and interior body reveals a few encircling fabric lines (Figure 7.6), and therefore may suggest the use of wound method. For two blue beads (JXL06 and JXL29), it is hard to determine the manufacturing method through microscopic observation, which made it

difficult to assign any of them to a particular group.

Table 7.4: The groups and manufacturing methods of selected samples from Jiuxianglan (JXL).

Group (n ¹)	Colour	Shape	Manufacturing method	End roundness (n*)	Image
JXL-R1 (6)	Red.	Short tubular or oblate.	Drawn.	Round (6).	
	JXL01, JXL02, JXL10, JXL22, JXL34, JXL35.				
JXL-O1 (3)	Orange.	Short tubular or oblate.	Drawn.	Round (3).	
	JXL24, JXL25, JXL27.				
JXL-Y1 (10)	Yellow.	Short tubular, long tubular or oblate.	Drawn.	Round (10).	
	JXL03, JXL05, JXL07, JXL12, JXL15, JXL19, JXL20, JXL32, JXL33, JXL38.				
JXL-G1 (8)	Green.	Short tubular, long tubular or oblate.	Drawn.	Round (8).	
	JXL08, JXL09, JXL11, JXL13, JXL14, JXL23, JXL30, JXL31.				
JXL-G2 (1)	Green.	Unidentifiable.	Wound?	Round (1).	
	JXL26.				
JXL-B1 (6)	Blue.	Short tubular, long tubular or oblate.	Drawn.	Round (6).	
	JXL04, JXL16, JXL17, JXL18, JXL21, JXL28.				
no group (2)	Blue.	n/a	Unidentifiable.	n/a	
	JXL06, JXL29.				

1: n = quantity.

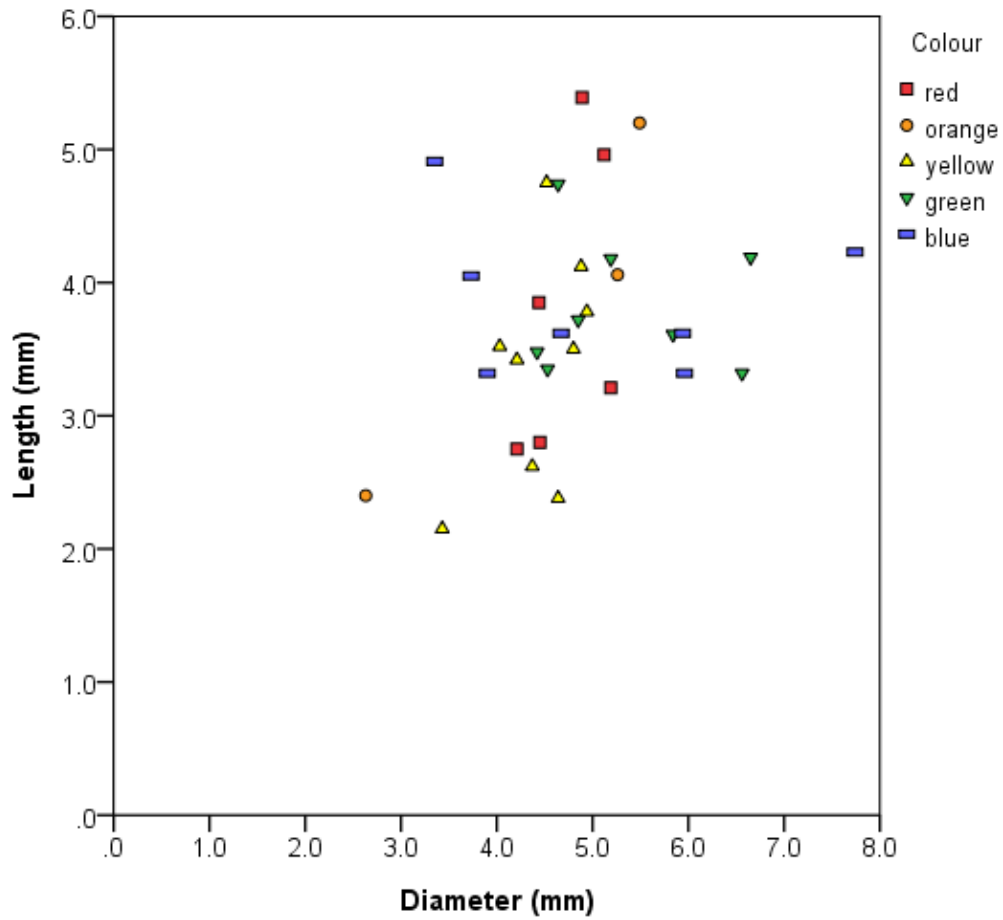


Figure 7.5: The size of glass beads from Jiuxianglan.

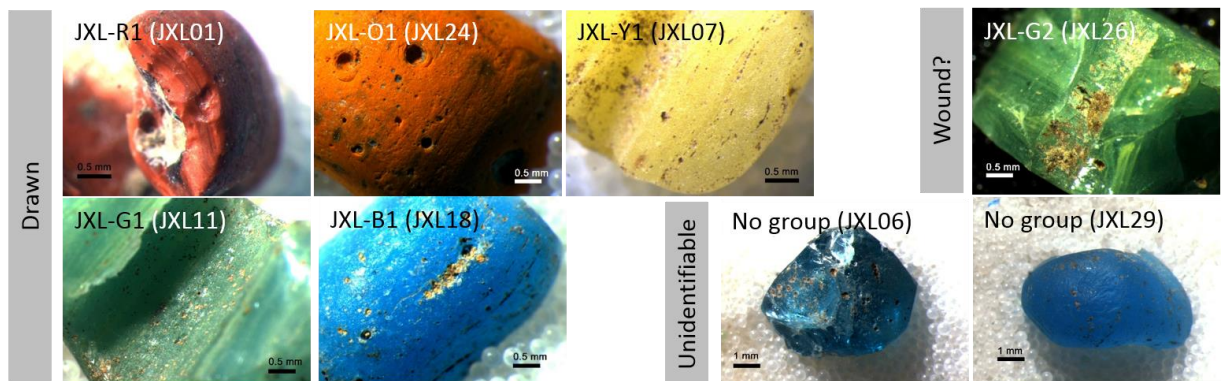


Figure 7.6: Optical microscopic observation reveals the manufacturing methods for Jiuxianglan beads.

In the red beads, blackish streaks are often noticed, and in the green beads, yellowish streaks can be seen. The optical microscopic examination clearly indicates that these blackish or yellowish streaks are not intentionally added on the bead surface for decoration, as they can also be observed from the interior body through the fragmented surface (Figure 7.6).

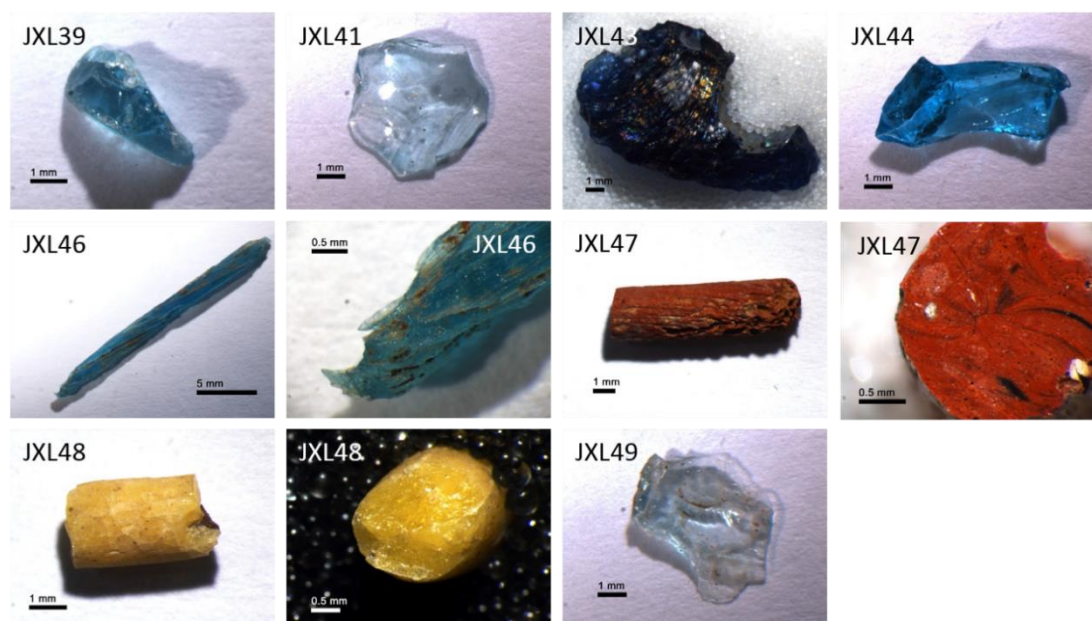


Figure 7.7: The analysed glass waste from Jiuxianglan.

Glass waste

In terms of the glass waste from Jiuxianglan, it can be seen from Figure 7.7 that the shapes of the waste do not suggest the use of the ‘lada’ technique for producing drawn beads. None of the waste resembles, for example, the ‘horns’, the ‘pulled tubes’ and the ‘caught knots’ suggested by Peter Francis as indicative evidence of the ‘lada’ drawn method (Francis 1990). There are no remains of glass tubes found at Jiuxianglan, and only red, yellow and blue (a few are aqua) glass waste was found. From Figure 7.7 it can be seen that JXL46, JXL47 and JXL48 are all glass rods rather than tubes. The image of JXL46 further indicates the pulled-off end of the glass rod. Together with the evidence which shows the bead encircling the tip of a mandrel

(Figure 2.2 (b)), it is likely that wound method rather than drawn method was used for bead production at Jiuxianglan. Therefore, the identification of the wound method through the examination of glass waste shows an inconsistency with the finished drawn glass beads in this research.

7.6. Guishan, southern Taiwan (late 1st millennium AD)

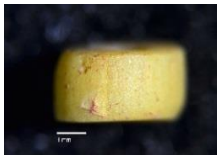
At Guishan, red (22.0%, n = 27), yellow (26.0%, n = 32), green (22.0%, n = 27), blue (17.9%, n = 22) and dark blue (11.4%, n = 14) beads are found in similar proportions (Figure 7.1). The only orange bead is actually a red bead covered with an orange surface (GS-O1, Table 7.5). Interestingly, although in small quantities, glass beads similar to the orange bead were unearthed from Phum Snay, Cambodia (350 BC-AD 200) (Carter 2013: 307 and Figure 7.15 in the cited work), Angkor Borei (Cambodia, 200 BC-AD 200), Kuala Selinsing (Malaysia, 9th-10th century AD), Samatra (Indonesia, the 9th century AD) (Dussubieux 2001: 157) and other distant sites in South Asia (Dussubieux 2001: 157; Dussubieux and Gratuze 2013). However, it is not known whether the orange-red bead at Guishan possesses the dark glass core mentioned in Dussubieux (2001: 157) and Dussubieux and Gratuze (2013).

Glass beads from Guishan have been divided into 9 groups based on their colours and manufacturing methods (Table 7.5). It is difficult to determine the manufacturing methods used to produce two samples GS095 (yellow) and GS119 (dark blue), and their physical appearances do not resemble other beads. Therefore, they are labelled as 'no group'.

Short tubular, long tubular and oblate are the three most common shapes of glass beads at Guishan, and a different 'biconical' shape is found in some yellow beads (GS-Y2 group). Figure 7.8 shows the size of all Guishan beads and, except for GS-Y2, GS-G2, GS-DB1 groups and a

few red beads, most beads have the diameters between 3-5.5 mm and the lengths between 1.5-5 mm. Glass beads in the GS-G2 group are small, with a length of 1-1.5 mm and a diameter of 2.5-3 mm, in comparison to the GS-G1 group. Some red beads have the shape of a long tube, with a length in the range of 6-8 mm. There is no difference in the manufacturing methods and physical appearances (e.g. hue of colour, texture of bead surface) of these long tubular red beads, and therefore they are thought to be in the same group as other red beads. Glass beads within the GS-Y2 group have a wider diameter (6-7.5 mm) due to their biconical shape. The GS-DB1 group, however, is rather different from other glass beads from Guishan as they are larger (length 3.5-6.5 mm and diameter 5.5-8 mm). GS-Y2 and GS-DB1 groups are only identified from Guishan in this current research.

Table 7.5: The groups and manufacturing methods of all Iron Age beads from Guishan (GS).

Group (n ¹)	Colour	Shape	Manufacturing method	End roundness (n ¹)	Image
GS-R1 (27)	Red.	Short tubular, long tubular or oblate.	Drawn.	Round (23) or tapered (4).	
	GS004, GS007, GS010, GS014, GS018, GS019, GS023, GS024, GS038, GS047, GS050, GS051, GS055, GS063, GS070, GS071, GS072, GS073, GS074, GS075, GS078, GS079, GS084, GS091, GS102, GS110, GS111.				
GS-O1 (1)	Orange + red.	Long tubular.	Drawn.	Round.	
	GS015.				
GS-Y1 (26)	Yellow.	Short tubular, long tubular or oblate.	Drawn.	Round (11) or tapered (15).	
	GS003, GS005, GS008, GS011, GS017, GS020, GS022, GS030, GS062, GS064, GS067, GS069, GS081, GS082, GS083, GS085, GS086, GS087, GS088, GS089,				

Group (n ¹)	Colour	Shape	Manufacturing method	End roundness (n ¹)	Image
	GS090, GS092, GS093, GS094, GS107, GS112.				
GS-Y2 (5)	Yellow.	Biconical.	Unidentifiable.	Round (2) or tapered (3).	
	GS028, GS029, GS040, GS041, GS113.				
GS-G1 (20)	Green.	Short tubular or oblate.	Drawn.	Round (26) or tapered (1).	
	GS001, GS006, GS016, GS021, GS026, GS027, GS031, GS032, GS034, GS035, GS036, GS044, GS045, GS052, GS103, GS104, GS106, GS109, GS115, GS123.				
GS-G2 (7)	Green.	Oblate.	Drawn.	Round.	
	GS037, GS065, GS101, GS108, GS116, GS117, GS118.				
GS-B1 (18)	Blue.	Short tubular, long tubular or oblate.	Drawn.	Round.	
	GS002, GS009, GS012, GS013, GS025, GS033, GS039, GS042, GS043, GS046, GS049, GS053, GS054, GS066, GS105, GS120, GS121, GS122.				
GS-B2 (4)	Blue.	Short tubular.	Wound?	Round (3) or tapered (1).	
	GS048, GS076, GS077, GS080.				
GS-DB1 (13)	Dark blue.	Short tubular or oblate.	Drawn.	Round.	
	GS056, GS057, GS058, GS059, GS060, GS061, GS068, GS096, GS097, GS098, GS099, GS100, GS114.				
no group (2)	Yellow or dark blue.	n/a	n/a	n/a	
	GS095, GS119.				

1: n = quantity.

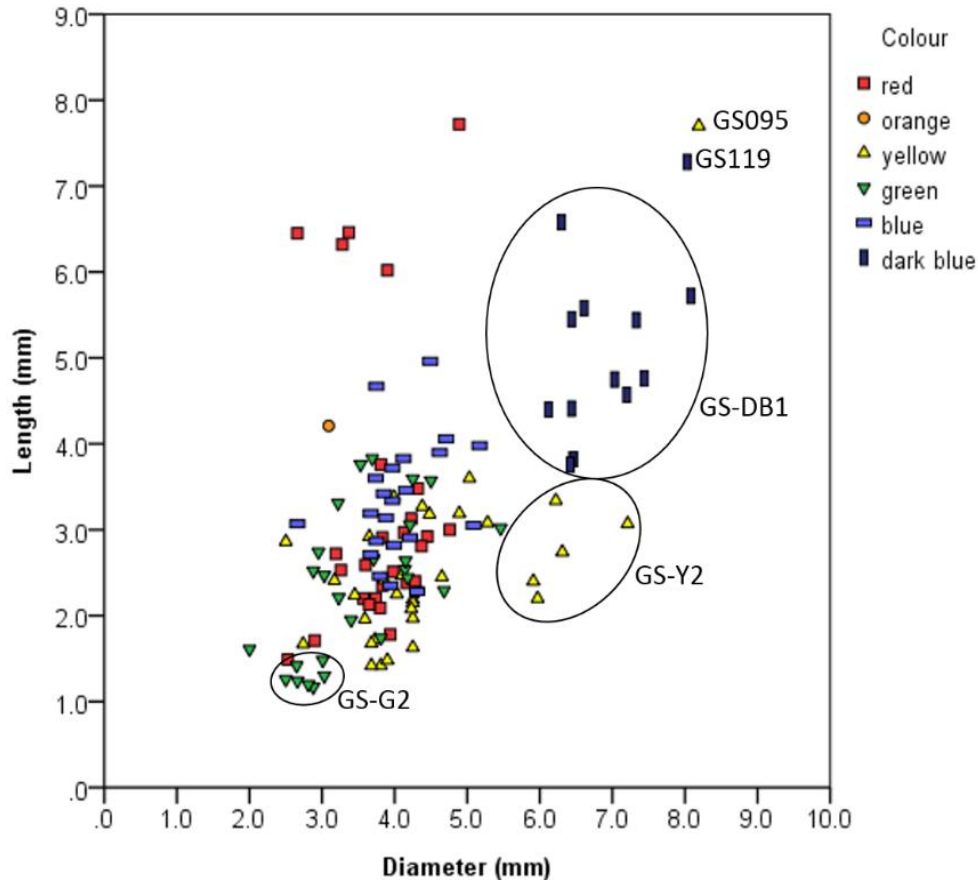


Figure 7.8: The size of all Iron Age glass beads from Guishan.

Figure 7.9 shows the results of microscopic observations of these beads. It is quite clear that the parallel fabric lines on the surface of red, orange, yellow (GS-Y1), green, blue (GS-B1) and dark blue beads indicate the use of drawn method, while the encircling lines on blue beads of GS-B2 group suggest the use of the wound method. Similar to the drawn red and green beads from Jiuxianglan, the blackish streaks on the red bead and the yellowish streaks on the green beads are found in samples from Guishan. The manufacturing method of the GS-Y2 group is unclear through microscopic observation. This is probably due to shaping after beadmaking in order to obtain the biconical shape, which may have erased the manufacturing marks on the bead surface.

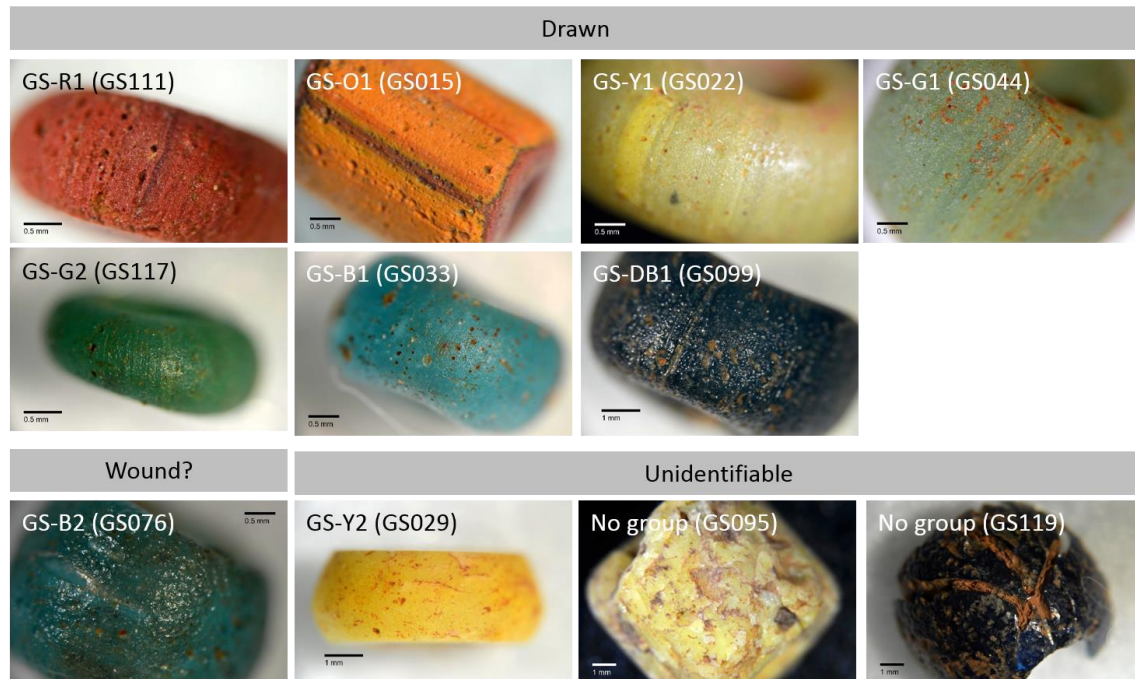


Figure 7.9: Optical microscopic observation reveals the manufacturing methods for Guishan beads.

7.7. Comparison of glass beads from Jiuxianglan and Guishan

As noted in Chapters 2.4 and 2.5, previous research has suggested the interaction between Guishan and Jiuxianglan. The research has shown that glass beads from Jiuxianglan and most from Guishan have the shape and size of typical Indo-Pacific beads. However, a comparison between beads from the two sites has shown that, despite the similar texture of the bead surface, the beads from Guishan are generally slightly smaller than those from Jiuxianglan. The types of Guishan beads are also more diverse than those of Jiuxianglan. The GS-Y2, GS-G2 and GS-DB1 types are not seen at Jiuxianglan or in other sites studied. This does not indicate exchange of glass beads between Guishan and Jiuxianglan. A summary is provided in Table 7.6.

Table 7.6: A summary of comparing bead typology between Guishan and Jiuxianglan.

Similar types
All similar to typical Indo-Pacific drawn beads, excluding the three unique groups mentioned below, but generally the sizes of beads from Guishan are smaller than those from Jiuxianglan.
Unique types not found in other sites
Guishan: GS-Y2, GS-G2 and GS-DB1.

7.8. Daoye, southwestern Taiwan (2nd-6th century AD)

At Daoye, around 80% of the glass beads are blue or green (n = 50), and a few beads are yellow (11.3%, n = 7), red (6.5%, n = 4) or dark blue (1.6%, n = 1) (Figure 7.1). No orange beads were found from Daoye.

Except for DY08, which has a long tubular shape, 42 out of the 62 beads are short tubular, and the remaining samples are of an oblate shape. These short tubular or oblate beads generally have a length between 1-5 mm and a diameter between 2.5-5.5 mm (Figure 7.10). A closer examination indicates that most of the blue and yellow beads are larger than the red, green and dark blue beads, but there is no correlation between size and shape within a single colour group.

The optical microscopy shows the beads have parallel fabric lines, demonstrating that all the glass beads from Daoye are made by the drawn method (Figure 7.11). Because of the absence of distinct variations of shape and size, glass beads from Daoye are divided into 6 groups simply based on their colours (Table 7.7). DY08 is separated into a single group (DY-G2) because the long tubular shape and the green hue do not resemble other green beads at Daoye.

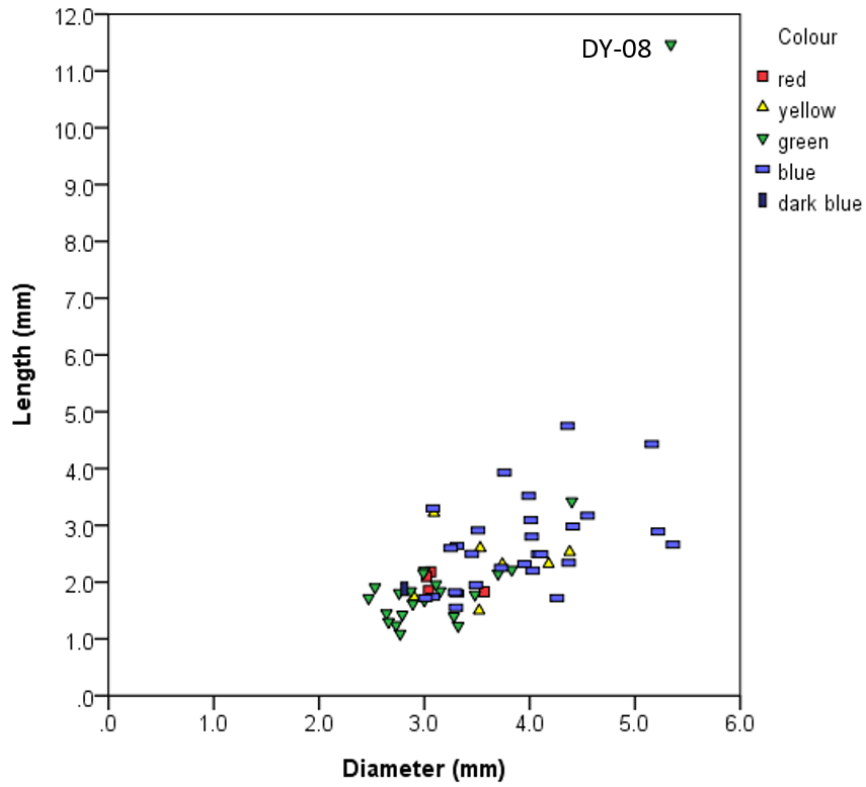


Figure 7.10: The size of all glass beads from Daoye.

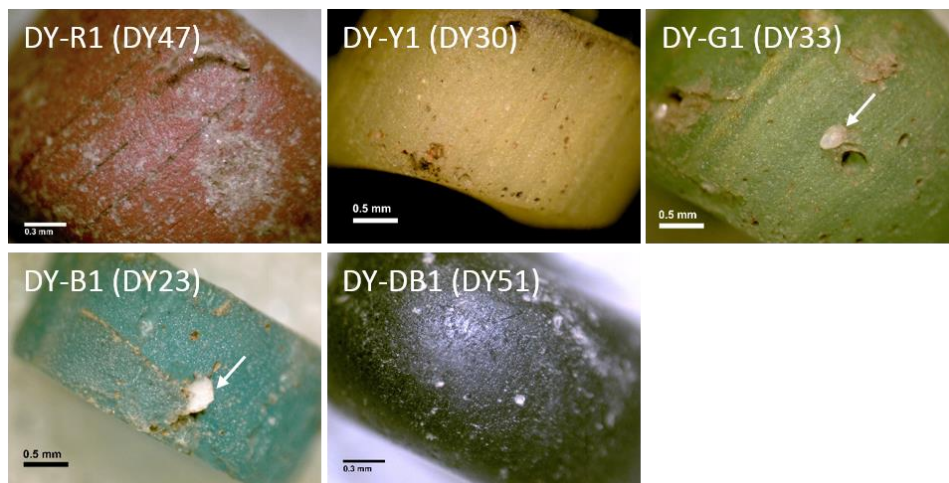
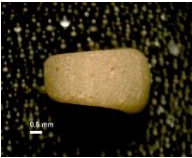
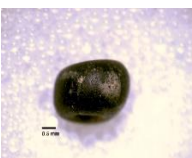


Figure 7.11: Optical microscopic observation reveals the parallel fabric lines and the quartz remains (arrow) in beads from Daoye.

Table 7.7: The groups and manufacturing methods of all beads from Daoye (DY).

Group (n ¹)	Colour	Shape	Manufacturing method	End roundness (n ¹)	Image
DY-R1 (4)	Red.	Short tubular or oblate.	Drawn.	Round (3) or tapered (1).	
DY-Y1 (7)	Yellow.	Short tubular or oblate.	Drawn.	Round (4) or tapered (3).	
DY-G1 (21)	Green.	Short tubular or oblate.	Drawn.	Round (18) or tapered (3).	
DY-G2 (1)	Green.	Long tubular.	Drawn.	Round (1).	
DY-B1 (28)	Blue.	Short tubular or oblate.	Drawn.	Round (23) or tapered (5).	
DY-DB1 (1)	Dark blue.	Oblate.	Drawn.	Round (1).	

1: n = quantity.

7.9. Wujiancuo, southwestern Taiwan (5th-8th century AD)

At Wujiancuo, 64.1% of glass beads are blue (n = 25), and there are small proportions of green (20.5%, n = 8), dark blue (10.3%, n = 4), red (2.6%, n = 1) and yellow (2.6%, n = 1) beads (Figure 7.1). As at Daoye, no orange beads were found at Wujiancuo. Around 80% of glass beads from Wujiancuo are short tubular, and a few are oblate or long tubular. Figure 7.12 shows that most glass beads from Wujiancuo have a length between 1-4 mm and a diameter between 1.5-5 mm.

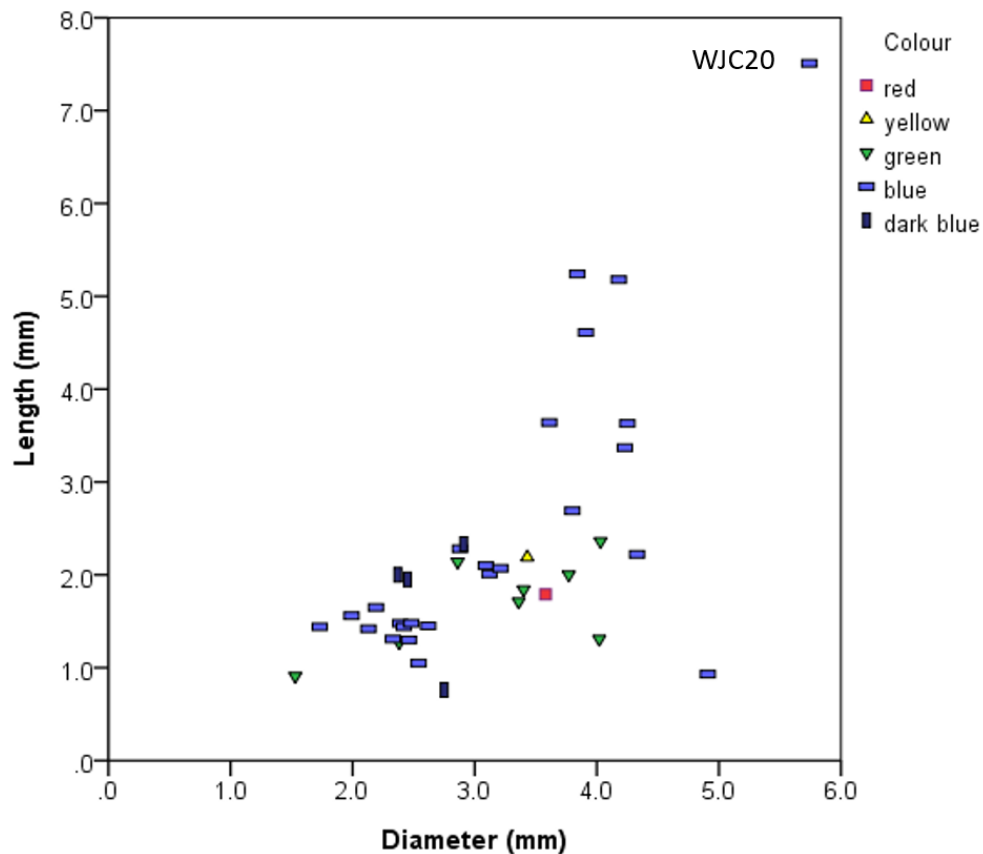
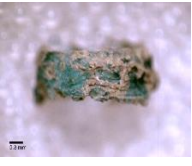


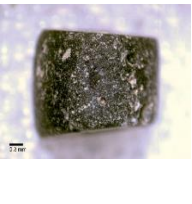
Figure 7.12: The size of all Iron Age glass beads from Wujiancuo.

Six groups of glass beads have been identified based on their colours and manufacturing methods (Table 7.8). Three samples, WJC19, WJC20 and WJC28, cannot be assigned to any of the defined typological groups. The different size and shape of WJC20 indicates that this sample

does not belong to the same group as the other blue beads from Wujiancuo. Figure 7.12 shows that WJC20 (length = 7.51, diameter = 5.74) is obviously larger than the other beads. The colour of this sample is nearly turquoise blue, which is different from the other azure blue beads from Wujiancuo. Also, the manufacturing methods of WJC19 and WJC28 cannot be determined through microscopic observation, and therefore it is not possible to determine their typological classification.

Table 7.8: The groups and manufacturing methods of all Iron Age beads from Wujiancuo (WJC).

Group (n ¹)	Colour	Shape	Manufacturing method	End roundness (n ¹)	Image
WJC-R1 (1)	Red.	Short tubular.	Drawn.	Tapered.	
	WJC47.				
WJC-Y1 (1)	Yellow.	Short tubular.	Drawn.	Tapered.	
	WJC59.				
WJC-G1 (8)	Green.	Short tubular or oblate.	Drawn.	Round (2) or tapered (6).	
	WJC13, WJC14, WJC17, WJC23, WJC44, WJC45, WJC46, WJC57.				
WJC-B1 (11)	Blue.	Short tubular or long tubular.	Drawn.	Round (5) or tapered (6).	
	WJC12, WJC15, WJC16, WJC18, WJC21, WJC22, WJC24, WJC25, WJC26, WJC27, WJC38.				
WJC-B2 (11)	Blue.	Short tubular.	Wound?	Tapered.	
	WJC39, WJC48, WJC49, WJC50, WJC51, WJC52, WJC53, WJC54, WJC55, WJC56, WJC58.				

Group (n ¹)	Colour	Shape	Manufacturing method	End roundness (n ¹)	Image
WJC-DB1 (4)	Dark blue.	Short tubular.	Drawn.	Round (1) or tapered (3).	
					WJC40, WJC41, WJC42, WJC43.
No group (3)	Blue.	n/a	n/a	n/a	
					WJC19, WJC20, WJC28.

1: n = quantity.

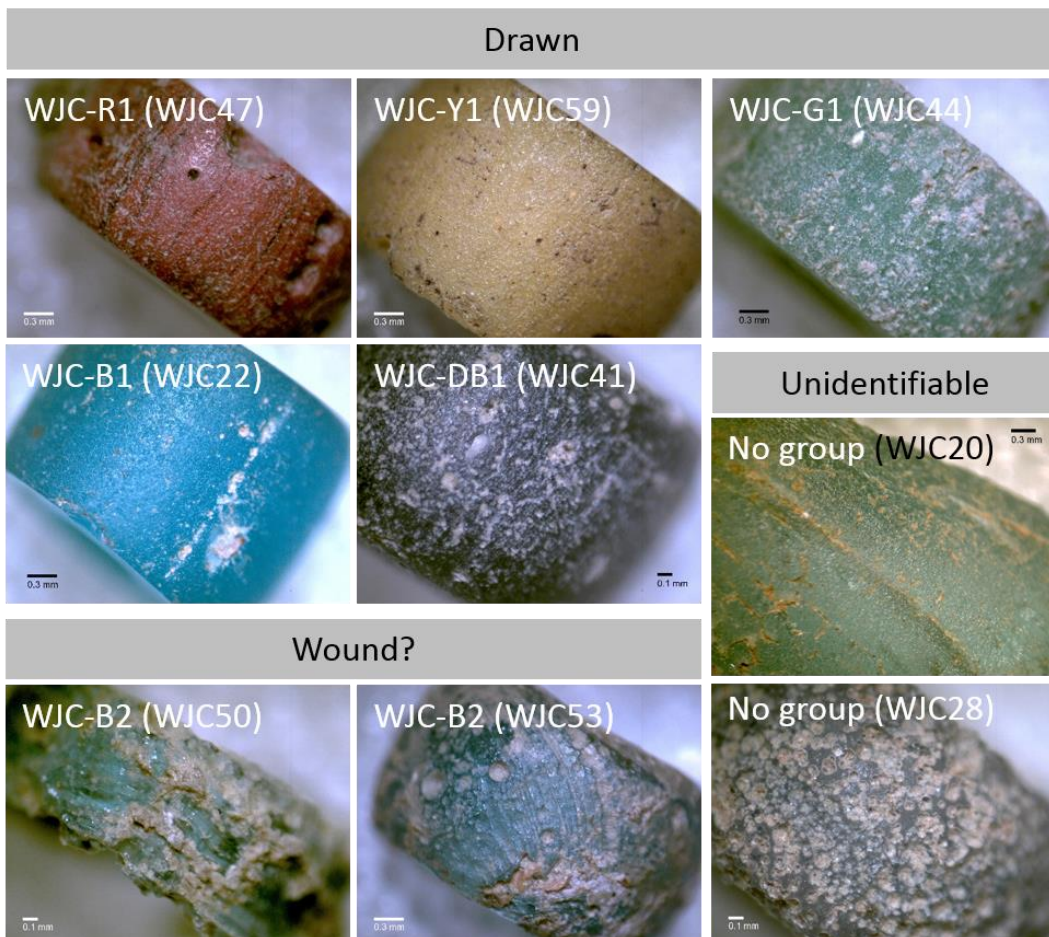


Figure 7.13: Optical microscopic observation showing the manufacturing methods for Wujiancuo beads.

Within the blue beads, two apparent groups (WJC-B1 and WJC-B2) can be observed. Glass beads of WJC-B1 group usually have a wall thickness of 0.5mm or less, and microscopic observation showing parallel fabric lines and bubbles indicates that these beads were made by drawn method (Figure 7.13). Glass beads similar to WJC-B1 are frequently reported in other contemporary Iron Age sites in Taiwan (e.g. Jiuxianglan, Daoye, Guishan and Xiliao). In terms of the WJC-B2 group, glass beads within this group are generally smaller, with a length between 1-2.2 mm and diameter between 2-3.2 mm. It is noteworthy that glass beads in the WJC-B2 group have extremely thin wall thicknesses of around 0.3mm or less. Microscopic observation suggests it is quite possible that the WJC-B2 group were wound-made, as the encircling fabric lines and bubbles can be seen from the bead surface.

The WJC-B2 type is only presently found at Wujiancuo. The identification of the wound method in the WJC-B2 group, together with the thin wall thickness, seems to indicate a similarity to the GS-B2 group at Guishan (see section 7.6). However, a closer investigation reveals that the WJC-B2 group generally has a thinner diameter than GS-B2 (> 0.3 mm), and the overall size of WJC-B2 is rather smaller than GS-B2 (length of 2.5-3.5 mm and diameter of 3.5-4.0 mm). Therefore, this result indicates that WJC-B2 and GS-B2 are different at the Wujiancuo and Guishan and may not be considered of the same typology.

7.10. Xiliao, southwestern Taiwan (6th-14th century AD)

The data relating to the Xiliao beads are from the published excavation report, and the analysis presented here is based on this description and the colour plates of 13 glass beads provided in the report (Chen and Cheng 2011; Liu 2011e). Unfortunately, no typological grouping can be made for Xiliao beads in this research, as this requires detailed investigation and measurement of the bead assemblages.

Figure 7.1 shows that the majority of beads are blue (38.7%, n = 24) and dark blue (19.4%, n=12), with small amounts of red (12.9%, n = 8), green (9.7%, n = 6) and yellow (6.5%, n = 4) beads. There are 8 beads described as ‘greenish blue’ or ‘bluish green’ in the excavation report. The lack of colour plates for these beads made it difficult to identify the precise colour, and therefore they are labelled as ‘blue or green’ in the pie chart. In comparison to the Daoye and Wujiancuo sites in southwestern Taiwan, a larger proportion of translucent dark blue beads have been unearthed from Xiliao.

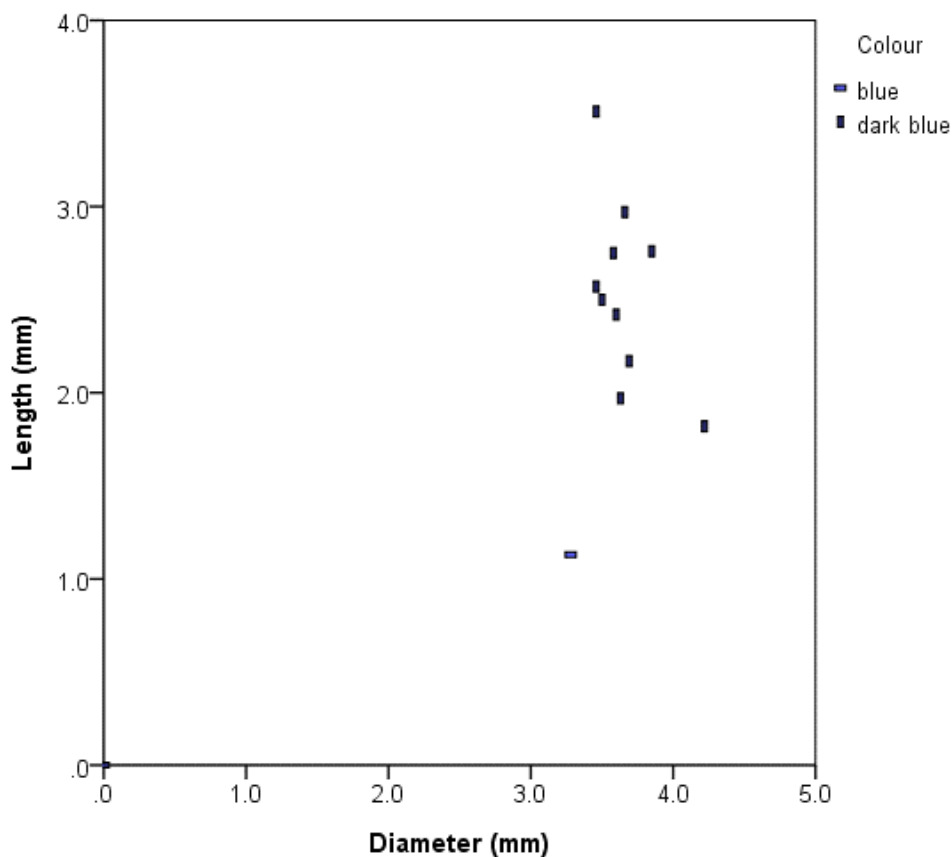


Figure 7.14: The size of glass beads from Xiliao. (Data collected from Chen and Cheng (2011).)

Figure 7.14 shows the size of 13 beads from the report. Together with the rough measurement from colour plates, the length of Xiliao beads are generally around 1-3 mm with a diameter of around 2-5 mm, which do not reveal distinct differences between these and the beads from Daoye and Wujiancuo. Based on the excavation report, most glass beads from Xiliao are short

tubular, with a tapered end.

7.11. Comparison of beads from Daoye, Wujiancuo and Xiliao

The material culture from Daoye, Wujiancuo and Xiliao all show the characteristics of the Niao Song Culture in southwestern Taiwan and are geographically close (Chapters 2.6, 2.7 and 2.8). However, the typological study here does not suggest close similarity of bead shapes from the three sites. It is notable that a larger proportion of glass beads from Wujiancuo and Xiliao have tapered ends, in comparison to those from the adjacent Daoye site. The tapered end roundness probably suggests that these beads might be re-heated for less time or at a lower temperature, ground or polished to obtain less round edges, and therefore indicates the possibility of slightly different treatments of glass beadworking for some of the beads. Generally, glass beads from the earlier site Daoye (2nd-6th century AD) fit the typical shape of Indo-Pacific glass beads as from Guishan and Jiuxianglan. These Indo-Pacific beads can also be found at the later Wujiancuo site (5th-8th century AD), but with different degrees of end roundness. However, the WJC-B2 type from Wujiancuo is a style that does not resemble the typical Indo-Pacific beads. At Xiliao (6th-14th century AD), the shape of glass beads does not reveal much variation suggesting a common source, but glass beads of dark blue colour are not common in Indo-Pacific drawn beads. The different chronologies of Daoye, Wujiancuo and Xiliao may explain the differences in the types between bead assemblages, which probably suggests a temporal shift of bead shape in southwestern Taiwan, in association with different supply sources of glass beads at different times.

Table 7.9: A summary of comparing bead typology between Daoye, Wujiancuo and Xiliao.

Similar types
<ol style="list-style-type: none"> 1. At Daye and Wujiancuo, all similar to Indo-Pacific drawn beads, except for WJC-B2, but with different degrees of end roundness. 2. There may be similar Indo-Pacific beads from Xiliao, but the exact typology is unknown.
Unique types not found at other sites
Wujiancuo: WJC-B2.
Others
<p>The dark blue short tubular glass beads from Xiliao are not seen at Daoye and Wujiancuo. This is also not typical Indo-Pacific drawn bead.</p>

7.12. Summary

This chapter discusses the typology of glass beads from Kiwulan, Jiuxianglan, Guishan, Daoye, Wujiancuo, Shisanhang and Xiliao. Glass beads studied in this research are all monochrome beads without further decoration, but careful investigation has suggested the differentiation between sites/regions. Glass beads found at Kiwulan (northeastern Taiwan) and Shisanhang (northern Taiwan) show more similarities to each other compared to the beads from other study sites in this research, and many of the beads from these two sites are not currently found in other regions (e.g. LL02, LL04, LL08 and LL10 types at Kiwulan; Type 1-3, Type 3-3, Type 5, Type 6, Type 7, Type 11, Type 15 and Type 16 at Shisanhang). Some similar types can be found at Kiwulan and Shisanhang (e.g. the LL02 type at Kiwulan and Type 5/6/7 at Shisanhang; the LL05 type at Kiwulan and Type 9 at Shisanhang). In southwestern Taiwan, the dominance of short tubular shapes at Daoye, Wujiancuo and Xiliao can be seen through the pie charts shown

in Figure 7.15, and a higher proportion of short tubular beads with tapered ends are found at the Wujiancuo and Xiliao sites, compared to Daoye. For the Jiuxianglan (southeastern Taiwan) and Guishan (southern Taiwan) sites, the results suggest that more diverse types of beads can be found at Guishan than at Jiuxianglan, but generally the shapes of glass beads from Jiuxianglan show more similarity to Guishan than other sites in this research. Additionally, a higher proportion of oblate beads can be found at Jiuxianglan and Guishan than in the sites in southwestern Taiwan, as shown in Figure 7.15.

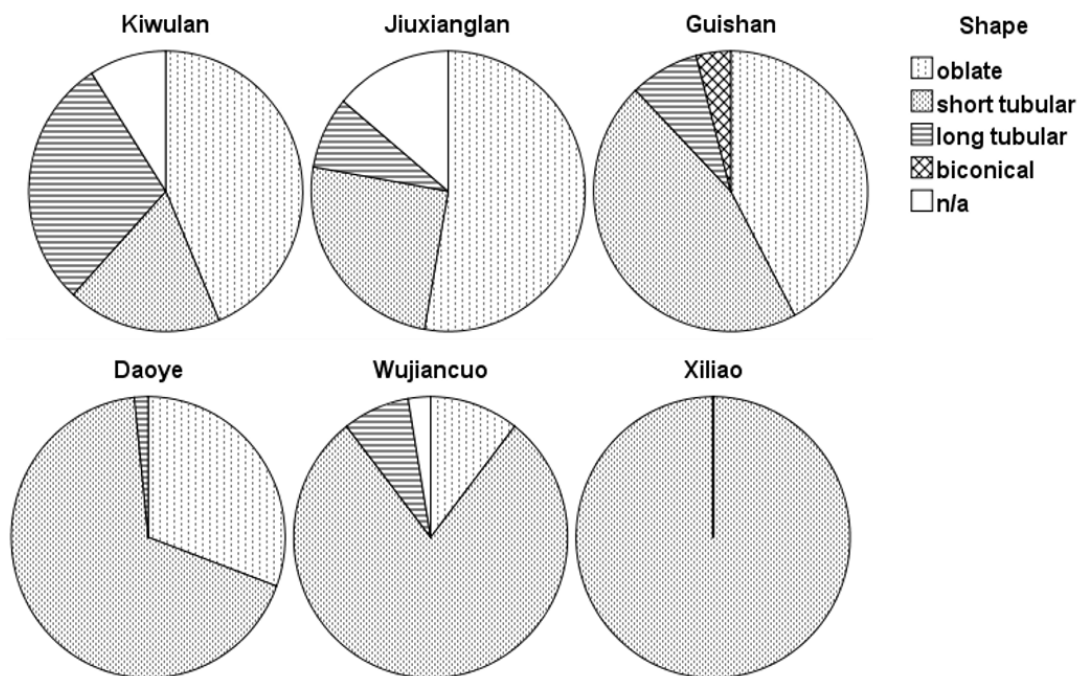


Figure 7.15: The proportion of bead shapes from each site.

In addition to the bead shapes, the bead colours also show regional differences (Figure 7.1). In northern and northeastern Taiwan, the dominance of orange, yellow, blue, and dark blue beads, together with the rather small percentage of red beads, is more significant than in other regions, and no green beads were found at Kiwulan and Shisanhang. In southwestern Taiwan, Daoye, Wujiancuo and Xiliao generally share more similarities of the colour distributions of the glass beads. Figure 7.1 shows that more green, blue and dark blue beads than red and yellow beads

are found in southwestern Taiwan, and no orange beads were reported from Daoye, Wujiancuo and Xiliao. In southeastern and southern Taiwan, Figure 7.1 shows that a higher percentage of red beads are found at Jiuxianglan and Guishan than other sites, and similar proportion of yellow, green and blue beads can also be seen at the two sites. This regional differentiation may be associated with the regional exchange network. Whether or not a similar pattern can be seen in the chemical composition will be explored in Chapters 8 and 9, and these results will be discussed in detail in Chapter 11.

Furthermore, the investigation of glass waste at Jiuxianglan reveals the use of the wound method for bead production, which is inconsistent with the majority of drawn beads at the same site. Whether this result suggests that the wound-made beads at Kiwulan, Guishan and Wujiancuo were produced at Jiuxianglan will be further investigated in Chapters 8 and 9 when the chemical composition and microstructure of this waste are examined.

However, it should be noted that a broad temporal scale is considered in this research, which has an effect on the interpretation of small scale differences within and between site(s). At present, it is not possible to narrow down the chronological interval within each site to understand any potential temporal shift of typology. It is hoped that, with future research, there will be a more detailed understanding of chronological transitions within specific site or culture and each site and its material culture will be more closely dated.

8. Results: chemical composition – part I: overview and m-Na-Al glass

8.1. Introduction

The results of the chemical compositions of the beads are divided into two chapters because of the complexity and number of chemical types observed. The beads from Kiwulan, Jiuxianglan, Daoye, Wujiancuo and Guishan are analysed in this research, while the data from Shisanhang and Xiliao are taken from the published excavation reports and interpreted alongside the new dataset. Considering the complexity of chemical and microstructural data, the results of the chemical analysis are discussed by chemical and colour groups rather than site by site. This chapter presents an overview of chemical groups of glass beads (section 8.2) and the findings which show the most predominant one glass composition found: m-Na-Al glass (section 8.3). The results of v-Na-Ca (plant ash) glass, other glasses and the summary are provided in Chapter 9. The full chemical analytical results are given in Appendix 2.

8.2. An overview of the chemical groups

Five chemical groups of glass beads have been identified in this research: m-Na-Al glass, v-Na-Ca glass (also known as plant ash glass), mineral soda lime silica glass (SLS glass), potash glass and lead silicate glass. The average base composition of the different chemical groups at each site is provided in Table 8.1. Here, the base composition includes the 7 major and minor elements (as oxides) in the glass (8 oxides in the lead silicate glass), normalised to 100%, in order to discuss the raw materials used for glass production without the influence from any intentionally added components such as colourants or opacifiers (Brill 1999: 9). A detailed

review of the chemical characteristics of each group and their potential raw materials is provided in Chapter 5. For m-Na-Al, v-Na-Ca and SLS glass, the amount of Na₂O (average 13-20%) demonstrates the use of soda as the flux in glass production. Figure 8.1 shows the bi-plot of Al₂O₃-(MgO+K₂O), and it can be seen clearly that m-Na-Al glass and v-Na-Ca glass are the two dominant chemical groups found here. Table 8.1 and Figure 8.1 show that m-Na-Al glass here generally contains greater than 5% Al₂O₃, less than 1% MgO and less than 3% K₂O. The high Al₂O₃ content in the m-Na-Al glass is associated with the use of granite sand (Dussubieux *et al.* 2010). The v-Na-Ca glass here generally contains more than 3% MgO and less than 3% Al₂O₃. The SLS glass contains less than 1% MgO and K₂O. In general, the lower amount of MgO (typically <1.5%) in m-Na-Al glass and SLS glass may suggest a mineral source of soda flux, while for v-Na-Ca glass, with MgO greater than 1.5%, may suggest the addition of soda from a vegetal source.

Table 8.1 and Figure 8.1 show that in the potash glass, the concentration of potash is higher than 15%, and MgO is less than 1.5%. This low amount of MgO in the potash glass may suggest that alkali was derived from a mineral source. The lead silicate glass seems to be clustered within v-Na-Ca glass with respect to MgO+K₂O in Figure 8.1, but the particularly high concentration of PbO (34.30% in the base composition, Table 8.1) shows it is different from the v-Na-Ca glass, a feature which cannot be seen clearly in the Al₂O₃-(MgO+K₂O) bi-plot. It should be mentioned that Shisahang and Xiliao samples were analysed in different labs (Chapter 6), so some chemical differences may reflect inter-lab comparability of data. Unfortunately, the original reports of Shisanhang and Xiliao data do not provide analytical information of any standard, which has hindered detailed comparison on the inter-lab comparability. Therefore, the discussion using Shisanhang and Xiliao data is carried out with caution in this thesis in order to avoid over-interpretation.

There is a different distribution of glass colours in each chemical group, in particular the m-Na-Al and v-Na-Ca glass. As shown in Figure 8.2, similar proportions of red, orange, yellow, green and blue colours are found in the m-Na-Al glass, while in v-Na-Ca glass, yellow, blue and dark blue colours dominate. Variable chemical and microstructural characteristics are found between colour groups and chemical groups, and the complexity and heterogeneity of glass is observed particularly in the m-Na-Al glass. This is discussed in more detail in section 8.3 and Chapter 9.

Table 8.1: The average base composition of each chemical group at Kiwulan, Shisanhang, Jiuxianglan, Guishan, Daoye, Wujiancuo and Xiliao.

Site (n) ¹	Artefact	SiO ₂ (%)	Al ₂ O ₃ (%)	Na ₂ O (%)	K ₂ O (%)	MgO (%)	CaO (%)	FeO (%)
<i>m-Na-Al glass</i>								
Kiwulan (9)	Bead	63.93±2.46	12.12±0.90	15.52±3.12	2.03±0.45	0.85±0.88	3.50±0.34	2.04±0.72
Shisanhang (20)	Bead	66.14±2.96	10.11±1.76	15.34±2.34	2.28±0.32	0.85±0.30	3.20±0.63	2.07±0.88
Jiuxianglan (35)	Bead	62.65±2.25	12.09±1.52	18.57±1.50	2.43±0.61	0.49±0.39	2.48±0.70	1.28±0.41
Jiuxianglan (5)	Glass waste	65.33±4.11	9.50±3.01	19.78±1.21	2.10±0.53	0.28±0.10	2.03±0.24	1.00±0.24
Guishan (54)	Bead	65.40±2.71	10.50±1.92	18.30±3.01	1.73±0.74	0.50±0.40	2.45±0.66	1.11±0.68
Daoye (8)	Bead	66.76±2.53	9.23±1.32	17.35±2.24	2.39±0.70	0.56±0.57	2.45±1.15	1.26±0.59
Wujiancuo (3)	Bead	68.95±2.76	8.27±2.16	16.73±1.11	2.37±1.01	0.25±0.14	2.26±0.98	1.18±0.48
Xiliao (2)	Bead	68.9±1.8	9.2±0.1	14.6±1.1	1.9±1.1	nd	4.1±0.5	1.4±1.4
<i>v-Na-Ca glass</i>								
Kiwulan (18)	Bead	66.81±1.35	2.39±0.49	15.51±0.88	2.89±0.34	4.23±0.95	7.14±1.11	1.03±2.86
Shisanhang (26)	Bead	67.53±2.03	1.78±0.52	16.10±1.30	3.04±0.63	4.53±1.01	5.89±1.11	1.13±0.85
Jiuxianglan (3)	Glass waste	63.62±2.47	2.98±1.36	18.04±2.14	2.75±0.14	4.65±1.19	6.69±1.93	1.27±0.44
Guishan (10)	Bead	67.40±1.23	3.02±0.18	18.55±2.13	1.74±0.72	3.16±0.46	5.36±1.06	0.77±0.63
Wujiancuo (1)	Bead	70.01	3.05	13.10	1.82	3.22	7.89	0.91
Xiliao (11)	Bead	68.6±1.2	3.0±0.7	13.9±0.8	3.3±0.7	4.2±0.6	5.8±0.4	1.2±0.2
<i>potash glass</i>								
Jiuxianglan (1)	Bead	80.99	1.90	0.44	15.05	0.18	0.99	0.45
Shisanhang (1)	Bead	67.06	1.61	2.67	18.77	1.12	7.96	0.80
<i>SLS glass</i>								
Guishan (1)	Bead	69.81	1.84	21.69	nd	0.36	5.41	0.90
Shisanhang (1)	Bead	71.43	2.09	15.36	0.50	0.62	8.22	1.79
<i>Lead silicate glass</i>								
Shisanhang (1) ²	Bead	44.79	2.07	9.23	1.92	2.74	3.39	0.96

1: n = sample quantity.

2: PbO = 34.30% in base composition.

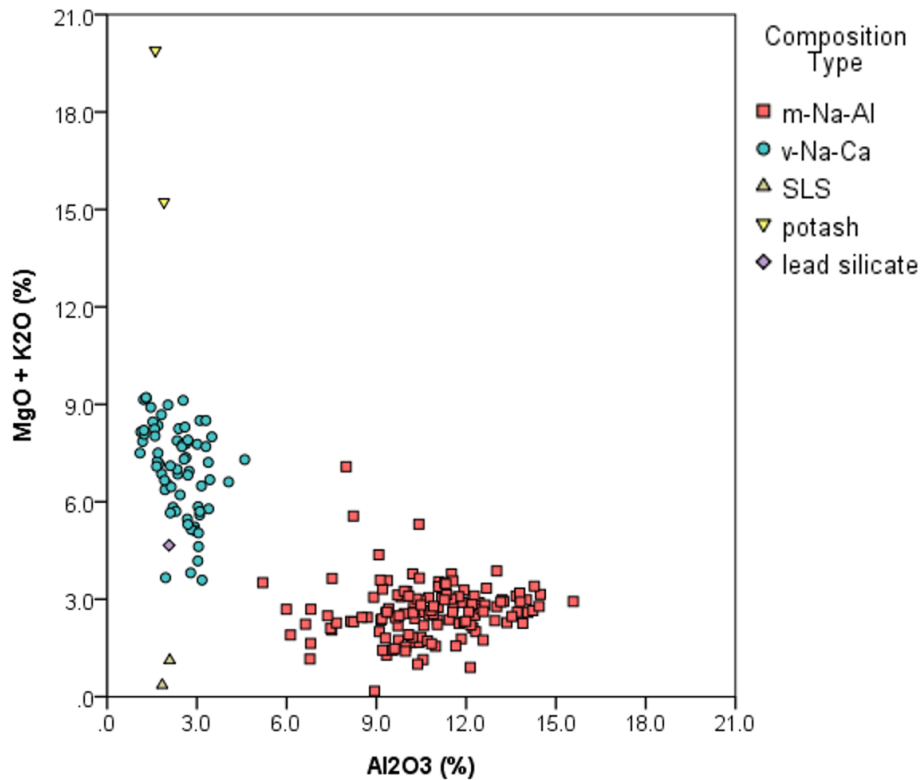


Figure 8.1: Al_2O_3 -($MgO+K_2O$) bi-plot showing the chemical groups of beads from Kiwulan, Shisanhang, Jiuxianglan, Guishan, Wujiancuo, Daoye and Xiliao (base compositions).

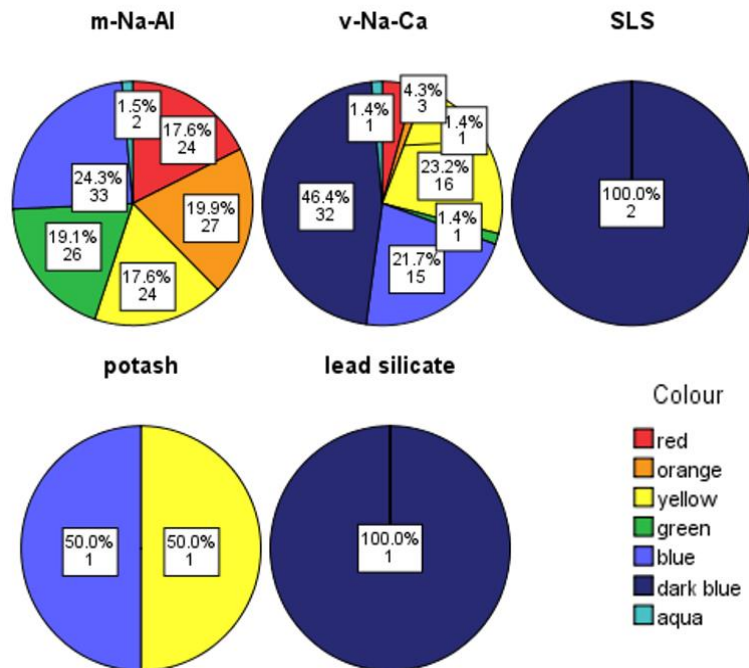


Figure 8.2: The distributions of colours in each chemical group for all the sites studied.

8.3. M-Na-Al glass

8.3.1. Chemical composition related to the glass melt

8.3.1.1. The sub-groups

Five sub-groups of m-Na-Al glass have been reported by Dussubieux *et al.* (2010) (Table 8.2, Chapter 5.2.1). In this research, it is found that the m-Na-Al glass shows an average CaO concentration of around 2-3%, which suggests a similarity to the m-Na-Al 1, m-Na-Al 2 and m-Na-Al 3 sub-groups reported by Dussubieux (Table 8.1 and Table 8.2). Considering the geographical and chronological distribution of these three reported sub-groups, the m-Na-Al glass identified in this research is more likely to belong to the m-Na-Al 1 and m-Na-Al 3 groups, in which Ba (barium), U (uranium) and Cs (caesium) are suggested to be diagnostic trace elements.

Further investigation has revealed that the concentration of Ba in the m-Na-Al glasses from Taiwan in this research is around 0.1% (1040ppm) on average, while U is generally around 8 ppm. This result indicates that the m-Na-Al glass may belong to the low-uranium-high-barium (lU-hBa) m-Na-Al 1 sub-group, which was widespread around the South China Sea for a relatively long period. Figure 8.3 shows a bi-plot of Ba-U in these analysed glasses and the average value of Ba and U in the reported m-Na-Al 1 and 3 sub-groups. A variable concentration of Ba from 0.04-0.25% and the U content below 20 ppm can be seen in the analysed glass, but generally most of the samples are clustered within the range of m-Na-Al 1 sub-group.

Table 8.2: Average base composition of the five sub-groups of m-Na-Al glass (Dussubieux et al. 2010).

	SiO ₂ (%)	Na ₂ O (%)	MgO (%)	Al ₂ O ₃ (%)	K ₂ O (%)	CaO (%)	FeO (%)	Regions and periods
mNA 1	63.5 ± 4.9	17.3 ± 3.5	0.9 ± 0.9	10.4 ± 2.2	2.9 ± 1.1	3.1 ± 1.6	2.1 ± 1.4	South Asia-Sri Lanka Southeast Asia 4 th c. BC-5 th c. AD 4 th c. BC-10 th c. AD
mNA 2	63.6 ± 3.9	18.5 ± 2.7	1.2 ± 1.5	7.7 ± 1.8	2.4 ± 0.9	3.5 ± 0.9	3.2 ± 1.2	Africa West coast of India 9 th -19 th c. AD
mNA 3	67.9 ± 2.4	14.9 ± 2.3	1.3 ± 0.2	7.3 ± 0.7	3.3 ± 1.0	3.0 ± 1.0	2.4 ± 1.2	Southeast Asia 4 th -3 rd c. BC
mNA 4	67.2 ± 3.4	17.8 ± 2.1	1.4 ± 0.4	7.4 ± 1.2	2.5 ± 0.06	0.8 ± 0.2	3.2 ± 2.6	Southeast Asia Kenya 14 th -19 th c. AD
mNA 5	62.3 ± 1.7	17.1 ± 1.2	1.6 ± 0.2	10.0 ± 0.8	1.4 ± 0.3	5.0 ± 0.6	2.3 ± 0.6	Turkey 12 th -14 th c. AD

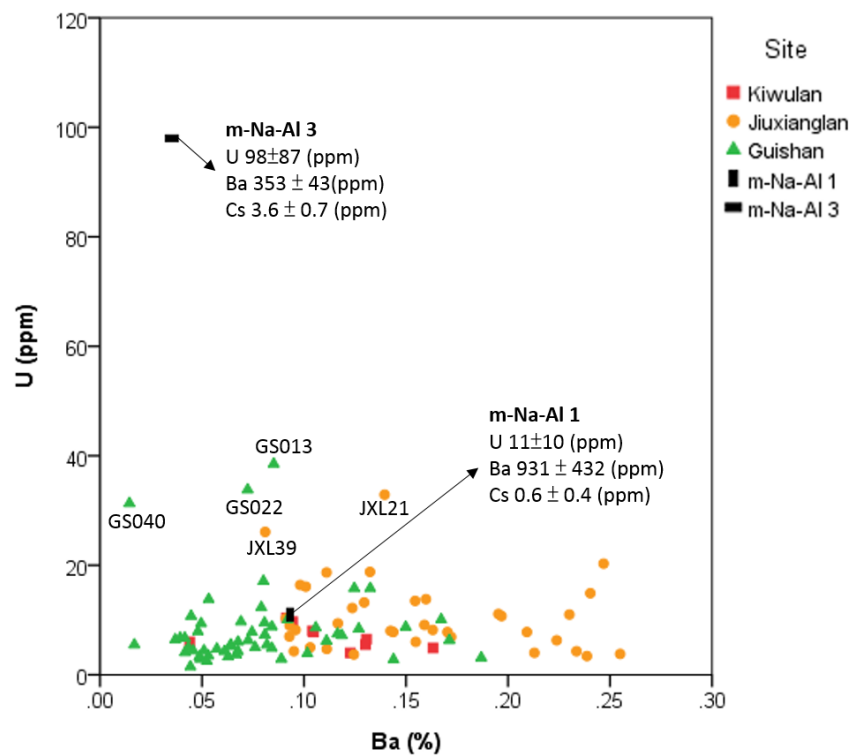


Figure 8.3: The Ba-U bi-plot of m-Na-Al glass.

Samples JXL21, JXL39, GS013, GS022 and GS040 show slightly higher U and in some cases lower Ba in comparison to other samples. Closer examination confirms that JXL21, JXL39, GS013 and GS022 also belong to the m-Na-Al 1 group based on the Cs content. The reported concentration of Cs is around 4 ppm in m-Na-Al 3, while in m-Na-Al 1 it generally averages less than 1 ppm. The low concentration of Cs in JXL21 (<LLD), JXL39 (<1 ppm), GS013 (<1 ppm) and GS022 (~1 ppm) indicates that that the four samples are m-Na-Al 1.

GS040 is more difficult to place within a group, as the concentration of Cs (~3 ppm) is higher than the typical m-Na-Al 1 glass. Also the base composition of Al₂O₃ (5%) is lower and MgO (1.3%) is slightly higher, and smaller amounts of Sr (strontium, 60 ppm) and Zr (zirconium, 63 ppm) are found in GS040 compared to the typical m-Na-Al 1 glass (Sr 373±145 ppm, Zr 561±420 ppm). These latter two elements are also slightly lower than those in the m-Na-Al 3 glass (Sr 132±31 ppm, Zr 193±27 ppm). Although the trace elemental pattern of U, Cs, Sr and Zr seem to fall into the low end of m-Na-Al 3 glass, the accepted date of m-Na-Al 3 glasses (4th-3rd century BC) is earlier than the date of Guishan (late 1st millennium AD) where GS040 was found. In addition, no yellow beads like that of GS040 made of m-Na-Al 3 glass have previously been reported (Dussubieux *et al.* 2010; Lankton and Dussubieux 2013). This makes it difficult to assign GS040 to any known sub-group of m-Na-Al glass.

It is noted that, although Figure 8.3 would suggest the separation of samples from Jiuxianglan and Guishan based on Ba contents, a closer examination reveals that the variable Ba contents may be associated with particular colours in some cases (more details in section 8.3.1.5). Therefore, the Ba contents of the Jiuxianglan and Guishan samples may not explicitly indicate different provenances for the glasses from the two sites.

8.3.1.2. The MgO-FeO and MgO-CaO correlation

It has been reported that in the m-Na-Al 1 group, the red and orange glasses generally contain greater concentrations of MgO, FeO and CaO compared to the blue glass, and clear positive correlations between MgO, FeO and CaO can be observed particularly in the orange glass (Dussubieux 2001: 115-118; Dussubieux *et al.* 2010). Similarly, in this research, greater concentrations of MgO, FeO and CaO can also be found in the red and orange glasses, and generally the blue and aqua glasses contain the lowest values of MgO, FeO and CaO (Figure 8.4 and Figure 8.5). However, the results suggest that the positive correlation between MgO, CaO and FeO is not clear in the red and orange glasses.

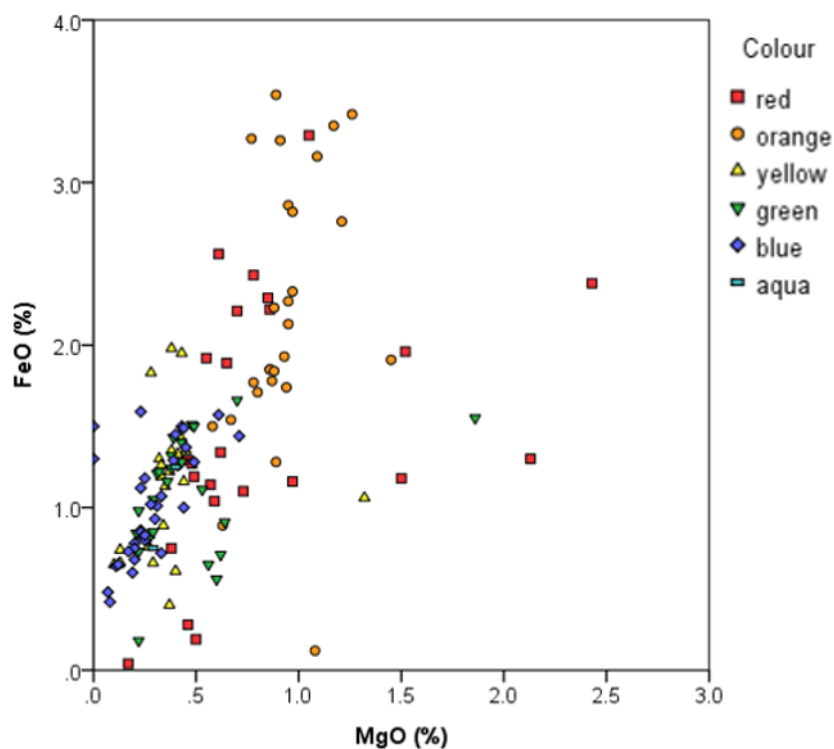


Figure 8.4: The MgO-FeO bi-plot of m-Na-Al glass by colour.

The bi-plots of MgO-FeO and MgO-CaO are shown in Figure 8.4 and Figure 8.5, respectively.

In the bi-plot of MgO-FeO, there is no strong correlation between MgO and FeO in the red

glass ($R^2 = 0.140$) and orange glass ($R^2 = 0.113$). Similarly, in the bi-plot of MgO-CaO, the R^2 value of 0.256 and 0.209 respectively in the red and orange glass indicates a weak correlation of MgO and CaO. These results do not match the strong positive correlation between MgO, FeO and CaO identified in Dussubieux (2001: 115-118).

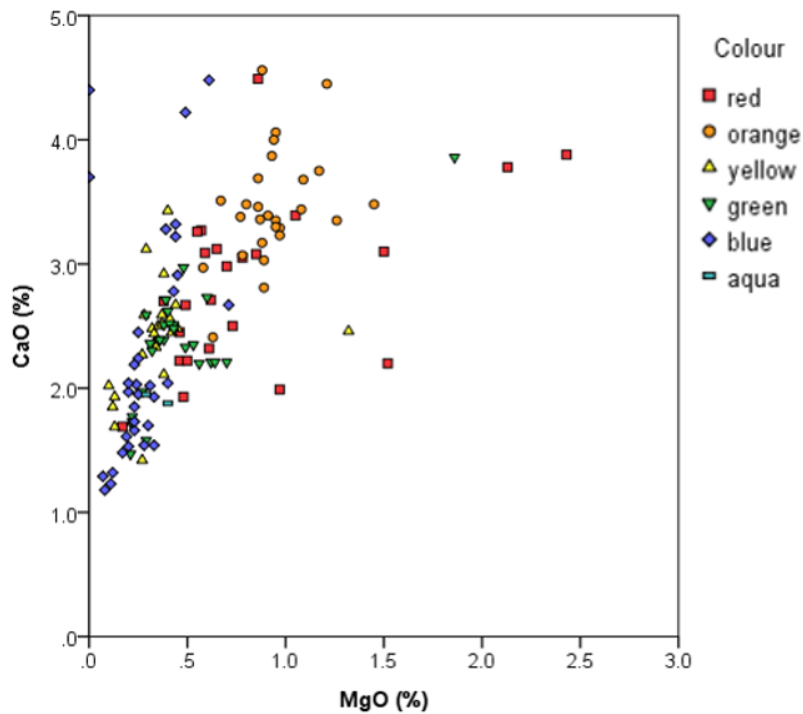


Figure 8.5: The MgO-CaO bi-plot of *m-Na-Al* glass by colour.

The enrichment of MgO, FeO and CaO in the orange and red glass had been tentatively attributed to the intentional introduction of a raw material containing iron and apatite, where Fe is thought to be used as reducing agent in the production of red and orange glasses (Dussubieux 2001: 155-156; Dussubieux *et al.* 2010: 1650). This may be possible in some cases, but the microstructure of the red and orange glass and the variable concentration of elements such as Pb (lead), Sn (tin), Zn (zinc), Ni (nickel) and Co (cobalt) in the red and orange glasses suggest that the production of these colours may be more complicated than previously assumed (sections 8.3.2.2 and 8.3.2.3). Overall, these results demonstrate that the relationship between

MgO, FeO and CaO is complicated and cannot be associated with a single type or source of raw material based on our current understanding of m-Na-Al glass.

8.3.1.3. The Fe, Ti, Sc, V and Nb relationship

Ti (titanium), Sc (scandium), V (vanadium) and in some cases Fe in glass are likely to be introduced from a sand source, and a correlation between these elements would probably confirm this assumption (Wedepohl *et al.* 2011).

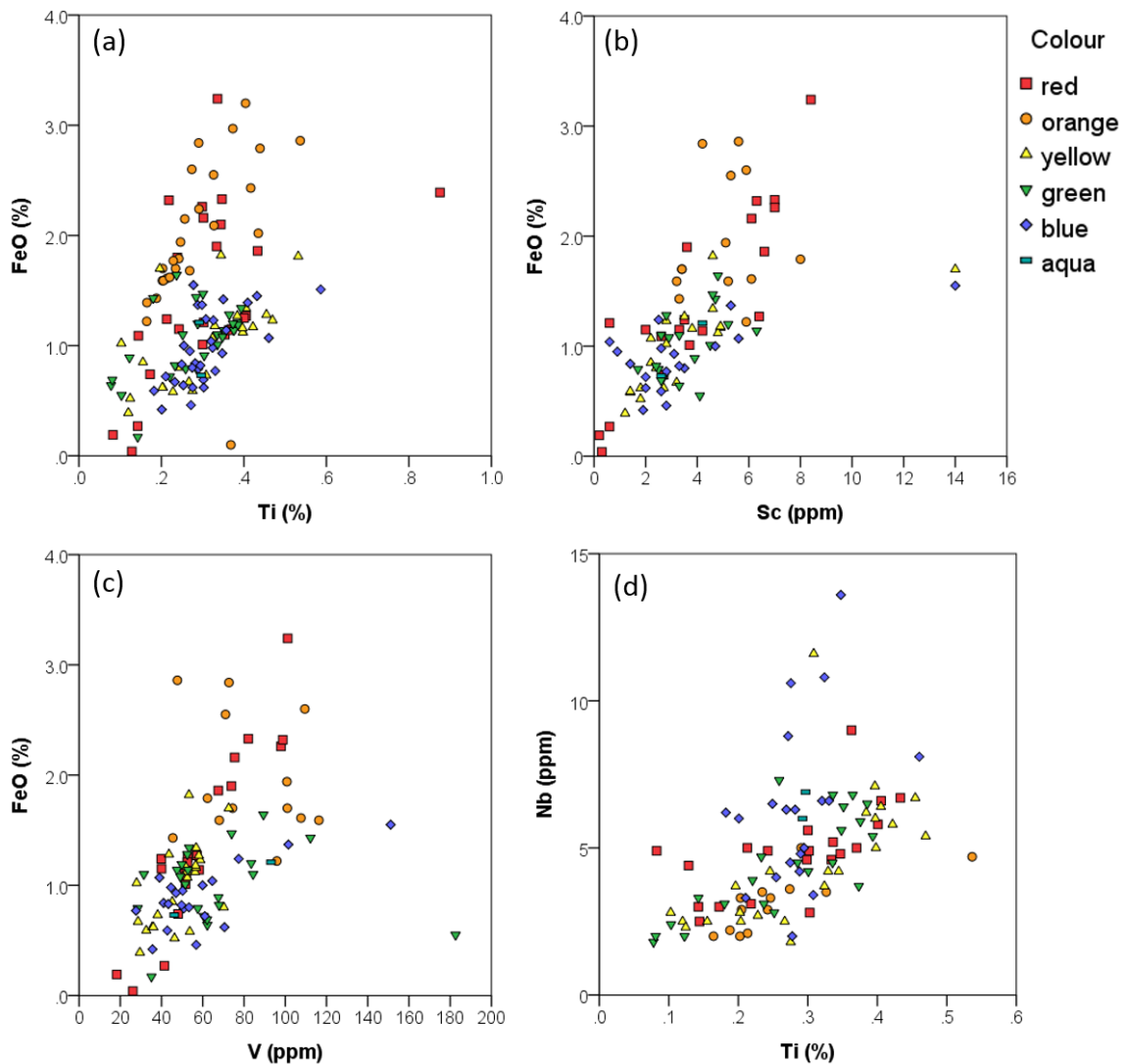


Figure 8.6: The bi-plots of (a) Ti-FeO, (b) Sc-FeO, (c) V-FeO and (d) Ti-Nb of m-Na-Al glass.

The bi-plots of Ti-FeO, Sc-FeO and V-FeO are shown in Figure 8.6 (a), (b) and (c). A Sc content lower than 8 ppm and a V content between 20-120 ppm generally match concentrations seen in granitic sands (Mielke 1979). In these glasses, generally elevated FeO is in association with increasing Ti, Sc and V. In the red and orange glasses, overall higher contents of FeO (> 1%), Sc (> 4 ppm) and V (> 50 ppm) can be observed compared to the other colours of glass (Figure 8.6 (b) and (c)), but the content of Ti does not show differences between colour groups (Figure 8.6 (a)). In most cases, Sc and V may be introduced from an Fe-bearing ingredient (associated with sands). Ti may be introduced with Fe as well, but the different Ti-FeO relationship between colour groups (Figure 8.6 (a)) may suggest potentially different raw materials or recipes containing Fe and Ti for producing different colours of glass.

In Figure 8.6 (d), an elevated level of Nb (niobium), generally higher than 6 ppm, is found in most blue and aqua glasses. Nb may be associated with the Ti-bearing mineral (e.g. titanite or Fe-Ti oxide), and this result may suggest a different sand source (or other raw material) used for the production of blue glass. Together with the Ti-FeO bi-plot (Figure 8.6 (a)), this may indicate that the sand used for producing the blue glass has more rutile (Rehren 2016, *pers. comm.*).

The variable contents of FeO, Ti, Sc, V and Nb and their relationships between different colours reveals the complexity and heterogeneity of the sand, or other raw materials, used for the production of m-Na-Al glass. It is rather difficult at this stage to know the explicit reasons for these variations, as this would need a better understanding on the source of sand and flux (therefore the glass melt) used in glass production. In addition, the variation seen between colour groups probably also indicates that a certain degree of compositional difference can be contributed from the addition of colourants, and this also requires more investigation in terms of the colouring of m-Na-Al glass.

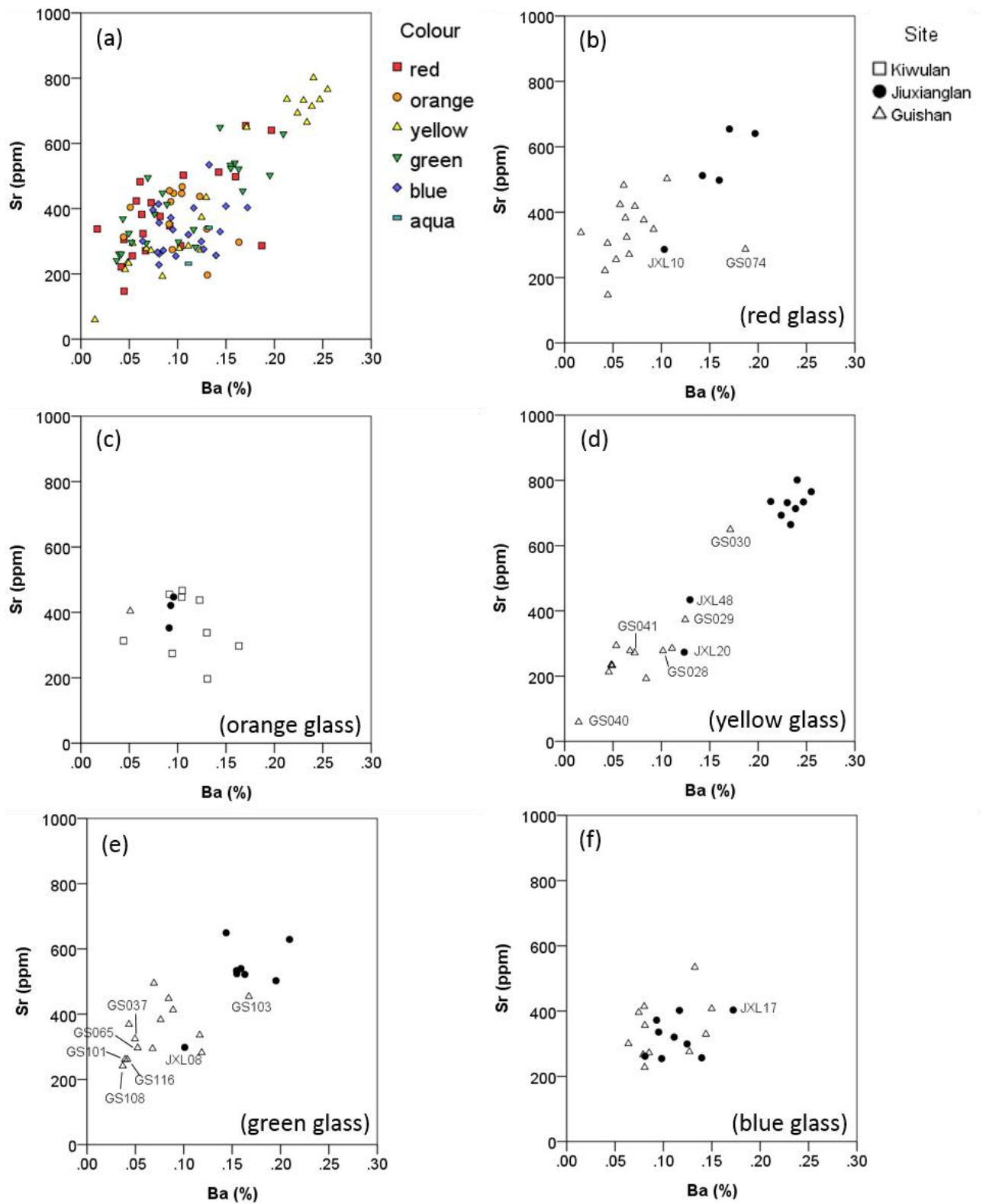


Figure 8.7: The Ba-Sr bi-plots of *m*-Na-Al glass.

8.3.1.4. The Zr-Hf relationship

The strong positive correlation between Zr (zirconium) and Hf (hafnium) ($R^2 = 0.860$) is found in all colours of glass. Zr is commonly present in zircon ($ZrSiO_4$) in granitic sand, and occurs with Hf. The Zr/Hf ratio of these samples generally ranges from 30-60, suggesting that zircon is from granitic sources (Wang *et al.* 2010). Furthermore, the presence of un-melted zircon is frequently identified in the m-Na-Al glass across all sites through microstructural analysis (see section 8.3.2.1).

8.3.1.5. The Ba-Sr relationship

Figure 8.3 has shown that some m-Na-Al glass contains a higher Ba content, and a closer look reveals that these Ba-rich samples are restricted to only some samples (mostly yellow and green glass, but a few blue and red glass). In these glasses, the Ba is associated with a higher concentration of Sr (Figure 8.7) when Ba is higher than 0.15% and Sr above 550 ppm.

It can be seen in Figure 8.7 (a) that lower Ba and Sr values are found in the orange glass, aqua glass and most of the blue glass. There is no differentiation of Ba and Sr content in the orange and blue glass from different sites (Figure 8.7 (c) and (f)). However, most yellow, green, and red glasses from Jiuxianglan contain more Ba and Sr in comparison to samples from Guishan (Figure 8.7 (b), (d) and (e)), which may suggest the potential different sources of glass beads from Jiuxianglan and Guishan.

In the red and green beads, differences can be seen between Jiuxianglan and Guishan samples. The red glass JXL10 is the only red sample from Jiuxianglan that shows low Ba and Sr contents, clustering with most samples from Guishan, while the red sample GS074 has a higher

concentration of Ba in comparison to other Guishan samples (Figure 8.7 (a)). Figure 8.7 (e) also shows that most Jiuxianglan green samples, excluding JXL08, contain higher Ba and Sr contents than the green samples from Guishan (except GS103). It is also noted that, within the Guishan green bead assemblage, the lowest Ba and Sr contents are found in the samples of the GS-G2 typological group (GS037, GS065, GS101, GS108 and GS116) (Figure 8.7 (e)).

Different Ba-Sr contents can also be seen between the yellow glass from Jiuxianglan and Guishan. The samples from Jiuxianglan contain a high concentration of Ba and Sr (except JXL20 and JXL48), and one sample GS030 from Guishan has high Ba and Sr contents (Figure 8.7 (d)). At Guishan, GS028, GS029 and GS041 belong to the GS-Y2 typological group. They have moderate Ba and Sr contents at similar levels to JXL20 and JXL48, and are slightly higher than most yellow glass of GS-Y1 style from Guishan.

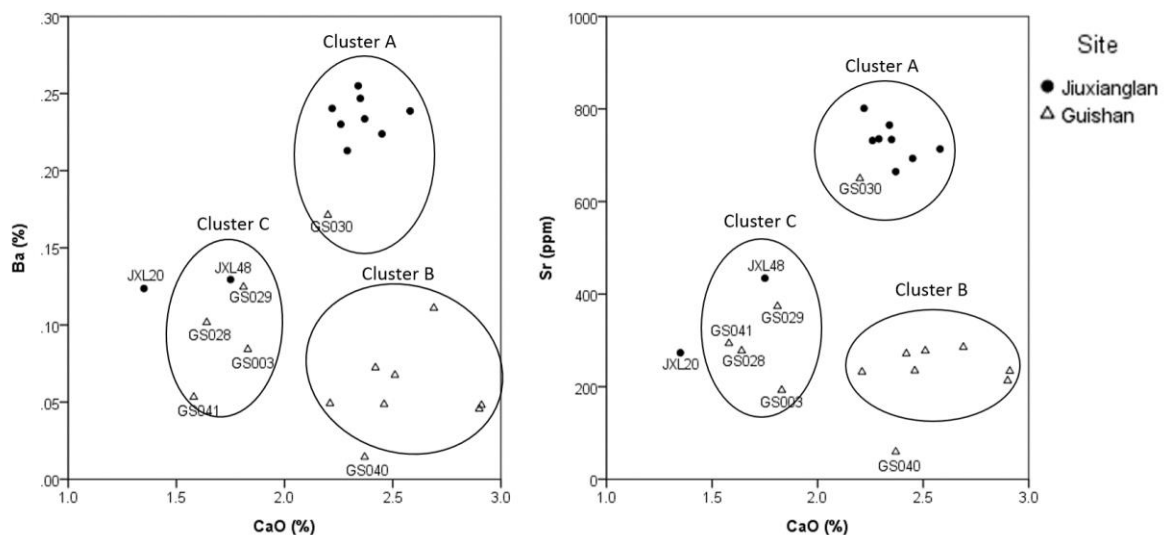


Figure 8.8: The CaO-Ba and CaO-Sr bi-plots of yellow m-Na-Al glass.

A clearer grouping of the yellow glass can be seen from the CaO-Ba and CaO-Sr bi-plots shown in Figure 8.8. Here, cluster A (high CaO, high Ba and high Sr) contains predominantly Jiuxianglan samples and one Guishan sample (GS030), cluster B (high CaO, low Ba and low

Sr) contains mostly Guishan samples belonging to the GS-Y1 typological group (excluding GS030 and GS040), and cluster C (low CaO, low Ba and low Sr) contains the Guishan samples of the GS-Y2 typological group and one sample (JXL48) from Jiuxianglan. JXL20 and GS040 are regarded as outliers, as the elemental pattern is not always consistent with a particular cluster. Although the elevated CaO-Ba and CaO-Sr relationship in cluster A and cluster C and the level of Sr at a few hundred ppm (Freestone *et al.* 2003a) might suggest sands containing carbonate rocks, the Ba content in these samples is much higher than that in carbonate rocks (average 100 ppm) (Mielke 1979) and a CaO/Sr ratio lower than 122 does not suggest an additionally introduced calcareous source of limestone (Wedepohl *et al.* 2011: 96-97).

There are two possible reasons for the enrichment of Ba and Sr in the m-Na-Al glass: (1) Some Ba and Sr in the m-Na-Al glass may be introduced as impurities from an impure granitic sand – e.g. an average range of 100-440 ppm for Sr and 420-840 ppm for Ba are reported in granitic rocks (Mielke 1979). Some granitic sands which are rich in minerals such as plagioclase may introduce more Ba and Sr. However, plagioclase will contribute only a few hundred ppm into the bulk composition (Iizuka 2016, *pers. comm.*). (2) Ba and Sr may be attributed to some Pb-bearing ingredients which also contain Ba and Sr. The red, green and yellow glasses rich in Ba and Sr generally contain greater concentrations of PbO (less distinct in the red glass). Although this association can probably be attributed to some Pb²⁺ substitution for Ca²⁺ in plagioclase, there is no clear relationship between the substitution (Heier 1962). Alternatively, sulphidic lead ores (galena, PbS) often accompany the precipitation of barite (BaSO₄) and/or celestine (SrSO₄) (Iizuka 2016, *pers. comm.*) and Sr²⁺ can sometimes substitute for Ba²⁺ in barite.

Lead tin oxide is often used as colourant in both yellow and green glass (see 8.3.2.5 and 8.3.2.6), and a strong positive Ba-Sr correlation in yellow and green glass can be seen in Figure 8.7 (d) and (e) ($R^2 = 0.935$ in yellow glass and 0.622 in green glass). Therefore, one possible

explanation for the higher Ba and Sr content in yellow and green glass may be the Pb-containing raw materials. For the red, blue and again green glass coloured by copper, it is possible that Ba is also associated with copper due to the co-occurrence of barite in copper and/or lead deposit, and in this research barite is found in one blue and one green glass from Jiuxianglan (see sections 8.3.2.4 and 8.3.2.6).

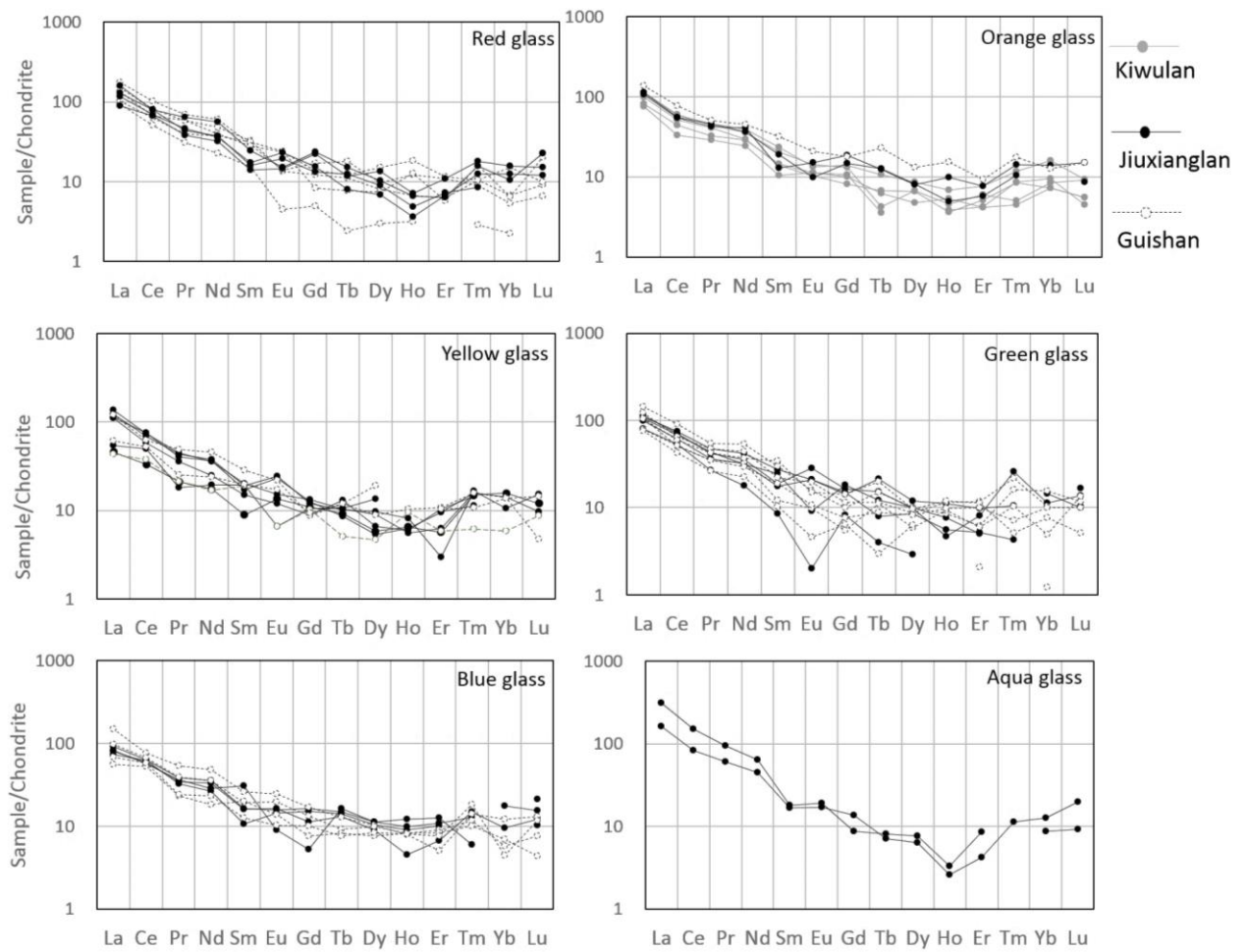


Figure 8.9: Some examples of the chondrite normalisation of the rare earth elemental pattern in the red, orange, yellow, green and blue glass. (Chondrite value using McDonough and Sun (1995).)

8.3.1.6. The rare earth elements

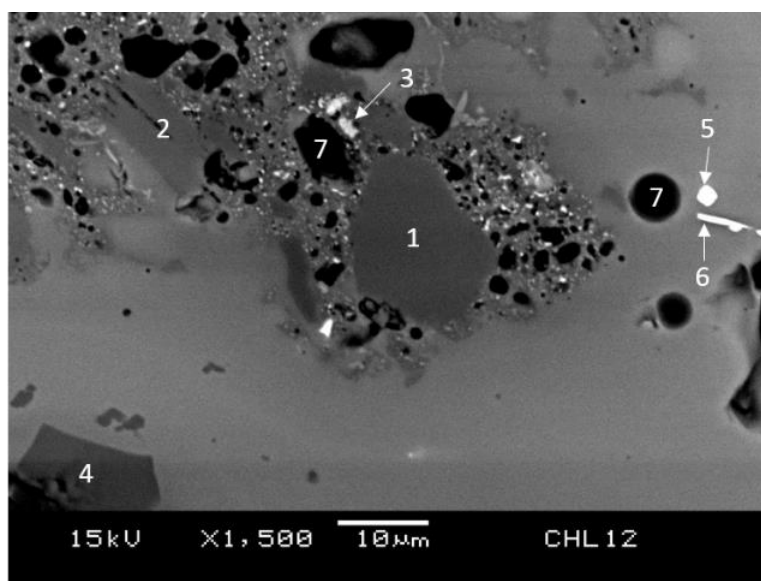
The rare earth element (REE) values have been normalised to chondrite values (chondrite data from McDonough and Sun (1995)) (Figure 8.9). Generally, a moderate enrichment of light rare earth elements (LREE) over heavy rare earth elements (HREE) can be seen, although a fluctuating level of HREE is also observed. The existence of heavy minerals in the sand, such as zircon, may result in an increased HREE concentration in the glass (Brems and Degryse 2014: 71). In the orange glass, a slightly lower value of HREE is found in samples from Kiwulan compared to those from Jiuxianglan and Guishan, but no distinct differentiation can be seen in the red, yellow, green and blue glass. A variable Eu anomaly is seen in all colours (Figure 8.9). The slight positive Eu anomaly may suggest the use of a plagioclase-rich sand (Wedepohl *et al.* 2011). Overall, this result, together with the fluctuating HREE concentration, indicates a variable mineral component in the sand.

8.3.2. Microstructure and colourant

8.3.2.1. The glass matrix

The microstructural analysis of m-Na-Al glass frequently shows the remains of undissolved minerals. For example, in Figure 8.10, plagioclase, alkali feldspar, Fe-Ti oxide minerals and voids/bubbles (labels 1-3 and 7) in the glass matrix can be seen. It also shows newly formed crystals precipitated from the glass matrix (Figure 8.10, label 4) or those related to the colouring (Figure 8.10, labels 5 and 6). These mineral residues are introduced mainly from the sand, suggesting the sand is relatively impure and variable in composition. These mineral remains, in particular the feldspar, suggest a low melting temperature for glassmaking. This is consistent with the results seen in the $\text{Na}_2\text{O}-\text{Al}_2\text{O}_3-\text{SiO}_2$ ternary phase diagram (Figure 8.11), where it can

be seen that most samples fall into the albite region, within a temperature range of 800-1000°C. This is supported by ethnographic studies of glassmaking at Jalesar in northern India, where m-Na-Al glass is produced at a temperature under 900°C (Sode and Kock 2001). The low melting temperature alongside an alumina-rich matrix leads to a higher viscosity of m-Na-Al glass, and therefore bubbles are difficult to remove and mineral residues remain un-melted in the glass which can be observed microscopically.



1: plagioclase. 2: alkali feldspar. 3: Fe-Ti oxide. 4: sodalite. 5: lead tin oxide. 6: SnO₂. 7: voids or bubbles. (JXL12, yellow.)

Figure 8.10: An example of mineral relics in the m-Na-Al glass (JXL12).

Plagioclase and alkali feldspar are the most frequent mineral residues found in the m-Na-Al glass (Figure 8.12), and plagioclase is slightly more common than alkali feldspar. The SEM-EDS analysis further shows that most of the plagioclase and alkali feldspar show a solid solution, rich in sodium, that is close to the albite endmember. This shows that the sand used in making m-Na-Al glass is rich in plagioclase and alkali feldspar, and particularly abundant in soda. Furthermore, it indicates that the sand itself already contains some soda that can act as flux. However, some additional soda flux may still be necessary for glassmaking. In this research,

the atomic percent of the plagioclase identified is more consistent, generally with around 5-6% Na, 2-3% Ca, 10% Al, 21% Si and 61% O (Figure 8.12 (a)). However, a more variable atomic percent is found between Na and K in alkali feldspar, with a combined atomic percent of around 8% alkali, 8% Al, 23% Si and 61% O (Figure 8.12 (b)-(e)).

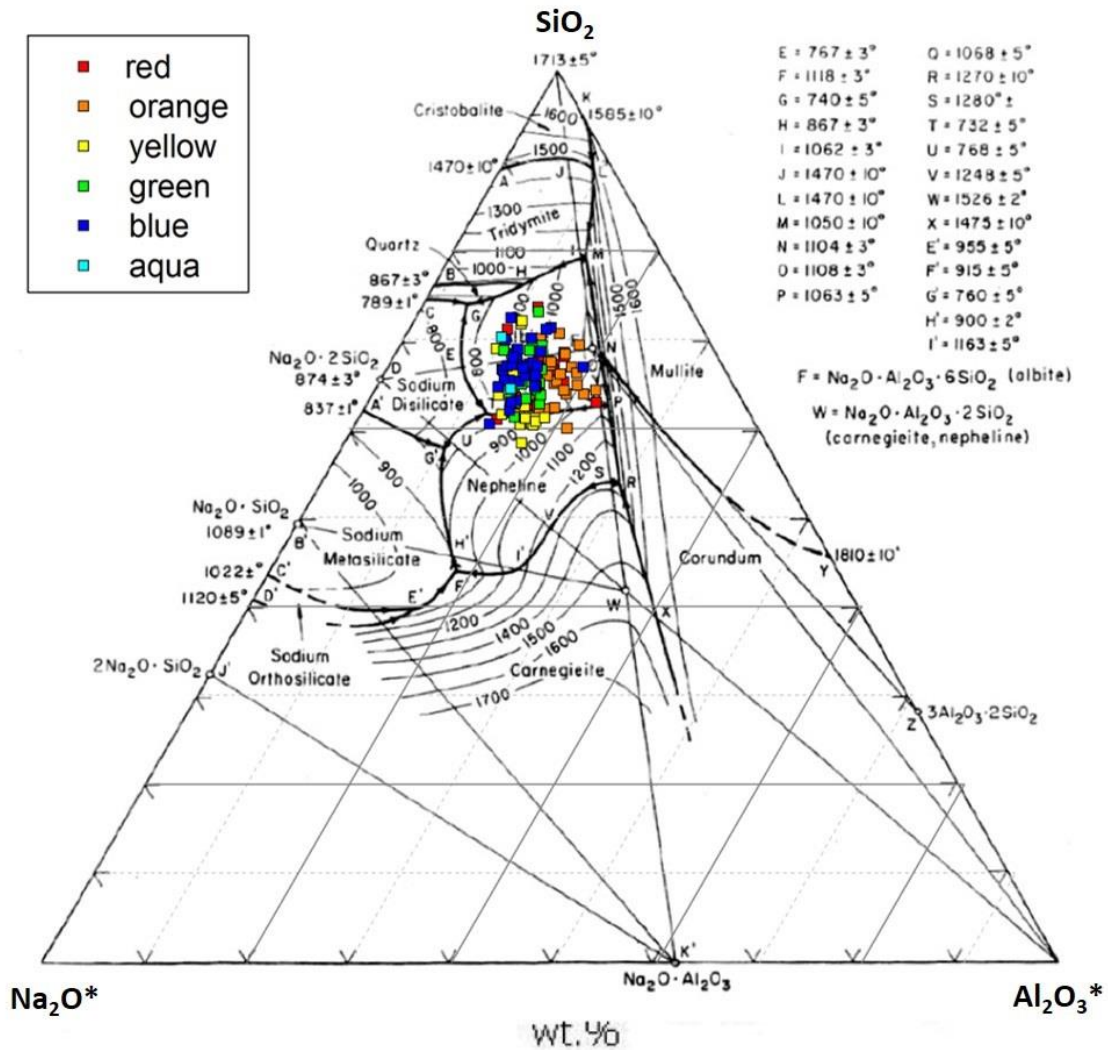


Figure 8.11: A plot of *m*-Na-Al glasses in the Na₂O-Al₂O₃-SiO₂ phase diagram. The oxides from the base composition are further reduced into three components (SiO₂, Al₂O₃* and Na₂O*) – the FeO, MgO and CaO are transmuted to Al₂O₃ (labelled Al₂O₃*), using a transmuting factor of 0.71, 1.26 and 0.91, respectively (Rehren 2016, pers. comm.). The K₂O is incorporated into Na₂O (labelled Na₂O*) transmuted by the factor of 0.66. The base phase diagram is from Levin and McMurdie (1959: 27).

In addition to the feldspar, some accessory minerals are observed which were also probably introduced from the sand. Zircon ($ZrSiO_4$) is often found in the m-Na-Al glass, with the atomic percent of 18% Zr, 15% Si and 67% O (Figure 8.13 (a)). Most of the zircon identified has an oval shape and sometimes round- or square-shaped zircon is also found. Occasionally large Fe-Ti oxide residues, possibly ilmenite, clustered near feldspar or quartz can be seen (Figure 8.13 (b)), and in sample GS103, the mineral kyanite, surrounded with sodalite crystals, is found (Figure 8.13 (c)).

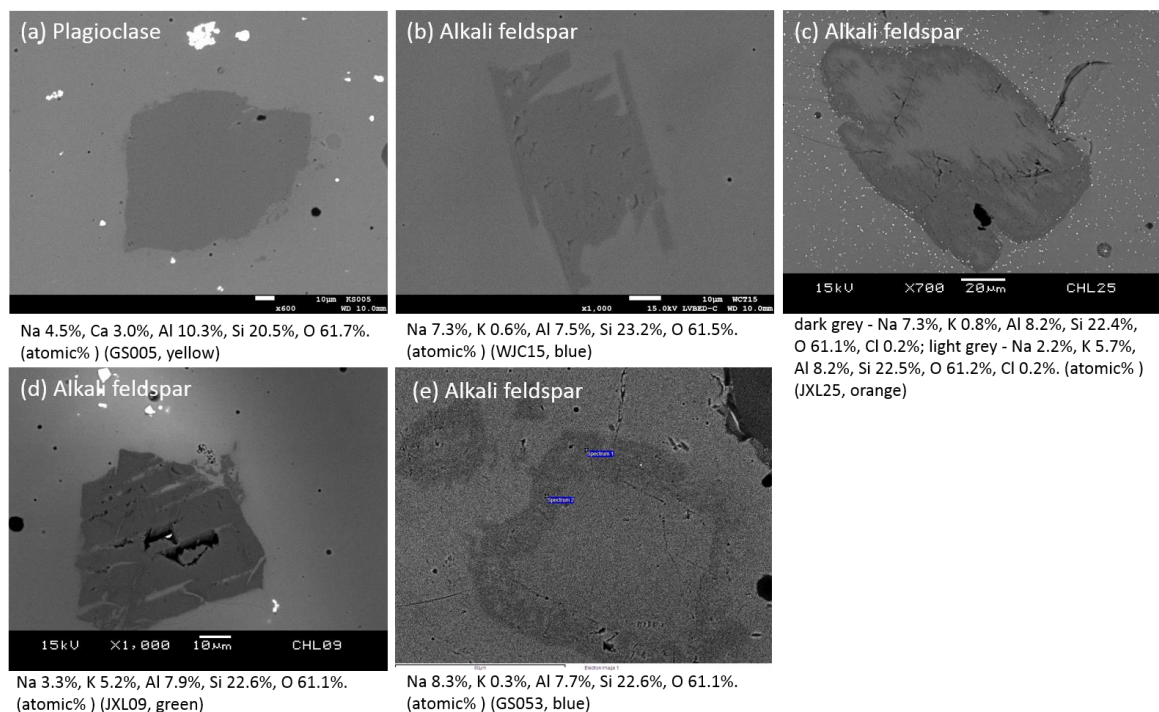


Figure 8.12: A series of feldspar relics identified in the m-Na-Al glass. ((a): GS005; (b): WJC15; (c): JXL25; (d): JXL09; (e): GS052.)

The microstructural analysis also reveals remnants of the colourants used. Generally, copper-based compounds are used to produce red, orange and blue glasses, lead tin oxide is found in yellow glass, and in the green glass both copper oxide and lead tin oxide have been identified. This is discussed in sections 8.3.2.2 to 8.3.2.7.

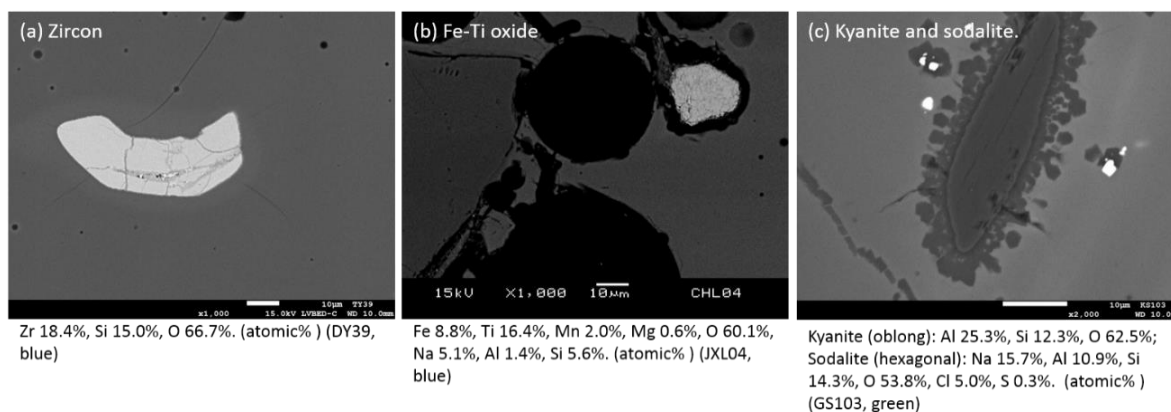


Figure 8.13: The remains of accessory minerals identified in the *m-Na-Al* glass. ((a): DY39; (b): JXL04; (c): GS103.)

8.3.2.2. The red glass

The red glass is coloured by cuprite (Cu_2O) and possibly pure copper (Cu), but is shown as CuO in the chemical data (Appendix 2). The samples from Jiuxianglan ($n = 6$), Guishan ($n = 15$) and Daoye ($n = 1$) contain CuO ranges from 0.9-1.8%, while a slightly higher CuO content of 2% and 3.5% is found in the Shisanhang samples ($n = 2$). The microstructural analysis carried out on a total of 10 samples from Jiuxianglan, Guishan and Daoye has shown the presence of copper sulphide (Cu_2S), cuprite and plenty of copper-based nano-particles which are not possible to analyse by SEM-EDS as they are too small (Figure 8.14).

In the glass matrix, fine bubbles are sometimes found, and occasionally there are large bubbles with a diameter of around a few hundred μm (Figure 8.14 (a)). Although blackish streaks are often observed in the red glass under the optical microscope, no distinct compositional or microstructural difference can be observed under SEM-EDS. More scientific investigation is necessary in order to understand the differences between the blackish streaks and the red areas.

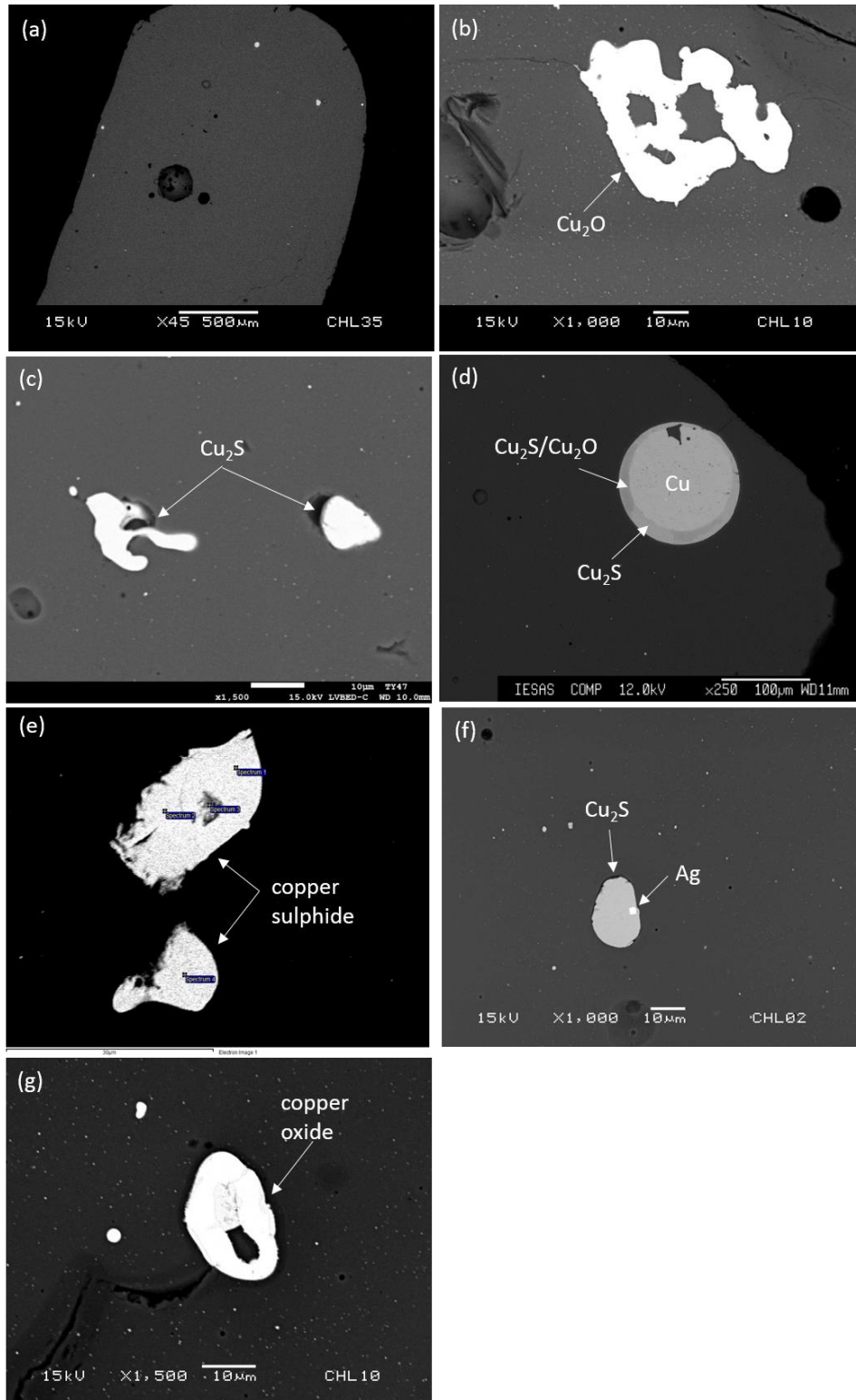


Figure 8.14: (a) An overview of the red glass; (b), (c), (d), (e), (f) and (g) the copper sulphide, copper oxide and metallic copper particles identified in the red glass. The chemical composition of inclusions shown in (d) is provided in Table 8.3. ((a): JXL35; (b): JXL10; (c): DY47; (d): GS004; (e): JXL34; (f): JXL02; (g): JXL10.)

Table 8.3: The composition of Cu, Cu₂S and Cu₂S/Cu₂O in Figure 8.14(d). (wt% by EPMA)

	Cu	S	Si	Al	Fe	Pb	Sn	O	Total
Cu	95.84	0.02	0.02	0.02	0.00	0.04	0.29	0.00	96.22
Cu ₂ S	80.13	18.73	0.03	0.03	0.12	0.21	0.05	0.14	99.44
Cu ₂ S/Cu ₂ O	80.07	14.47	0.06	0.00	0.21	0.09	0.00	4.61	99.51

Irregular or round droplets of copper sulphide and cuprite are frequently found in the red glasses (Figure 8.14). Copper sulphide is more common than copper oxide, and these particles are in some cases attached to small voids. The particles of copper oxide and copper sulphide are often present as irregular shapes (Figure 8.14 (b) and (d)), which may suggest their formation as crystals below the melting temperature of metallic copper (1083°C), instead of a liquid phase, (Freestone 1992). In rare cases, the particles of copper sulphide and copper oxide are present as round droplets, with a size of less than 30 μm in diameter, which suggest some were melted at a temperature higher than the melting point of metallic copper, and in this case the liquid copper forms the round droplet (Freestone 1992).

Interestingly, in sample GS004, a droplet of copper metal is found, with a diameter of around 100 μm , surrounded by a rim of copper sulphide and partially oxidised copper sulphide/copper oxide (Figure 8.14 (d), Table 8.3). Its particularly large size suggests it is less likely to be metallic copper precipitated from the glass matrix. It also shows a similarity to the desulphurised copper droplet of copper smelting matte prills (Hauptmann *et al.* 2003). If this is the case, it may be that the colouring mechanism of the red glass is similar to the co-smelting process of copper smelting, and the copper-based colourant may be a mixture of sulfidic copper and oxidic copper. In Figure 8.14 (e), (f) and (g), some small particles of copper sulphide and copper oxide are observed, and in Figure 8.14 (f) a silver inclusion is found within the copper sulphide particle. The morphology of particles in Figure 8.14 (e), (f) and (g) does not suggest

the precipitation of crystals, and therefore there is a possibility that these are un-melted relics of the colouring raw materials.

If a mixture of sulfidic copper and oxidic copper was used as colourant, the colouring of red glass probably would not need an abundant supply of charcoal. In the co-smelting reaction of sulfidic and oxidic copper ore, self-reducing takes place by the interaction between copper sulphide and copper oxide (Hauptmann *et al.* 2003). The process requires the supply of a flow of air so that the reaction between copper sulphide, copper oxide and oxygen produces cuprite or metallic copper which is responsible for the red colour in the glass, although the presence of metallic copper, possibly as nano-particles, cannot be detected by electron microprobe in this research.

It is possible that the copper-based colourant added to the red glass is derived from the waste or by-products of sulfidic/oxidic copper smelting, such as matte. Matte is an intermediate product of sulfidic copper ore smelting, and is a mixture of copper sulphide and/or iron sulphide which can be used for further smelting to produce pure copper metal. However, Early Bronze Age craftspeople may not have been aware of the copper contents in matte and discarded it with the slag (Hauptmann *et al.* 2003). Although the typically greater concentration of FeO in the red glass requires more investigation, the matte is likely to introduce some FeO when added as colourant, which may lead to the higher FeO content in red glass. Some FeO may be incorporated into the glass melt, enhancing the precipitation of cuprite or metallic copper in the red glass (Freestone 1987).

The use of metallurgical by-product or waste for red glass production has been proposed by Freestone *et al.* (2003b) and Peake and Freestone (2012) in opaque red glass of the late pre-Roman Iron Age and Anglo-Saxon (the 5th to the 7th century AD) period, respectively. In these

cases, the use of slag is proposed. In Peake and Freestone (2012), Fe- and Ca-rich inclusions associated with slag were found, but these inclusions were not reported in Freestone *et al.* (2003b). In the two cases, elevated levels of FeO were also identified in the red glass. The use of copper smelting slag is considered as less possible in this research, as the slag contains negligible contents of copper, and there are no Fe- or Ca-rich inclusions observed in the red glass in this research. However, the possibility of using matte as raw material for colouring suggests the connection between the glass production and the copper production, although one can imagine that the amount of matte required for producing the red glass is relatively small considering the small volume of red glass bead. Overall, this is probably as a result of selection or processing of raw materials for red glass production, but requires further study.

It is also likely that impurities such as Pb (lead), Sn (tin), Co (cobalt), Ni (nickel), Zn (zinc), As (arsenic), Ag (silver) and Sb (antimony) might have been introduced from raw materials of colourant, and incorporated into the glass melt during the colouring process. Table 8.4 shows that the red glass is rich in Ni (average 150 ppm) and Zn (average 120 ppm) in comparison to the copper-coloured green and blue glasses, although the range is variable. Most of the red glass from Guishan and Jiuxianglan has Ni concentrations less than 120 ppm, but particularly high values are found in GS019 (290 ppm) and GS023 (1100 ppm) from Guishan.

A bronze source of copper-based colourant is considered as less likely. The content of SnO₂ is less than 0.3% (mostly around 0.1%) and PbO less than 1.5%, with a varied CuO/SnO₂ ratio from 6 to 130. It is only in another sample, JXL22, that a cluster (ca. 60 μm) of nodular and acicular tin oxide is seen. Although tin oxide crystals in these glasses may suggest the copper source is related to bronze, its rare presence and the low contents of SnO₂ (0.06%) and PbO (0.61%) in the same sample indicates that bronze was not the principal source of the copper-based colourant for producing the red glass in this research.

Table 8.4: The average, maximum and minimum value of PbO (%), SnO₂ (%), Co (ppm), Ni (ppm), Zn (ppm), As (ppm) and Sb (ppm) in m-Na-Al glass coloured by Cu-based colourants.

		red (n=24)	orange (n=27)	green (n=26)	blue (n=33)
PbO (%)	Mean	0.36	0.47	2.25	0.18
	Max	1.65	1.96	5.62	1.35
	Min	0.00	0.00	0.60	0.00
SnO ₂ (%)	Mean	0.10	0.36	0.23	0.05
	Max	0.28	1.34	0.45	0.15
	Min	0.00	0.01	0.07	0.00
Co (ppm)	Mean	14.0	33.7	7.5	5.2
	Max	34.3	156.8	12.8	14.4
	Min	0.9	5.0	1.5	0.0
Ni (ppm)	Mean	149.6	182.4	44.1	27.6
	Max	1106.5	1331.4	171.2	238.6
	Min	3.8	13.6	4.8	1.5
Zn (ppm)	Mean	121.5	493.4	45.1	82.2
	Max	1246.5	1925.8	113.4	842.9
	Min	0.0	0.0	11.0	0.0
As (ppm)	Mean	25.7	230.9	17.1	17.5
	Max	86.3	1166.2	43.5	41.9
	Min	2.5	11.5	2.8	4.3
Ag (ppm)	Mean	10.7	61.3	7.3	8.3
	Max	23.9	261.6	17.3	13.7
	Min	0.9	3.1	2.0	3.4
Sb (ppm)	Mean	10.7	61.3	7.3	8.3
	Max	23.9	261.6	17.3	13.7
	Min	0.9	3.1	2.0	3.4

8.3.2.3. The orange glass

In the orange glass, a higher CuO content, between 3-8%, is found than in the red glasses. In orange glass, it has been noted cuprite and metallic copper provide the orange colour (Ahmed

and Ashour 1981). Microstructural analysis was carried out on 3 beads from Jiuxianglan and 4 beads from Kiwulan, and this has revealed differences between the two sites.

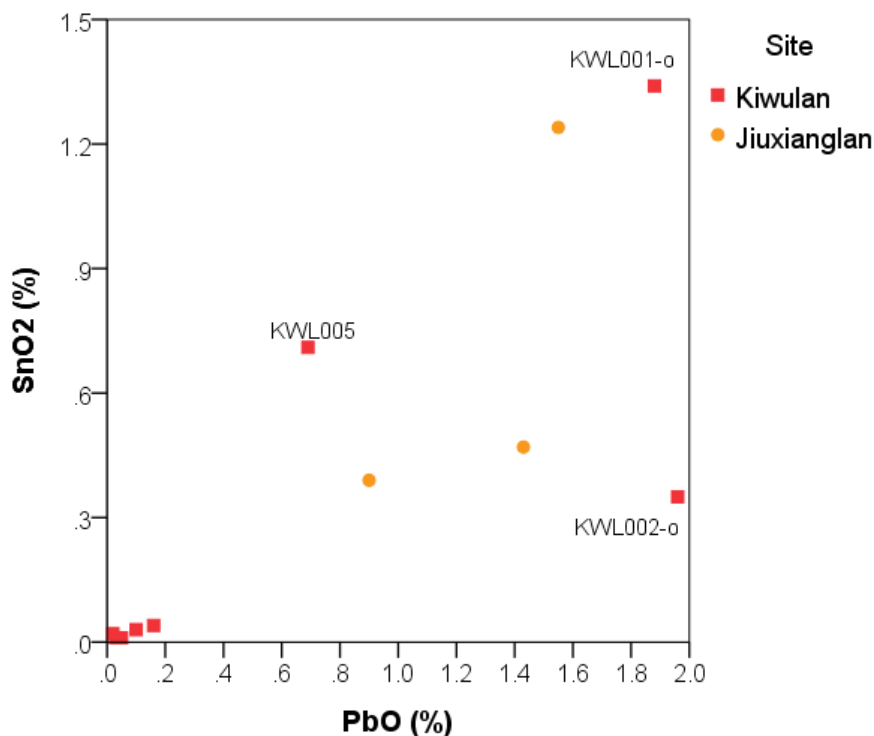


Figure 8.15: The PbO-SnO₂ bi-plot of orange glass from Kiwulan and Jiuxianglan.

The 3 samples of orange glass from Jiuxianglan all have high SnO₂ and high PbO contents compared to most Kiwulan samples (Figure 8.15). JXL25 from Jiuxianglan contains a large inclusion (ca. 450 μm in length) which is rich in copper and contains tin (Figure 8.16 (a)). Further investigation has shown that this inclusion is probably an oxidised Cu-containing component surrounded by a rim which is rich in CuO and SiO₂ (Figure 8.16 (b) / Table 8.5, label 1-4). A couple of small crystals embedded within the inclusion are found to have around 16% Cu, 52% Sn and 40% O (Figure 8.16 (c), (d) / Table 8.5, label 5 and 7), which indicates it may be an oxidised bronze-like inclusion or bronze slag. A CuO prill is also found in proximity to the bronze-related inclusion in JXL25 (Figure 8.16 (e) / Table 8.5, label 10). Occasionally, acicular or nodular tin oxide is observed in the orange glass from Jiuxianglan (Figure 8.16 (f)

and (g)), and large crystals of copper oxide with different degrees of oxidation (Cu/O atomic ratio in the range of 0.9-1.6) are often found, either linearly distributed in the glass matrix or precipitated within the voids (Figure 8.16 (h)).

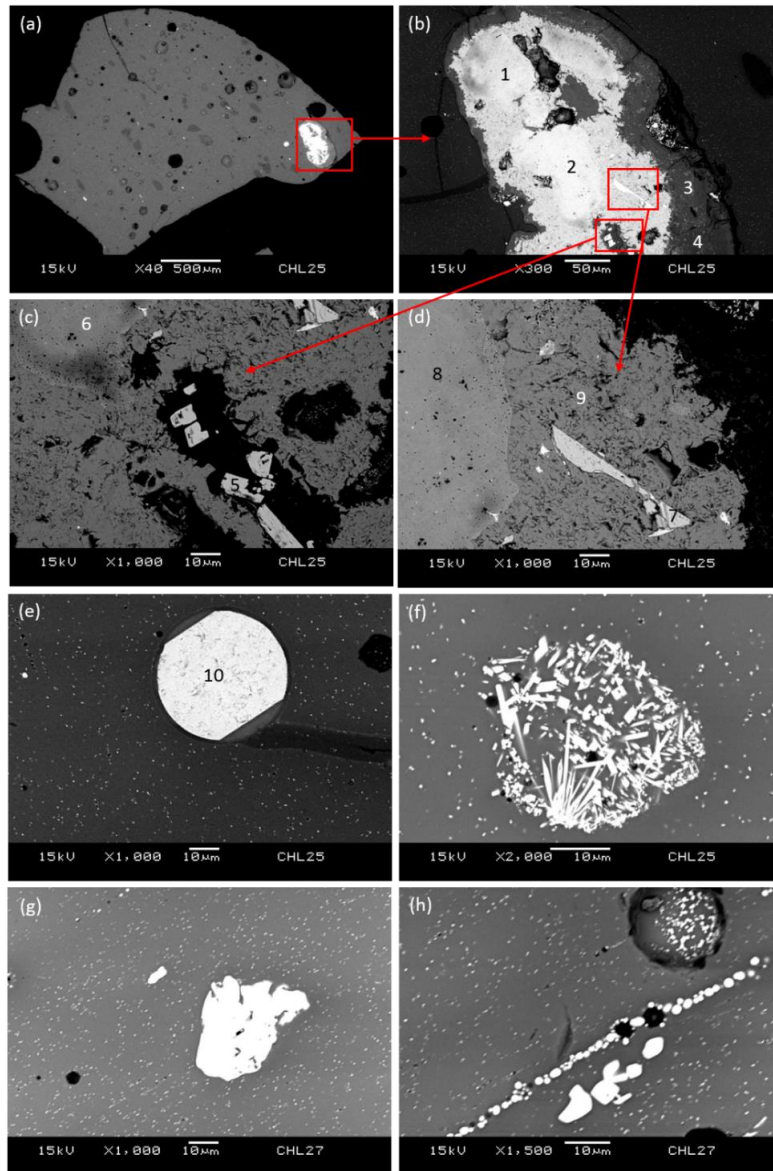


Figure 8.16: Inclusions or crystals identified in the orange glass. (a) the cross-section of JXL25; (b) the bronze-related prill; (c) and (d) the oxidised Cu/Sn in the prill; (e) the CuO prill, which is the bright round particle to the left of the bronze-related prill in (a); (f) acicular tin oxide; (g) nodular tin oxide; (h) Cu_2O crystal. (The composition of particles labelled from 1 to 10 is shown in Table 8.5. ((a)-(f): JXL25; (g)-(h): JXL27.)

In JXL24, optical microscopic observation reveals some reddish streaks in the orange glass (Figure 8.17 (a)). The microstructural analysis indicates the orange part is a dense distribution of fine copper particles, while in the red part a cluster of larger copper oxide particles is found as dendritic forms or concentrated within the voids (Figure 8.17 (b)). The SEM-EDS further shows a higher CuO content in the orange section (ca. 11%) than the red section (ca. 9%).

The presence of the bronze-related inclusion, together with the higher SnO₂ and PbO contents in the orange glass from Jiuxianglan, suggests that the inclusion is likely to be introduced as bronze slag or oxidised bronze. Therefore, it is possible that the colourant used for producing the orange glass from Jiuxianglan may be derived from sources related to bronze production or bronze artefacts. In this case, the Sn content in the bronze behaves as reducing agent to produce cuprite or metallic copper, which generates the colour hues between red-orange (Bring and Jonson 2007). The orange hue is achieved by a greater concentration of cuprite or metallic copper and also the smaller grain size of cuprite. The glassmaker might not have been aware of the interaction which produced the colour, but have been aware that specific colouring additives produced specific colours.

There has been a long debate about the role of tin as a reducing agent in glass, and it is still not fully understood (e.g. Durán *et al.* 1984; Ishida *et al.* 1987; Capatina 2005; Bring and Jonson 2007). Generally, it is assumed that tin is in the form of Sn²⁺ (SnO) in the glass which reduces the Cu²⁺ to Cu⁺ or metallic copper. It is thought tin protects the metallic copper from oxidation to Cu²⁺, and in this case it is the metallic copper dispersed through the glass that contributes to the colour (Capatina 2005). Alternatively, it has also been suggested that tin acts as redox buffer to regenerate the Cu⁺, which forms the colloidal Cu₂O that is responsible for the colour (Durán *et al.* 1984). A detailed investigation of the colouration mechanism is not the focus of this research, and the SEM-EDS analysis also limits further understanding in terms of the form of

copper-based nanoparticles dispersed in the glass matrix. However, this result has shown the potentially different raw materials used as colourants for the red and orange glasses from Jiuxianglan, where the orange glass may be produced by deliberately introduction of bronze-related materials due to its tin content while the red glass appears to be coloured in a different fashion, although with copper-containing raw materials.

Table 8.5: The chemical composition of the particles labelled 1 to 10 in Figure 8.16 (b)-(e).

(wt%)

Label	Cu	Sn	Na	Al	Si	Cl	Ca	O	Total	Note
1	86.9			0.8	3.1	0.5		7.4	98.6	CuO/Cu?
2	86.4			0.6	2.8			6.8	96.6	CuO/Cu?
3	29.4		1.2	0.7	15.0	0.5	0.4	30.0	77.2	
4	27.7			0.8	13.6			28.6	70.6	
5	15.4	51.5	1.3		2.6			39.4	110.2	Oxidized Cu/Sn?
6	86.3				2.8			6.3	95.3	CuO/Cu?
7	17.9	52.2	1.2		2.0			40.6	114.0	Oxidized Cu/Sn?
8	86.9				3.0			6.6	96.4	CuO/Cu?
9	81.6			0.7	2.6			15.3	100.2	CuO
10	80.0		3.7	1.7	5.9			19.0	110.2	CuO

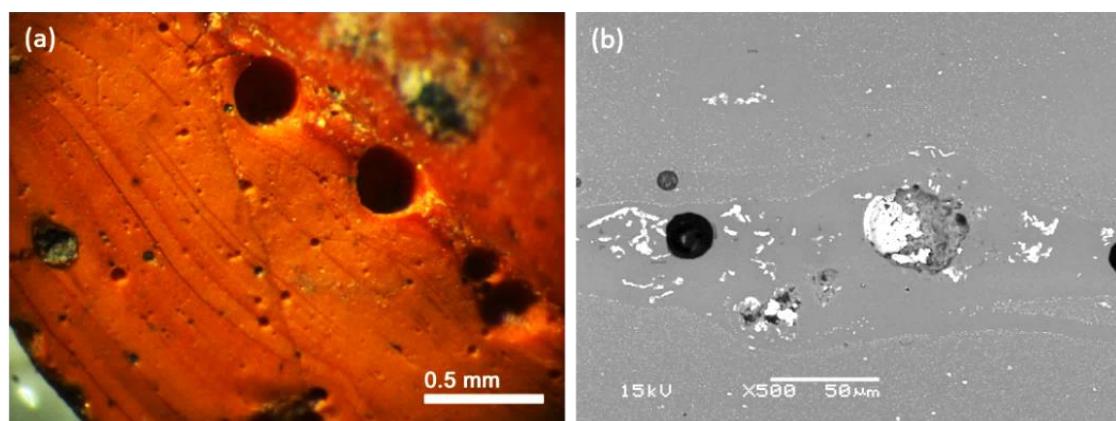


Figure 8.17: The cross-section of orange glass (JXL24). (a) the reddish streaks in the orange glass can be observed under optical microscope; (b) the BSE image shows the cluster of large copper oxide particles in the reddish streak (middle) and the absence of fine copper particles in comparison to the orange area (top and bottom).

All the orange glasses from Kiwulan, except for KWL001, KWL002 and KWL005, contain relatively low concentrations of PbO (<0.2%) and SnO₂ (<0.1%) (Figure 8.15). The microstructural analysis has shown that copper-based nano-particles are dispersed in the glass matrix, and there are several large copper-based crystals linearly distributed over the matrix or in the voids. A closer look reveals that some of the large crystals (ca. 2-3 μm) are metallic copper Figure 8.18 (a) and (b). The smaller copper-based particles often contain oxygen, although there may be contribution of oxygen from the glass matrix due to the electron beam size (Figure 8.18 (c)).

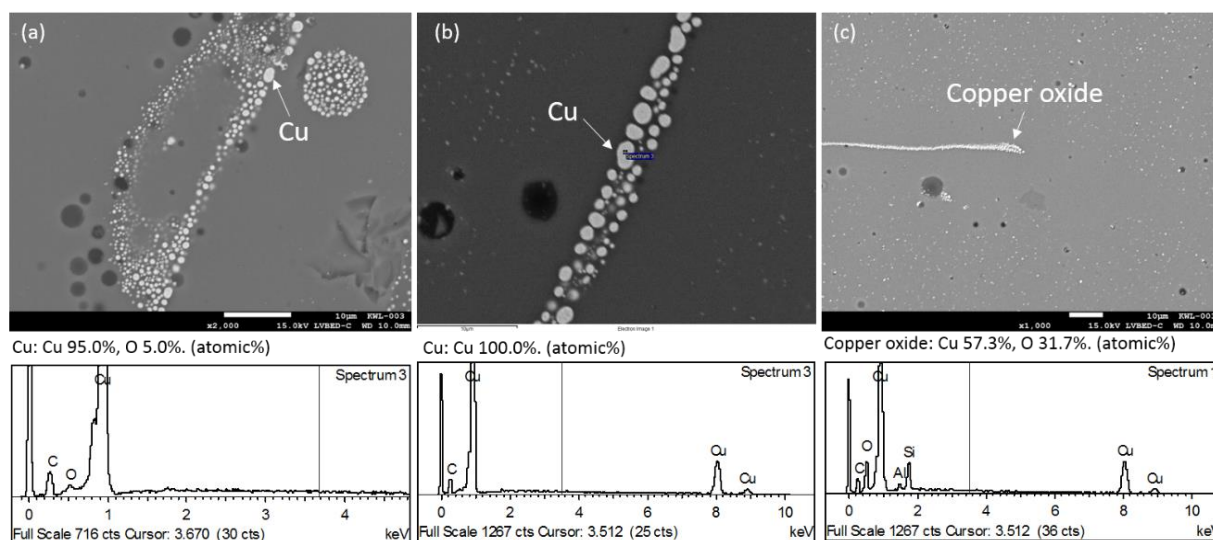


Figure 8.18: (a) and (b): the metallic copper crystals identified in KWL003; (c) the copper oxide identified in KWL004.

However, in KWL005, a higher PbO content of 0.7% and SnO₂ of 0.7% is found and a cluster of copper oxide (ca. 62% Cu and 38% O in atomic%) and tin oxide (21% Sn and 79% O in atomic%) inclusions is observed in this sample (Figure 8.15 and Figure 8.19). These inclusions probably indicate the decomposition and/or incomplete melting of a bronze-related compound during glass production, as in the case seen in the orange glass from Jiuxianglan. The presence of the decomposed inclusions, together with the significant PbO and SnO₂ concentrations in

KWL005, suggest that different copper-based ingredients were used to produce the orange colour in this sample, compared to the other samples from Kiwulan.

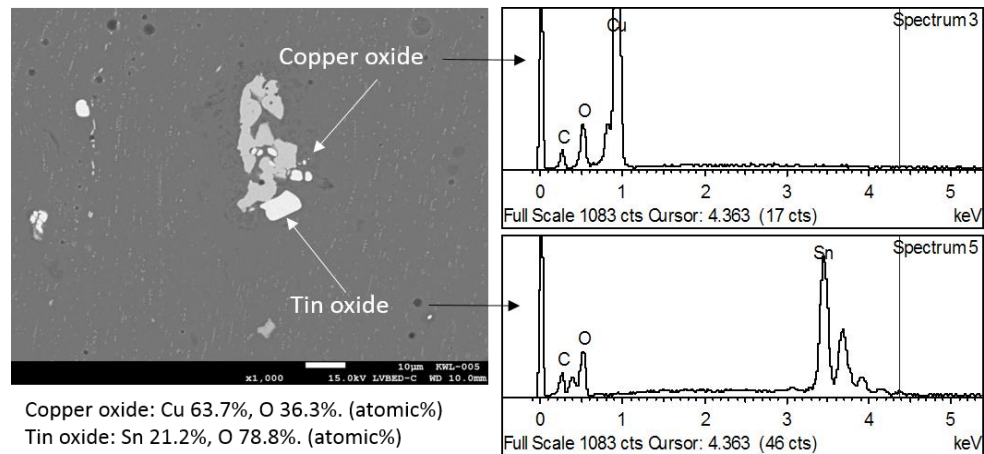


Figure 8.19: The inclusion of copper oxide and tin oxide seen in KWL005, showing possibly the decomposition of bronze.

The analysed orange glass from Kiwulan shows that a copper-based and almost tin-free compound was used (except for KWL001, KWL002 and KWL005). Although it is not possible to know exactly the form of raw materials introduced, it is likely that the source is related to copper smelting, as seen in the red glass from Jiuxianglan. Therefore, some FeO in the orange glass may be attributed to the use of copper matte or the tool of iron tongs. The original copper component may contain copper sulphide and/or copper oxide. With better control of the air flow and heat treatment than the glass seen from Jiuxianglan, it is possible that the copper sulphide fully reacted to cuprite or metallic copper in the orange glass, which explains why no inclusions of copper sulphide are seen in the orange glass from Kiwulan. The precipitation of large metallic copper crystal observed in some of the orange glasses in Kiwulan is therefore possibly due to the longer processing time, either heating or cooling, that allows the nucleation and growth of crystals. The significant amount of FeO in the orange glass probably also helped to enhance the nucleation and growth of cuprite or metallic copper crystals (Freestone 1987). Based on the co-

smelting concept discussed for the red glass (section 8.3.2.2), this process generates SO₂ gas; the more copper sulphide changes to cuprite or metallic copper, the more SO₂ gas is emitted. The emission of SO₂ gas in excess of the solubility in the glass melt may lead to many fine bubbles, as observed in the glass matrix of these orange glass beads, which are often located near the voids or clusters of copper-based crystals.

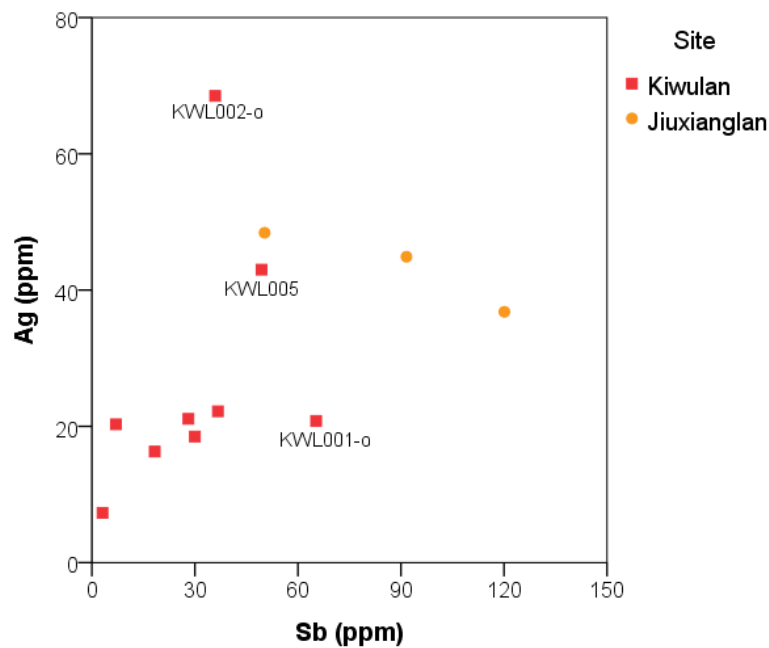


Figure 8.20: The Sb-Ag bi-plot of orange glass from Kiwulan and Jiuxianglan

This result indicates the different choices of colourants in the production of orange glasses from Jiuxianglan and Kiwulan – one with bronze-related copper and the other with tin-free copper. In either case, impurity metals from the original copper ores (Co (cobalt), Ni (nickel), Zn (zinc), As (arsenic), Ag (silver) and Sb (antimony)) may be introduced with the colourants. It can be seen from Table 8.4 that generally higher contents of Co, Ni, Zn, As, Ag and Sb are found in the orange glass than in other colours. A closer investigation has shown that the copper-containing ingredients used for producing orange glass from Kiwulan and Jiuxianglan, respectively, may have different sources. The tin-free samples from Kiwulan contains less Ag

(<25 ppm) and Sb (<40 ppm), while the tin-rich samples from Kiwulan (KWL005) and Jiuxianglan show Ag contents higher than 35 ppm and Sb higher than 50 ppm (Figure 8.20). In the tin-rich samples, the samples from Jiuxianglan have relatively high Zn concentrations (>700 ppm) in comparison to the low value in sample KWL005 from Kiwulan (75 ppm). The greater amounts of Ag, Sb and Zn in these samples may be also associated with the Sn, as these metals often occur as a complex in the tin ore deposits.

In addition to the monochrome orange glass, sample KWL001 from Kiwulan shows an inter-layer of red glass between the outer orange glass and the inner blue glass. Another similar sample, KWL002, also has an orange surface, but the inner core indicates a complicated combination of different materials. In the orange glass surface in both samples, generally a higher content of PbO (ca. 2%), SnO₂ (<1%), Zn (ca. 670 ppm), Ag (ca. 45 ppm) and Sb (ca. 50 ppm) is observed (Figure 8.15 and Figure 8.20), which shows a similarity to the orange glass coloured by bronze-related raw materials discussed above from Jiuxianglan. The SEM-EDS analysis of KWL001 shows that the orange and red glasses are made of m-Na-Al glass, while the inner blue glass is made of v-Na-Ca glass. In terms of KWL002, the results seem to suggest the mixing of glass and 'earth' materials (clay and/or sand). The detailed microstructure of this type of glass will be described together in the section on v-Na-Ca glass (Chapter 9.2.2.4).

Although no microstructural analysis has been carried out on orange glasses from Guishan and Shisanhang, the variable composition of the samples from Guishan and Shisanhang also suggests raw materials used for producing orange glass were complex. GS015 is the only bead from Guishan that shows a red glass core covered by an orange glass surface. It is noted that the orange glass contains relatively high Ni (1300 ppm), As (1200 ppm) and Sb (260 ppm) in comparison to the orange glass from other sites. The PbO and Zn compositions of the orange glass from Shisanhang are taken from the published report (Tsang and Liu 2001: 91-106),

which suggests the orange glasses do not contain a significant content of PbO, except for SSH-B008. Five samples contain Zn higher than 0.9%, while negligible amounts of Zn are reported in the other samples. Some of this chemical data suggests the presence of Cu-rich particles, in which the Cu contents of around 98% and Zn of around 1% is reported (Tsang and Liu 2001: 96, 103 and 105).

8.3.2.4. The blue glass

The blue glass is coloured by cupric copper, Cu^{2+} (Weyl 1976), and the CuO ranges from 0.2-2%. Microstructural analysis was carried out on 10 samples from Jiuxianglan, 2 samples from Guishan, 3 samples from Daoye and 3 samples from Wujiancuo. Generally, the glass matrix is quite homogenous in comparison to the red and orange glass, but occasionally has bubbles and un-melted inclusions of silica, feldspar or zircon.

As the matrix is relatively homogeneous, it is less easy to identify the form of colourant used. However, in JXL28, a cluster of copper oxide and acicular tin oxide is present (Figure 8.21), identified by spot analysis by SEM. The presence of copper and tin oxides may suggest that bronze was used for colouring some blue m-Na-Al glass. In contrast, tin oxide was found in JXL16, JXL17 and WJC15 samples, in the form of acicular, nodular and triangular crystals, respectively.

The remains of prismatic barite (BaSO_4) inclusions are found in JXL17 (Figure 8.22). The barite may be unintentionally introduced with a copper ore or with less purified copper-containing raw materials during the colouring process; as yet the sources of raw materials cannot be identified.

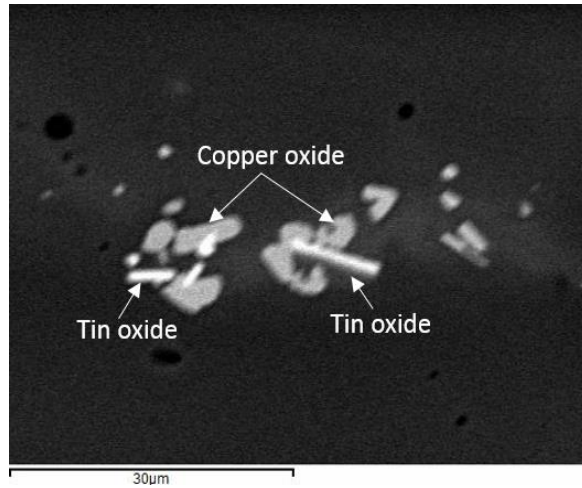


Figure 8.21: The cluster of copper oxide and tin oxide seen in JXL28, showing possibly the decomposition of bronze.

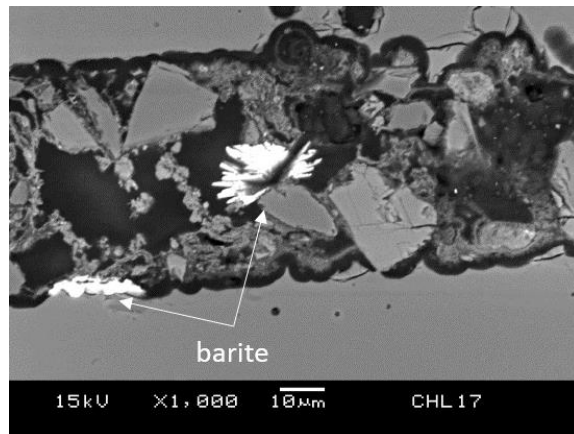


Figure 8.22: The inclusions of barite in JXL17.

Co (cobalt), Ni (nickel), Zn (zinc), As (arsenic), Ag (silver) and Sb (antimony) are also found in the blue glass but at lower concentrations than are found in the copper-coloured red and orange glass (Table 8.4) as might be expected as due to the lower concentrations of copper in the blue glasses. A closer examination reveals that the blue glass from Guishan generally contains a higher As content (>15 ppm) than those from Jiuxianglan (<15 ppm), and therefore may suggest different sources of colourants in the blue glasses from the two sites and hence different provenances.

It is noteworthy that the two blue glass *waste* fragments from Jiuxianglan have a different microstructure to the blue beads. The glass matrix is relatively homogeneous with the absence of bubbles and almost no silica or feldspar remains. The glass waste is visibly transparent, but the beads are opaque. This may suggest the beads and waste from Jiuxianglan are not related. As suggested in Chapter 7.5, this supports the idea that the evidence for local production of beads at Jiuxianglan is inconclusive.

8.3.2.5. The yellow glass

The yellow glass is coloured by lead tin oxide. PbO varies between 1-14% and SnO₂ is below 2%. Microstructural analysis was performed on 10 samples from Jiuxianglan, 4 samples from Guishan and 1 sample from Daoye.

Different microstructures are found in the yellow glass from Jiuxianglan, Guishan and Daoye. Figure 8.23 (a) shows an example of yellow glass from Jiuxianglan, which has a relatively heterogeneous matrix. The brighter matrix contains PbO as high as 9% and the darker matrix as low as 1%. It is quite common that the crystals of lead and tin cluster with nepheline crystals (NaAlSiO₄) (often tetragonal or hexagonal) in the brighter matrix, and occasionally a few hexagonal sodalite (Na₈Al₆Si₆O₂₄Cl₂) crystals are found near the lead tin oxide and nepheline (Figure 8.23 (a)). Another typical image of the aggregate of lead tin oxide and nepheline in Jiuxianglan samples is shown in Figure 8.23 (b), in which the small lead tin oxide crystals (<10 μm) spread around the large nepheline crystals (~300 μm). It is noteworthy that around 4-5 atomic% Si is found in the lead tin oxide (Sn ~14-15 at%, Pb ~20-21 at% and O ~58-59 at%). Therefore, it is likely that the lead tin oxide is in the form of Pb(Sn,Si)O₃ rather than PbSnO₃ (Heck *et al.* 2003; Welter *et al.* 2007). Sodalite crystals are also found in the dark matrix, and in some cases surrounding the even darker matrix which may be the partially melted mineral of

sodium aluminosilicate (Figure 8.23 (c)).

In the yellow glass from Daoye, a more homogeneous matrix is observed ($\text{PbO} \sim 3\%$), and there are no crystals of nepheline and sodalite clustering near the lead tin oxide (Figure 8.23 (d)). The lead tin oxide in the yellow glass from Daoye is also found to be $\text{Pb}(\text{Sn},\text{Si})\text{O}_3$.

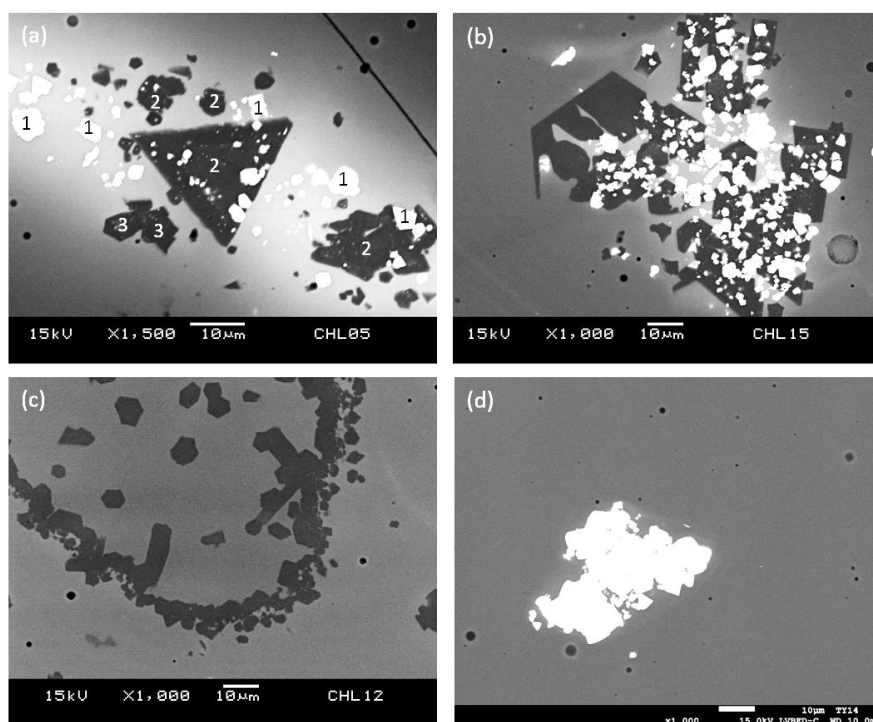


Figure 8.23: The inclusions and crystals in the yellow glass from Jiuxianglan. (a) the non-homogenous matrix and the cluster of lead tin oxide (1), nepheline (2) and sodalite (3) (JXL05); (b) the typical aggregate of lead tin oxide and nepheline crystals seen in Jiuxianglan samples (JXL15); (c) the cluster of sodalite crystal in the yellow glass from Jiuxianglan (JXL12); (d) the yellow glass from Daoye, showing the homogeneous matrix and the crystal of lead tin oxide (DY14).

These microstructural differences, between the yellow beads from Jiuxianglan and Daoye probably indicate different colouring processes or heat treatments for yellow glasses arriving at the two sites. For the yellow glass from Jiuxianglan, it is likely that the lead- and tin-containing

ingredient(s) was introduced to the glass frit (or glass melt), and then melted together. The sand used for making m-Na-Al glass is rich in alkali feldspar and plagioclase (close to the albite group), which forms the glass composition located in the albite region in the $\text{Na}_2\text{O}-\text{Al}_2\text{O}_3-\text{SiO}_2$ phase diagram (see section 8.3.2.1). Therefore, during the melting process, the Pb and Sn take the Si from the glass melt or un-melted sodium aluminosilicate, forming $\text{Pb}(\text{Sn},\text{Si})\text{O}_3$ in the final glass. The excess PbO dilutes the surrounding melt and therefore may facilitate the formation of nepheline crystals (Rehren 2016, *pers. comm.*). The presence of sodalite may be attributed to the raw materials which may have been in the form of chloride, sulphate or sulphide. The reaction between chloride, sulphate or sulphide and sodium aluminosilicate (nepheline or existing albite-like minerals) led to the conversion of sodalite (Saha 1961; Dumańska-Słowik *et al.* 2015). There are no tin oxide crystals observed in the yellow glass, which may suggest that the tin content is of a lower proportion compared to the Pb content and that the colouring process was conducted at a low temperature, possibly below 1000°C , as a high processing temperature may lead to the recrystallisation of tin oxide as a result of lead tin oxide dissolution (Tite *et al.* 2008).

In the sample from Daoye, the absence of nepheline and sodalite suggests that lead- and tin-bearing material(s) may have been added as a single component to raw glass or a more vitrified glass frit which contains fewer silica or feldspar relics. In this case, some pre-treatments such as calcination of lead tin oxide compound may have been performed (Heck *et al.* 2003). Similarly, there are no tin oxide crystals in the yellow glass from Daoye, and therefore a lower temperature of colouring process, mentioned above, might have been practiced (Tite *et al.* 2008).

The four samples from Guishan show two different microstructures corresponding to the two typological groups. In GS005 and GS022 (GS-Y1 type), there is almost no nepheline and sodalite clustered with the lead tin oxide, and the lead tin oxide is in the form of $\text{Pb}(\text{Sn},\text{Si})\text{O}_3$.

This demonstrates that the colouring process of the Guishan yellow glass of GS-G1 type is similar to that of Daoye rather than Jiuxianglan. The occasional presence of small nepheline crystals ($<10\ \mu\text{m}$) within the areas rich in lead tin oxide may result from the reaction between lead tin oxide and the relics of sodium aluminosilicate in the glass matrix.

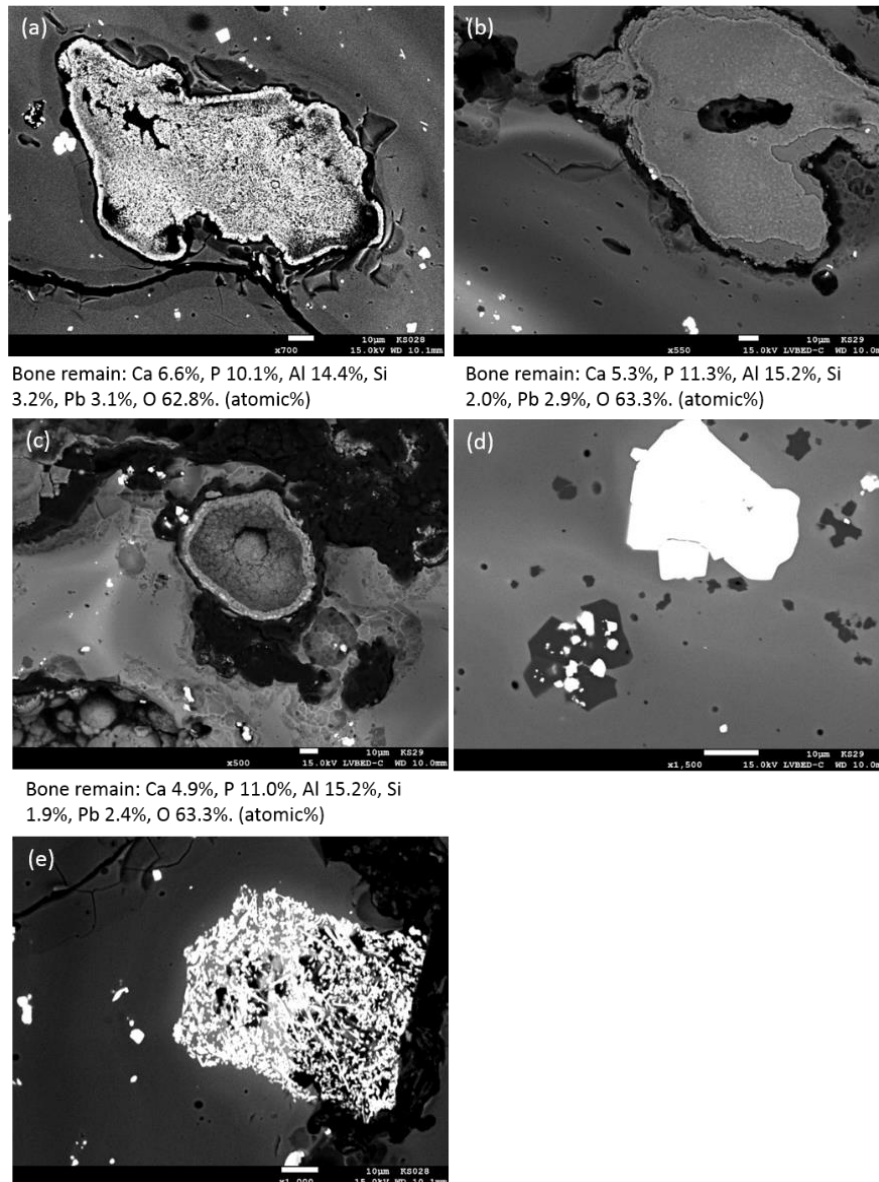


Figure 8.24: Inclusions and crystals in GS028 and GS029. (a): the bone ash remains in GS028; (b) and (c): the bone ash remains in GS029; (d): the nodular lead tin oxide (bright crystal) and sodalite (dark crystal) in GS029; (e): the acicular lead tin oxide (bright crystal) and sodalite (dark crystal within the acicular lead tin oxide) in GS028.

From Guishan, GS028 and GS029 samples, which belong to GS-Y2 group, show a different microstructure. Inclusions which are rich in phosphorous and calcium are present, and the porous texture of these inclusions suggests these are bone ash (Figure 8.24 (a)-(c)). SEM-EDS analysis has shown that the bone ash remains contain CaO around 8% and P₂O₅ around 25%, which are higher than the CaO and P₂O₅ contents in the glass matrix (CaO ~3% and P₂O₅ is not detected). This indicates that there is no significant contribution of Ca and P from the bone ash remains to the glass matrix. The unconnected boundary between the bone ash remains and the matrix suggest the bone ash remains may be a later addition after glassmaking or glass colouring. The purpose of using this type of material is unclear, but it may be to increase the opacity – GS028 and GS029 are fully opaque even under strongly transmitted light, while the other yellow glass beads look semi-translucent. Alternatively, it may be used for the shaping during beadmaking, as the two beads are both biconical in shape with quite a sharp angle at the base.

Aggregates of lead tin oxide (nearly cubic in shape) and sodalite are found in both GS028 and GS029 (Figure 8.24 (d)), and in GS028 there are clusters of acicular lead tin oxide and sodalite (Figure 8.24 (e)). As in the other yellow glasses analysed, tin oxide is absent in the two samples. This may indicate a colouring process similar to that of the Jiuxianglan samples – the raw materials containing lead and tin were introduced to the glass frit or melt to produce the yellow glass. The different microstructures of lead tin oxide in these samples probably resulted from the heat treatment during colouring and the heating and cooling duration.

8.3.2.6. The green glass

The green glass is coloured by copper oxide and lead tin oxide. The content of CuO ranges from 0.25% to 1.5%. SnO₂ is between 0.05-0.5% and PbO between 0.5-6%. Microstructural analysis was carried out on 9 samples from Jiuxianglan, 3 samples from Guishan and 3 samples

from Daoye. The results reveal the possible raw materials in terms of colourants, and also indicate the complexity of discussing green glass colouring processes which may be any one of the following: (1) mixing yellow glass and blue glass, (2) adding yellow colourant to blue glass or vice versa, (3) adding lead-, tin- and copper-bearing materials respectively into the raw glass, glass frit or glass batch. Therefore, the following results focus on the discussion of raw materials used in colouring rather than the colouring process of green glass.

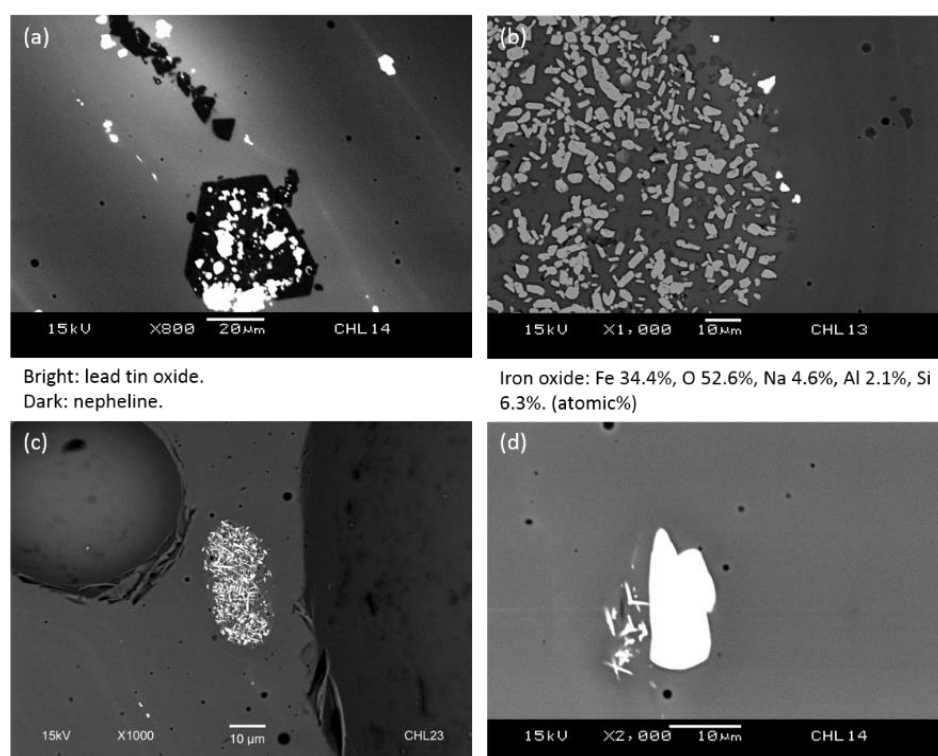
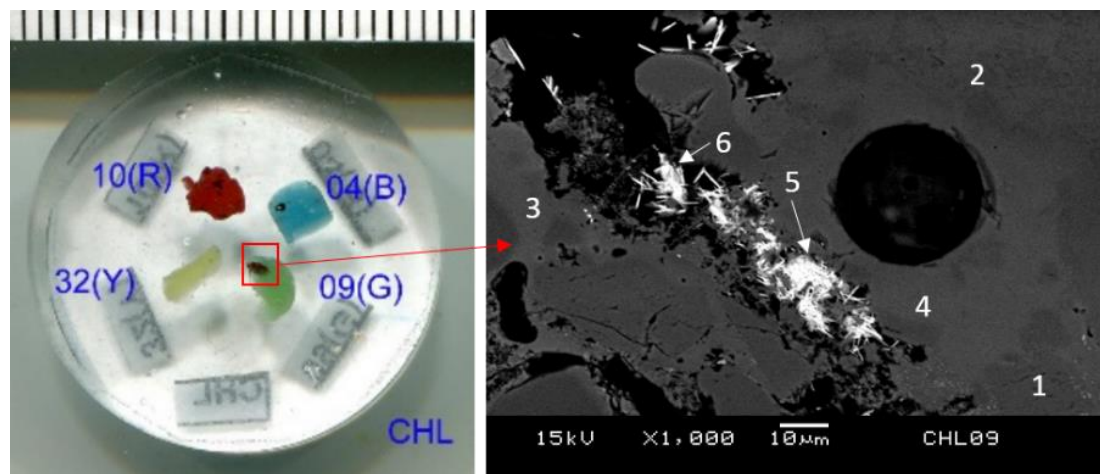


Figure 8.25: The microstructure of green glass from Jiuxianglan. (a) The heterogeneous glass matrix dispersed with lead tin oxide (bright crystals) and nepheline (dark crystals); (b) iron oxide inclusions; (c) and (d) tin oxide crystals. ((a) and (d): JXL14; (b): JXL13; (c): JXL23.)

In the green glass from Jiuxianglan, a relatively heterogeneous matrix is observed. As shown in Figure 8.25 (a), the bright matrix contains PbO as high as 10%, while the dark matrix has PbO at less than 4%. Similar to the yellow glass from this site, the aggregates of lead tin oxide and nepheline, and in some cases sodalite, crystals disperse throughout the bright matrix. The

SEM-EDS analysis shows that the lead tin oxide is $\text{Pb}(\text{Sn},\text{Si})\text{O}_3$, as also seen in the yellow glass. In JXL13, a cluster of sub-angular iron oxide inclusions is found (Figure 8.25 (b)). These iron oxide inclusions are likely to be the hammer scale from tools. Crystals of tin oxide, which are mostly of acicular shape, are occasionally found in the green beads (Figure 8.25 (c) and (d)). The presence of tin oxide crystals could be associated with the intentional use of a tin-bearing ingredient used to produce lead tin oxide in the yellow glass, or with the raw material of colouring blue glass.



Weight%											
	SiO_2	Al_2O_3	Na_2O	MgO	K_2O	CuO	TiO_2	FeO	SO_3	Cl	Total
1	67.1	21.0	10.5		1.4						100.0
2	54.8	20.1	15.6		2.1	1.3		3.2	2.3	0.5	100.0
3	71.1	12.6	8.9	0.9	3.6			2.9			100.0
4	62.3	13.7	12.1	1.6	2.3		2.4	5.2		0.4	100.0
Atomic%											
	Ba	Ca	S	O	Na	K	Al	Si			
5	8.9	1.2	11.8	64.8	3.6	0.6	2.6	6.6			
6	8.0	1.2	11.3	64.8	4.1		3.1	7.6			

Figure 8.26: The inclusion of barite found in JXL09 (1: sodium aluminosilicate; 2-4: glassy matrix; 5-6: barite.)

It is noteworthy that, in JXL09, a visible red inclusion is found within the green glass (Figure 8.26). A closer look at this area reveals the absence of any lead tin oxide, but shows it is rich in

partially dissolved sodium aluminosilicate (Figure 8.26, label 1), and the glassy areas shows a heterogeneous distribution of CuO, TiO₂, FeO and SO₃ (Figure 8.26, labels 2-4). An interesting find is the presence of prismatic barite crystals within the inclusion (Figure 8.26, labels 5-6). This probably suggests that the red inclusion is a relic of non-oxidised matte. If it is the case, the production of green glass requires a more oxidised atmosphere to generate the Cu²⁺ ions, although this cannot be confirmed here without further analysis. However, this result suggests that a potential copper source from copper matte is likely for the production of the green glass from Jiuxianglan.

In the three samples from Guishan and the three samples from Daoye, two different microstructures are found within the beads from a single archaeological site. The two different microstructures possibly suggest different production processes of lead tin oxide within the glass as discussed in the yellow glass (section 8.3.2.5).

At Guishan, GS001 and GS037 show a homogeneous glass matrix dispersed with small crystals of lead tin oxide (Pb(Sn,Si)O₃), and there is no nepheline or sodalite clustered with the lead tin oxide (Figure 8.27 (a)). Also, a relic of copper oxide is found in GS001 (Figure 8.27 (b)). Similarly, in DY14 and DY42-1 from Daoye, there are clusters of lead tin oxide dispersed on a homogeneous matrix, and an absence of nepheline (Figure 8.28 (a)).

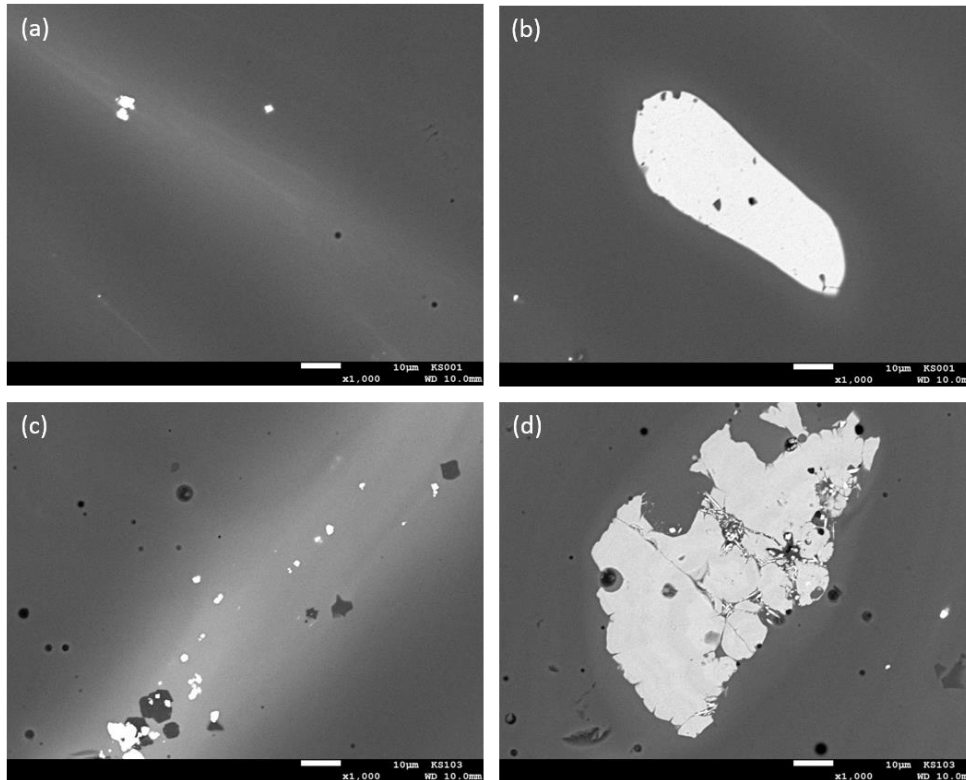


Figure 8.27: The microstructure of green glass from Guishan. (a) the lead tin oxide (bright crystal) dispersed throughout the glass matrix in absence of sodalite (GS001); (b) the inclusion of copper oxide in GS001; (c) the cluster of lead tin oxide (bright crystal) and sodalite (dark crystal) in the glass matrix (GS103); (d) the tin-rich inclusion in GS103.

A different microstructure is observed in GS103 from Guishan where the matrix is heterogeneous due to the uneven distribution of PbO which can be as high as 15% in the PbO-rich area. A cluster of lead tin oxide and sodalite crystal is also found in GS103 (Figure 8.27 (c)). In DY33 from Daoye, an aggregate of lead tin oxide and nepheline is found, but the matrix of DY33 is more homogeneous in comparison to GS103 (Figure 8.28 (b)).

Tin-rich inclusions are found in samples from Guishan and Daoye, but the components may suggest different sources. In GS103 from Guishan, a tin-rich inclusion contains 10 at% Sn, 15 at% Ca, 1 at% Mg, 8 at% Al, 6 at% Si and 60 at% O (Figure 8.27 (d)). In DY42-1 from Daoye,

another relic of a tin-rich inclusion is found, which unlike the tin-rich inclusion in GS103, is rich in Fe, Ni and Zn, and surrounded with tiny tin oxide crystals (Figure 8.28 (c)). The presence of a tin-rich inclusion may suggest that the tin-bearing ingredient is added directly to the glass, possibly from the raw materials used to produce lead tin oxide. Their different chemical compositions probably suggest that varied sources or types of tin-containing materials were used in glasses produced at different sites.

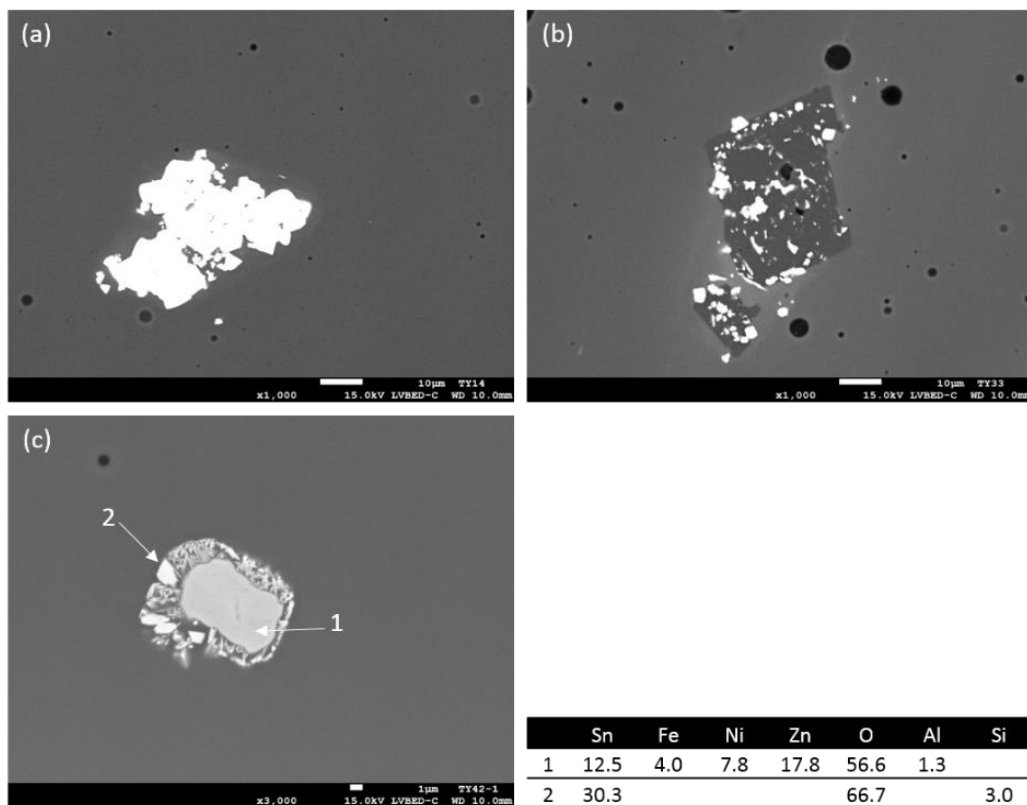


Figure 8.28: The microstructure of green glass from Daoye. (a) The lead tin oxide without nepheline in DY14; (b) the lead tin oxide (bright crystal) and nepheline (dark crystal) in DY33; (c) the tin remains in TY42-1. (The table shows the atomic% of inclusions in (c).)

8.3.2.7. The aqua glass

Only two aqua glasses, JXL41 and JXL49, were analysed; both are *waste* glasses from Jiuxianglan and are m-Na-Al glass. JXL41 has 0.2% CuO and 1.2% FeO, while in JXL49 negligible amounts of CuO and FeO were found. The two samples are fully transparent, with no silica relics but a few zircons (Figure 8.29). The lack of bubbles and silica relics indicates that the microstructure of aqua glass waste does not resemble the microstructure of the glass beads from Jiuxianglan. Although one can argue that the aqua glass may be used as a base for the colouring, there are no supporting archaeological finds related to colouring at the site, nor aqua coloured beads. This raises a question about the relationship between the glass beads and glass waste from Jiuxianglan.

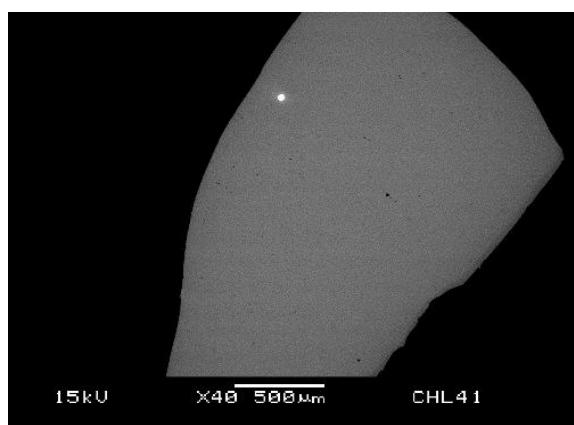


Figure 8.29: The relatively homogeneous matrix in the aqua glass from Jiuxianglan (JXL41).

The bright inclusion is zircon.

9. Results: chemical composition – part II: v-Na-Ca glass, other glass composition and summary

9.1. Introduction

This chapter discusses the result of v-Na-Ca glass (section 9.2), potash glass, soda lime silica glass and lead silicate glass (section 9.3) and culminates with a summary of the chemical analysis. An overview of chemical groups and the results of m-Na-Al glass is provided in Chapter 8, and the chemical composition of each sample is provided in Appendix 2.

9.2. v-Na-Ca glass

9.2.1. Chemical composition related to the base glass

V-Na-Ca glass, found around the South China Sea region, is often thought to be of Western Asian origin, and three primary sub-groups have been recently suggested (Dussubieux and Allen 2014; Dussubieux 2014) (Table 9.1 and Chapter 5.2.3). The average composition of v-Na-Ca glass from each site is shown in Table 8.1. A closer comparison between the characteristic chemical compositions of the glass from the study sites and the reported sub-groups, however, reveals a rather complex pattern. As shown in Figure 9.1, a broad similarity can probably be identified with the glass analysed here and the reported v-Na-Ca 2 and v-Na-Ca 3 sub-groups based on the contents of Ti (titanium) and Zr (zirconium) (Figure 9.1 (d)), but there are overlaps in the minor and major compositions between these groups (Figure 9.1 (a), (b) and (c)). Essentially, the samples analysed do not fit well with the sub-groups reported by Dussubieux.

Table 9.1: The characteristic chemical composition of Southeast Asian v-Na-Ca glass sub-groups reported in Dussubieux (2014).

SiO ₂ (%)	Al ₂ O ₃ (%)	Na ₂ O (%)	K ₂ O (%)	MgO (%)	CaO (%)	Ti (%)	Zr (ppm)
v-Na-Ca 1 (lowest Al ₂ O ₃ , highest CaO, fairly high Ti and Zr)							
65.7±2.90	1.4±0.40	16.4±1.90	2.6±0.80	3.5±1.20	7.2±1.70	0.11±0.05	287±183
v-Na-Ca 2 (highest Na ₂ O, highest MgO, lower CaO)							
66.6±4.00	2.4±0.60	17.6±2.70	2.00±0.30	4.9±1.00	4.50±0.70	0.10±0.03	94±27
v-Na-Ca 3 (lowest Na ₂ O, moderate Al ₂ O ₃ and CaO, relatively low Ti and Zr)							
66.40±3.80	2.20±0.70	14.60±1.50	3.00±0.40	4.20±0.70	6.30±1.10	0.04±0.02	53±35

However, some chemical differences can be observed between samples found at Guishan, Kiwulan and Shisanhang. Figure 9.1 (a) shows that samples from Guishan generally contain higher Al₂O₃ (>2.5%), while those from Shisanhang have lower Al₂O₃ (<2%) than Guishan and most Kiwulan samples. The samples from Kiwulan contain moderate Al₂O₃ (1.5-3%) and some of them cluster with Shisanhang samples. In Figure 9.1 (b), the Guishan samples contain lower MgO (<3.5%) and K₂O (<2.5%), and the Shisanhang samples have higher MgO (>4%) and K₂O (>2.5%). The Kiwulan samples have moderate MgO and K₂O, and again generally cluster with Shisanhang samples. In Figure 9.1 (c), the Guishan samples show a negative linear CaO-Na₂O correlation not seen in other samples.

These differences taken together probably indicate different sources of glass arriving at Guishan, Kiwulan and Shisanhang as they do not conform to a single analytical group. In particular, the varied MgO-K₂O pattern may suggest the use of different plant species and/or plants procured from different geological environments.

The samples from Xiliao contain MgO higher than 3.5%, K₂O higher than 3% and Na₂O lower than 15%, which more or less cluster with Kiwulan and Shisanhang samples, but a higher value of Al₂O₃ (>2%) is found in the samples from Xiliao. WJC20, from Wujiancuo, is an outlier and has Al₂O₃ at 3%, K₂O at 1.8% and MgO at 3%. The three Jiuxianglan samples (JXL43, JXL46 and JXL47), which are all glass waste, show a dispersed range of chemical compositions and therefore no clear grouping of these glasses can be suggested for this site.

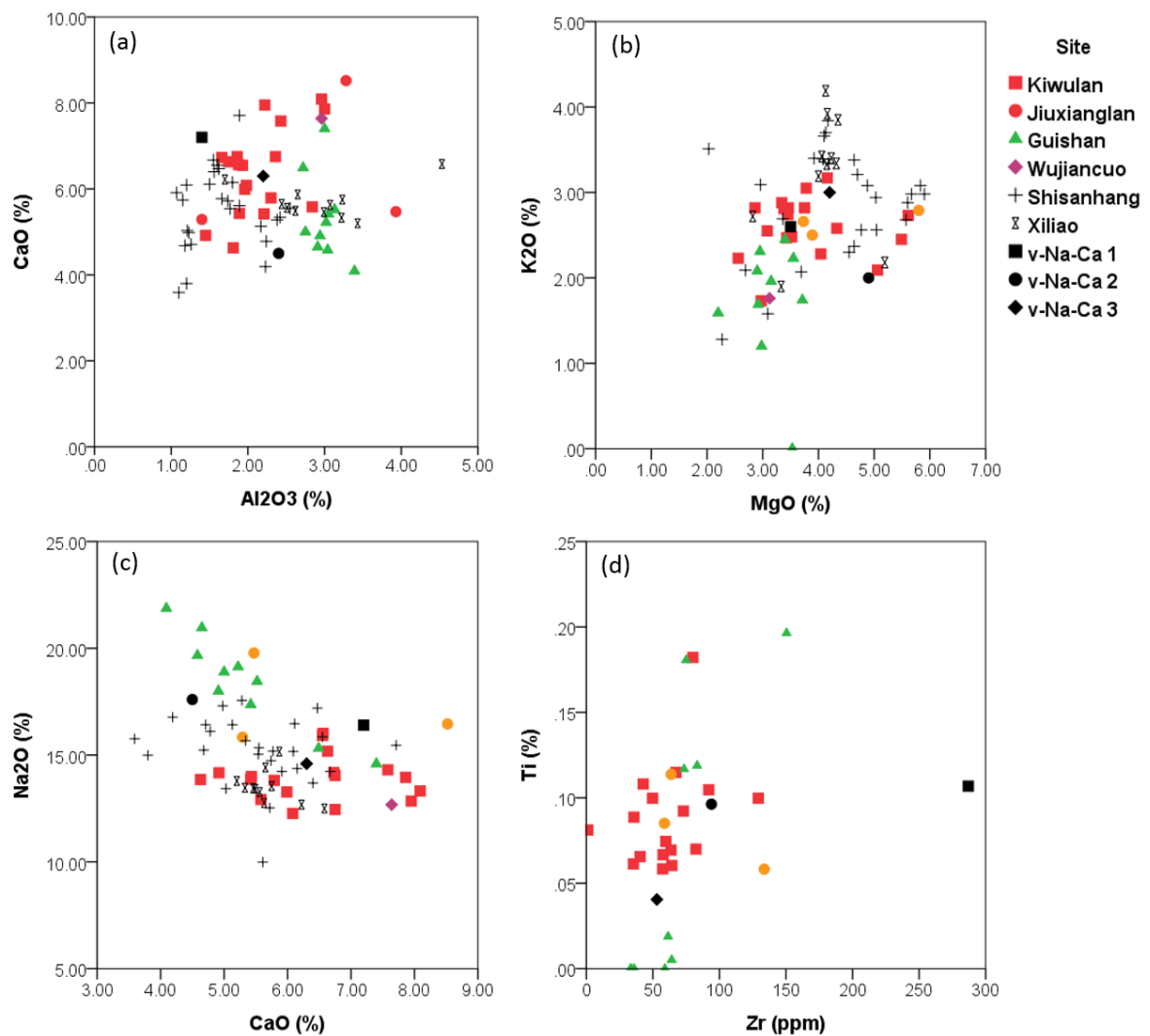


Figure 9.1: The bi-plots of (a) Al₂O₃-CaO, (b) MgO-K₂O, (c) CaO-Na₂O and (d) Zr-Ti in v-Na-Ca glass. The black symbols show the average value of the v-Na-Ca 1, v-Na-Ca 2 and v-Na-Ca 3 sub-groups.

9.2.1.1. The Al₂O₃, Zr and Ce relationship

Figure 9.2 shows the bi-plots of Al₂O₃-Ce and Zr-Ce in samples from Kiwulan, Guishan and Jiuxianglan. Most of the samples contain Ce concentrations higher than 7 ppm and Zr higher than 30 ppm, except for the sample KWL006 (KWL-LL04 style). In the yellow glass of LL05 type from Kiwulan and the blue glass of GS-B2 type from Guishan, a generally rough linear Al₂O₃-Ce correlation can be observed, which may indicate the introduction of Ce mainly with Al₂O₃ from the sand (Mirti *et al.* 2009: 1066). This correlation, however, is not observed in the Guishan samples of GS-DB1 type (dark blue glass).

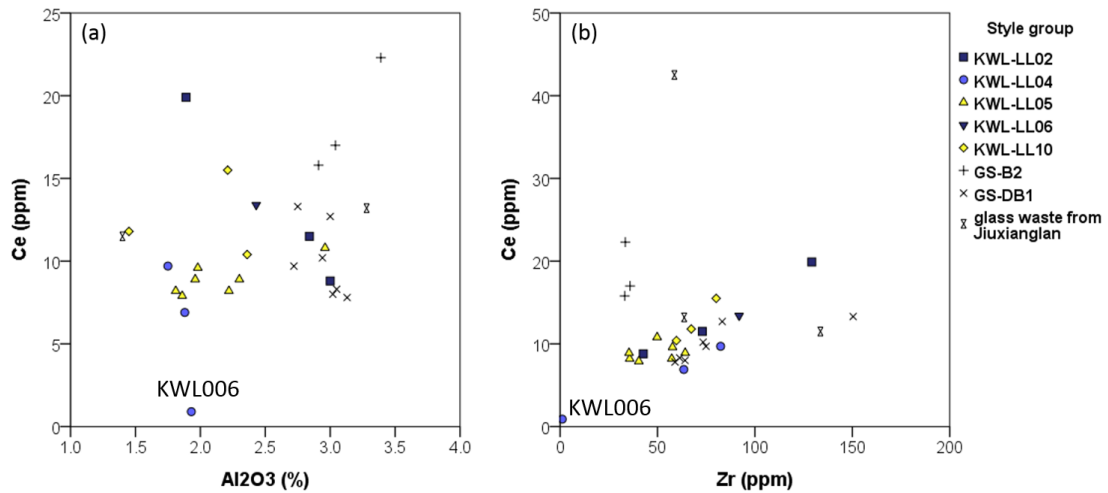


Figure 9.2: The bi-plots of Al₂O₃-Ce and Zr-Ce in the v-Na-Ca glass. The symbol colours of Kiwulan samples present the colour of sample in each typological group. JXL46 has relatively high Ce content (42.5 ppm) and is not shown here

A linear correlation is seen for the samples in the Zr-Ce bi-plot with the exception of GS-B2 type (Figure 9.2 (b)), and this elevated Zr content is also correlated with the Ti content. This is particularly noteworthy in the samples from Guishan, where the different Al₂O₃-Ce and Zr-Ce patterns may suggest the use of different sand sources for GS-B2 and GS-DB1 types.

A dispersed pattern is also seen in the *waste* from Jiuxianglan. One sample has relatively high values of Ce (40 ppm), while the other two have Ce contents around 13 ppm. Therefore, no similar groups can be identified within the samples from Jiuxianglan or between Jiuxianglan and the other sites.

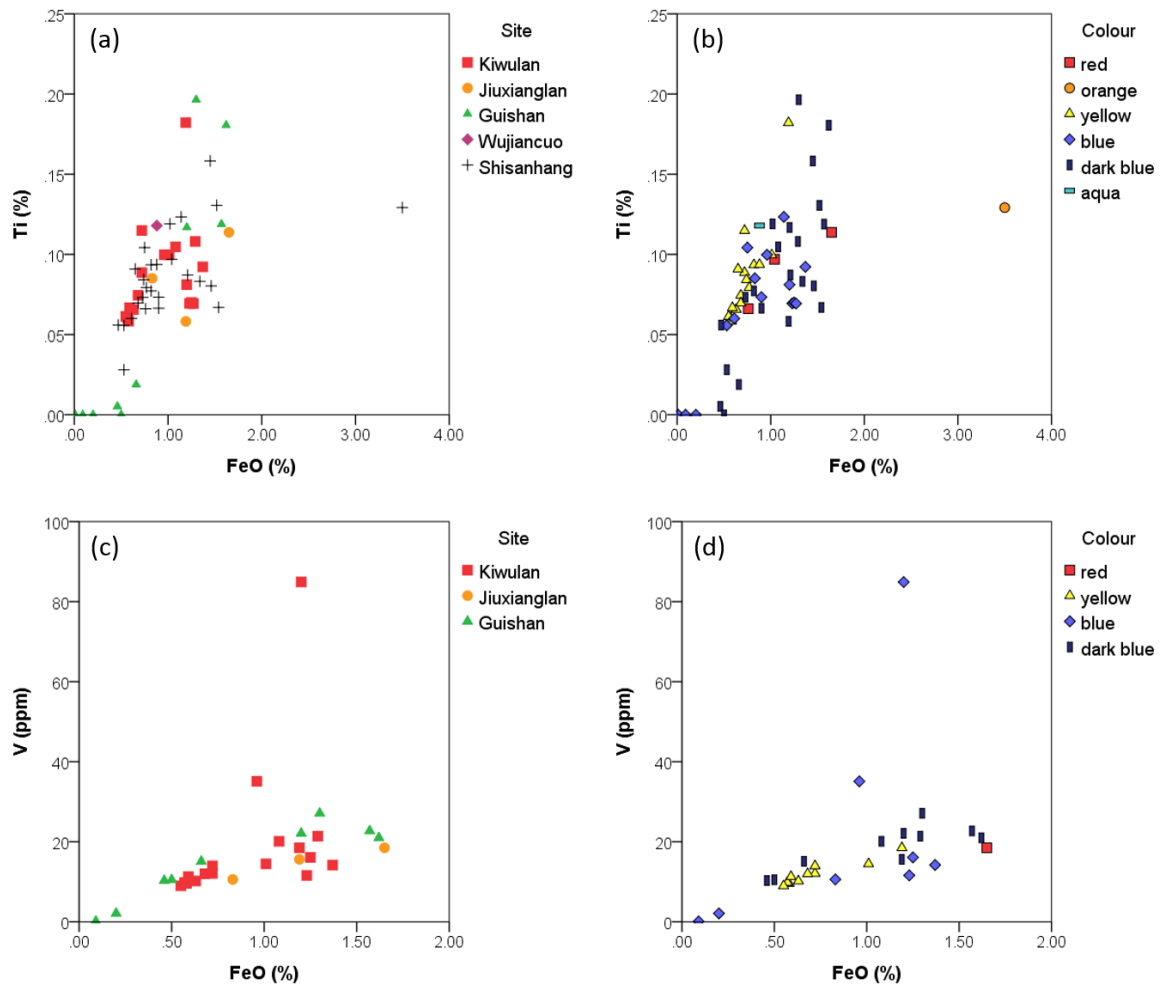


Figure 9.3: The bi-plot of FeO-Ti and FeO-V in the *v*-Na-Ca glass. (a) and (c) by site, (b) and (d) by colour.

9.2.1.2. The FeO, Ti and V relationship

In the FeO-Ti and FeO-V bi-plots (Figure 9.3), a rough linear FeO-Ti and FeO-V correlation is observed. A closer investigation reveals a strong correlation particularly in the yellow glass

from Kiwulan and Shisanhang ($R^2 = 0.744$ in FeO-Ti and 0.889 in FeO-V) (Figure 9.3 (b) and (d)). This may suggest that the principal FeO content in the yellow glass is derived from an impure sand containing Fe-bearing ingredients. If this is case, the slightly elevated contents of FeO in the v-Na-Ca glass in this research differ from the contents of unintentionally added FeO in the Western Asian soda plant ash glass (typically <1%) (e.g. Freestone and Gorin-Rosen 1999; Mirti *et al.* 2008; Mirti *et al.* 2009).

9.2.1.3. The MnO contents

An examination of the FeO-MnO relationship has shown that the dark blue glass from Guishan contains low MnO (<0.3%), while for the dark blue samples from Kiwulan, Shisanhang and Xiliao, MnO is higher than 0.5% (Figure 9.4 (a) and (b)). The FeO contents, however, do not show variations. The low MnO contents in the Guishan samples may suggest an unintentional addition with the colourant (see below), whilst the higher values may suggest MnO was deliberately added (Sayre 1963; Brill 1988; Jackson 2005), and it may be associated with the introduction of a base glass chunk/fragment used to be coloured. This suggests a different source of the dark blue glass beads at Guishan compared to Kiwulan, Shisanhang and Xiliao.

The deliberate addition of MnO in the base glass is more obviously identified in the yellow glass. Figure 9.4 (b) and (c) shows that the yellow glass from Kiwulan and Shisanhang contains MnO and FeO above 0.5% (except for KWL013 and KWL-GB-1468). Two samples of SSH-Type14 from Shisanhang have MnO concentrations above 2%. MnO is not used for producing yellow glass, in which the colourant is usually lead tin oxide (see section 9.2.2.2). Therefore, it is very likely that manganese was introduced as a decolourant in the base glass (Sayre 1963; Chapter 4.2). In this case, this may suggest that the imported v-Na-Ca glass was recycled or re-melted for the local production of glass beads around the South China Sea. A comparison

between the yellow glass made of v-Na-Ca and m-Na-Al glass could support such assumption. Figure 9.4 (d) shows that the v-Na-Ca glass (except KWL013 and KWL-GB-1468) contains a higher MnO content than the m-Na-Al glass.

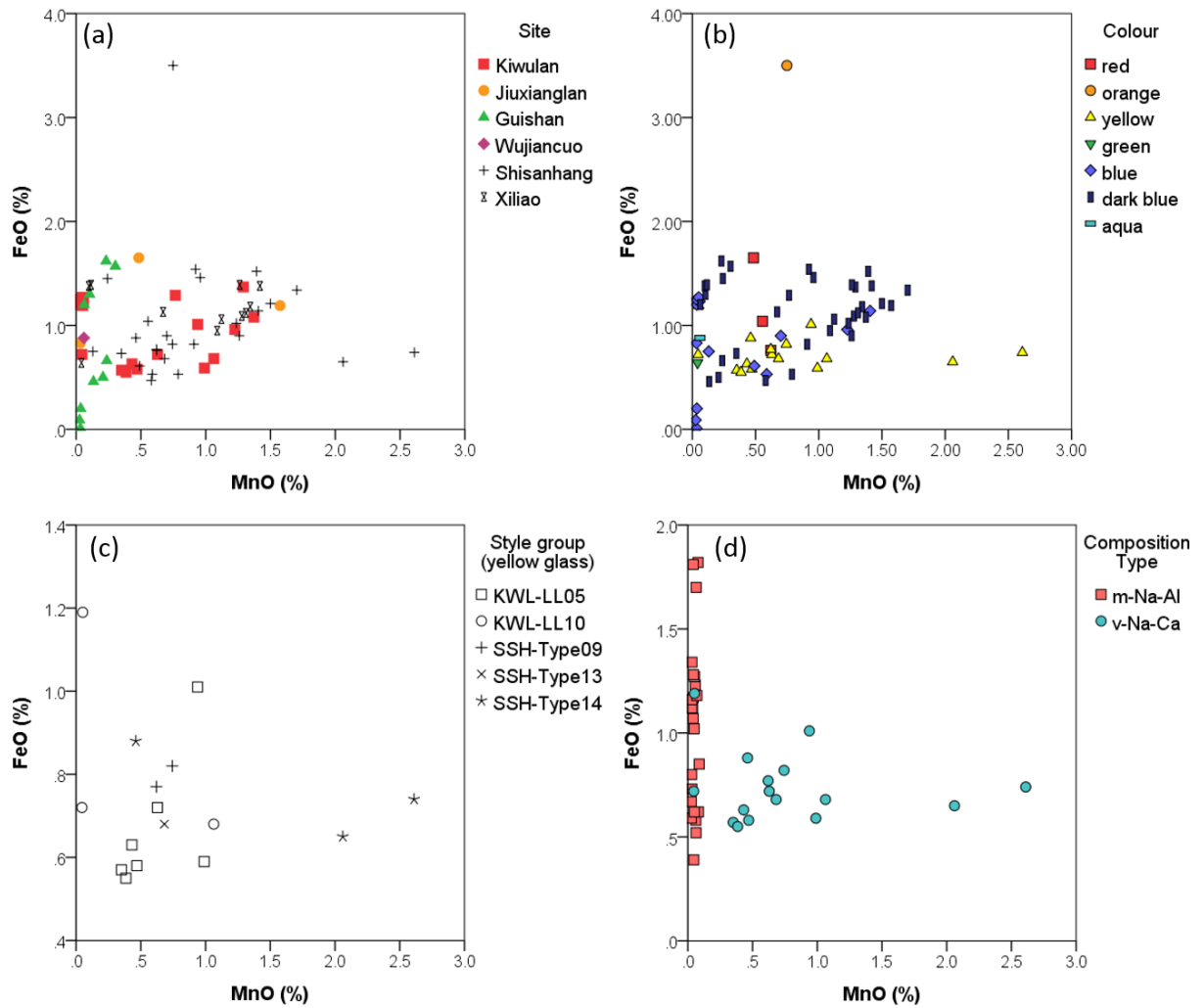


Figure 9.4: The bi-plots of FeO-MnO in the v-Na-Ca glass: (a) by site; (b) by colour; (c) yellow glass only; (d) yellow glass by chemical group.

9.2.2. Microstructure and chemistry of the colourants

The matrix of the v-Na-Ca glass is relatively homogeneous compared to the m-Na-Al glass.

The inclusions or crystals seen under the SEM are mostly associated with the colourants.

Therefore, the following section is structured by colour.

9.2.2.1. The red glass

Three red v-Na-Ca glasses, including 2 glass beads from Shisanhang and 1 glass waste fragment from Jiuxianglan, are coloured by Cu_2O (cuprite), but even though the copper content is shown as CuO in the chemical data (Appendix 2). In the two Shisanhang samples the, content of CuO is less than 0.3%, but it is 1.3% in the Jiuxianglan sample.

The microstructure of the red v-Na-Ca and m-Na-Al glasses are similar, both contain a few bubbles of less than $50\ \mu\text{m}$ diameter and many copper-based nano sized particles, which could be cuprite or metallic copper, dispersed through the matrix. Large inclusions of Cu_2S ($\sim 10\ \mu\text{m}$) are also found in the red glass, as shown in Figure 9.5. This suggests that the source of colourant and the colouring processes may be similar in the two glass types (see 8.3.2.1).

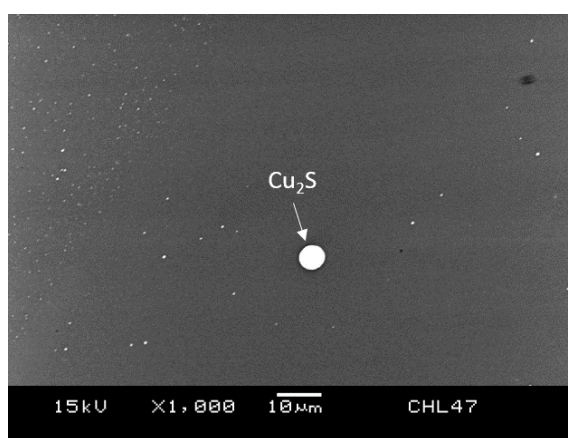


Figure 9.5: The Cu_2S particle in the red v-Na-Ca glass waste from Jiuxianglan (JXL47).

Table 9.2 shows the copper-containing glasses contain trace concentrations of PbO , SnO_2 , Co , Ni , Zn , As , Ag and Sb . Higher Sb is found in the red v-Na-Ca glass (JXL47) in comparison to the red m-Na-Al glass (1-25 ppm, Table 8.4). This discrepancy may be due to the use of different copper sources for colouring the two glasses or different base glasses, one containing antimony.

Table 9.2: The average, maximum and minimum value of PbO (%), SnO₂ (%), Co (ppm), Ni (ppm), Zn (ppm), As (ppm) and Sb (ppm) in v-Na-Ca glass coloured by Cu-based colourant.

		Red (n=1)	Blue (n=9)	Dark blue (n=11)
PbO (%)	Mean	0.34	0.25	0.16
	Max.		2.02	0.69
	Min.		0.00	0.02
SnO ₂ (%)	Mean	0.06	0.02	0.00
	Max.		0.13	0.02
	Min.		0.00	0.00
Co (ppm)	Mean	5.3	100.1	399.3
	Max.		348.8	850.0
	Min.		0.0	5.9
Ni (ppm)	Mean	53.2	14.2	48.7
	Max.		30.0	97.1
	Min.		0.0	31.4
Zn (ppm)	Mean	51.9	72.6	308.2
	Max.		245.3	1353.3
	Min.		2.1	8.2
As (ppm)	Mean	31.2	15.4	13.7
	Max.		44.8	42.0
	Min.		4.7	4.2
Ag (ppm)	Mean	8.4	3.6	1.1
	Max.		19.0	3.7
	Min.		0.3	0.1
Sb (ppm)	Mean	114.6	4.5	3.8
	Max.		12.4	11.0
	Min.		0.3	0.8

9.2.2.2. The yellow glass

The yellow v-Na-Ca glass is coloured by lead tin oxide, and contains PbO (6-12%) and SnO₂ (below 0.5%). In this research, yellow v-Na-Ca glass is only found in beads from Kiwulan and Shisanhang. Microstructural analysis was conducted on 10 samples from Kiwulan.

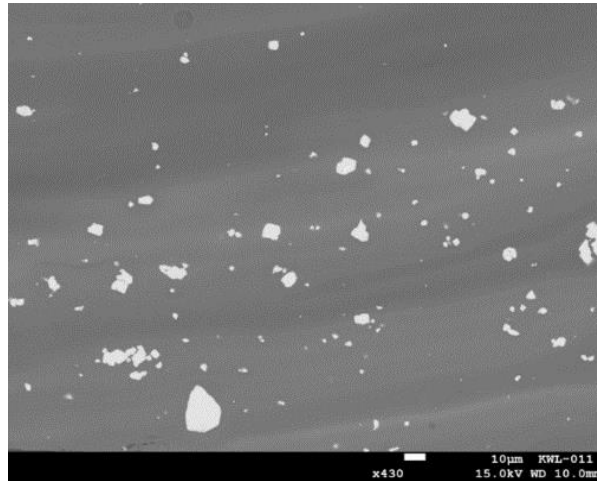


Figure 9.6: The non-homogeneous matrix of yellow v-Na-Ca glass (KWL011). The white crystals are lead tin oxide.

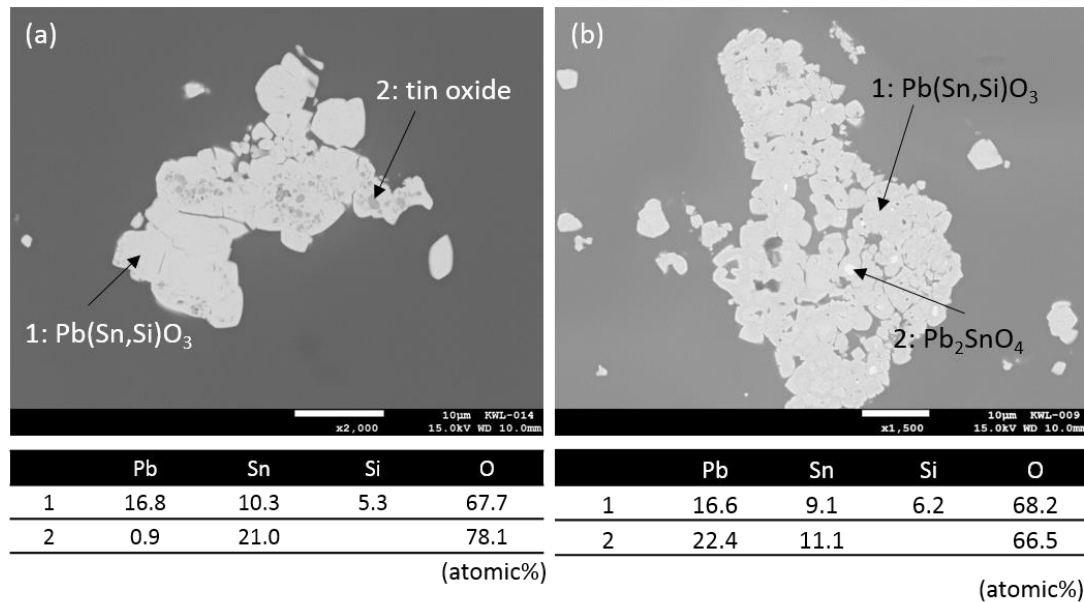


Figure 9.7: The crystals related to the yellow colourant in the v-Na-Ca glass. (a) the lead tin oxide (1) and tin oxide crystals (2) (KWL014); (b) The $Pb(Sn,Si)O_3$ (1) and Pb_2SnO_4 (2) crystals (KWL009).

Figure 9.6 shows the yellow glasses exhibit a heterogeneous matrix. The bright matrix contains higher concentrations of PbO (~18%) compared to the dark matrix (~9%). As in the case of m-Na-Al glass, the lead tin oxide is found to be $Pb(Sn,Si)O_3$.

The microstructure suggests the possible addition of a lead tin oxide yellow colourant into the glass to produce yellow glass. Figure 9.7 (a) shows the tin oxide phase within $\text{Pb}(\text{Sn},\text{Si})\text{O}_3$ in some cases. This is similar to the observation reported in Heck *et al.* (2003), in which the tin oxide is found within the core of lead tin oxide crystals and the authors suggest the introduction of lead tin yellow pigment into the base glass. In some samples, the presence of (possibly) a Pb_2SnO_4 phase (Pb/Sn atomic ratio of 2) is observed in the $\text{Pb}(\text{Sn},\text{Si})\text{O}_3$ crystal (Figure 9.7 (b)). In most of the samples, the lead tin oxide crystal seldom clusters with any silicate crystals, the only exception being KWL010, in which an aggregate of lead tin oxide and wollastonite is found.

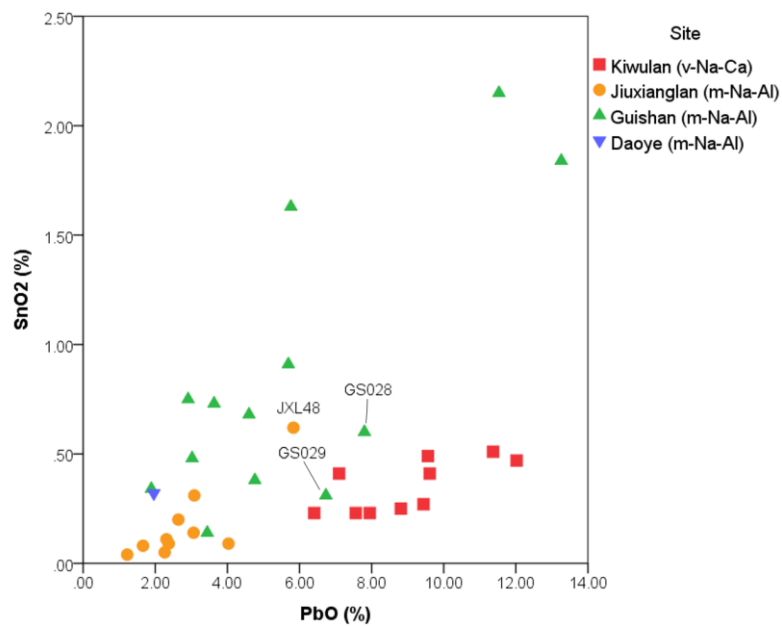


Figure 9.8: The PbO-SnO_2 bi-plot of the yellow v-Na-Ca and m-Na-Al glass.

A closer comparison between the PbO and SnO₂ contents of yellow v-Na-Ca glass and m-Na-Al glass has indicated there may be different recipes used for lead tin oxide colourants in the beads found at different sites. Figure 9.8 shows the v-Na-Ca glass from Kiwulan contains higher PbO and the PbO/SnO₂ ratio is between 15 and 35. The m-Na-Al glass from Jiuxianglan has lower values of PbO and SnO₂, and a more dispersed range of PbO/SnO₂ ratio from 10 to 45.

The Daoye and Guishan samples (all m-Na-Al glass) cluster and a wider range of PbO and SnO₂ is found, but with a ratio of less than 8 (except GS028 and GS029 (of the GS-Y2 type) which have higher ratios). These differences in the PbO-SnO₂ relationship in the yellow v-Na-Ca glass and m-Na-Al glass are probably associated with the use of different recipes of lead tin oxide used to produce the yellow colour. In the case of the m-Na-Al glass, the varied PbO-SnO₂ pattern seen between sites, and between the bead types in Guishan, is consistent with the microstructural results which may indicate different traditions of producing yellow glass using different raw materials and possibly different production technologies (Chapter 8.3.2.5). Therefore, the yellow glass beads from different sites may have different origins.

Another difference between the yellow v-Na-Ca and m-Na-Al glass is the content of Sb. Figure 9.9 (a) shows higher contents of Sb (10-130 ppm) and MnO (>0.3%) are found in the v-Na-Ca glass compared to the m-Na-Al glass (except KWL013 and KWL-GB-1468). The MnO content is thought to be related to the base glass used (see section 9.2.1). The presence of Sb, however, is more complex. The slightly elevated level of Sb does not suggest intentional addition and might reflect the recycling of v-Na-Ca glass fragments of Western Asian origin in Southeast Asian workshops, although the level of Sb is usually relatively low at trace elemental level or even not detected in contemporary Sassanian or Islamic glass (Brill 1999; 2001; Mirti *et al.* 2008; Mirti *et al.* 2009). Alternatively, the presence of antimony in v-Na-Ca glass may be associated with lead tin oxide used to colour the glass. In the SnO₂-Sb and PbO-Sb bi-plots shown in Figure 9.9 (b) and (c), Sb is generally correlated with PbO and SnO₂ in the v-Na-Ca glass. Similar to the Sb concentration, contents of As (>10 ppm), Ni (>10 ppm) and Zn (>30 ppm) are also higher in the v-Na-Ca glass than in the m-Na-Al glass (Figure 9.9 (d), (e) and (f)), which suggests two possibilities: (1) a different geological deposit/source of lead tin oxide is used in the yellow v-Na-Ca glass compared to m-Na-Al glass, or (2) the elevated levels of these elements are attributed to recycled base glasses. As yet the interpretation is inconclusive

but may be elucidated with the discovery and analysis of production debris (although as yet, there is little evidence for this). It also requires a greater understanding of the raw materials used to produce lead tin oxide in contemporary Western Asia, as these yellow v-Na-Ca glass beads may have been imported as finished objects from Western Asia to the South China Sea region.

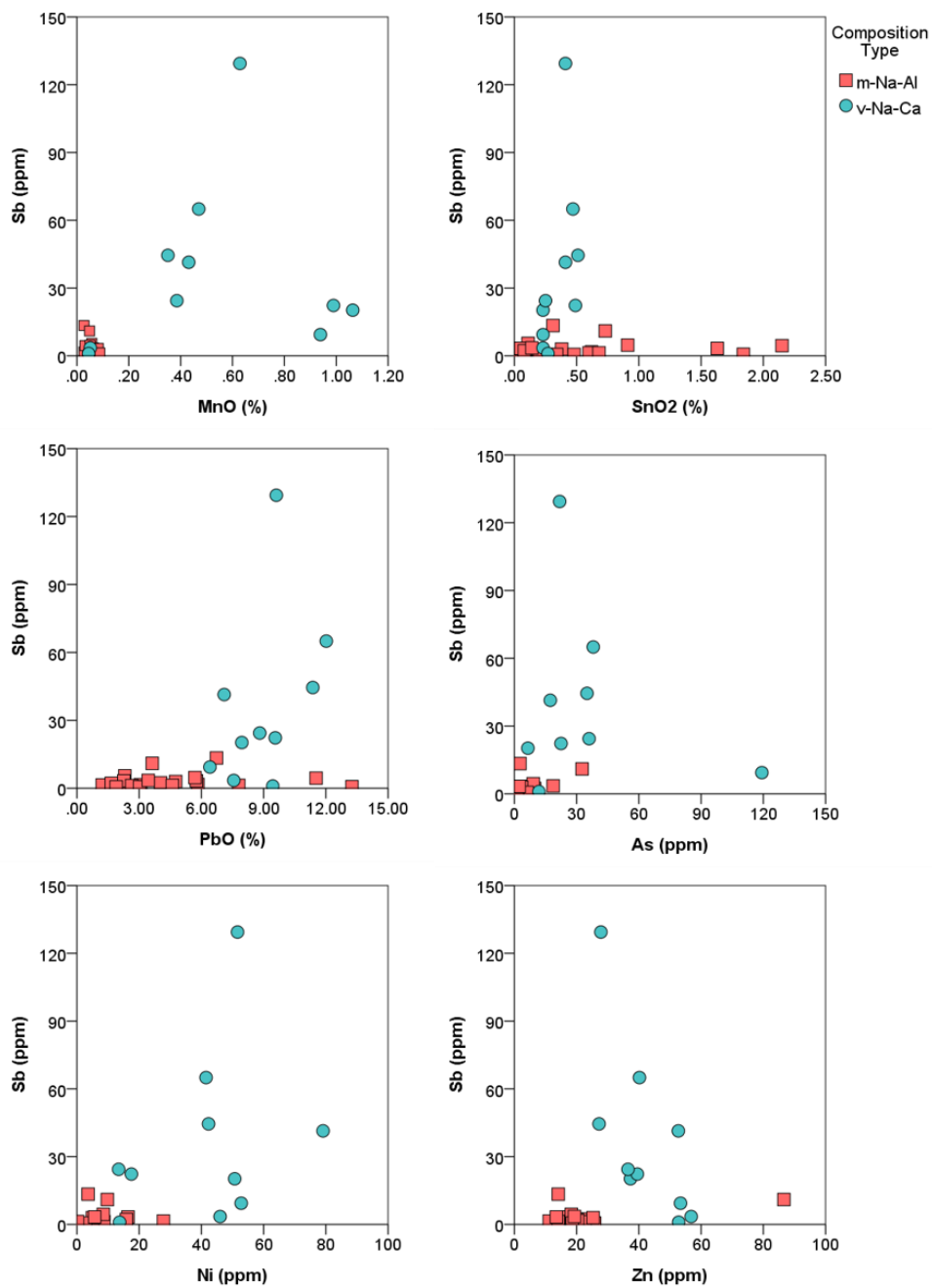


Figure 9.9: The bi-plots showing (a) MnO-Sb, (b) SnO₂-Sb, (c) PbO-Sb, (d) As-Sb, (e) Ni-Sb

and (f) Zn-Sb of the yellow v-Na-Ca and m-Na-Al glass.

9.2.2.3. The light blue and dark blue glass

The light blue glass is coloured by copper oxide. The light blue beads from Guishan (n = 3) contain CuO at around 0.4%, while beads from Kiwulan have lower CuO concentrations of around 0.1%. The CuO-Co bi-plot (Figure 9.10) shows that two light blue beads of KWL-LL04 type (KWL-GB305-1 and KWL007) contain a higher Co concentration of 90 and 140 ppm than the other light blue beads, suggesting that cobalt may also contribute to the blue tint of these two samples. For the other samples, the light blue beads from Shisanhang (n=5) show a CuO content lower than 0.2%, but the Co content was not analysed in the original report (Tsang and Liu 2001: 91-106). The light blue glass waste from Jiuxianglan contains a high concentration of CuO (~1%) and negligible Co content.

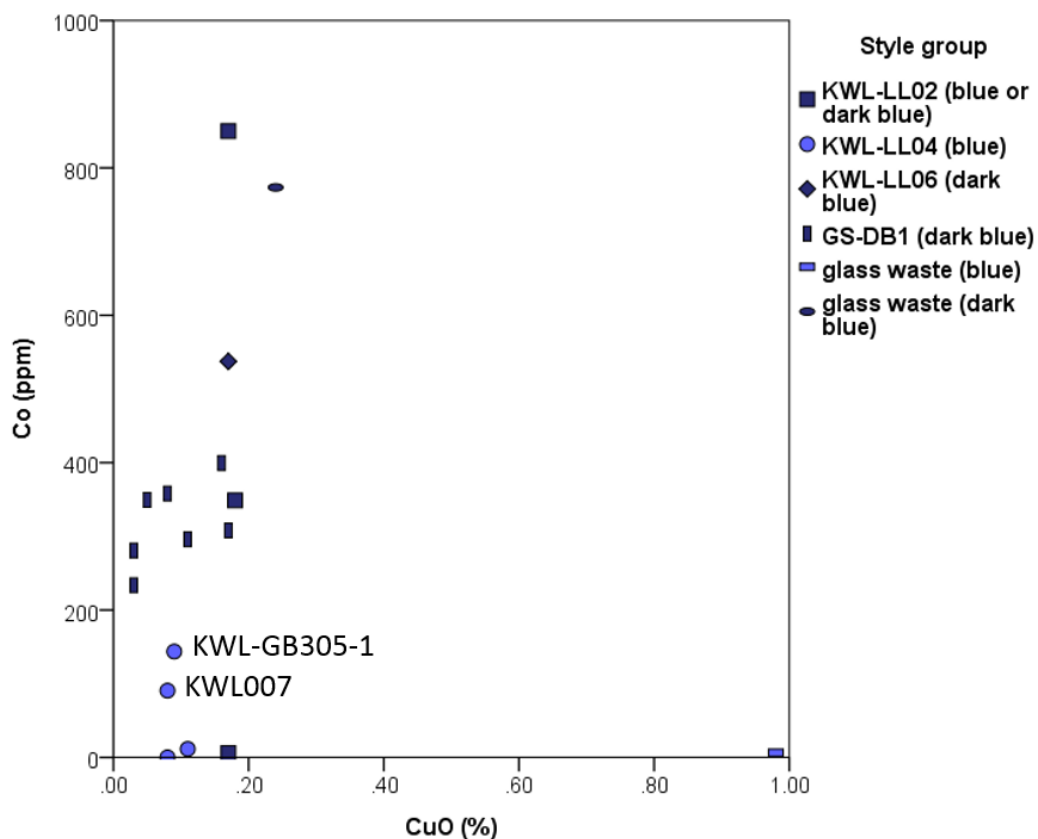


Figure 9.10: The CuO-Co bi-plot of blue and dark blue v-Na-Ca glass.

The dark blue glass is coloured by cobalt, which ranges between 200-400 ppm in the Guishan beads ($n = 7$), 350-850 ppm in the Kiwulan beads ($n = 3$) and is 770 ppm in the *waste* from Jiuxianglan (Figure 9.10). No cobalt concentrations were analysed in glass beads from Shisanhang (Tsang and Liu 2001: 91-106) and Co was not detected in beads from Xiliao (possibly because Co is below detection by XRF) (Chen and Cheng 2011).

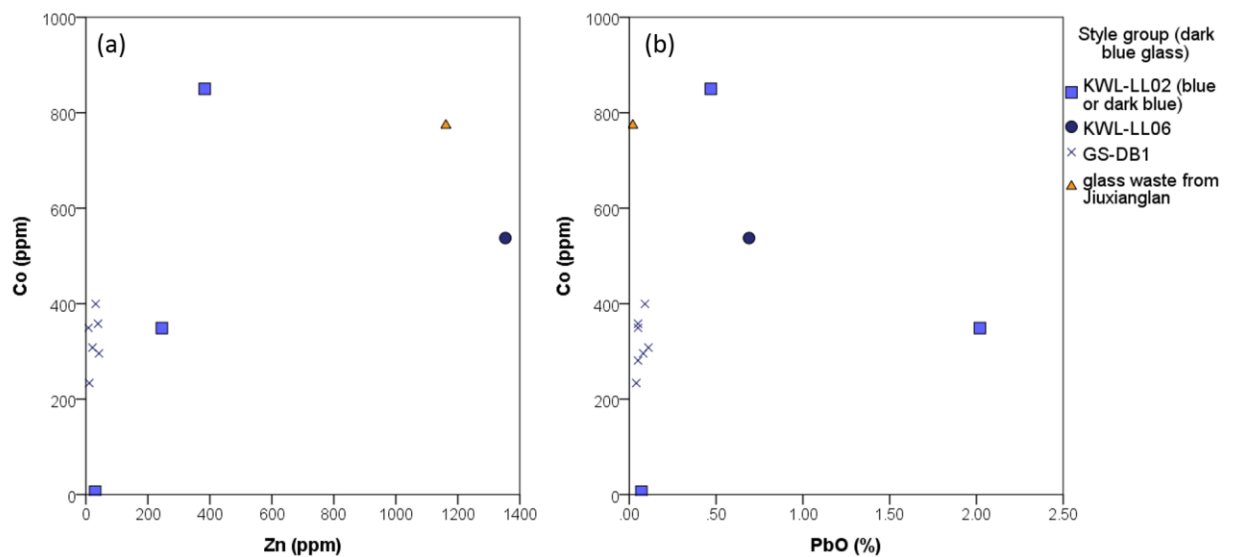


Figure 9.11: The Co-Zn and PbO-Zn bi-plots of blue and dark blue v-Na-Ca glass.

The differentiation between dark blue samples from Kiwulan, Guishan and Jiuxianglan can be observed in the chemical composition. The concentrations of Zn and PbO show different patterns in the dark blue glasses from Guishan, Kiwulan and Jiuxianglan. Figure 9.11 (a) shows the Guishan samples contain almost negligible level of Zn, while dark blue beads from Kiwulan and dark blue glass waste from Jiuxianglan have Zn concentrations above 200 ppm. Low concentrations of PbO are found in the dark blue beads from Guishan and the dark blue glass waste from Jiuxianglan, but higher concentrations, at around 0.5%, are found in two samples from Kiwulan (Figure 9.11 (b)). This suggests that the dark blue glass waste from Jiuxianglan does not match any of the dark blue glass beads analysed in this research. The relatively high PbO concentration (~2%) in sample KWL002 (KWL-LL02 type) from Kiwulan is attributed to

the presence of lead tin oxide (see below), and therefore it is not relevant to the discussion of cobalt sources here.

These chemical differences possibly suggest different geological sources of cobalt ores used in colouring the dark blue glass (e.g. Gratuze *et al.* 1996). Considering the chronology and location of Guishan (late 1st millennium AD, southern Taiwan) and Kiwulan site (7th-12th century AD, northeastern Taiwan), this suggests different origins for the dark blue glass beads at the two sites. This difference in provenance of the beads may be attributed to the supply of dark blue glass at different periods in the South China Sea network or to the different exchange partners between local areas in Taiwan and the South China Sea. Taken together with the possible recycling or re-melting of v-Na-Ca glass discussed in section 9.2.1.3, this also raises an issue in terms of the nature of the exchange of glass between Southeast Asia and Western Asia and the possibility that dark blue glass may have been produced using local raw materials in Southeast Asia. However, there is a lack of information about which cobalt ores were exploited in ancient Western Asia or Southeast Asia, which hinders further discussion of the origin of dark blue glass around the South China Sea region.

Microstructural analysis was performed on 7 samples: 3 light blue beads from Kiwulan and 1 light blue waste from Jiuxianglan, 2 dark blue beads from Guishan and 1 dark blue waste from Jiuxianglan. All have homogeneous matrices displaying little microstructural information to allow comparison. However, two samples of KWL-LL02 type (KWL001 and KWL002) from Kiwulan with a dual colour system did display microstructural features and will be addressed in the next section.

9.2.2.4. The glass with an orange surface and blue body (KWL-LL02 type)

KWL-LL02 typological group is an unusual style of glass bead. It has an orange surface but a glass- or clay/sand-made body. This type has only been found at Kiwulan and Shisanhang in Iron Age Taiwan; the full typological information for these beads is provided in Chapter 7.2. Two samples (KWL001 and KWL002) of KWL-LL02 type were analysed under the electron microscope. The results reveal that the orange surface is made of m-Na-Al glass in both samples (section 8.3.2.3, p178). In KWL001, a red interlayer can be seen, which has a m-Na-Al glass composition. The inner core body of KWL001 is made of v-Na-Ca glass, while in KWL002 a more complicated situation is observed.

Figure 9.12 shows the results of line analysis on KWL001. It can be seen quite clearly that the outer surface is rich in Al_2O_3 and PbO, while the inner body is rich in MgO. Different CuO concentrations can also be found between the outer surface and the inner body - generally higher CuO is found in the surface area, which declines from the red interlayer to the blue body.

The BSE image is provided in Figure 9.13, and the chemical composition analysed by SEM-EDS is shown in Table 9.3. In Figure 9.13 (a), two distinct sections can be observed. The upper bright grey area is the orange surface, showing an abundance of white particles of copper oxide. The lower dark grey area is the blue body, where a relatively homogeneous matrix is found. A closer look at the red interlayer between the orange surface and the blue body shows that copper oxide particles are hardly found in the red interlayer compared to the orange surface. This microstructural result is consistent with the observation on orange and red m-Na-Al glass discussed in sections 8.3.2.2 and 8.3.2.3.

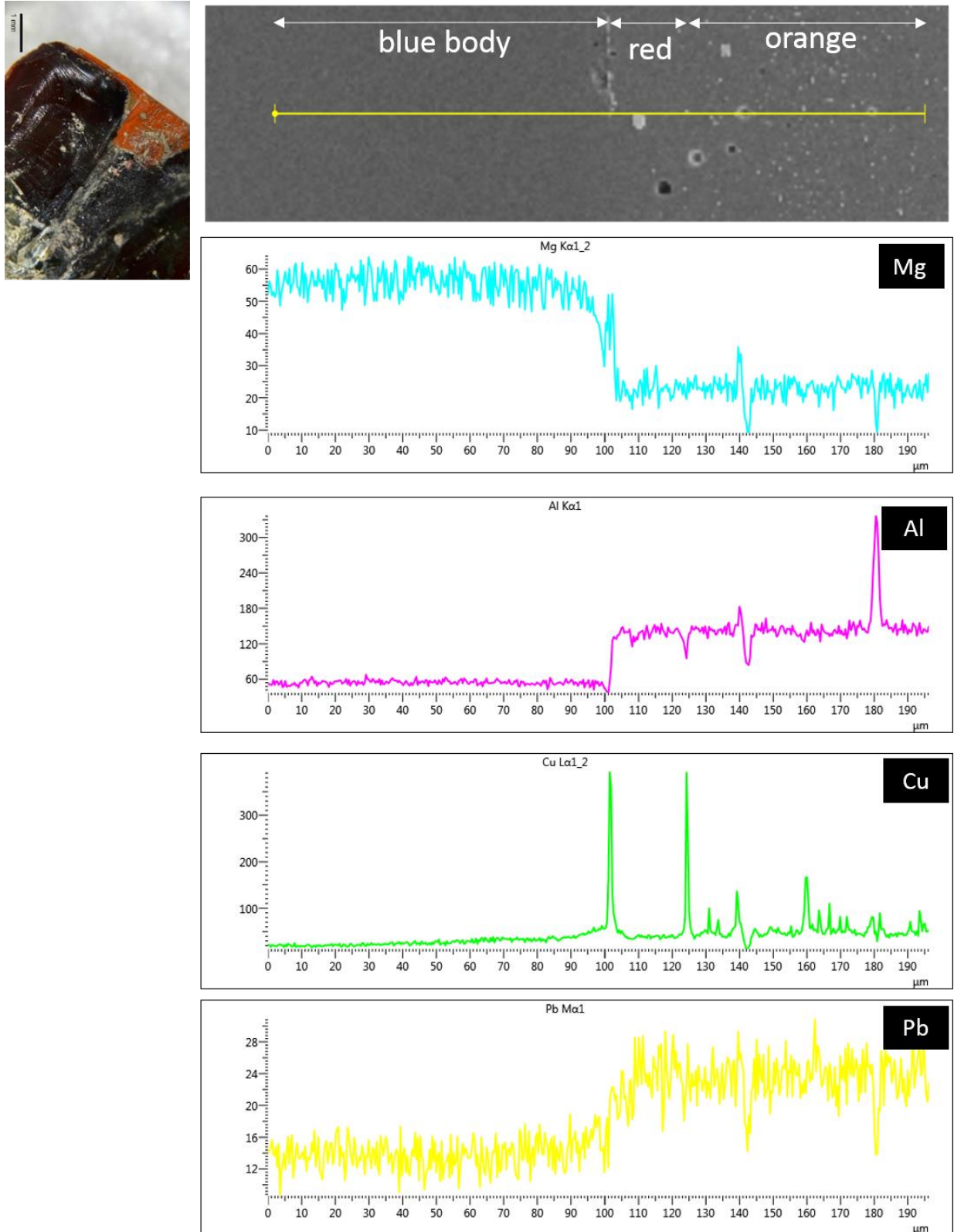


Figure 9.12: The SEM-EDS line analysis of KWL001, showing the distribution of Mg, Al, Cu and Pb.

Table 9.3 shows that the orange surface contains 12% Na₂O, 10% Al₂O₃, 0.7% MgO, 2% PbO and 9% CuO, which fits the typical composition of orange m-Na-Al glass. The red interlayer also shows the characteristics of m-Na-Al glass, with Na₂O of 11%, Al₂O₃ of 10%, MgO of 0.6%, PbO of 1.5% and a slightly lower CuO content of 5%. As for the blue body, the Na₂O content of 12-15% and both Al₂O₃ and MgO of around 3% demonstrate that it is made of v-Na-Ca glass.

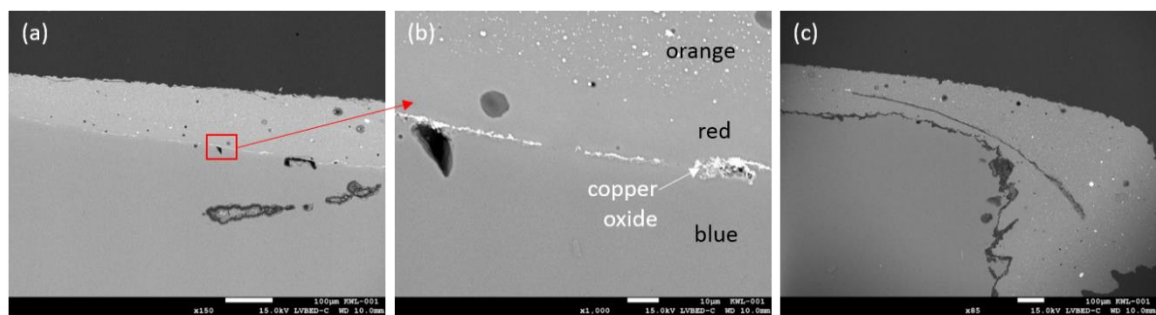


Figure 9.13: The microstructure of KWL001. (a) The upper bright grey layer is the orange surface, while the lower dark grey area is the blue body; (b) a closer look at the interface has shown the aggregates of copper oxide between the red and blue glass; (c) some areas show the loose adherence between surface and body.

Table 9.3: SEM-EDS analysis on different sections of KWL001. (wt%)

	SiO ₂	Al ₂ O ₃	Na ₂ O	K ₂ O	MgO	CaO	FeO	TiO ₂	CuO	SnO ₂	PbO	SO ₃	Cl
orange surface	56.1	9.6	11.9	3.1	0.7	2.9	3.0	1.0	8.8	1.8	2.0		0.7
red interlayer*	60.3	10.0	10.9	3.5	0.6	2.9	2.8	1.1	5.4	2.0	1.6		0.7
blue inner body close to the interlayer*	63.7	2.7	12.1	2.6	2.9	7.2	1.0		6.6			0.2	0.8
blue inner body	65.3	3.0	15.2	3.2	3.5	8.5	0.6						0.7

*: spot analysis

In the blue body, the area closest to the red interface contains higher CuO (Table 9.3 and Figure 9.12). The CuO content of the blue body far from the interface is below the detection limit of

SEM-EDS, but the EPMA result has shown a concentration of 0.2%. This result suggests the diffusion of some copper oxide from the interlayer of the red m-Na-Al glass to the body of the v-Na-Ca glass. In fact, aggregates of copper oxide are frequently identified between the red and blue glass and a tightly combined interface is seen between the m-Na-Al and v-Na-Ca glass (Figure 9.13 (b)). In other areas, a loose adherence between the m-Na-Al and v-Na-Ca glass has been observed, suggesting a lack of interaction between the two types of glass at the boundary.

The line analysis for KWL002 is shown in Figure 9.14. The outer orange surface is Al_2O_3 -rich and MgO-poor, while the inner body shows the reverse. A slight decrease in CuO concentration is also observed from the surface to the body. The line analysis of the PbO content, however, has shown that the orange surface is composed of a PbO-rich outer layer and a PbO-poor inner layer. It also shows that some of the inner body contains PbO-rich areas.

From the chemical composition shown in Table 9.4, it can be confirmed that the orange surface is made of m-Na-Al glass, with a Na_2O content of around 13%, Al_2O_3 of around 10% and MgO of 0.6%. The PbO-rich sub-layer contains PbO of 4%, while the PbO-poor sub-layer has higher FeO of 3% and slightly higher Cl at 0.6%. In terms of the inner body, the microstructural analysis surprisingly reveals a relatively heterogeneous microstructure that may indicate the mixing of v-Na-Ca glass and some other earth materials which may be clay or sand (Figure 9.15). Generally, a glassy matrix is found, and the chemical composition of around 14% Na_2O , 2% Al_2O_3 and 5% MgO suggests a similarity to the v-Na-Ca glass. The SEM-EDS analysis indicates that a higher CuO content can be detected in the areas close to the interface (Table 9.4) as in the case in KWL001, and a 'cluster' of copper oxide can also be found at the interface (Figure 9.15 (a)). Also, PbO-rich areas are frequently found in the inner body, containing lead tin oxide ($\text{Pb}(\text{Sn},\text{Si})\text{O}_3$) (Table 9.4 and Figure 9.15 (a)).

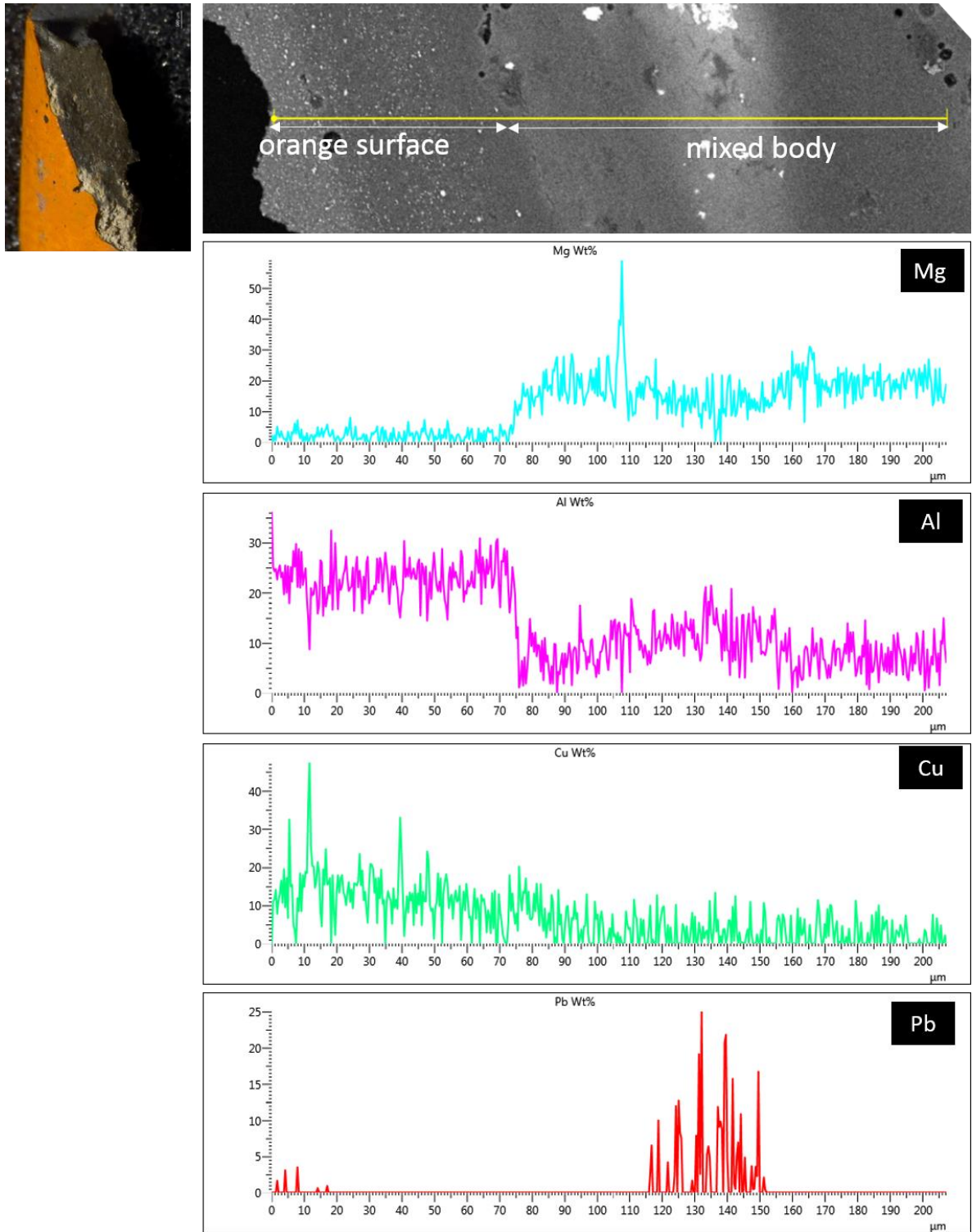


Figure 9.14: The SEM-EDS line analysis of KWL002, showing the distribution of Mg, Al, Cu and Pb.

Table 9.4: SEM-EDS analysis on different sections of KWL002. (wt%)

	SiO ₂	Al ₂ O ₃	Na ₂ O	K ₂ O	MgO	CaO	FeO	CuO	PbO	Cl
Pb-rich outer surface	57.0	10.8	12.4	2.1	0.6	3.5		9.4	4.0	
Pb-poor outer surface	58.4	9.5	12.9	2.4	0.6	2.8	3.0	9.9		0.6
inner body close to the interface*	67.5	1.4	13.4	2.6	5.9	5.6		2.7		0.9
inner body	67.0	1.6	15.5	3.4	6.3	5.5				0.7
inner body, lead-rich*	60.9	2.8	13.9	2.5	4.9	7.9			6.3	0.8

*: spot analysis

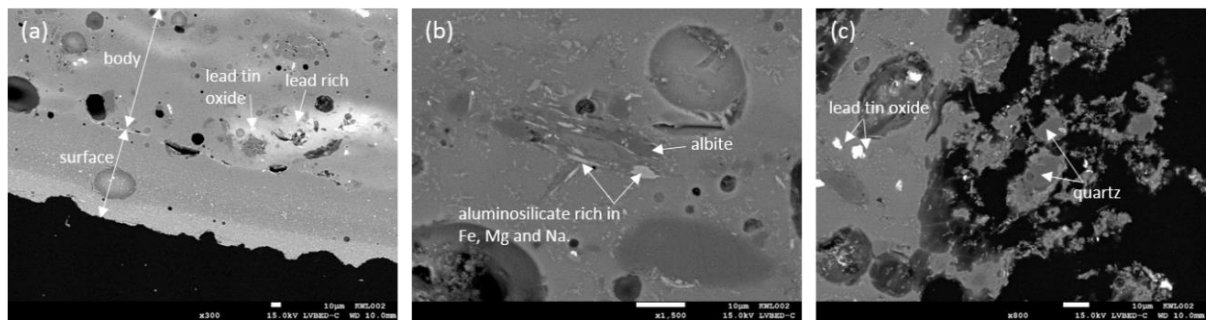


Figure 9.15: The microstructure of KWL002. (a) The lower bright grey layer and dark grey layer are the orange surface with different concentrations of PbO, while the upper area is the body with the mixture of glass and 'sand' materials; (b) minerals such as albite and aluminosilicate rich in Fe, Mg and Na are distributed over the glass body; (c) the area far from the orange surface shows a relatively loose structure, with a frequent presence of silica or silicate (not shown).

The texture of the interior body of KWL002 is less similar to pure glass (see image in Figure 9.14). The microstructure of the inner body of KWL002 indicates that it was made of a combination of different materials including glass or some earth materials such as sand or clay. The PbO-rich feature and presence of lead tin oxide in this inner body area suggest the potential

mixing with glass coloured by lead tin oxide, as this component does not naturally occur in sand. The potential use or recycling of other coloured glass fragments could also be supported by the high Co content (350 ppm) detected by LA-ICP-MS in the bulk composition. In addition, mineral inclusions of albite, apatite and aluminosilicate rich in Fe, Mg and Na are often dispersed through the inner body (Figure 9.15 (b), apatite not shown here). In the areas far from the orange surface, a relatively 'loose' and porous structure is observed, and the presence of silica and silicate minerals is common (Figure 9.15 (c)).

The microstructural results of KWL001 and KWL002 suggest that the orange bead of the KWL-LL02 type were deliberately made, and there seems to be no restrictions in the materials used for producing the core body. This can be further supported by another sample, KWL-GB-605 of the KWL-LL02 type. Although no microstructural analysis was carried out on the bead, it has a core body made of dark blue v-Na-Ca glass with a relatively high content of Co (850 ppm). It is therefore very likely that the three beads of KWL-LL02 style have three different types of core body – KWL001 with blue glass, KWL002 with mixture of glass, clay or sand, and KWL-GB-605 with dark blue glass. Comparing this to the similar bead from Shisanhang in northern Taiwan, possibly indicates the circulation of this kind of orange bead in northeastern and northern Taiwan, from present evidence.

This finding raises questions about the production and consumption of these particular glass beads and of glass used to make the beads around the South China Sea region. Glass beads of the KWL-LL02 type are less well-reported around the South China Sea, and although their origin is still unclear, it can now be shown that this type of bead is made of two different chemical groups of glass – the m-Na-Al glass and the v-Na-Ca glass. This result suggests that the workshop producing this type of bead might have been supplied with glass of the two chemical compositions. Both these chemical groups are common around the South China Sea,

and therefore this connection is worthy of further investigation.

9.2.2.5. The green glass

Only one green bead made of v-Na-Ca glass was analysed and it originated from the Xiliao site. The data for this bead is derived from published results and therefore no microstructural analysis information is available. The published XRF analysis reveals that this green bead contains Na₂O of 12.5%, Al₂O₃ of 4.5% and MgO of 4%. An FeO content of 0.6% is reported, but the CuO content is below the detection limit.

9.2.2.6. The aqua glass

The only aqua v-Na-Ca glass bead (WJC20) analysed is from the Wujiancuo site. It contains Na₂O of 13%, Al₂O₃ of 3% and MgO of 3%. The slightly bluish green tint can probably be attributed to the FeO concentration of 0.9% and CuO of 0.1%. The microstructural analysis has shown it has a relatively homogeneous matrix, and therefore no further information in terms of the colourant raw material can be inferred. However, it is noteworthy that WJC20 is larger than most of the v-Na-Ca beads identified in this research and is larger than most other glass beads from Wujiancuo (see Chapter 7.9), and therefore may have a different provenance.

9.3. Other chemical groups

9.3.1. Potash glass

The two potash glasses in this research are from Jiuxianglan (JXL38) and Shisanhang (SSH-B024); JXL38 is unearthed from Jiuxianglan and is the only analysed Jiuxianglan glass bead found in a mortuary context. The K₂O contents are 13.5% in JXL38 and 18% in SSH-B024. The base composition of the two samples (Table 8.1) shows similar Al₂O₃ contents but very

different CaO contents – JXL38 contains Al_2O_3 of 2% and CaO of 1%, while SSH-B024 has Al_2O_3 of 1.6% and higher CaO of 8%. This suggests that SSH-B024 is probably similar to the m-K-Ca sub-group (see Chapter 5.2.2), but it is difficult to assess the sub-group for JXL38, as the microstructure demonstrates heavy weathering throughout (see below) and therefore the chemical composition may not reflect the initial composition of the fresh glass.

The SSH-B024 bead is blue glass coloured by CuO (~1%), and there is no microstructural information from the published report (Tsang and Liu 2001: 96). Microstructural analysis was carried out on JXL038. This bead looks like yellow glass from the surface, but further investigation has shown that the inner area is greenish (Figure 9.16 (a)). The result shows different compositions in the outer and inner areas (Figure 9.16 (b)). The inner greenish area is coloured by lead tin oxide and copper oxide (PbO 3.5%; SnO_2 0.1%; CuO 2%), and lead tin oxide is clustered with K-feldspar. The outer yellowish section, however, has low K_2O value and slightly higher SiO_2 , and is in absence of lead tin oxide (Figure 9.17). A lower un-normalised total is also found in the outer yellowish section (~83%). Therefore, it is likely that JXL38 was originally of a green colour rather than yellow, and the outer surface is weathered (not deliberately decorated).

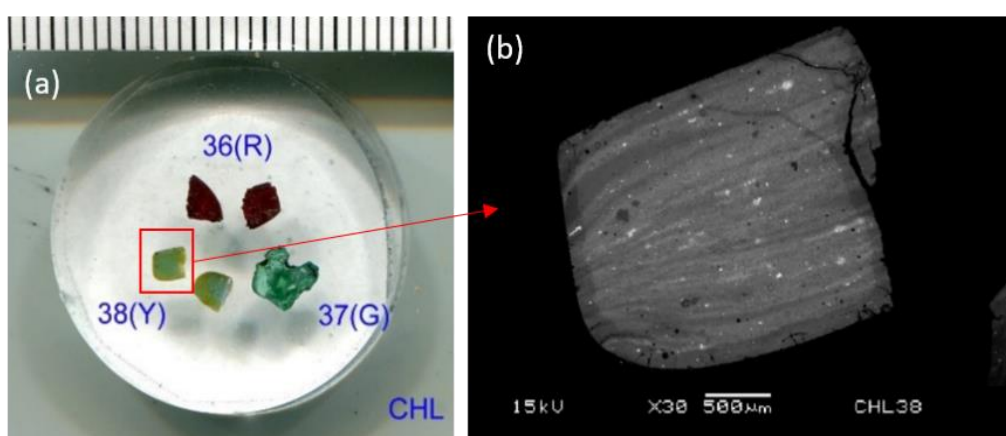


Figure 9.16: (a) The yellowish outer area and greenish inner area in JXL38; (b) the BSE image shows compositional differences in the two areas.

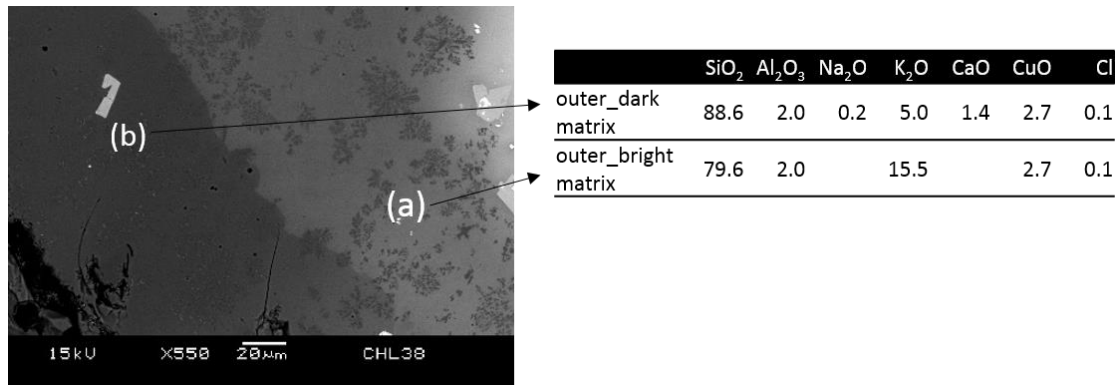


Figure 9.17: (a) The microstructure of the greenish area and the composition of the matrix; (b) the microstructure of the yellowish area and the composition of the matrix

9.3.2. Soda-lime-silica glass (SLS glass)

There are two samples made of mineral soda-lime-silica (SLS) glass: one bead from Guishan (GS119) and the other bead from Shisanhang (SSH-B047). Table 8.1 shows that the Guishan sample contains Na₂O of 22% and CaO of 5%, while the Shisanhang sample contains lower Na₂O of 15. % and higher CaO of 8%. The two samples both contain MgO at less than 1%, demonstrating the characteristics of a mineral source of soda flux. No microstructural analysis has been carried out on any SLS glass.

The two glass beads are dark blue. GS119 is coloured by Co (cobalt), with a significant concentration of 1300 ppm. CuO (0.3%) and MnO (0.4%) are also found in GS119, and there are negligible concentrations of PbO (0.2%), Sn (<LLD), Zn (25 ppm), As (6 ppm) and Sb (3 ppm). The analysis of SSH-B047 is taken from the published report (Tsang and Liu 2001: 94) which shows a CuO concentration of 0.2%, particularly high Zn at 0.2% and MnO at 0.1%. It is likely that cobalt contributes to the dark blue colour, but unfortunately cobalt was not analysed for.

The chemical composition of the base glass and colourant of both GS119 and SSH-B047 may

suggest different sources of the SLS glass. They are also of different styles, GS119 has an oblate shape and is particularly thin which differs from the other dark blue glass beads made of v-Na-Ca glass (Chapter 7.6). SSH-B047 belongs to the SSH-Type 1, which are divided into three sub-groups. Although the specific shape of SSH-B047 was not mentioned in the report, the colour plates of each sub-group do not suggest these are similar in shape to GS119 (Chapter 7.3). However, it is worth mentioning that SSH-B047 is the only SLS glass reported within the SSH-Type 1 group, and all the other samples are v-Na-Ca glass.

9.3.3. Lead silicate glass

SSH-B057 is the only lead silicate glass bead in this assemblage and it has been previously published. It belongs to the SSH-Type 10 from Shisanhang (Tsang and Liu 2001: 102). Table 8.1 shows that this sample has SiO₂ of 45%, Na₂O of 9%, K₂O of 2% and PbO of 34% in the base composition. According to the colour plate in the excavation report, SSH-B057 is dark blue or blue. The CuO concentration is 1.6% and MnO is 0.2%, but the cobalt content is not available. Lead silicate glass is not a typical composition in contemporary Southeast Asia but is associated with glass production in China (Chapter 5.3.1). Therefore, the presence of lead silicate glass in Shisanhang suggests the potential interaction between this site and China, although this must remain tentative with only one sample represented.

9.4. Summary

Chapters 8 and 9 discuss the results of chemical composition and microstructure of glass samples from Kiwulan, Shisanhang, Jiuxianglan, Guishan, Daoye, Wujiancuo and Xiliao. It is obvious that m-Na-Al glass and v-Na-Ca glass are the two dominant chemical groups found in prehistoric Taiwan. Most of the m-Na-Al glass reported here belongs to the m-Na-Al 1 sub-group, which is currently the largest group of m-Na-Al glass identified in the South China Sea

region (Dussubieux *et al.* 2010; Dussubieux and Gratuze 2010). The v-Na-Ca glass (plant ash glass), conversely, is a type that is less well studied in contemporary Southeast Asia, although recent research has started to acknowledge its increasing presence in the South China Sea region from the late 1st millennium AD onwards (Lankton and Dussubieux 2013; Dussubieux and Allen 2014). Whilst the v-Na-Ca glass in this research shows different major and minor compositional pattern (e.g. MgO-K₂O and CaO-Na₂O relationships) between the study sites, the results do not fit well into any sub-groups of v-Na-Ca glass recently reported by Dussubieux and Allen (2014) and Dussubieux (2014).

This research shows the complexity of chemical composition and microstructure in m-Na-Al glass, which is associated with sand and colourant raw materials. The sand, likely granite sand, used for producing m-Na-Al glass is rich in plagioclase and alkali feldspar, suggesting that a certain amount of soda in the m-Na-Al glass is from sand. The presence of plagioclase in the sand may introduce more Ba and Sr to the glass melt, and therefore a high Ba content is observed in the m-Na-Al glass analysed in this research. However, the greater concentration of Ba in some yellow glass from Jiuxianglan (and a few green, red and blue beads) may be further attributed to the use of Pb-bearing ingredient as colourant, in which Ba co-occurred with Pb in the geological deposits. In the green, red and blue glass coloured by copper, it is also likely that higher Ba content resulted from the co-occurrence of barite in the copper/lead ores, as prismatic crystals of barite are observed in the m-Na-Al glass in this research.

In the m-Na-Al glass, an elevated level of MgO, FeO and CaO is found in red and orange glass, as reported in Dussubieux (2001: 115-118) and Dussubieux *et al.* (2010), but there is no strong linear correlation between them. This suggests that MgO, FeO and CaO contents in the red and orange m-Na-Al glass did not derive from a single source. Some FeO content may be introduced from sand, as the elevated FeO level is in association with increasing concentrations of Ti, Sc

and V in all colours of m-Na-Al glass, and inclusions of Fe-Ti oxide are occasionally found by SEM-EDS. In the red and orange glass, it is possible that additional FeO contents were introduced by the use of matte as colourants or by the copper or bronze hammer scale. This may indicate a link between the glass and copper production around the South China Sea or South Asia, but the small quantities of copper-containing ingredients needed for producing the red and orange glass may not suggest a large scale of organisation between the two craft productions. In fact, this link between glass and metallurgical production is seen in many societies, such as Late Bronze Age Egypt (Rehren 1998), pre-Roman Iron Age Britain and Ireland (Freestone *et al.* 2003b) and early medieval England (Peake 2012; Peake and Freestone 2014).

In terms of v-Na-Ca glass, generally the microstructure of glass is not as heterogeneous as that of m-Na-Al glass, and most of the mineral relics or crystals are related to colourants rather than the raw materials of the base glass. However, the chemical composition reveals possibly different sources, in terms of raw materials of base glass, between or within site(s), and also the potential recycling of v-Na-Ca glass. For example, the difference between sites is seen in the Al₂O₃ contents (high in Guishan but low in Shisanhang) and the MgO-K₂O relationship (both low in Guishan, moderate in Kiwulan and high in Shisanhang), which may suggest different raw materials, such as sands or plant species, or recipes used for producing the raw glass. Alternatively, the different Al₂O₃-Ce and Zr-Ce patterns in the light blue and dark blue beads made of v-Na-Ca glass at Guishan suggest different sand sources were used for producing light blue and dark blue glass beads unearthed from a single site, which may indicate a diverse supply network. The possible recycling or re-melting of v-Na-Ca glass is seen from the elevated MnO content, particularly in the yellow glass which is not coloured by an Mn-based ingredient. It is also likely that the slightly higher amounts of Sb, As, Ni and Zn in the yellow v-Na-Ca glass, compared to the yellow m-Na-Al glass, resulted from glass recycling, but this requires more

understanding of glass production around the South China Sea region, the movement of raw glasses and recycling practices.

The types of colourants in the m-Na-Al glass and v-Na-Ca glass do not reveal significant differences. Cuprite are associated with the red colour in m-Na-Al and v-Na-Ca glass. The orange beads made of m-Na-Al glass are also coloured by cuprite. The yellow colourant lead tin oxide, precisely $\text{Pb}(\text{Sn},\text{Si})\text{O}_3$, is identified in both m-Na-Al glass and v-Na-Ca glass. The light blue beads of the two compositional groups are mainly coloured by copper oxide, but in some cases of v-Na-Ca glass there may be a contribution from cobalt. The dark blue glass, made of v-Na-Ca glass, is coloured by cobalt.

However, the trace elemental pattern and microstructure of glass beads within a single colour have shown differences related to the sources of colourant raw materials or colouring methods. One example is the orange m-Na-Al glass from Jiuxianglan and Kiwulan. The orange glass from Jiuxianglan is probably coloured by a bronze-related ingredient, while most samples from Kiwulan may suggest the use of copper matte. Another example can be seen in the dark blue v-Na-Ca glass from Kiwulan and Guishan. The low concentrations of Zn and PbO in the Guishan samples demonstrate different sources of cobalt ore compared to the dark blue beads from Kiwulan. The microstructure of lead tin oxide in both m-Na-Al and v-Na-Ca yellow glass is another example, and here the results suggest different colouring methods. The frequent presence of nepheline crystals (and sometimes sodalite) with lead tin oxide in the yellow m-Na-Al glass from Jiuxianglan may indicate the introduction of lead- and tin-bearing raw materials respectively, while the near absence of this microstructural feature in the yellow m-Na-Al glass from Daoye and Guishan (GS-Y1 type) and the yellow v-Na-Ca glass from Kiwulan suggests lead tin oxide may be introduced as a single component.

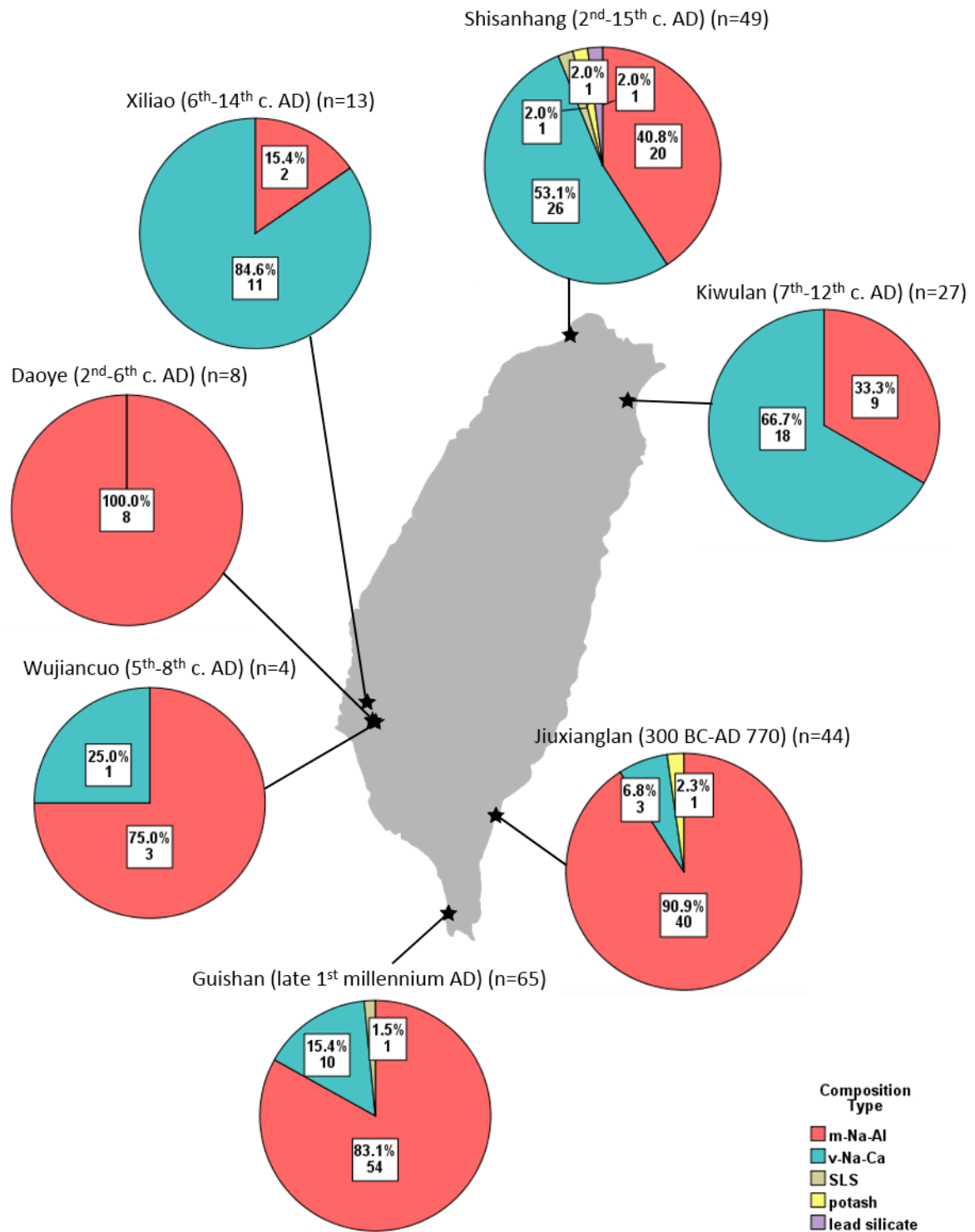


Figure 9.18: The distribution of chemical groups at Shisanhang, Kiwulan, Jiuxianglan, Guishan, Wujiancuo, Daoye and Xiliao.

It is the combined chemical composition and microstructural analysis of glass beads which reflects any regional differentiation in terms of the source(s) of raw materials or use of different

colouring methods. This regional differentiation is also seen in the proportion of chemical groups identified at each site (Figure 9.18). Larger proportions of m-Na-Al glass by site are found at Jiuxianglan (southeastern Taiwan) and Guishan (southern Taiwan) than at Kiwulan (northeastern Taiwan), Shisanhang (northern Taiwan) and Xiliao (southwestern Taiwan). At Kiwulan and Shisanhang, a similar proportion of m-Na-Al glass and v-Na-Ca glass is observed at both sites. This generally matches the regional differentiation observed in the typological study in this research (Chapter 7.12), and therefore may suggest the exchange of glass beads within a particular geographic region (see discussion in Chapter 11). However, the different chemical compositions and microstructures of the beads found throughout the different regions in Taiwan, together with the results from the typological study, suggest less inter-regional circulation of glass beads in the 1st millennium AD within Taiwan. This may indicate that glass beads, as imported objects, were regarded as prestige or inalienable goods within the society. In fact, the context of bead distributions at each site also indicates the possibility of different social structures within and between sites, and this will be explored in the next chapter.

Another important finding of the chemical analysis is the paradox seen between the Jiuxianglan glass beads and waste. The glass waste from Jiuxianglan is composed of both m-Na-Al glass and v-Na-Ca glass. In the m-Na-Al glass, the chemical composition and microstructure of yellow, blue and aqua glass *waste* do not show any similarity to the m-Na-Al glass *beads* from Jiuxianglan. The yellow glass waste from Jiuxianglan (JXL48) has a similar elemental pattern to the GS-Y2 bead type from Guishan, but the microstructure does not always show consistency with the beads. Moreover, no glass beads made of v-Na-Ca glass from Jiuxianglan were found in any of the samples analysed despite the presence of waste of this composition. Similarly, the elemental compositions of red, blue and dark blue v-Na-Ca glass waste does not suggest close similarity to the composition of the v-Na-Ca glass beads from other sites in this research, even for glass beads from the nearby Guishan site. Therefore, at present no beads can be identified

in Taiwan which might have been made with this waste glass. This paradox is also noted in the typological study in Chapter 7.5. It must be noted, however, that this may be explained by the biased sampling of the glass beads, as only a rather small proportion of bead samples ($n = 44$) were selected in comparison to the thousands of beads unearthed from Jiuxianglan. Nevertheless, the evidence presented here does not support the proposition of local production of beads at Jiuxianglan. Nor does it indicate the export and exchange of glass beads made locally at Jiuxianglan to other contemporary sites in Taiwan.

10. Results: the distribution of beads by context

10.1. Introduction

This chapter discusses the bead distributions from each site in relation to their finds context. This will be achieved using the contextual information provided by the excavation reports and excavators and the groupings of beads into different stylistic and compositional types. A comparison between sites will also be provided in an attempt to understand the consumption of glass beads at different sites or regions to assess any social or cultural differences. However, due to the limited information provided by the excavation reports relating to different (securely dated) settlement contexts in the study sites, the discussion is mostly based on evidence unearthed from burial contexts which are discussed in more detail.

10.2. Kiwulan, northeastern Taiwan (7th-12th century AD)

Eleven out of 35 burials were found with grave goods in the Lower Cultural Layer from Kiwulan, and glass beads were unearthed from 6 burials (section 2.2). The grave goods from each burial and the gender/age of the deceased are listed in Table 10.1. The table shows that glass and agate beads are the most common types of grave goods. Grave M043 has the greatest variety of bead types and relatively large quantities of grave goods, including many glass beads (not mentioned in the report, but more than 30 pieces based on examination), glass earrings, agate beads and bronze bells. The glass beads were mostly found near the mandible of the body. Unfortunately, the gender and age of the deceased could not be identified in most cases (see Table 10.1). In the 11 burials with grave goods, only 2 of them are reported with a confirmed age – burial M038 is an adult and burial M066 a child (Table 10.1).

Table 10.1: Grave goods found from the burials in the Lower Cultural Layer in Kiwulan.

(Adapted from Chen et al. (2008b) and Chen et al. (2008c).)

Grave goods	Burials	Mortuary code	Gender	Age
6 small glass beads.	1	M038	Unknown	Adult
26 agate beads. Many small glass beads (quantity not mentioned). 3 bronze bells. 2 glass earrings.	1	M043	Unknown	Unknown
2 agate beads. 2 small glass beads.	1	M066	Unknown	Child, ~11 yrs
2 agate beads. Small beads (quantity or type not mentioned).	1	M076	Unknown	Unknown
1 small glass bead.	2	M113 M124	Unknown Unknown	Unknown Unknown
1 pottery jar.	1	M050	Unknown	Unknown
1 pottery bottle. 1 pottery jar.	1	M052	Unknown	Unknown
1 pottery bottle. 1 small grindstone.	1	M056	Unknown	Unknown
1 iron-wire ornament.	1	M130	Unknown	Unknown
1 lithic hammer.	1	M131	Unknown	Unknown
None.	24			
Total	35			

The distribution of glass beads from the Lower Cultural Layer is shown in Figure 10.1. It can be seen that 5 out of 6 burials with glass beads are located in regions A and D, and a concentrated

distribution can also be observed.

A large proportion (~90%) of glass beads were unearthed from non-burial contexts in the Lower Cultural Layer (section 2.2.1). The pits where the glass beads were found are also listed in Figure 10.1. However, almost all of the beads from non-burial contexts were found in a ‘Featured Context’ (named 現象 in the original report) labelled H204 in the pit P187, to the southeast. The finds in H204 include many glass beads, agate beads, potsherds, fragmented slabs and slabs with perforation holes.

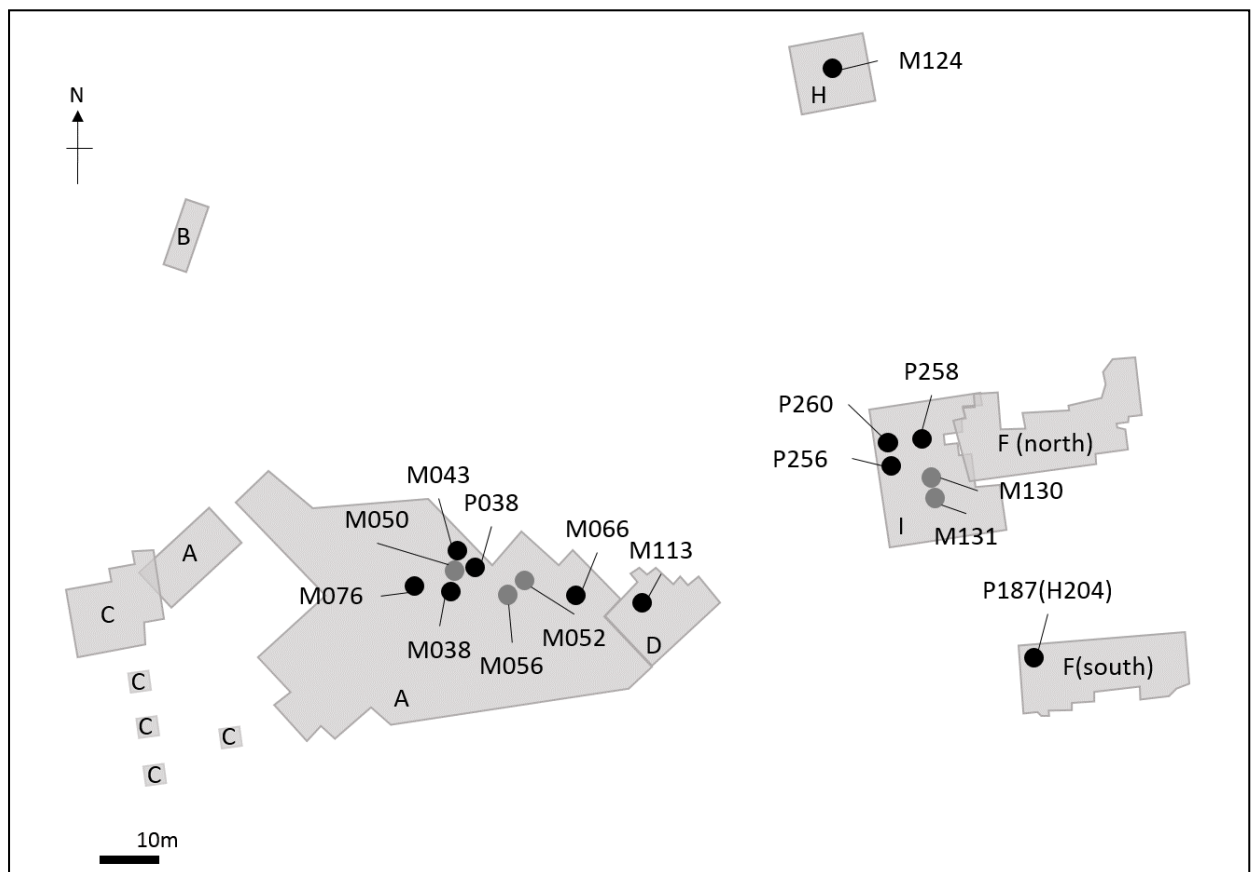


Figure 10.1: The distribution of glass beads from the Lower Cultural Layer at Kiwulan. (Black dot labelled with M: burials with grave goods which contain glass beads; grey dots labelled with M: burials with grave goods but no glass beads; black dots labelled with P: non-burial context with glass beads.) (Background map redrawn from Chen et al. (2008a: 18).)

A closer examination of the typology and chemical compositions of the beads, between the burial and non-burial contexts, has shown little differentiation. Table 10.2 shows the typological groups of glass beads in each burial and in the non-burial contexts. It can be seen that LL01, LL02, LL03, LL04, LL05 and LL06 typological groups are found in both contexts (particularly M043 and H204). LL03 type is made of m-Na-Al glass and LL04, LL05 and LL06 are made of v-Na-Ca glass (Chapters 8 and 9), which suggests that there are no significant differences in bead style and composition from burial or non-burial contexts at this site. As for the minor typological groups, LL07 (unknown composition), LL08 (unknown composition) and LL10 (v-Na-Ca glass) are also found in both contexts (Table 7.1, Table 10.2 and Chen *et al.* 2008e: 26-28), while LL09 (unknown composition), LL11 (unknown composition) and LL12 (unknown composition) are only recovered from two burials M038 and M043. The quantities of LL09, LL11 and LL12, however, are relatively small (generally <5 pieces).

Table 10.2: The typological groups of glass bead in each burial and in the non-burial context of P187(H204), P038, P250, P256, P258 and P260.

Location	Bead types
M043	LL01, LL03, LL04, LL05, LL06, LL07, LL09, LL10, LL12
M038	LL05, LL07, LL09, LL11
M066	LL02, 1 dark blue bead, barrel shape (no group)
M076	2 bead fragments which may belong to LL2 (orange surface but yellow body)
M113	LL11
M124	LL09
P187(H204)	LL01, LL02, LL03, LL04, LL05, LL06
P038	LL02
P250	LL02
P256	LL01, LL02, LL08
P258	LL01
P260	LL07

Burial M043 displays a wide diversity and large quantity of beads; together with the large proportion of other burials without grave goods, it raises issues about the status of the burials at the site. It is quite possible that the inequalities in the provision of grave goods may reflect some social differentiation. As suggested in Chapters 8 and 9, glass beads from Kiwulan are exotic objects; therefore, the diversity and quantity of grave goods in M043, in particular the presence of non-local materials, represents the investment of more resources in mortuary practice than the other burials, and this is often regarded as an indicator of potential social hierarchy or a reflection of the social identity of the individual (Pearson 2003; Drennan *et al.* 2010).

The function of H204 is another interesting issue. H204 actually includes the trenches P194, P187 and P179 working from north to south, and a large number of glass beads accompanied by agate beads were unearthed, particularly from P187. Burial M120 was found on the north side of H204, distributed across P194 and P187. The burial M120 and the glass beads in P187 were recovered from layers in the same chronological level (Chen *et al.* 2008a: 158) and so may be related. However, the absence of a human skeleton except for a single human tooth from M120, alongside the presence of animal teeth, raises questions about the relationship of the two contexts of H204 and M120. Although it cannot be confirmed here, the presence of large quantities of glass beads and agate beads in H204 possibly suggests that this area may be a ritual or ceremonial location related to M120. Or it is possibly more likely that the glass beads from H204 belong to the grave of M120, even though the excavation report questions M120 as a burial (Chen *et al.* 2008c).

10.3. Shisanhang, northern Taiwan (2nd-15th century AD)

Glass beads from Shisanhang were recovered from burials and settlement areas, but the total number of beads recovered from different contexts was not provided in the excavation report (Tsang and Liu 2001: 91-106). A rough distribution of the glass beads on the site can be inferred from the analytical report in Tsang and Liu (2001: 91-106), and this is shown in Figure 10.2. This shows that most of the samples analysed in the report were from sections B, C and H. Only one bead was excavated from section E, and this is the lead silicate glass. It has been suggested in the excavation report that sections B and C may represent the earlier Iron Age occupation, sections D and E may reveal the expansion of settlement from around the 5th century AD onwards, and section H probably shows the later development in the late prehistoric period (Tsang and Liu 2001: 32). The presence of a lead silicate glass bead in section E may indicate the interaction of Han people in the later period, although this interpretation is tentative based on one analysed sample. However, the distribution of glass beads in sections B, C and H shows a more ambiguous pattern probably due to the relatively long time span of the site. With the lack of detailed stratigraphic information and contexts of beads found, it is hard to interpret the detailed temporal and spatial differentiation of glass beads found from Shisanhang. Nevertheless, the presence of non-local objects in grave goods, including glass beads, glass bracelets, glass earrings and foreign coinage (Chapter 2.3), reflects not only the dynamic economic activities at Shisanhang but also the social organisation displayed to bring these goods to site from elsewhere, potentially through long distance exchange network(s).

Although this research has suggested some glass beads from Kiwulan share similar typology and chemical compositions to those from Shisanhang (Chapters 7.4, 8, and 9), previous research has suggested differences in the mortuary practices between Kiwulan and Shisanhang. It has been mentioned in Chiu (2004: 37) that ‘...only the non-local artefacts such as glass earrings,

glass beads and agate beads are similar to those found from Shisanhang in terms of the typology and colours, but the other aspects such as pottery and mortuary practices are quite different.’ At Shisanhang, sideways flexed burials toward the southwest have been identified. Although the poor condition of human remains from burials at Kiwulan had made it difficult to analyse the body arrangement, the research by Chiu (2004: 72) does not suggest the sideways flexed burials in the Lower Cultural Layer at Kiwulan. C-14 dating has shown intensive occupation during 5th-10th centuries AD at Shisanhang (Tsang and Liu 2001: 31-32), a date range which overlaps with the Lower Cultural Layer at Kiwulan (9th-12th century AD). Although Kiwulan is located in the defined broad geographic region of the Shisanhang Culture, this result probably suggests different social characteristics, in terms of the burial practice, between the Lower Cultural Layer at Kiwulan and Shisanhang.

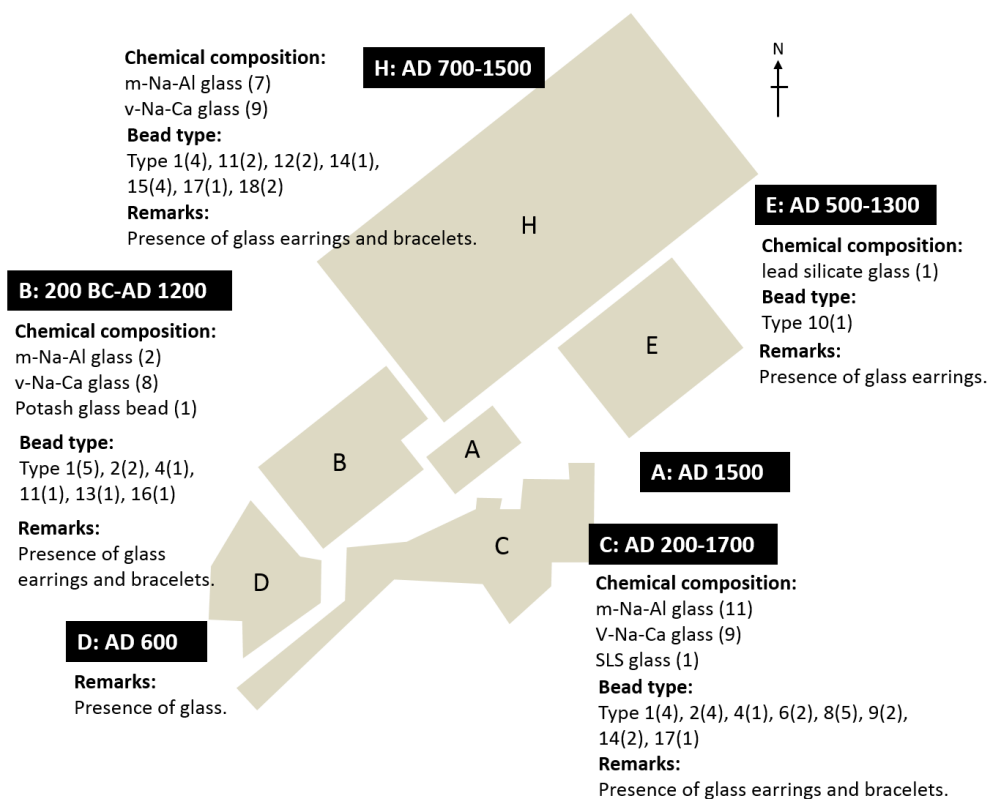


Figure 10.2: The distribution of glass beads from Shisanhang. The labels A, B, C, D, E and H indicate the excavated sections. The number within the brackets is the quantity of beads. (Background image redrawn from Tsang and Liu (2001).)

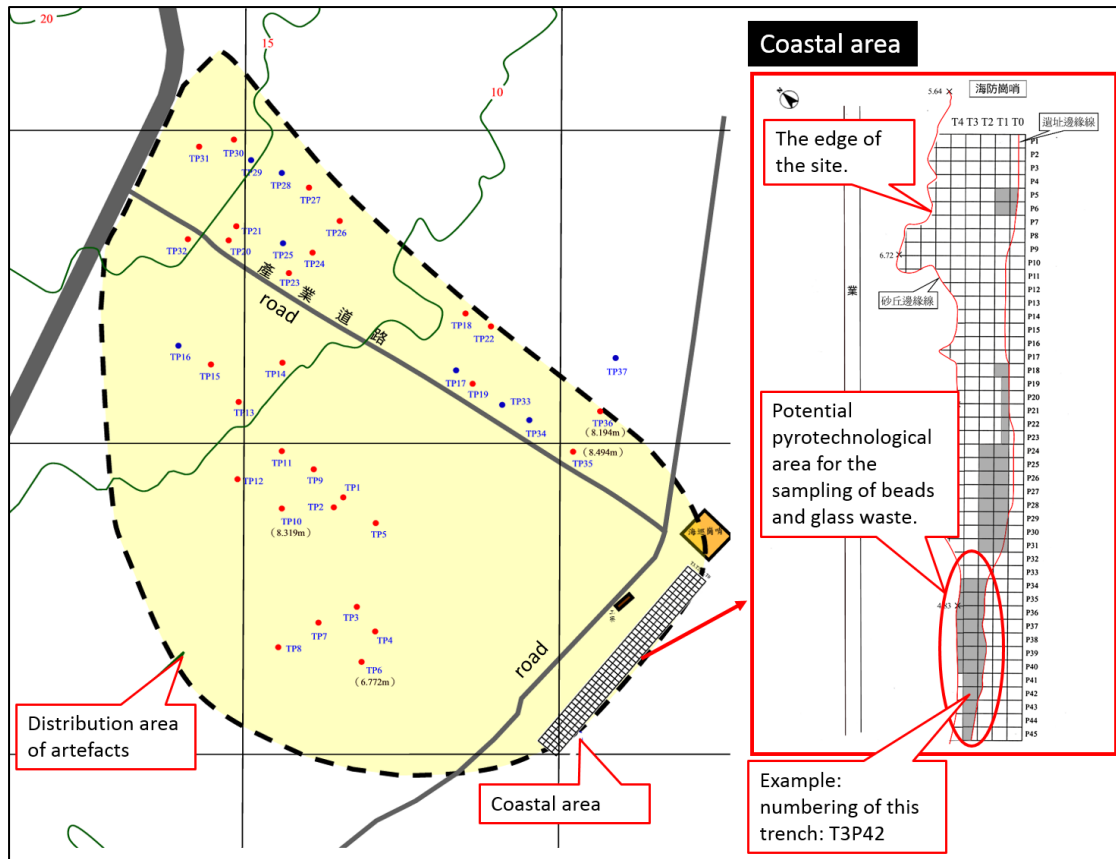


Figure 10.3: Map of Jiuxinaglan, showing the coastal area where the potential pyrotechnological activities are suggested and where the beads sampled in this research were found. (Background map: courtesy of Mr. Kun-Hsiu Lee.)

10.4. Jiuxianglan, southeastern Taiwan (300 BC-AD 770)

Glass beads were found predominantly from the coastal area at Jiuxianglan, where it was suggested pyrotechnological activities, including glass beadmaking, were practiced (Lee 2010: 29, and see Chapter 2). The map of Jiuxianglan showing the location of the coastal area is given in Figure 10.3, and this research focuses on the bead assemblage and glass waste found from the suggested pyrotechnological location in the coastal area. The grid shown in the coastal area in Figure 10.3 represents the trenches excavated (grey shading), and the numbering is provided on the top and right side of the grid. A highlighted example is shown on the right for pit T3P42, with a code of T3 on the top and P42 on the right.

Figure 10.4 shows the spatial distribution of glass beads from each trench in the coastal area. The image in the upper right corner in Figure 10.4 shows the relative location of trenches where glass beads were unearthed (red), the gravel structure which is suggested to be the potential furnace (black) and the location of burned clay (orange). It can be seen that most of the glass beads were found in trenches T2P38, T2P39, T4P36 and between T3P34 and T3P40, near the location of the burned clay and gravel structure. The proportion of different bead colours, however, does not show any spatial differentiations.

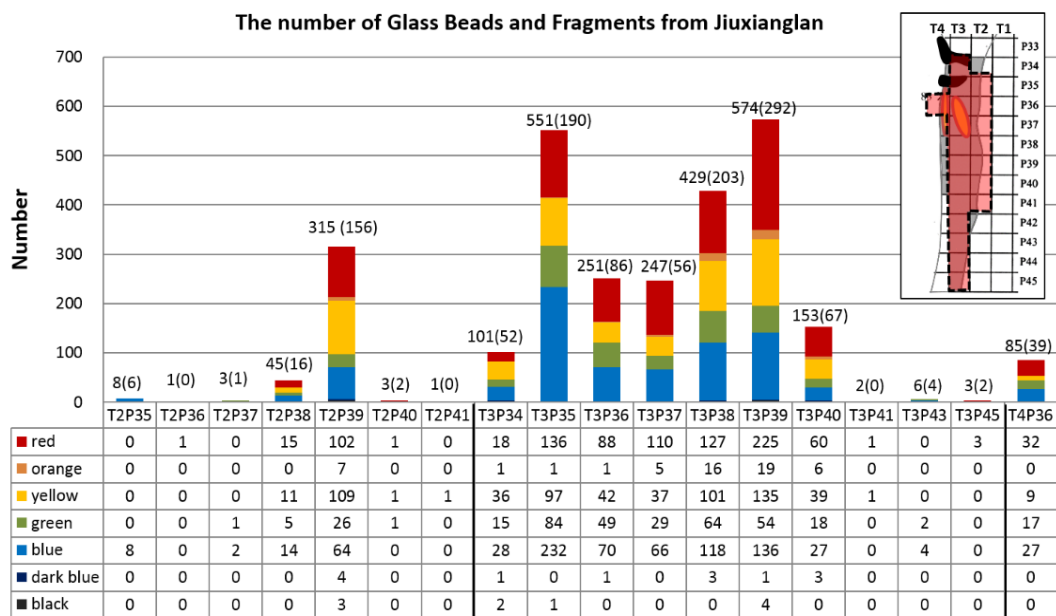


Figure 10.4: The distribution and quantity of glass bead in each trench. The location of trenches where glass beads were unearthed (red area) and the potential region of pyrotechnological activities (black symbol as potential furnace and orange symbol as burned clay) are shown in the upper right of the figure, and the number in the brackets represents the quantity of bead fragments.

The distribution of glass waste is shown in Figure 10.5, which mostly comes from T2P39 and T3P38-T3P40. This represents a slightly southward distribution compared to the glass beads.

The spatial distribution in terms of the proportion of different colours does not show significant differences between either trenches.

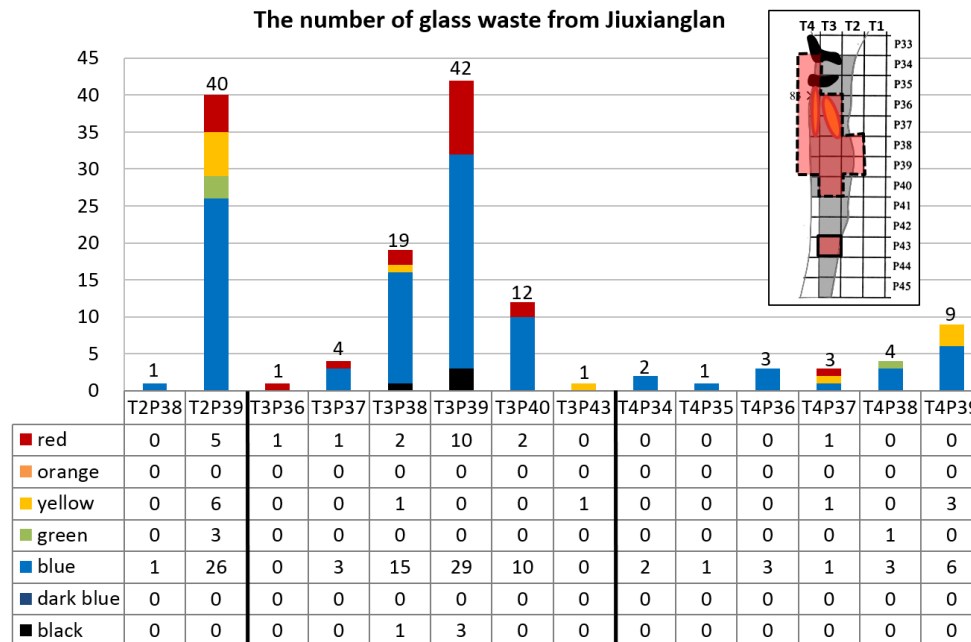


Figure 10.5: The distribution and quantity of glass waste in each trench. The location of trenches where glass waste was unearthed (red area) and the potential region of pyrotechnological activities (black symbol as potential furnace and orange symbol as burned clay) are shown in the upper right of the figure.

Much of the glass waste comprises relatively small fragments, with a total weight of glass waste of less than 30g. In comparison to the large numbers of glass beads unearthed in nearby areas, the very small quantity and weight of glass waste probably does not suggest large scale glass bead production at Jiuxianglan, although it could be possible that not much waste was left. This result also corroborates the paradox seen in the typology and chemical composition between glass beads and waste as discussed in Chapters 7.7.5, 8 and 9, i.e. the compositions and manufacturing methods of the two groups are not the same. The distribution, typology and chemical composition of glass beads and waste do not necessarily rule out the possibility of

bead production at some level, but there is no strong indication of a large scale local bead production at Jiuxianglan, and the presence of a large quantity of 'exotic' glass beads near the gravel structure requires more investigation.

In contrast, 19 burials from Jiuxianglan contain grave goods, and glass beads were recovered from 9. Some of these contained multiple burials in a single grave. According to the results reported in Lee (2010: 180-187), a great variety of grave goods were found, including glass, agate, shell and nephrite beads, pottery vessels, and bronze and iron artefacts.

A differentiation of types and quantities of grave goods between burials can be observed. For example, the burial B2 contains the greatest variety of grave goods (9 types consisting of 53 pieces) including 9 glass beads, 10 shell beads, 13 clay beads, 6 fishbone beads, 6 lithic arrow heads, 1 lithic adze, 2 clay spindle whorls, 4 pottery vessels and 2 face-covering potsherds. Other examples of the variability of grave goods between different burials can be seen in B1 and B10. The burial B1 contains 3 pottery vessels and 2 face-covering potsherds, while in B10 there are 45 glass beads and 4 clay spindle whorls. There are also different distributions of bead quantities between burials. Burial B5 contains the largest quantity of glass beads totalling 316, 45 glass beads were recovered from both B10 and B13, and the remaining 6 burials contained 2-15 glass beads as grave goods. This represents an inequality in the provision of grave goods, but in contrast with Kiwulan, the centralised distribution of glass beads and other grave goods in a single burial is less distinct here at Jiuxianglan.

The information provided relating to age and gender of the inhumations remains unclear, which has hindered further interpretation in terms of the relationship between grave goods and the social status or identity of the deceased. However, this result still suggests some social differentiation at Jiuxianglan (even if this is only related to gender or age which cannot be

determined at this stage). What might be inferred tentatively from this difference between the sites is that the mortuary practices, reflected by the distribution of glass beads and other grave goods, may indicate a different social organisation and social structure between the two sites, Jiuxianglan and Kiwulan.

10.5. Guishan, southern Taiwan (late 1st millennium AD)

In Guishan, glass beads were excavated from three burials. Multiple bodies were found in a single burial, with 4 bodies in Burial 1, 2 bodies in Burial 2 and 3 bodies in Burial 3 (unpublished report, Li 2014, *pers. comm.*). Pottery jars and tooth ornaments were also recovered as grave goods, but the exact number is not given in the report. The quantity and colour distribution of the glass beads in each burial are provided in Figure 10.6. It can be seen that relatively large quantities of glass beads were unearthed from Burial 1 and Burial 2 compared to Burial 3, and all of the dark blue beads and GS-Y2 beads were excavated only from Burial 1. It has been shown in Chapters 8 and 9 that GS-B2 and GS-DB1 are v-Na-Ca glass while the other typological groups are m-Na-Al glass. Both the two chemical groups are found from Burial 1 and Burial 2. This indicates that there is no significant differentiation of bead composition, and hence general provenance of the beads, from different burials. They reflect similar exchange activities. The glass beads were mostly found near the femur, the rib or the phalanges of the body (Li 2014, *pers. comm.*).

According to the unpublished report, 1 sub-adult and 2 adults (possibly 1 male and 1 female) are confirmed in Burial 1. One individual in Burial 2 may be female, while in Burial 3 there is one female adult. The gender and age of the remaining individuals are unknown.

At Guishan, the deceased were buried in stone slab coffins with the body arrangement showing

an extended supine or prone burial. The use of stone slab coffins and the extended supine body arrangement shows a cultural affinity to the Sanhe Culture at Jiuxianglan (sections 3.3.1.2 and 3.3.1.3), suggesting similar burial practices between the two cultures. However, at present it is more difficult to interpret any social differentiation within Guishan and link it to a similar social structure at Jiuxianglan, based on the three burials. Nevertheless, in the two sites the presence of glass beads as grave goods indicates the investment of energy to acquire ‘exotic’ objects and place them in the mortuary context, and the difference in the number of beads between the three burials from Guishan is clear (and not necessarily linked to the number of bodies in each grave). Despite the lack of typological and chemical differentiation of beads between the burials, the difference seen from bead quantities may tentatively suggest differences in status at Guishan.

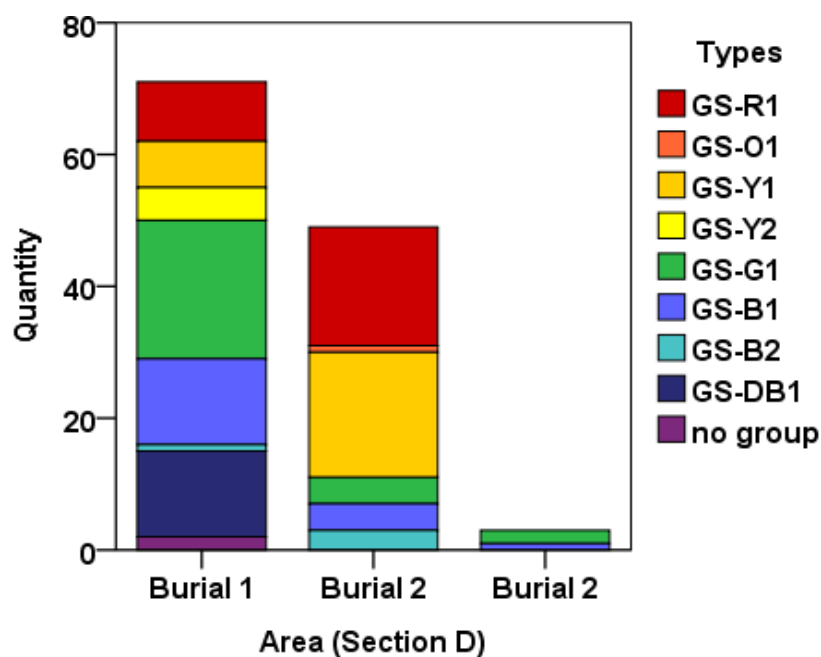


Figure 10.6: The quantity and colour of glass beads in the three burials from Guishan.

10.6. Daoye, southwestern Taiwan (2nd-6th century AD)

In Daoye, glass beads were unearthed from mortuary contexts and middens. The distribution of glass beads is provided in Figure 10.7, and it can be seen that there is no distinct difference in

the quantity and colour of glass beads recovered from burials or middens (Figure 10.7). This result in conjunction with the lack of chemical or typological differences of beads between the two contexts (Chapters 7.8, 8 and 9) suggests that there is no difference between different contexts. The Daoye beads are mostly made of m-Na-Al glass and the most distinct physical and chemical differences relate to the colour of the beads and not the shape.

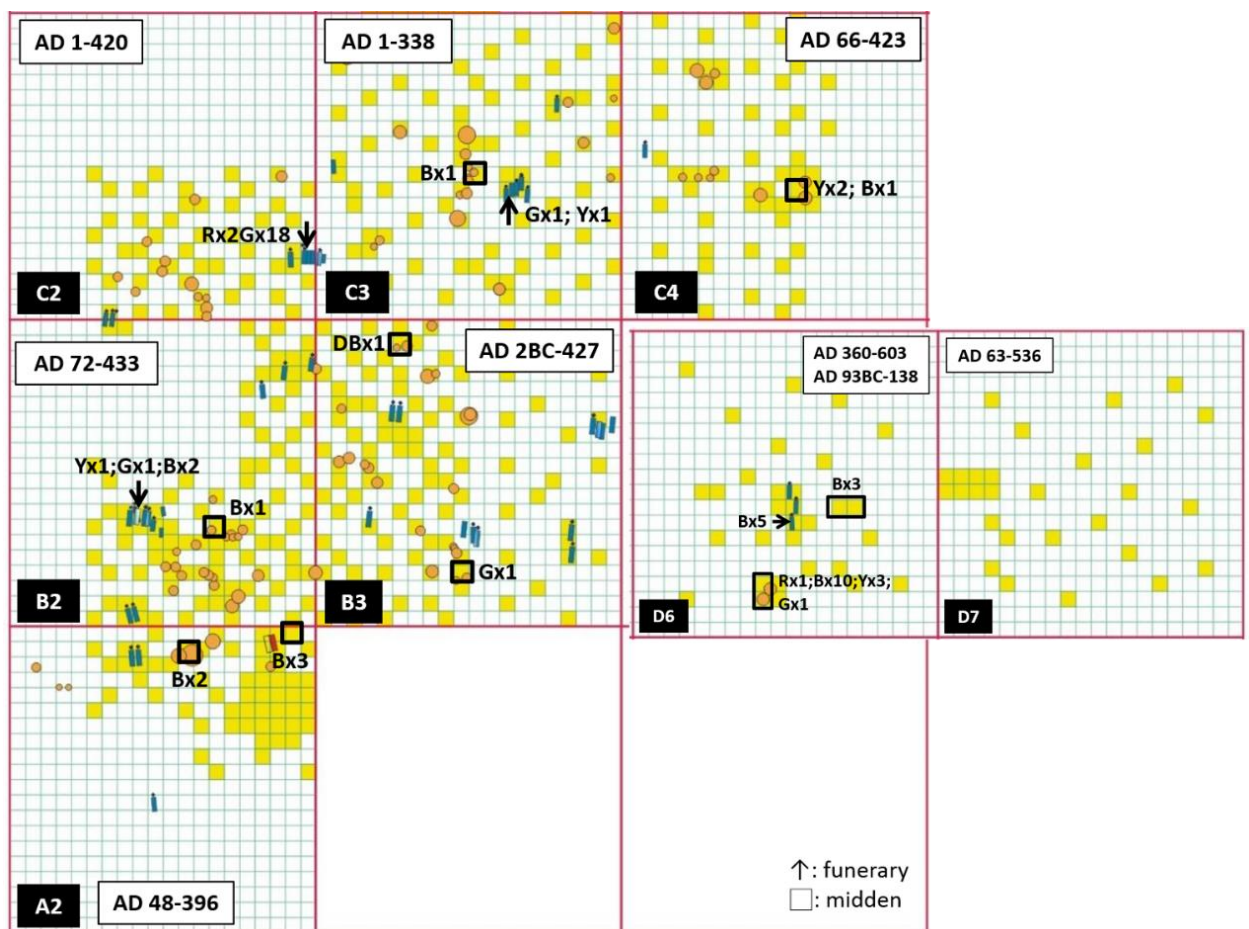


Figure 10.7: The distribution of glass beads at Daoye (Yellow square: excavated trench. Orange circle: midden. Blue symbol: burial. R: red bead. Y: yellow bead. G: green bead. B: blue bead.) (Background map: courtesy of Professor Kuang-Ti Li and Professor Cheng-Hwa Tsang.)

The centralised distribution of glass beads within a single burial is rarely observed at Daoye. As noted in Chapter 2.6, 38 out of 47 burials were found with grave goods, but the quantity of

beads per burial is small. Extended supine inhumation is the main burial practice at Daoye, and the age and gender remain unknown for most burials. However, according to the unpublished excavation report (Tsang and Li 2010), the burial with one glass bead in the C2 area is an infant, and in the burial, 2 red and 18 green beads were found (Figure 10.7). The two burials in C3 and D6 are both adults. One yellow and 1 green glass bead were unearthed from the burial in C3, together with a few clay beads and clay bracelets. In the burial in D6, 5 blue glass beads were recovered. The presence of non-local glass beads at the site suggests acquisition of exotic objects either before or after death (based on our present understanding of provenance). However, the low quantity and variety of grave goods throughout the site probably indicates a lack of elaborate adult burials and wealthy child burials, and lesser degree of social hierarchy can be observed here. This together with the characteristic mortuary practices, such as the presence of burial clusters near the household area and the placement of a pot at the north side of the head, suggests a different social structure or religious practice at Daoye compared to Kiwulan, Jiuxianglan and Guishan; one which has fewer and simpler grave goods.

10.7. Wujiancuo, southwestern Taiwan (5th-8th century AD)

Similar to Daoye, glass beads were recovered from burials and middens at Wujiancuo, and the distribution is shown in Figure 10.8. Fifty-two out of 85 Iron Age burials contained grave goods in Wujiancuo, and 9 of them were interred with glass beads. Three burials (Burial 12 in KVIII, Burial 13 in TS1 and Burial 16 in TS1) have confirmed to have glass beads. According to the unpublished excavation report (Tsang *et al.* 2009), the other glass beads from burial context may be from the remaining single burial from KVIII (Burial 1) and 3 burials from TS1 (Burial 6, Burial 9 and Burial 14), but unfortunately the full information relating to the bead assemblage and its recovery context was not available. Further tracing back to the original excavation record, the 9 blue beads with missing contexts in TS1, noted in Figure 10.8, may be recovered from the

three burials (B6, B9 and B14) in this region. Also, the examination of the excavation records has shown that 1 bead is likely to be recovered from the Burial 1 in the KVIII region and 2 beads from the KVII region may be from the Burial 5. In terms of gender and age, it has been reported that the 9 burials containing glass beads include infant (n = 1), juvenile (n = 2) and adult (n = 2), with the gender of male (n = 3) or female (n = 2) (Tsang *et al.* 2009). This suggests no variability of glass beads in grave goods between ages and genders.

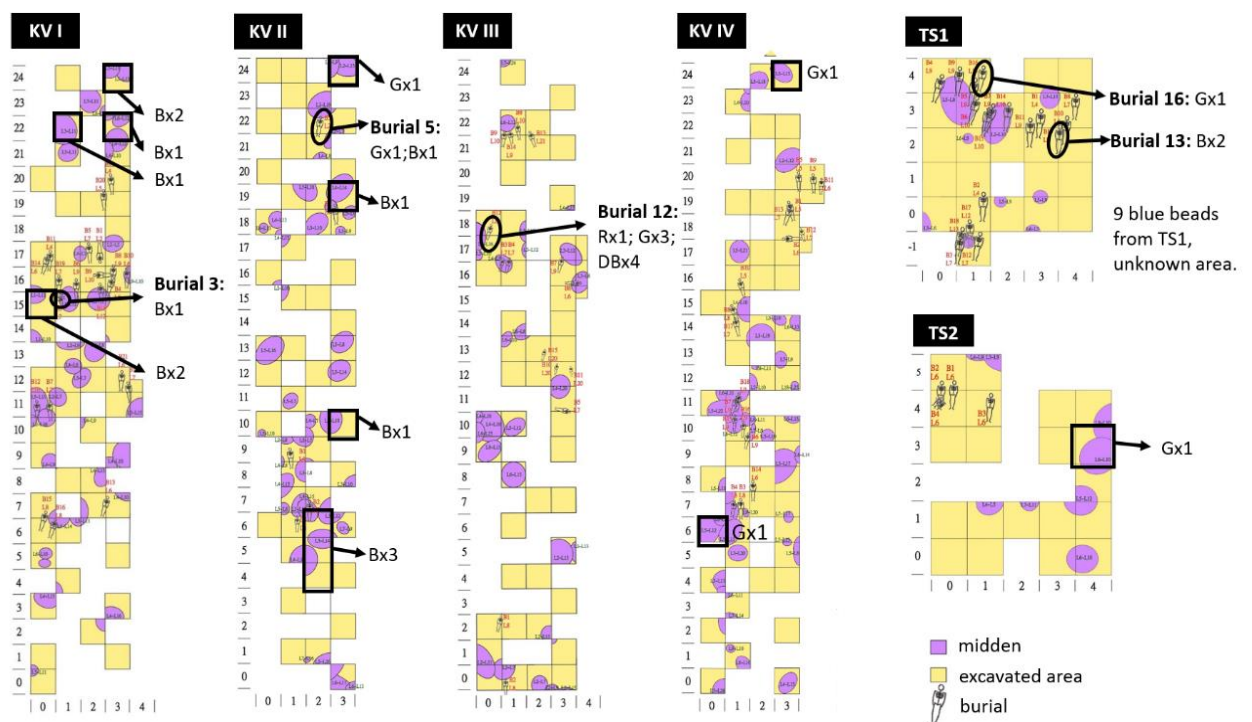


Figure 10.8: The distribution of glass beads from Wujiancuo. (R: red bead; G: green bead; B: blue bead.) (Background map: courtesy of Professor Kuang-Ti Li and Professor Cheng-Hwa Tsang)

It can be inferred from Figure 10.8 that there is no significant centralised distribution of glass beads which cluster with a single burial, and only small numbers of grave goods from most burials were reported (Tsang *et al.* 2009). For example, Burial 12 in the KVIII area contains 8 glass beads and 1 pottery jar, Burial 5 in the same region has 3 pottery jars, and Burial 9 in the

TS1 area contains 2 pottery jars, 6 clay bracelets and a few glass beads. Therefore, the mortuary practices show that grave goods in burials at Wujiancuo are sparse. This pattern shows similarities to those seen at Daoye.

At Wujiancuo, glass beads of the WJC-B2 type (Chapter 7.9) were all recovered from the TS1 area at this site, with 1 bead from Burial 13, 1 bead from Burial 16 and 9 beads from unknown locations in this area. The other typological group WJC-B1 is mostly found from burials or middens from the KVI and KVII areas, with only 1 sample found in Burial 13 in TS1. Furthermore, no other typological group has been identified in TS1. As discussed in Chapter 7.9, WJC-B1 type is drawn-made, while WJC-B2 is likely to be wound-made. The chemical composition of WJC-B1 is m-Na-Al glass (Chapter 8.3.2.4), but the chemical composition of WJC-B2 type is not known as it has not been analysed. However, the distribution of different types of blue beads within different areas at Wujiancuo (Figure 10.8) hardly suggests mortuary practice variability between different regions in this site, as a closer investigation does not reveal significant differences in terms of grave goods provision and burial practice between different areas. Therefore, this result suggests different sources of beads in TS1 compared to the other regions, and future research on the chemical composition may help to elucidate this issue.

10.8. Xiliao, southwestern Taiwan (6th-14th century AD)

Table 10.3 provides a list of the locations where glass beads were recovered from Xiliao. It can be seen that a rather small number of glass beads ($n = 7$) were found from 4 burials, but with no obvious concentrated distribution. Judging from the excavation report, generally only a low number of grave goods were recovered in burials throughout the site. For example, in burial M2 in the P24UexTP4L trench, the grave goods include 1 glass bead and 3 pottery vessels (Liu

2011b: 198), while burial M3 in the same trench has only 3 glass beads as grave goods (Liu 2011b: 200). In another burial which does not contain glass beads, in the U1-4-P83 trench, the deceased was interred with 2 clay beads and 1 pottery jar (Liu 2011b: 195). The presence of very few grave goods and fewer beads in burials mimics that at Daoye and Wujiancuo. As noted in Chapter 2.8, the burial tradition and its transition over time at Xiliao is similar to that observed in the Niaosong Culture in the Tainan Science Park region (i.e. Daoye and Wujiancuo). The glass bead distributions in grave goods at Xiliao, together with the burial traditions, therefore may indicate a sharing of cultural characteristics with the Niaosong Culture in southwestern Taiwan.

Table 10.3: The location where the glass beads were unearthed from Xiliao (Liu 2011b).

Pit	Location	Colour*	Note
P74	L3b, F2	Rx1; Yx2; Bx1	
P89	L2d, F2-L4	Bx1	
P90	L3a, M2-L2	Bx1	
P91	L3c	Bx2	
P5	L3b, F1	Yx1	
P19	L2d, M1-L1	Rx2; DBx1	
P19	L2d, F6-L3	Yx1	
P19	L2d, F4-L1	Gx1	
P24UexTP2L	L2d, M1	Rx1	Burial
P24UexTP4L	L2c, M3	Rx1; Gx1; Bx1	Burial
P24UexTP4L	L2b, M2	Rx1	Burial
P24UexTP1R	L2c	Gx1	
P24UexTP2R	L3a, M1	Rx2	Burial
P26	L4c, F3	Bx14	
P11	L2c, F1-L1	Bx1; DBx1	
P14	L2d	DBx10	
P15	L2b, F2-L3	Bx1	
P16	L2a, F1	Gx1, BorGx8	
P16	L2a, F9	Bx1	
P16	L2b, F3	Gx1	
P16	L2b, F7	Bx1; Gx1	

*: R: red bead; Y: yellow bead; G: green bead; B: blue bead; DB: dark blue bead.

10.9. Summary

The investigation of glass bead distributions at each site has revealed different consumption patterns particularly relating to mortuary practices. In northeastern Taiwan, the centralised distribution of grave goods and glass beads in a single burial is significant at Kiwulan (9th-12th century AD). At Shisanhang (2nd-15th century AD, with principal occupation in 5th-10th century AD) in northern Taiwan, the lack of detailed contextual data of the analysed samples in the published report has made it hard to understand the consumption pattern of glass beads and the mortuary practice at this site, but previous research has suggested a difference in burial practice between Shisanhang and the Lower Cultural Layer at Kiwulan (Chiu 2004). Although Kiwulan and Shisanhang are both within the geographic area of Shisanhang Culture, these findings suggest that Kiwulan and Shisanhang may have different social characteristics and the traditional assumption that similar artefact types in the two regions represents a single cultural group needs more investigation. Conversely, the similarity of some bead types and compositions (Chapters 7.4, 8 and 9) between northern and northeastern areas may not reflect a sharing of cultural traits but should be regarded as a result of exchange activities between societies in northern and northeastern Taiwan (Chapters 11.2.3.2 and 11.3.1).

The uneven distribution of glass beads from mortuary contexts is also seen at Jiuxianglan (300 BC-AD 770) in southeastern Taiwan and Guishan (late 1st millennium AD) in southern Taiwan. In comparison to Kiwulan, the grave goods from Jiuxianglan do not reveal the centralised distribution of large numbers of beads in a single burial. Instead, more than one burial is found containing a variety of grave goods and some have large quantities of glass beads. At Guishan, 2 of the 3 burials were found with relatively large quantities of glass beads. This suggests the presence of wealthy burials and some social differentiation at Jiuxianglan and Guishan. However, it is hard to provide more detail relating to the potential similarity or differences of

each society at Jiuxianglan and Guishan due to limited information relating to mortuary practices.

At Doaye, Wujiancuo and Xiliao in southwestern Taiwan, the distribution of glass beads from mortuary contexts appears to reveal less inequality (although quantities are small). None of the burials at these sites show clustering of large numbers of beads or other grave goods within a single burial. The sites are linked by proximity, found in the same region, but also the chronology of Daoye, Wujiancuo and Xiliao overlaps, with dates of 2nd-6th century AD, 5th-8th century AD and 6th-14th century AD, respectively. The mortuary practice at the three sites all shows extended supine burials with the placement of pottery near the head, although the tradition of paving potsherds as grave goods appears to disappear later in the period (Chapter 2 and Chapter 4). Despite the similarities of mortuary practice in the three sites in southwestern Taiwan, the typology of glass beads from the three sites is not always consistent (Chapter 7.11), and the chemical composition has shown different proportions of m-Na-Al glass and v-Na-Ca glass at these sites (Chapter 9.4). Here the case in southwestern Taiwan is opposite to the situation seen in northern and northeastern Taiwan. A similar distribution pattern of glass beads and other grave goods in burials at the three sites of Daoye, Wujiancuo and Xiliao may serve as evidence of similar cultural, religious or social characteristics in southwestern Taiwan, possibly as a reflection of sharing group identities in this region. The differences seen in bead typology and chemical groups in the three sites possibly point to different mechanisms for the long distance exchange of glass beads over time, the control of resources and the social differentiation within each site compared to northern and northeastern Taiwan. This is further explored in Chapter 11.

The other noteworthy aspect is the discussion of glass bead production at Jiuxianglan. Large quantities of glass beads near the structure of what has been described by the excavators as a

furnace have been reported, while a more southward distribution is seen for the beadmaking waste. It is suggested here that the very small quantity and total weight of beadmaking waste does not support the possibility of large scale production of glass beadmaking at Jiuxianglan. This is supported by the results of typological and chemical analyses (Chapters 7.5, 8 and 9), which shows the two have different colour distributions and compositions, and further indicates that most of the Jiuxianglan beads analysed in this research are likely to be imported rather than locally produced.

11. Discussion: the exchange, consumption and production of glass beads in Taiwan and between Taiwan and the South China Sea region

11.1. Introduction

This chapter brings together the different elements of the results and discussion presented in Chapters 7, 8, 9 and 10, and revisits the research questions posed in Chapter 1. The exchange of glass beads is discussed first, with a focus on the regional and chronological patterns identified and their implications for the exchange networks operating within Taiwan and between those known from within the South China Sea region. Second, the social differentiation identified within and between site(s), reflected by glass beads, will be used to explore the different social and cultural practices in the use of exotic glass beads between sites and regions. Lastly, glass bead production at Jiuxianglan and around the South China Sea will be reflected upon, in an attempt to explore the potential raw materials and technical differentiation seen in the chemical and microstructural analysis. The map of study sites can be found in Figure 2.1 or Figure 3.1.

11.2. The exchange activities through time and by region

11.2.1. The chronological distribution

This research shows chronological differences in the distribution of glass beads in Iron Age Taiwan. Generally, m-Na-Al glass is found in early to mid-1st millennium AD, followed by v-Na-Ca glass from late 1st millennium AD onwards (Figure 11.1). M-Na-Al glass appears first

in the eastern coastal sites in Taiwan compared to other regions. This can be seen at Jiuxianglan (300 BC-AD 770) studied here and is supported by recent chemical analysis of glass beads from Huagangshan, a contemporary site in the east coast, where m-Na-Al glass has been found but v-Na-Ca glass is absent (Chao 2016, *pers. comm.*). The early presence of m-Na-Al glass is also seen at Daoye (2nd-6th century AD). The Guishan and Wujiancuo sites are of a late 1st millennium AD date, and a slightly elevated proportion of v-Na-Ca glass bead can be observed. In the later sites, generally those which extend into around the turn of the 1st millennium AD, v-Na-Ca glass becomes the main compositional type of the beads, and this can be seen at Kiwulan and Xiliao. This indicates a continuous import of m-Na-Al glass in early 1st millennium AD and the co-occurrence of v-Na-Ca glass in late 1st millennium AD in Iron Age Taiwan. Shisanhang (2nd-15th century AD) is a more complicated case, as it covers a very long chronological period. The identification of m-Na-Al glass at Shisanhang in northern Taiwan may suggest its early presence in this region, and future analysis combining a much more detailed stratigraphy and detailing specific locations of glass beads will help to elucidate the chronological sequence of the beads at this site.

The bead types found in Iron Age Taiwan reveal differences in terms of shape and colour distribution between sites/regions (Chapter 7.12). Here the bead typological differences generally match that seen in chemical composition. In the earlier sites Jiuxianglan and Daoye where m-Na-Al glass dominates, higher proportions of red, yellow and green beads are found (Figure 7.1). At Guishan, dated to late 1st millennium AD, the dominance of red, yellow and green colours is also seen in m-Na-Al glass. In the later sites Wujiancuo and Xiliao where the proportion of v-Na-Ca glass increases, higher proportions of blue and dark blue glass are seen. Similarly at Guishan (which chronologically overlaps with Wujiancuo and Xiliao), v-Na-Ca glass beads are found and all are blue or dark blue beads. No orange beads in v-Na-Ca glass are found at any of the sites where v-Na-Ca glass is present. Therefore, a virtual absence of red and

orange glass is seen in the v-Na-Ca composition in this research, suggesting a chronological difference of bead colours in association with the glass composition through time. This may further suggest a relationship between the colouring method and base glass composition over time and space (see section 11.4.4). At Kiwulan (7th-12th century AD) and Shisanhang (2nd-15th century AD), the m-Na-Al glass comprises orange beads and in the v-Na-Ca glass, blue and dark blue beads. However, the shapes and colours of beads from Kiwulan and Shisanhang are less similar to other bead assemblages from the other study sites in this research (Chapter 7.4), which can be attributed to the regional exchange in northern and northeastern Taiwan (section 11.2.3.2).

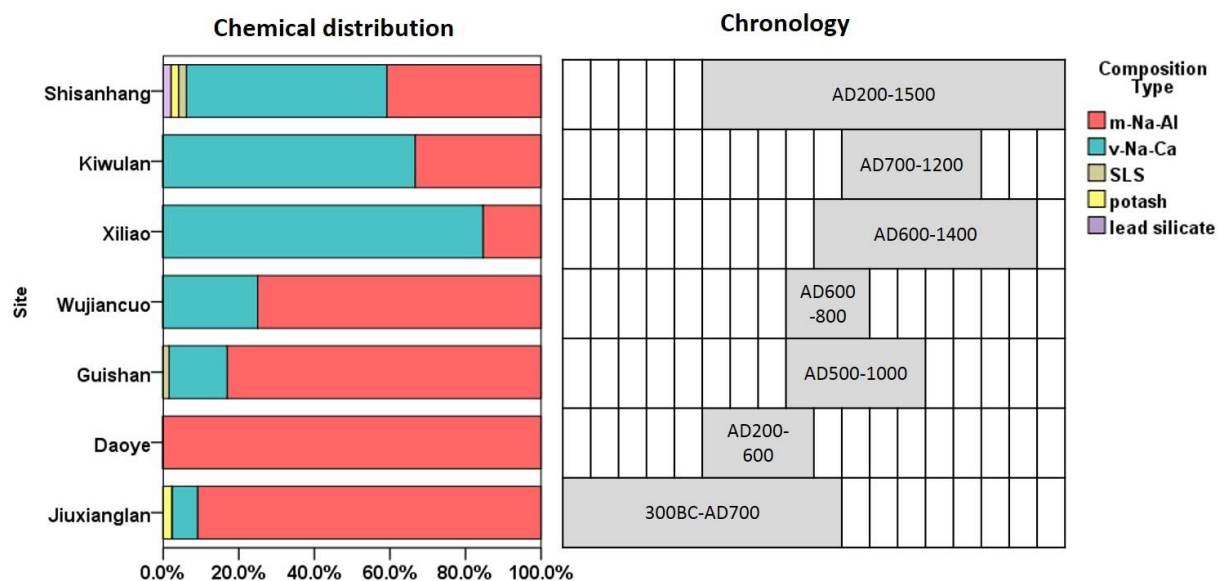


Figure 11.1: The chronological distribution of glass compositions from Shisanhang, Kiwulan, Jiuxianglan, Guishan, Wujiancuo, Daoye and Xiliao.

Although this research focuses on the period of the 1st millennium AD, another transition can probably be seen during early 2nd millennium AD, with the introduction of high lead glass of Chinese origin in Taiwan. Previous chemical analysis by Cui *et al.* (2008) on the Luliao beads (early 2nd millennium AD, label 15 in Figure 3.1) has suggested most beads at this site are composed of lead silicate glass and potassium lead silicate glass, and so a Chinese origin rather

than Southeast Asian origin is proposed. The glass beads from Luliao also exhibits a different style (e.g. the spiral coiled shape) that suggests the use of mainly the wound method (Ho and Liu 2005). Similarly, some of the glass beads from the Upper Cultural Layer at Kiwulan (the 14th century AD-early modern era) are of high lead glass and potassium lead silicate glass, and the typology of some beads resemble those from Luliao (Cheng 2007: 40; Chen *et al.* 2008e: 18-26). Therefore, integrating the data from Luliao and the Upper Cultural Layer at Kiwulan with the results of this research suggests that it is likely that glass beads of Chinese origin were imported into Taiwan at a slightly later date than the v-Na-Ca glass, in the 2nd millennium AD.

11.2.2. The regional distribution

This thesis has demonstrated that the typology and chemical composition of glass beads show regional differentiations (Chapters 7.12 and 9.4). In the southeast and the south, at Jiuxianglan (southeastern Taiwan, 300 BC-AD 770) and Guishan (southern Taiwan, late 1st millennium AD), m-Na-Al glass predominates and a similar colour distribution of red, yellow, green and blue beads is found (Figure 7.1 and Figure 9.18). However, the bead types and compositions at Guishan are more diverse than those at Jiuxianglan (Chapters 7.7 and 9.4). In southwestern Taiwan, Daoye (2nd-6th century AD) and Wujiancuo (5th-8th century AD) also show a predominance of m-Na-Al glass, while at Xiliao (6th-14th century AD) it is v-Na-Ca glass that dominates. The microstructures and types of glass beads do not suggest a close similarity of glass bead technologies between southwestern and eastern coastal Taiwan. One example can be seen in the yellow glass, in which different colouring processes are found in the Daoye samples compared to the Jiuxianglan samples. Unfortunately due to unexpected LA-ICP-MS instrumental failure in the final stages of this research, no trace elements were obtained, and therefore a more nuanced investigation of this material from Daoye could not be conducted. In the north, at Shisanhang (northern Taiwan, 2nd-15th century AD) and Kiwulan (northeastern

Taiwan, 7th-12th century AD), the typological studies discussed in Chapter 7.4 revealed distinct differences of bead types at the two sites compared to other regions in Taiwan. Here, this is mimicked in the similar distributions of the two major chemical groups, m-Na-Al glass and v-Na-Ca glass at both sites, indicating the participation in similar external exchange networks and/or the potential circulation of glass beads within this particular region (Figure 9.18).

As discussed in Chapter 3, archaeological research in northern and northeastern Taiwan has indicated the presence of the Shisanhang Culture in the Iron Age, while in southwestern Taiwan the Niaosong Culture has been identified. Research has also suggested a cultural affinity and the interaction between the Sanhe Culture at Jiuxianglan and the Guishan Culture at Guishan. The identification of typological and chemical differentiation in the beads between different regions in this research therefore fits within the different cultural regions identified in Iron Age Taiwan. These differences in bead supply could therefore be attributed to different exchange activities, in terms of the source of glass beads and the movement of traders, in each region. This is explored below.

11.2.3. Bead types and compositions over time and space

11.2.3.1. The cross-regional bead exchange network in Iron Age Taiwan

The different types and compositions of glass beads over time and space identified in this thesis suggest a transition of bead exchange activities in Iron Age Taiwan. The earlier presence of m-Na-Al glass and later the v-Na-Ca glass in Iron Age Taiwan in the 1st millennium AD matches our current understanding of the chronological sequence of glass compositions in the South China Sea network (Chapter 5). It suggests the supply of glass beads to Taiwan in this period is closely associated with the exchange network operating in the South China Sea region. The

early presence of m-Na-Al glass in eastern coastal Taiwan confirms that its import in early 1st millennium AD is very likely to be based on the established network of nephrite exchange around the South China Sea (Chapter 3.2). The increasing amount of v-Na-Ca glass in the later period in Taiwan could be attributed principally to the shift in glass supply within the South China Sea network (Lankton and Dussubieux 2006; Dussubieux and Gratuze 2010; Lankton and Dussubieux 2013). Specifically, the increasing proportion of v-Na-Ca glass in late 1st millennium AD in Southeast Asia is predominantly associated with a Western Asian origin (Dussubieux 2001; Lankton and Dussubieux 2006; see Figure 5.7.3 in Lankton and Dussubieux 2013), but there is no archaeological evidence to suggest interaction between Western Asia and Taiwan during this time period. Therefore, it is unlikely the v-Na-Ca glass was imported directly from Western Asia. The high percentage of v-Na-Ca glass in Taiwan in late 1st millennium AD is likely to be associated with the exchange activities between Taiwan and Southeast Asia in this period. Furthermore, the high lead glass found in early 2nd millennium AD may be of Chinese origin (Chapter 5.3), and this could be regarded as a result of growing interaction between Taiwan and China in this period. This early presence of high lead glass in the 2nd millennium seems to be distributed in western, northern and northeastern Taiwan, which suggests a change of the bead exchange network from a Southeast Asian-oriented link to a Chinese-oriented link at the turn of the 2nd millennium AD.

11.2.3.2. Glass bead exchange in northern and eastern coastal Taiwan

Liu (2010; 2011: 262) proposed an exchange network in the northern and eastern coastal region of Taiwan. The differentiation of bead typology and compositions seen in this research suggest possibly the circulation of glass beads in the northern part within this exchange network, but this is less evident in the southern part of the eastern coastal region.

The similar styles of beads seen at Shisanhang and Kiwulan may indicate an exchange network of glass beads in northern and northeastern Taiwan in the 1st millennium AD. This network is probably consistent with the geographic distribution of the Shisanhang Culture in this region (Figure 3.1). The ongoing excavations at Hanben (northeastern Taiwan) have revealed glass beads with a similar typology to those at Shisanhang (e.g. Type 3-1) and Kiwulan (e.g. LL01 type), and a cultural affinity to the Shisanhang Culture is suggested (Liu 2014; Gushi 2015). At another site, Chongde (7th-17th century AD), the archaeological record also suggests a similarity of the material to that of the Shisanhang Culture, and the types of Iron Age glass beads found at Chongde resemble those from Shisanhang (e.g. Type 1-3 and Type 5/6/7) and the Lower Cultural Layer at Kiwulan (e.g. LL02 and LL03) (Liu 2007; Wang 2013). This indicates the circulation of particular types of glass beads around northeastern Taiwan, and the existence of a linked exchange network within this region.

In terms of the material from Jiuxianglan in southeastern Taiwan and Guishan in southern Taiwan, the results generally show different chemical compositions and bead types to those seen from the northern sites which overlap chronologically (Chapters 7.12 and 9.4), indicating that beads were rarely exchanged between the southern and northern parts of this network. There is also a difference between the two southern sites, Jiuxianglan and Guishan. This can be observed, for example, in the yellow and green beads from the two sites, some of which are of different types, have a different composition (relating to the Ba-Sr relationships) and have different microstructures, suggesting they have different provenances (Chapters 7.7 and 8.3.1.5). Therefore, as these beads are quite dissimilar, it is less likely that beads were exchanged between the two sites, even though pottery types and other kinds of material culture do show similarities at the two sites which would indicate some contact (see Chapters 2.4 and 2.5).

Liu (2010) further attributes the exchange and presence of greyish pottery within the network to the non-local 'trading diaspora' from foreign countries around the South China Sea. Members of this trading diaspora exchanged goods with local societies, and gradually acculturated into the local societies in eastern and northern Taiwan. Whether or not the trading diaspora also imported glass beads is unclear. However, taken together with the exchange network, the trading diaspora and the regional differentiation of beads between the northern and southern parts within this proposed exchange network by Liu (2011: 262) reveal the presence of multi-scale interaction networks in northern and eastern coastal Taiwan.

11.2.3.3. Glass bead exchange in southwestern Taiwan

Glass bead exchange in southwestern Taiwan seems to show a different pattern. As suggested in the last section, Iron Age glass beads in northern and eastern coastal Taiwan may have been imported based on the established Neolithic nephrite network. The Neolithic nephrite objects found in southwestern Taiwan are thought to be imported from eastern regions through the upland route (Chapter 3.2). However, the dissimilarities of typology, chemical composition and microstructure seen in beads between southwestern and eastern Taiwan (sections 11.2.1 and 11.2.2) suggest beads may not have been exchanged between the two regions. Other pathways must then be explored.

It is therefore likely that Iron Age glass beads in southwestern Taiwan were exchanged through the long distance maritime trade route (the South China Sea) rather than the upland pathway within Taiwan as seen in the Neolithic nephrite exchange. The chronological differentiation is much clearer in the three sites in the southwestern region than in other regions (section 11.2.1). The earlier dominance of m-Na-Al glass at Daoye and later v-Na-Ca glass at Xiliao in southwestern Taiwan suggest that the supply of glass beads in this region in the 1st millennium

AD is closely tied to the South China Sea network, but the small quantity of glass beads from sites in southwestern Taiwan (Chapter 3.3.2.1) may indicate less intensive exchange in comparison to that seen in northern and eastern Taiwan.

The involvement of southwestern Taiwan within the South China Sea network can be traced back to the Neolithic period, through the exchange of greyish black pottery. Liu (2013a) has suggested an interaction between southwestern Taiwan and the eastern part of the South China Sea region based on the greyish black pottery exchange in the Neolithic period, which is different from the Iron Age greyish black pottery exchange in northern and eastern Taiwan (Chapter 3.3.1.1). Whether or not glass beads in southwestern Taiwan were introduced through exactly the same route/areas of the greyish black pottery exchange in the South China Sea region is less clear due to the lack of research on issues of exotic goods exchange between the two regions. However, the exchange of greyish black pottery demonstrates that southwestern Taiwan actively participated in the exchange activities in the South China Sea network prior to the Iron Age. Therefore, the direct import of glass beads from the South China Sea region is possible, and the interaction between the two regions is worthy of further investigation.

11.2.3.4. A prestige good exchange network?

The differences seen in glass beads between regions suggest that inter-regional re-distribution of glass beads is less evident in the coastal areas in Iron Age Taiwan. This is probably clearest by examining later v-Na-Ca glass. This research shows the regional differentiation in chemical composition, microstructure and typology of v-Na-Ca glass between the sites of Wujiancuo, Xiliao, Guishan, Kiwulan and Shisanhang (Chapters 7, 9.2 and 9.4); that is, despite all being on the coast and some with a relatively close proximity and with overlapping chronology, they show distinct differences in the bead assemblages. This differentiation can be attributed to the

exchange networks as discussed in previous sections (sections 11.2.3.1, 11.2.3.2 and 11.2.3.3), but it also suggests there may be control over bead exchange within a particular region or society. It is likely that glass beads were prestige goods, that access to them was restricted to specific social groups, and that bead exchange within a particular area was controlled.

This likely control over bead exchange is more evident in northern and northeastern Taiwan than in southwestern Taiwan. Greater social differentiation is seen at Kiwulan (northeastern Taiwan) and Shisanhang (northern Taiwan) compared to the sites in southwestern Taiwan (Chapters 10.2, 10.3, and 10.9). This suggests more social stratification at Kiwulan and Shisanhang where the presence and exchange of prestige goods may be an indication of cementing or establishing elite status and/or sharing 'elite symbols' between societies within this particular region (Junker 1999: 305-311; Bellina 2014) (more discussion on social differentiation in section 11.3). Therefore, in northern and northeastern Taiwan the bead exchange network may be part of a network of prestige goods exchange, and associated with greater socio-political complexity. Further discussion on this issue is not possible at present, as relevant research on prestige good exchange and social complexity is absent in Taiwan archaeology. However, the presence of regional prestige good exchange networks related to stratified societies is not a new concept (e.g. Brumfiel and Earle 1987; Junker 1999; Sherratt and Sherratt 1991; Dillan and White 2010; Carter and Lankton 2012; Bellina 2014; Carter 2015). A similar idea is provided in recent research by Carter and Lankton (2012) and Carter (2015) on Iron Age beads (both glass and agate/carnelian) from Thailand and Cambodia in Southeast Asia. In her research, Carter proposes the existence of a regional prestige good exchange network based on the changing types and compositions of beads between local areas, linking it to the control over exotic bead exchange by elites and the emergence of complex society over time and space in her study areas. The path of developing social complexity in Taiwan may not necessarily parallel that in Thailand or Cambodia, but Carter's research and the similar case

seen in northern and northeastern Taiwan demonstrate that bead exchange around the South China Sea region cannot simply be regarded as object exchange. Instead, this is embedded in multiscale economic and socio-political interaction between regions and societies.

11.3. Social differentiation reflected by the distribution of glass beads within different contexts

This thesis has demonstrated that the inequality of grave good provision is more obvious at Kiwulan (northeastern Taiwan), Jiuxianglan (southeastern Taiwan) and Guishan (southern Taiwan) than at Doaye (southwestern Taiwan), Wujiancuo (southwestern Taiwan) and Xiliao (southwestern Taiwan) (Chapter 10). At Shisanhang, the presence of exotic glass beads among the grave goods may reflect social hierarchy, but at present no definitive statement can be made as this requires more detailed information relating to the burial contexts. These regional differences have been found to echo the regional exchange network.

11.3.1. Social differentiation in northern and eastern Taiwan

In northern and eastern Taiwan, more glass beads were found, and these show a centralised distribution of glass beads in single or multiple burial(s) (Chapter 10). The burial practice at Kiwulan (northeastern Taiwan) shows a centralised distribution of glass beads with diverse grave goods in a single burial, while multiple rich burials were found at Jiuxianglan (southeastern Taiwan) and Guishan (southern Taiwan, but culturally similar to eastern Taiwan, see Chapter 3.3.1.3).

Although there is an absence of information relating to age and gender of the inhumations at many of the sites, the variation in grave good provisions still demonstrates social differentiation.

This research notes the prestige value of exotic glass beads in Iron Age Taiwan. In northern and eastern Taiwan, the presence of grave goods with larger quantities and more diverse ranges of beads may suggest an elaborate mortuary practice in relation to higher status of the deceased, as more energy was invested in the acquisition of grave goods (Pearson 2003; Drennan *et al.* 2010). In addition, the rich burials may suggest accessibility to prestige goods through exchange networks and their accumulation in particular social ranks (Junker 1999: 171-175). Therefore, the more distinct difference in numbers of beads and other grave goods in burial(s) at Kiwulan, Jiuxianglan and Guishan probably suggests a more stratified society at these sites than that at Daoye, Wujiancuo and Xiliao (see section 11.3.2). The diverse kinds of grave goods at Kiwulan and Jiuxianglan also indicate that the elites or high status individuals/groups at the two sites may have had access to a wider range of local and/or non-local prestige goods through exchange in regional networks or with the South China Sea network.

In the north of Taiwan, although both Kiwulan and Shisanhang are located in the geographic range of the Shisanhang Culture, the different mortuary practices, in terms of body arrangement between Kiwulan and Shisanhang, suggest variation in social organisation at the two sites (Chapter 10.3.). The information relating to burial practices at Shisanhang is incomplete, but the difference of social organisation between Kiwulan and Shisanhang can be inferred through the use of space at the two sites. Kiwulan has habitation and burial areas, while Shisanhang contains more spatial sectors such as habitations, burials, kilns and an iron smelting furnace and the scale of settlement is larger than that at Kiwulan (Chapters 2.2 and 2.3). This further indicates that Shisanhang is a site with more segmented activity areas, although there may be an effect of temporal scale in the use of space at Shisanhang. The spatial variations at the two sites may reflect different economic and social activities and social relations between sites or societies (Philippa-Touchais 2010). Taken together, the acquisition of prestige glass beads at Kiwulan and Shisanhang indicates degrees of social differentiation at both sites, but the much

larger quantities of beads and more segmented space at Shisanhang may suggest a different social structure, possibly more complex, at this site. Further research including detailed stratigraphic information from Shisanhang may make clear any chronological changes in the bead acquisition, the use of space or the related social and economic activities at this site. However, these factors taken together at the two sites demonstrate that the presence of similar bead types at Kiwulan and Shisanhang is not simply a phenomenon of the circulation of similar objects within a cultural group, but is likely a result of dynamic economic and socio-political interactions within northern and northeastern Taiwan.

11.3.2. Social differentiation in southwestern Taiwan

In southwestern Taiwan, the lack of a concentrated distribution of glass beads and other grave goods in specific burials suggests a different organisation of societies than that seen in northern and eastern Taiwan. In general, smaller numbers and varieties of glass beads and other grave goods are found in burials from Daoye, Wujiancuo and Xiliao compared to the sites in northern and eastern Taiwan (Chapters 10.6, 10.7 and 10.8). This suggests less participation in acquiring exotic glass beads in the South China Sea exchange network (see section 11.2.3.3), and also less demand for and possibly less access to non-local glass beads in these societies. This could be regarded as a result of the interplay between social practices and economic activities, as the increasing demand and exchange of exotic prestige goods are often associated with an emergent social hierarchy (Renfrew and Shennan 1982; Brumfiel and Earle 1987; Junker 1999: 144; Johnson and Earle 2000). Taken together, it may indicate that societies at Daoye, Wujiancuo and Xiliao in southwestern Taiwan was less stratified in comparison to Kiwulan, Shisanhang, Jiuxianglan and Guishan in the northern and eastern Taiwan in the Iron Age.

Further consideration of the chronology of Daoye (2nd-6th century AD), Wujiancuo (5th-8th

century AD) and Xiliao (6th-14th century AD) shows that there is no significant difference in the distribution pattern and diversity of grave goods at the three sites (Chapters 10.6, 10.7 and 10.8). This suggests that the increasing complexity of societies over time is less evident in southwestern Taiwan, and therefore may reflect stable economic relations and socio-political interactions in southwestern Taiwan in this period. Future research on the household distribution at each site, the social practice reflected by other categories of material culture and the exchange activities in southwestern Taiwan will further enhance this picture.

11.3.3. The analogy to aborigines in Taiwan

The lesser degree of social differentiation in southwestern Taiwan is analogous to the Siraya aborigines in this region. The Daoye, Wujiancuo and Xiliao sites in the southwest all show cultural affinities to the Niaocong Culture. The current Siraya aborigines, who are consumers of glass beads, in southwestern Taiwan are thought to be descendants of the Niaocong people (Tsang and Li 2013: 227). The record ‘An account of the Eastern Savages’ (*Dongfan Ji*, 東番記) written by Di Chen in 1603 in the Ming Dynasty, mentions the life and customs of the Siraya people, in southwestern Taiwan in the 17th century AD. This document provides an ethnohistoric parallel for the discussion of social differentiation in southwestern Taiwan in the Iron Age. His account notes the social structure of the southwestern inhabitants ‘...They sporadically distribute over regions of thousands of *li* [one *li* is around 0.5 kilometer], in several different groups as dorps [or villages]. The larger dorps have a population of around thousand people, while the smaller dorps are with 500 or 600 people. There is no chief. They elect the one with more children as the leader, following the leader’s order. ...’ This suggests a society which is less stratified, lacks hereditary status, and echoes the evidence seen of less social differentiation in sites in the southwest discussed above.

A similar parallel to current aborigines can also be seen at Jiuxianglan in southeastern Taiwan and Guishan in southern Taiwan. Although archaeologically Jiuxianglan is associated with the Sanhe Culture and Guishan is assigned as the Guishan Culture, they both show connections and parallels to the Paiwan aborigines in these areas (Li 2003; Lee 2006; Kuo 2008 and see Chapter 3.3.1.3). The Paiwan society is a ranked society with an inherited aristocracy (Chiang 1992; Hsu 2005: 31-34; Umass 2005). Within Paiwan, there is a tradition of using polychrome glass beads as heirlooms (Chapter 4.6). Glass beads are not simply regarded as ornaments but have particular social meaning. For example, some beads are used as a marker to legitimise status (e.g. the *makazaigao*, or *makacaingaw*, bead) (Hsu 2005: 81; Umss 2005) and some are used as a means of cementing socio-political alliances between societies by giving beads in gift exchange (e.g. the *palalivak* bead) (Umass 2005). It is unclear when the tradition of glass beads as heirlooms developed and it cannot be shown unequivocally in these Iron Age societies. However, the suggestion of ranked society and of the social relations reflected by glass beads in the Paiwan society serves as a good parallel for the discussion in section 11.3.1 of a potentially more stratified society observed through the variation of glass beads in mortuary contexts at these two sites.

11.4. Glass bead production in Taiwan and around the South China Sea

11.4.1. Glass bead production at Jiuxianglan

At Jiuxianglan, the presence of drawn glass beads along with the wound method used for the bead waste does not indicate local production of glass beads. There are no finished wound beads, and the chemical composition of the analysed glass beads does not show a similarity to the glass beadmaking waste (Chapters 8.3.2.7, 9.2.2.6 and 9.4). The areas where large quantities of glass beads were found have previously been suggested as the location of pyrotechnological

activities (Lee 2010: 29), but the evidence examined in this research does not support a large scale of bead production at this site (Chapter 10.4.). Therefore, this evidence, together with the rather small quantity of glass beadmaking waste, lead to the question as to whether this is specialisation in glass beadmaking at Jiuxianglan.

The presence of the wound method of bead production seen in the waste found at Jiuxianglan raises other issues relating to the source of this technology. It has been suggested that most of the Indo-Pacific glass beads were made by the drawn method (Francis 1990; 1991; 2002; Chapter 4.5.1), which differs from the wound method seen in the glass waste at Jiuxianglan. Although the existence of similar sandstone casting moulds found at Khao Sam Kaeo (mid-late 1st millennium BC) to those at Jiuxianglan has led to the suggestion that metalworking knowledge and finished beads were imported from mainland Southeast Asia to Jiuxianglan (Hung and Bellwood 2010; Hung and Chao *in press*; Chapter 3.3.1.2), the beadmaking technology at Khao Sam Kaeo is by the cold-working lapidary method rather than wound method (Lankton *et al.* 2008b; Bellina 2014; Chapter 4.5.3). At present there is an absence of wound beadmaking methods identified in mainland Southeast Asia in this period, and so there is no evidence the technique was transferred from mainland Southeast Asia. One possible provenance for this bead technology is China where the source of the wound method has been proposed (Francis 2002: 76-78 and Chapter 4.5.2). However, the presence of Chinese wound beads around the South China Sea region (ca. the 12th century onwards) (Francis 2002: 76-78) is later than the date of Jiuxianglan (300 BC-700 AD). The archaeological evidence also does not point to interaction between China and Jiuxianglan in the 1st millennium AD. Therefore, the potential source of this knowledge of wound beadmaking at Jiuxianglan remains unclear, but this probably indicates a diverse practice of beadmaking methods around the South China Sea and a possibility of variation in methods between sites. The lapidary beadmaking method from Khao Sam Kaeo (Lankton *et al.* 2008b; Bellina 2014) is one example, and another example can

be seen in the mosaic method of producing Jatim beads in East Java in the 1st millennium AD (Lankton *et al.* 2008a) (Chapter 4.5.3).

11.4.2. The production of m-Na-Al 1 glass around the South China Sea

This research has shown the chemical complexity and microstructural heterogeneity of m-Na-Al 1 glass between different sites (Chapters 8.3). As noted in Chapter 9.4, granite sand was probably used for the production of m-Na-Al 1 glass, and this kind of sand is widely distributed and contains a variety of components. The complexity of the chemical composition and the presence of some un-melted mineral relics dispersed over the glass matrix seen in the m-Na-Al 1 glasses here (Chapter 8.3) suggest that the sand may have been less refined before it was introduced into the glass melt, which supports the assumption made by Dussubieux *et al.* (2010). There may also be a possibility that some of the impurities seen in the glasses here were introduced from the soda efflorescence (such as *reh*) if additional soda was introduced in a lesser refined state too. The varied range of chemical compositions and the presence of mineral relics therefore raises issues in terms of the standardisation and specialisation of m-Na-Al 1 glass around the South China Sea or South Asia.

The ‘partial melting model’ and ‘total melting model’ are proposed in Rehren (2000a) and Rehren (2000b) for explaining the standardisation of glassmaking of HMG glass in Late Bronze Age Egypt and LMG glass in early Iron Age Europe and the Roman empire. The ‘partial melting model’ is characterised by the clustering of glass compositions close to the eutectic point in the ternary phase diagram, suggesting a more developed technology producing higher quality of glass, in which glass formation is controlled by the melting process rather than strict recipe. The ‘total melting model’ shows glass compositions widely dispersed near the eutectic point, indicating that the glassmaking requires careful selection of raw materials and may demonstrate

a lesser standardised production process which produces lower quality of glass.

The wide range of chemical composition seen in the m-Na-Al 1 glass therefore may reflect the ‘total melting model’ of glassmaking, as a varied composition can be observed in the plot of $\text{Na}_2\text{O}-\text{Al}_2\text{O}_3-\text{SiO}_2$ phase diagram (Figure 8.14, plotted by colour groups). Although not shown in Figure 8.14, the investigation by site in the $\text{Na}_2\text{O}-\text{Al}_2\text{O}_3-\text{SiO}_2$ phase diagram also reveals a dispersed distribution. This suggests that while there may be a shared knowledge of raw material selection or recipes in making this kind of glass, these glasses have a more variable composition. The microstructural results, showing mineral relics and bubbles (the presence of which varies between sites), indicates a low quality glass was produced. Therefore, it may suggest that the production process of m-Na-Al 1 glass is less standardised, lacking full control of production parameters. However, although production methods do not show a high degree of specialisation, the selection of similar raw materials implies that there may be a certain degree of craft specialisation of m-Na-Al 1 glassmaking, in terms of the shared knowledge of recipes or raw materials. In addition, despite its wide geographic and chronological distribution, evidence of primary production of m-Na-Al 1 glass has only so far been reported from South Asia (Dussubieux *et al.* 2010). This may suggest that this particular knowledge of raw materials or recipes is more accessible to the South Asian or South Asian-influenced craftspeople or workshops.

11.4.3. The production and recycling of v-Na-Ca glass around the South China Sea region?

This research has tentatively suggested that some imported v-Na-Ca glass may have been recycled in Southeast Asia based on the elevated level of some transitional metal elements which are irrelevant to the colouring (Chapters 9.2.1.3 and 9.2.2.2). Similarly in Chapter 9.2.2.4,

the core body of LL02 type at Kiwulan reveals the mixing of v-Na-Ca glass and sand/clay. The results therefore imply that there may be secondary production, including glass colouring and glass beadmaking, using v-Na-Ca glass around the South China Sea region. In the case of the LL02 type at Kiwulan, it further shows the combination of different materials/glasses including v-Na-Ca glass, m-Na-Al glass and sand/clay in glass bead production. In fact, there has been research suggesting the recycling of imported glass in East Java, and that these recycled glasses were coloured and used for producing glass beads locally (Lankton *et al.* 2008a; Chapter 4.5.3). Taken together, the possible existence of secondary glass production around the South China Sea may indicate that the local Southeast Asian craftspeople actively produced glass beads for particular local demand or for export to the South China Sea network. However, as v-Na-Ca glass is a less well-studied chemical group in the South China Sea region, this assumption requires more study.

11.4.4. Linking the red and orange glass colouring to base chemical groups

Lastly, one interesting aspect noticed in the research is the different colour distributions in the m-Na-Al and v-Na-Ca glasses. Overall, a relatively higher percentage of red and orange glass is found in the m-Na-Al glass than in v-Na Ca glass (Figure 8.2, and see Dussubieux *et al.* (2010) and Dussubieux and Allen (2014)). Considering the technological origin of the two types of glass and the chronological sequence (Chapters 5.2.1 and 5.2.3), this might suggest a South Asian-oriented tradition of colouring red and orange glass. The near absence of red and orange glass beads in v-Na-Ca glass could suggests two scenarios: (1) the glass colouring workshops making these beads did not have the tradition or knowledge of making red and orange glass. This implies that the workshops using v-Na-Ca glass did not know the South Asian tradition of glass production, and so the knowledge of producing red and orange glass is restricted to South Asian-oriented workshops. (2) This may be a result of glass bead supply in late 1st millennium

AD in the South China Sea network. In this case, the demand and accessibility of bead colours in local societies may be affected by the supply of glass bead exchange in different periods. The restricted distribution of red and orange beads between different compositions shows the potential interplay between production and exchange of glass beads in different periods in the South China Sea region, and it is hoped that future research on varied colours will help enhance our current picture.

12. Conclusions and future prospects

Based on the study of typology, chemical composition, microstructure and context of glass beads from 7 Iron Age sites (Kiwulan, Shisanhang, Jiuxianglan, Guishan, Daoye, Wujiancuo and Xiliao) in Taiwan, this research has suggested glass beads as prestige goods in early Iron Age Taiwan (the 1st millennium AD). More surprisingly it has identified regional and chronological distributions of glass beads, which may be associated with the cultural, economic and socio-politic interactions by regions and through time.

This research has demonstrated that the exchange of glass beads in early Iron Age Taiwan is linked to the South China Sea network, as the transition of glass compositions in this period matches those seen in the South China Sea region. The early import of glass beads is seen in eastern coastal Taiwan, witnessed by the arrival of m-Na-Al glass in early 1st millennium AD, and later the presence of v-Na-Ca glass in late 1st millennium AD is seen across different regions in Taiwan.

Within Taiwan, the inter-regional exchange between different regions in the 1st millennium AD is less evident. This suggests that glass beads were regarded as prestige goods in local societies or within particular regional exchange networks in this period and within cultural/social groups. More intensive exchange of glass beads is found in northern and eastern Taiwan than in southwestern Taiwan, which may be a feature of the availability of glass beads through supply networks, or alternatively may be explained by social factors.

By studying glass bead distributions from mortuary contexts, this research has shown that sites in the north (Kiwulan and Shisanhang), the east (Jiuxianglan) and the south (Guishan) of

Taiwan may be more stratified than sites in the southwest (Daoye, Wujiancuo and Xiliao). Those sites or regions which show greater social complexity, as seen in the numbers and distribution of glass beads within mortuary contexts, also reveal intensive regional exchange of beads. Therefore, it is concluded that the exchange of glass beads in early Iron Age Taiwan should be regarded as a result of the interplay between economic and socio-political practices within and between sites/regions.

The findings of this research do not support the local production of the beads and large scale bead production at Jiuxianglan, and the technological origin of the wound beadmaking method at this site remains unclear. However, the chemical and microstructural analysis of glass beads from sites throughout Taiwan has allowed a greater understanding of the production of m-Na-Al glass and v-Na-Ca glass in the South China Sea region. It is suggested that the knowledge of raw materials or recipes of m-Na-Al glass may have been shared between South Asian-oriented workshops, but the production process is not very standardised. The relevant knowledge of m-Na-Al glass production and particularly the colouring of red and orange glass is probably restricted to South Asian or South Asian-influenced workshops. As for the v-Na-Ca glass, there is some evidence that this glass was recycled for the production of beads somewhere around the South China Sea region.

Future prospects

Whilst this research has demonstrated that the combination of typological, chemical, microstructural and contextual investigation of early Iron Age glass beads from Taiwan is imperative to gain a better understanding of exchange networks and supply and use of beads, future research is always necessary.

1. It has been suggested tentatively that there was a transition of bead exchange in Taiwan from the South China Sea-oriented to the Chinese-oriented network in the turn of the 2nd millennium AD. Future analysis of glass beads from the later period will help to test the assumption.
2. More detailed analysis alongside a better understanding of the context of the materials at Jiuxianglan will be helpful to understand the nature of bead production which has taken place at this site.
3. Detailed stratigraphic data and use of space in archaeological sites in Taiwan will give an insight to the study of prestige value of glass beads and the way these beads materialised into the cultural and social context.
4. It is hoped that future works on the combined microstructural and chemical analysis of glass beads from more sites in Taiwan or around the South China Sea will provide a more comprehensive picture of glass bead exchange and production in these regions.

Bibliography

- Ahmed, A. A. and Ashour, G. M. 1981. Effect of heat-treatment on the crystallization of cuprous-oxide in glass. *Glass Technology*, 22: 24-33.
- An, J. 2000. *A Brief History of Glasswares in China*. Beijing: Encyclopedia of China Publishing House.
- An, J. 2005. Ancient glass technology in the Wei, Jin and Southern-Northern Dynasties. In: Gan, F. (ed.) *Development of Chinese Ancient Glass*, pp. 113-127. Shanghai: Shanghai Scientific and Technological Literature Publishing House Co., Ltd.
- Basa, K. K., Glover, I. and Henderson, J. 1991. The relationship between early Southeast Asian and Indian glass. *Bulletin Indo-Pacific Prehistory Association*, 10: 366-385.
- Beck, H. C. 1928. I.—Classification and nomenclature of beads and pendants. *Archaeologia (Second Series)*, 77: 1-76.
- Bellina, B. 2003. Beads, social change and interaction between India and South-east Asia. *Antiquity*, 77: 285-297.
- Bellina, B. 2014. Maritime silk roads' ornament industries: socio-political practices and cultural transfers in the South China Sea. *Cambridge Archaeological Journal*, 24: 345-377.
- Bellina, B. and Glover, I. 2011. Ban Don Ta Phet and Khao Sam Kaeo: the earliest Indian contacts re-assessed. In: Manguin, P.-Y., Mani, A. and Wade, G. (eds.) *Early Interactions between South and Southeast Asia*, pp. 17-46. Singapore: ISEAS - Yusof Ishak Institute.
- Bellina, B. and Silapanth, P. 2006. Khao Sam Kaeo and the upper Thai peninsula: understanding the mechanisms of early trans-Asiatic trade and cultural exchange. In: Bacus, E. A., Glover, I. C. and Pigott, V. C. (eds.) *Uncovering Southeast Asia's Past - Selected papers from the Tenth Biennial Conference of the European Association of Southeast Asian*

- Archaeologists*, pp. 379-392. Singapore: NUS Press.
- Brems, D. and Degryse, P. 2014. Trace elements in sand raw materials. In: Degryse, P. (ed.) *Glass Making in the Greco-Roman World*, pp. 69-85. Belgium: Leuven University Press.
- Brill, R. H. 1970. The chemical interpretation of the texts. In: Oppenheim, A. L., Brill, R. H., Barag, D. and Saldern, A. v. (eds.) *Glass and Glass Making in Ancient Mesopotamia*, pp. 105-128. Corning, New York: Corning Museum of Glass.
- Brill, R. H. 1972. A chemical-analytical round-robin on four synthetic ancient glasses. *International Congress on Glass, Artistic and Historical Communications, Versailles, Sept.–Oct. 1971*. Institut de Verre, Paris.
- Brill, R. H. 1987. Chemical analysis of some early Indian glasses. In Bhardwaj, H. C. (ed.) In: *Archaeometry of Glass. Proceedings of the XIV International Congress on Glass, New Delhi, 1986*, pp. 1-25. Calcutta: Indian Ceramic Society.
- Brill, R. H. 1988. Scientific investigations of the Jalame glass and related finds. In: Weinberg, G. D. (ed.) *Excavations at Jalame, site of a glass factory in late Roman Palestine*, pp. 257-294. Columbia, MO: University of Missouri Press.
- Brill, R. H. 1995. Scientific research in early Asian glass. In: *Proceedings of XVII International Congress on Glass*, pp. 270-279. Beijing: Chinese Ceramic Society.
- Brill, R. H. 1999. *Chemical Analyses of Early Glasses*, Vol. 2. New York: The Corning Museum of Glass.
- Brill, R. H. 2001. Some thoughts on the chemistry and technology of Islamic glass. In: Carboni, S. and Whitehouse, D. (eds.) *Glass of the Sultans*, pp. 25-45. New York: The Metropolitan Museum of Art.
- Brill, R. H., Barnes, I. L. and Joel, E. C. 1991a. Lead isotope studies of early Chinese glass. In: Brill, R. H. and Martin, J. H. (eds.) *Scientific Research in Early Chinese Glass*, pp. 65-83. New York: The Corning Museum of Glass.

- Brill, R. H., Fenn, P. M. and Lange, D. E. 1995. Chemical analyses of some Asian glasses. In: *Proceedings of XVII International Congress on Glass*, pp. 463-468. Beijing: Chinese Ceramic Society.
- Brill, R. H., Tong, S. S. C. and Dohrenwend, D. 1991b. Chemical analyses on some early Chinese glasses. In: Brill, R. H. and Martin, J. H. (eds.) *Scientific Research in Early Chinese Glass*, pp. 31-58. New York: The Corning Museum of Glass.
- Bring, T. and Jonson, B. 2007. Colour development in copper ruby alkali silicate glasses. Part 1. The impact of tin (II) oxide, time and temperature. *Glass Technology: European Journal of Glass Science and Technology Part A*, 48: 101-108.
- Brumfiel, E. M. and Earle, T. K. 1987. Specialization exchange and complex societies: an introduction. In: Brumfiel, E. M. and Earle, T. K. (eds.) *Specialization Exchange and Complex Societies*, pp. New York: Cambridge University Press.
- Bulbeck, D. 2002. Indigenous Traditions and Exogenous Influence in the early History of Peninsular Malaysia. In: Glover, I. and Bellwood, P. (eds.) *Southeast Asia: from Prehistory to History*, pp. 314-336. New York: RoutledgeCurzon.
- Capatina, C. 2005. The study of copper ruby glass. *Ceramics*, 49: 283-286.
- Carter, A. K. 2010. Trade and exchange networks in Iron Age Cambodia: preliminary results from a compositional analysis of glass beads. *Bulletin of the Indo-Pacific Prehistory Association*, 30: 178-188.
- Carter, A. K. 2013. *Trade, exchange, and socio-political development in Iron Age (500 BC - AD 500) mainland Southeast Asia: An examination of stone and glass beads from Cambodia and Thailand*. PhD unpublished thesis, Department of Anthropology, the University of Wisconsin-Madison.
- Carter, A. K. 2015. Beads, exchange networks and emerging complexity: a case study from Cambodia and Thailand (500 BCE–CE 500). *Cambridge Archaeological Journal*, 25: 733-757.

- Carter, A. and Lankton, J. W. 2012. Analysis and comparison of glass beads from Ban Non Wat and Noen U-Loke. In: Higham, C. and Kijngam, A. (eds.) *The Origins of Angkor: The Iron Age: Summary and Conclusions*, Vol. 6, pp. 91-114. Bangkok: Fine Arts Department of Thailand.
- Chao, C.-Y., Liu, Y.-C. and Chung, K.-F. 2013. On "Upper Huakangshan Culture": a proposal. *Field Archaeology of Taiwan*, 16: 53-79.
- Chao, C.-Y. and Wang, K.-W. 2012. The appearance of glass beads in prehistoric Taiwan and their significance in the South China Sea region: A Pilot Study. In: *International Conference on Cross-regional Comparison of Ancient Migration and Exchange Patterns*. Taipei: Research Center for Humanities and Social Sciences, Academia Sinica.
- Chen, C.-L. 1966. The study of ancient glass beads in the Paiwan aborigines in Taiwan and the deduction of their emergence. *Journal of Archaeology and Anthropology*, 28: 1-6.
- Chen, C.-L. 1968. *Material Culture of the Formosan Aborigines*. Taipei: The Taiwan Museum.
- Chen, K.-T. 2000. *Ancient Iron Technology of Taiwan*. PhD unpublished thesis, Department of Anthropology, Harvard University.
- Chen, K.-T. and Cheng, C.-F. 2011. Preliminary scientific analysis of glass artefacts unearthed from Xiliao. In: Liu, Y.-C., Chen, K.-T., Liu, Y.-S. and MOTC, D. G. o. H. (eds.) *Reports of the Salvage Excavation at Xiliao*, part 2, pp. 25-67. Tainan: Directorate General of Highways, MOTC.
- Chen, Y.-B. 2006. The significance of excavation in Kiwulan in the archaeological research in Lanyang Plain. *Yilan Literature Series*, 27: 11-25.
- Chen, Y.-B., Chiu, S.-J. and Li, C.-Y. 2008a. *The Salvage Excavation at Kiwulan Site*, Vol. 1. Yilan: Lanyang Museum.
- Chen, Y.-B., Chiu, S.-J. and Li, C.-Y. 2008b. *The Salvage Excavation at Kiwulan Site*, Vol. 2. Yilan: Lanyang Museum.

- Chen, Y.-B., Chiu, S.-J. and Li, C.-Y. 2008c. *The Salvage Excavation at Kiwulan Site*, Vol. 3. Yilan: Lanyang Museum.
- Chen, Y.-B., Chiu, S.-J. and Li, C.-Y. 2008d. *The Salvage Excavation at Kiwulan Site*, Vol. 4. Yilan: Lanyang Museum.
- Chen, Y.-B., Chiu, S.-J. and Li, C.-Y. 2008e. *The Salvage Excavation at Kiwulan Site*, Vol. 6. Yilan: Lanyang Museum.
- Chen, Y.-M. 2008. Regional interaction and the formation of cultural groups: a perspective from the Orchid Island. In: *Culture Creativity and Social Practice*. Taipei: Institute of Ethnology, Academia Sinica.
- Cheng, C.-F. 2007. *Studies of Glass Beads Excavated from Kivulan and Shenei Site, Taiwan*. MA unpublished thesis, Institute of Anthropology, National Tsing Hua University.
- Chiang, B. 1992. The social anthropological research on Paiwan aborigines, part I: 1895-1971. *Newsletter of Taiwan History Field Research*, 24: 27-47.
- Chiu, H.-L. 2004. *Investigations of Mortuary Behaviors and Cultural Change of the Kivulan Site in I-Lan County, Taiwan*. MA unpublished dissertation, Department of Anthropology, National Taiwan University.
- Cui, J., Ho, C.-K., Liu, K.-H. and Wu, X. 2008. Scientific analysis on some ancient glass beads from Taiwan. *Cultural Relics in Southern China*, 4: 109-114.
- de Beauclair, I. 1972. Jar burial on Batel Tobago Island. *Asian Perspectives*, 15: 167-176.
- DeCorse, C. R., Richard, F. G. and Thiaw, I. 2003. Toward a systematic bead description system: a view from the Lower Falemme, Senegal. *Journal of African Archaeology*, 1: 77-110.
- Drennan, R. D., Peterson, C. E. and Fox, J. 2010. Degrees and Kinds of Inequality. In: Price, T. D. and Feinman, G. (eds.) *Pathways to Power*, pp. 45-76. Springer New York.
- Dillian, C. D. and White, C. L. 2010. *Trade and Exchange: Archaeological Studies from History and Prehistory*. New York: Springer.
- Dumańska-Słowik, M., Heflik, W., Pieczka, A., Sikorska, M. and Dąbrowa, Ł. 2015. The

- transformation of nepheline and albite into sodalite in pegmatitic mariupolite of the Oktiabrski Massif (SE Ukraine). *Spectrochimica Acta Part A: Molecular and Biomolecular Spectroscopy*, 150: 837-845.
- Durán, A., Fernández Navarro, J. M., García Solé, J. and Agulló-López, F. 1984. Study of the colouring process in copper ruby glasses by optical and EPR spectroscopy. *Journal of Materials Science*, 19: 1468-1475.
- Dussubieux, L. 2001. *L'apport de l'blation laser couplée à l'ICP-MS à la caractérisation des verres: application à l'étude du verre archéologique de l'Océan Indien*. PhD unpublished thesis, Université d'Orléans.
- Dussubieux, L. 2009. LA-ICP-MS analysis of African glass beads: Laboratory inter-comparison with an emphasis on the impact of corrosion on data interpretation. *International Journal of Mass Spectrometry*, 284: 152-161.
- Dussubieux, L. 2014. Compositional analysis of ancient glass fragments from Si Pamutung, North Sumatra. In: Perret, D. (ed.) *History of Padang Lawas, North Sumatra*, pp. 379-389. Paris: Association Archipel.
- Dussubieux, L. and Allen, J. 2014. Compositions of glass artifacts from Malaysia New data from the sites of Pengkalan Bujang and Sungai Mas. In: Perret, D. and Jaafar, Z. B. (eds.) *Ancient Glassware in Malaysia: The Pengkalan Bujang Collection*, pp. 119-161. Kuala Lumpur: Department of Museums Malaysia.
- Dussubieux, L. and Gratuze, B. 2010. Glass in Southeast Asia. In: Bellina, B., Bacus, E. A., Pryce, T. O. and Christie, J. W. (eds.) *50 Years of Archaeology in Southeast Asia: Essays in Honour of Ian Glover*, pp. 246-259. Bangkok: River Books.
- Dussubieux, L. and Gratuze, B. 2013. Glass in South Asia. In: Janssens, K. (ed.) *Modern Methods for Analysing Archaeological and Historical Glass*, Vol. 2, pp. 399-413. New York: John Wiley & Sons, Ltd.
- Dussubieux, L., Gratuze, B. and Blet-Lemarquand, M. 2010. Mineral soda alumina glass:

- occurrence and meaning. *Journal of Archaeological Science*, 37: 1646-1655.
- Francis, P. 1990. Glass beads in Asia. Part one. Introduction. *Asian Perspectives*, 28: 1-21.
- Francis, P. 1991. Beadmaking at Arikamedu and beyond. *World Archaeology*, 23: 28-44.
- Francis, P. 2002. *Asia's Maritime Bead Trade: 300 B.C. to the Present*. Honolulu: University of Hawai'i Press.
- Freestone, I. C. 1987. Composition and microstructure of early opaque red glass. In: Bimson, M. and Freestone, I. C. (eds.) *Early Vitreous Materials, Occasional Paper No.56*, pp. 173-191. London: British Museum.
- Freestone, I. C. and Gorin-Rosen, Y. 1999. The great glass slab at Bet Shearim, Israel: an early Islamic glassmaking experiment? *Journal of Glass Studies*, 41: 105-116.
- Freestone, I. C., Leslie, K. A., Thirlwall, M. and Gorin-Rosen, Y. 2003a. Strontium isotopes in the investigation of early glass production: Byzantine and early Islamic glass from the Near East. *Archaeometry*, 45: 19-32.
- Freestone, I. C., Ponting, M. and Hughes, M. J. 2002. The origins of Byzantine glass from Maroni Petrera, Cyprus. *Archaeometry*, 44: 257-272.
- Freestone, I. C., Stapleton, P. and Rigby, V. 2003b. The production of red glass and enamel in the Later Iron Age, Roman and Byzantine periods. In: Entwistle, C. (ed.) *Through a Glass Brightly: Studies in Byzantine and Medieval Art and Archaeology presented to David Buckton*, pp. 142-154. Oxford: Oxbow Books.
- Fu, X. and Gan, F. 2006. Chemical composition analysis of some ancient glasses unearthed from southern and southwestern China. *Sciences of Conservation and Archaeology*, 18: 6-13.
- Gan, F. 2007. Ancient Chinese glass and ancient Silk Road - keynote speech of the 2004 Urumchi Symposium on Ancient Glasses in Northern China. In: Gan, F. (ed.) *Study on Ancient Glass along the Silk Road - Proceedings of 2004 Urumqi Symposium on Ancient Glass in Northern China and 2005 Shanghai International Workshop of*

- Archaeology of Glass*, pp. 1-29. Urumqi, China: Fudan University Press.
- Glover, I. and Bellina, B. 2011. Ban Don Ta Phet and Khao Sam Kaeo: the earliest Indian contacts re-assessed. In: Manguin, P.-Y., Mani, A. and Wade, G. (eds.) *Early Interactions between South and Southeast Asia: Reflections on Cross-cultural Exchange*. Singapore: SEAS.
- Glover, I. and Henderson, J. 1995. Early glass in South and South East Asia and China. In: Scott, R. and Gyu, J. (eds.) *China and Southeast Asia: Art, Commerce and Interaction*, pp. 141-169. London: Percival David Foundation of Chinese Art.
- Gratuze, B. 1999. Obsidian characterization by Laser Ablation ICP-MS and its application to prehistoric trade in the Mediterranean and the Near East: sources and distribution of obsidian within the Aegean and Anatolia. *Journal of Archaeological Science*, 26: 869-881.
- Gratuze, B., Soulier, I., Blet, M. and Vallauri, L. 1996. De l'origine du cobalt : du verre à la céramique. *Revue d'Archéométrie*: 77-94.
- Gorin-Rosen, Y. 2000. The ancient glass industry in Israel: summary of finds and new discoveries. In: Nenna, M.-D. (ed.) *La Route du Verre: Ateliers Primaires et Secondaires du Second Millénaire av. J.-C. au Moyen Âge*, pp. 49-63. Lyon: Maison de l'Orient Méditerranéen.
- Guido, M. 1978. *The glass beads of the prehistoric and Roman periods in Britain and Ireland*. London: Society of Antiquaries of London.
- Guido, M. 1999. *The Glass Beads of Anglo-Saxon England c.AD 400-700: A Preliminary Visual Classification of the More Definitive and Diagnostic Types*. Suffolk: St Edmundsbury Press Ltd.
- Gushi. 2015. *Even the head of Hualian County does not know - how the Hanben site on the Suhua Highway project changes our understanding of Taiwan history?* [Online]. Available: <http://gushi.tw/archives/18732>.

- Hauptmann, A., Rehren, Th. and Schmitt-Strecker, S. 2003. Early Bronze Age copper metallurgy at Shahr-i Sokhta (Iran), reconsidered. In: Stöllner, T., Körlin, G., Steffens, G. and Cierny, J. (eds.) *Man and Mining - Mensch und Bergbau*, pp. 197-213. Bochum: Deutsches Bergbau-Museum.
- Heck, M., Rehren, Th. and Hoffmann, P. 2003. The production of lead–tin yellow at Merovingian Schleithem (Switzerland). *Archaeometry*, 45: 33-44.
- Heier, K. S. 1962. Trace elements in feldspars - a review. *Norsk Geologisk Tidsskrift*: 415-454.
- Henderson, J. 1985. The raw materials of early glass production. *Oxford Journal of Archaeology*, 4: 267-291.
- Higham, C. 2004. Mainland Southeast Asia from the Neolithic to the Iron Age. In: Glover, I. and Bellwood, P. (eds.) *Southeast Asia: from Prehistory to History*, pp. 41-67. New York: RoutledgeCurzon.
- Ho, C.-K. and Liu, K.-H. 2005. *The Illustrated Handbook of Artefacts from Luliao site*. Taichung: National Museum of Natural Science.
- Hou, D. 2005. Ancient glass technology in the pre-Qin and Han Dynasty. In: Gan, F. (ed.) *Development of Chinese Ancient Glass*, pp. 80-112. Shanghai: Shanghai Scientific and Technological Literature Publishing House Co., Ltd.
- Hsu, M.-C. 2005. *Glass Beads in Paiwan*. Taipei: Daw Shiang Publishing Co. Ltd.
- Hu, C.-Y. 2012. Comparative analysis of glass beads used among Austronesian groups in Taiwan: some thoughts on forms, values and materiality. *Journal of Archaeology and Anthropology*, 76: 97-134.
- Huang, S.-C. and Liu, Y.-C. 1980. *Inspections and Suggestions on the Renovation of Important Historic Sites in Taiwan: The Archaeological Sites and the Ancient Aboriginal Communities*. Taipei: Tourism Bureau, MOTC.
- Huang, S.-C., Chen, Y.-B. and Yen, H.-C. 1987. *Report of Archaeological and Ethnographic Investigations in the Kenting National Park on Southern Tip of Taiwan.*, Bingdong,

- Taiwan: Kenting National Park Headquarters, Construction and Planning Administration, Ministry of the Interior, Taiwan.
- Huang, T.-X. 1982. *Niaosong Relic of Yongkang Rural Township, Tainan County*. MA unpublished dissertation, Department of Archaeology, National Taiwan University.
- Huang, Q. 1988. Study on ancient glass in Guangxi. *Archaeology*, 3: 264-276+295.
- Huang, Q. 2003. Study on the ancient glass wares discovered in Guangxi. In: Gan, F. (ed.) *Study on Ancient Glass in Southern China - Proceedings of 2002 Nanning Symposium on Ancient Glasses in Southern China*. Shanghai: Shanghai Scientific and Technological Publishers.
- Huang, Q. 2005. Ancient glass technology in the south and south-west of China. In: Gan, F. (ed.) *Development of Chinese Ancient Glass*, pp. 182-199. Shanghai: Shanghai Scientific and Technological Literature Publishing House Co., Ltd.
- Hung, H.-C. 2012. Taiwan nephrite overseas and their Beinan cultural characteristics. *Field Archaeology in Taiwan*, 15: 19-40.
- Hung, H.-C. and Bellwood, P. 2010. Movement of raw materials and manufactured goods across the South China Sea after 500 BCE: from Taiwan to Thailand, and Back. In: Bellina, B., Bacus, E. A., Pryce, T. O. and Christie, J. W. (eds.) *50 Years of archaeology in Southeast Asia: essays in honour of Ian Glover*, pp. 234-245. Bangkok: River Books.
- Hung, H.-C. and Chao, C.-Y. In press. Taiwan's early metal age and engagement with world trading systems. *Antiquity*.
- Hung, H.-C. and Iizuka, Y. In press. Nephrite and mica industries: A link towards the Austronesian world. In: Bellina, B. (ed.) *Excavation Report of Khao Sam Kaeo Site, Peninsula Thailand*.
- Hung, H.-C., Iizuka, Y., Bellwood, P., Nguyen, K. D., Bellina, B., Silapanth, P., Dizon, E., Santiago, R., Datan, I. and Manton, J. H. 2007. Ancient jades map 3,000 years of prehistoric exchange in Southeast Asia. *PNAS*, 104: 19745-19750.

- Hung, H.-C., Nguyen, K. D., Bellwood, P. and Carson, M. T. 2013. Coastal Connectivity: Long-Term Trading Networks Across the South China Sea. *The Journal of Island and Coastal Archaeology*, 8: 384-404.
- Hung, L.-Y. and Ho, C.-K. 2007. New light on Taiwan highland prehistory. *Bulletin of the Indo-Pacific Prehistory Association*, 26: 21-31.
- Iizuka, Y. and Hung, H.-C. 2005. Archaeomineralogy of Taiwan nephrite: sourcing study of nephritic artifacts from the Philippines. *Journal of Austronesian Studies*, 1: 33-79.
- Ishida, S., Hayashi, M., Takeuchi, N. and Wakamatsu, M. 1987. Role of Sn²⁺ in development of red color during reheating of copper glass. *Journal of Non-Crystalline Solids*, 95: 793-800.
- Jackson, C. M. 2005a. Glassmaking in Bronze-Age Egypt. *Science*, 308: 1750-1752.
- Jackson, C. M. 2005b. Making colourless glass in the Roman period. *Archaeometry*, 47: 763-780.
- Jackson, C. M., Nicholson, P. T. and Gneisinger, W. 1998. Glassmaking at Tell el-Amarna: an integrated approach. *Journal of Glass Studies*, 40: 11-23.
- Jackson, C. M. and Smedley, J. W. 2004. Medieval and post-medieval glass technology: melting characteristics of some glasses melted from vegetable ash and sand mixtures. *Glass Technology*, 45: 36-42.
- Janowski, M. 1998. Beads, prestige and life among the Kelabit of Sarawak, east Malaysia. In: Sciaman, L. D. and Eicher, J. B. (eds.) *Beads and Bead Makers*, pp. 213-246. Oxford: Berg.
- Johnson, A. W. and Earle, T. K. 2000. *The evolution of human societies: from foraging group to agrarian state*. Stanford: Stanford University Press.
- Junker, L. L. 1999. *Raiding, Trading, and Feasting: The Political Economy of Philippine Chiefdoms*. Honolulu: University of Hawai'i Press.
- Kidd, K. E. and Kidd, M. A. 1970. A classification system for glass beads for the use of field

- archaeologists. In: *Canadian Historic Sites: Occasional Papers in Archaeology and History*, pp. 45-89. Ottawa: National Historic Sites Service.
- Kuo, S.-C. 2008. The origin of Paiwan based on archaeological evidence in the late prehistoric period in southern Taiwan. In: *Annual Meeting of Anthropology and Ethnology in Taiwan 2008: The Cross-boundary and Challenge of Anthropology*. Taipei: Institute of Ethnology, Academia Sinica.
- Kuo, S.-C. 2015. The context of Zhongguang site in the northern East Rift Valley. In: *Annual Meeting of Taiwan Archaeology 2014*. Taipei: Institute of History and Philology, Academia Sinica.
- Lankton, J., Dussubieux, L. and Rehren, Th. 2008a. A study of mid-first millennium CE Southeast Asian specialized glass beadmaking traditions. In: Bacus, E., Glover, I. and Sharrock, P. (eds.) *Interpreting Southeast Asia's Past: Monument, Image and Text: Selected Papers from the 10th International Conference of the European Association of Southeast Asian Archaeologists*, pp. 335-356. Singapore University Press.
- Lankton, J. W. and Dussubieux, L. 2006. Early glass in Asian maritime trade: a review and an interpretation of compositional analyses. *Journal of Glass Studies*, 48.
- Lankton, J. W. and Dussubieux, L. 2013. Early glass in Southeast Asia. In: Janssens, K. (ed.) *Modern Methods for Analysing Archaeological and Historical Glass*, Vol. 2, pp. 415-443. New York: John Wiley & Sons, Ltd.
- Lankton, J. W., Dussubieux, L. and Gratuze, B. 2008b. Glass from Khao Sam Kaeo: transferred technology for an early Southeast Asian exchange network. *Bulletin de l'Ecole Française d'Extrême-Orient 2006*, 93: 317-351.
- Lankton, J. W., Ige, O. A. and Rehren, Th. 2006. Early primary glass production in southern Nigeria. *Journal of African Archaeology*, 4.
- Lee, K.-S. 2002. The new discoveries and issues of Beinan. *Taitung Historical Journal*, 7: 40-71.

- Lee, K.-S. 2005a. Glass materials from Jiuxianglan site and the relevant research questions. In: *Foreign Substances in Taiwan: Beads and Penannular Jade Ring*, pp.95-120. Taipei: Institute of History and Philology.
- Lee, K.-S. 2005b. *The Report of the Salvage Excavation at Jiuxianglan, Taitung County*. Taitung: Taitung County Government.
- Lee, K.-S. 2006. The salvage excavation and the important findings at Jiuxianglan, Taitung County. In: *Annual Meeting of Taiwan Archaeology 2005*, pp.12-1 – 12-30. Taitung: National Museum of Prehistory.
- Lee, K.-S. 2007. *The Report of the 2nd Salvage Excavation at Jiuxianglan, Taitung County*. Taitung: Taitung County Government.
- Lee, K.-S. 2010. *The Salvage Excavation Report of Jiuxianglan, Taitung, Vol. 1 - Cultural Layer and Funerary*. Taitung: Taitung County Government and National Museum of Prehistory.
- Lee, K.-S. 2015. The sandstone casting mould from *Jiuxianglan*: a pilot study of the meaning and origin. In: *Annual Meeting of Taiwan Archaeology 2014*, pp. 160-201. Taipei: Institute of History and Philology, Academia Sinica.
- Lee, K.-S. and Yeh, M.-C. 2001. *The History of Taitung: The Prehistory*. Taitung: Taitung County Government.
- Levin, E. M. and McMurdie, H. F. 1959. *Phase Diagrams for Ceramists: Part II*. Ohio: The American Ceramic Society.
- Li, F. 1999. *Elemental and Isotopic Analysis of Ancient Chinese Glass*. MPhil unpublished thesis, University of Hong Kong.
- Li, K.-C. 1999. *The Prehistoric Cultures in Kenting National Park*. Taipei: Council for Cultural Affairs, Executive Yuan.
- Li, K.-C., Cheng, Y.-S. and Ling, P.-C. 1985. *Reports of Archaeological Investigations in the Kenting National Park on the Southernmost of Taiwan*. Taipei: Department of

Anthropology, National Taiwan University.

- Li, K.-T. 1993. *Reports of Archaeological Investigations of the Site at National Marine Biology Museum and Kuei-shan Site*. Kaohsiung: Planning Bureau of National Marine Biology Museum.
- Li, K.-T. 1994. *Coastal Adaption in Southern Taiwan: A Case Study of Guishan Site and Eluanbi II Site*. Kaohsiung: Planning Bureau of National Marine Biology Museum.
- Li, K.-T. 1995. *The Comparative Study of Prehistoric Settlement in Hengchun Peninsula: A Case Study of Guishan Site and Eluanbi II Site*. Kaohsiung: Planning Bureau of National Marine Biology Museum.
- Li, K.-T. 2001. The significance of perforated human teeth unearthed from Kuei-shan Site, near the southern tip of Taiwan. *Bulletin of the Institute of History and Philology, Academia Sinica*, 72: 699-722.
- Li, K.-T. 2003. Ceramic remains from Kueishan and discussions relating to the relationship of Formosan aborigines in southern Taiwan. *Bulletin of the National Museum of Natural Science*, 16: 79-90.
- Li, K.-T., Chen, W. and Tsang, C.-H. 2008. The ancient environment of archaeological sites in Tainan Science Park and the coastline change in the southwestern plain in the Holocene period. In: *Annual Meeting of Anthropology and Ethnology in Taiwan 2008: Cross-boundary and Challenge of Anthropology*. Taipei: Institute of Ethnology, Academia Sinica.
- Li, Q., Zhang, B., Gan, F., Chen, H., Ma, B. and Gu, D. 2003. Analytical results of chemical composition of some ancient glasses unearthed from southern China by PIXE technique. In: Gan, F. (ed.) *Study on Ancient Glass in Southern China - Proceedings of 2002 Nanning Symposium on Ancient Glasses in Southern China*. Shanghai: Shanghai Scientific and Technological Publishers.
- Lien, C.-M. 1998. An analytical study on prehistoric Pei-nan jades. In: Deng, C. (ed.) *East*
270

- Asian Jade: Symbol of Excellence*. pp. 350-367. Hong Kong: Centre for Chinese Archaeology and Art, CUHK.
- Lin, S.-F., Chen, Y.-B., Chiu, S.-J. and Li, C.-Y. 2012. The prehistoric people in Kiwulan and the natural landscape. In: Li, S.-y. and Hsu, M.-c. (eds.) *The 9th International Symposium on Yilan Research: Tracing Kiwulan*. Yilan: Archives of Yilan History.
- Liu, K.-H. 1986. On the religious of Niasong Culture from the perspective of archaeological remains. *Man and Culture*, 22: 20-29.
- Liu, K.-H. and Ho, C.-K. 2005. Carnelian beads and glass beads in Luliao site, Shalu, Taichung. In: *Foreign Substances in Taiwan: Beads and Penannular Jade Ring*, pp. 202-210. Taipei: Institute of History and Philology, Academia Sinica.
- Liu, Y.-C. 1999. *The Existing Unknown*. Taichung County: The Cultural Center of Taichung County.
- Liu, Y.-C. 2001. The significance of excavation at Lalu. In: *The Post-921 Earthquake Reconstruction of Society and Culture*, pp. 405-435. Taipei: Institute of Ethnology, Academia Sinica.
- Liu, Y.-C. 2003. The prevailing duration and the related issues of Taiwan jade artefacts. In: Tsang, C.-h. (ed.) *Prehistory and classical civilization - papers from the third International Conference on Sinology (history Session)*, pp. 45-82. Taipei: Academia Sinica Press.
- Liu, Y.-C. 2005. From jade to glass and agate: the transition of prehistoric decoration items in Taiwan. In: *Foreign Substances in Taiwan: Beads and Penannular Jade Ring*, pp. 211-226. Taiwan.
- Liu, Y.-C. 2006a. The geographic boundary the related interaction of cultural groups from an archaeological perspective: a perspective from the mountainous region in eastern Chianan Plain. In: *Reconstructing Siraya: The Conference of Pinpu Groups in Tainan*, pp. 169-191. Tainan: Tainan County Government.

- Liu, Y.-C. 2006b. Preliminary examination on the manufacturing techniques and research methods of jade in Taiwan. In: Hsu, Z., Zhang, Z. and Yang, J. (eds.) *Archaeology of the New Century: Multi-interaction of Culture, Region and Ecology*, pp. 471-496. Beijing: The Forbidden City Publishing House.
- Liu, Y.-C. 2007. *Human activity along the Liwu stream in Taroko: the sustainable management, the aborigines and the national park*. Hualian, Taiwan: The Taroko National Park.
- Liu, Y.-C. 2010. The study of the interaction between people in eastern Taiwan in the late prehistory. *The 17th Academic Lecture, Institute of History and Philology, Taiwan*. Taiwan.
- Liu, Y.-C. 2011a. Exploring the settlement of Niaosong Culture: a case study of Xiliao. In: Liu, Y.-C., Chen, K.-T., Liu, Y.-S. and MOTC, D. G. o. H. (eds.) *Reports of the Salvage Excavation at Xiliao*, part 2, pp. 1-25. Tainan: Directorate General of Highways, MOTC.
- Liu, Y.-C. 2011b. *Reports of the Salvage Excavation at Xiliao*, part 1, Vol. 1. Tainan: Directorate General of Highways, MOTC.
- Liu, Y.-C. 2011c. *Reports of the Salvage Excavation at Xiliao*, part 1, Vol. 2. Tainan: Directorate General of Highways, MOTC.
- Liu, Y.-C. 2011d. *Reports of the Salvage Excavation at Xiliao*, part 1, Vol. 3. Tainan: Directorate General of Highways, MOTC.
- Liu, Y.-C. 2011e. *Reports of the Salvage Excavation at Xiliao*, part 3, Vol. 1-12. Tainan: Directorate General of Highways, MOTC.
- Liu, Y.-C. 2011f. *The History of Taiwan: The Archaeological Records of the Inhabitants*. Nantou: Taiwan Historica.
- Liu, Y.-C. 2013a. Jade production and resource competition in prehistoric Taiwan. In: Chen, K.-T. and Tsang, C.-H. (eds.) *New Lights on East Asian Archaeology*, pp. 199-237. Taipei: Academia Sinica.

- Liu, Y.-C. 2013b. A study of the Tamalin Culture and discussion of related issues. In: Chen, K.-T. (ed.) *Rethinking East Asian Archaeology - Memorial Essay Collection for the Tenth Anniversary of Kwang-Chih Chang's Death*, pp. 83-107. Taipei: Institute of History and Philology, Academia Sinica.
- Liu, Y.-C. 2013. The preliminary study of greyish black pottery in late Neolithic Age in Taiwan. *The 7th Academic Seminar at the Institute of History and Philology, Academia Sinica*.
- Liu, Y.-C. 2014. The significance of Hanben site. In: *The 1st Symposium on the Engineering and Techniques of the Suhua Highway*. Taipei: Suhua Highway Improvement Engineering Office.
- Liu, Y.-C. and Chao, C.-Y. 2010. *The Salvage Excavation at Huagang Junior High School: Metal Age Period*. Hualien, Taiwan: Hualien County Cultural Affairs Bureau.
- Liu, Y.-C. and Chung, K.-F. 2014. The report of the investigation on Pinlin Site in Hualien in 2012. In: *Annual Meeting of Taiwan Archaeology 2013*. Taipei: National Taiwan University.
- Liu, Y.-C. and Yen, T.-Y. 2000. *The Context and Geographic Distribution of Prehistoric Sites in Taitung County: The Eastern Region of Coastal Mountain Range and the Green Island*. Taitung: Taitung County Government.
- Liu, Y.-C., Tseng, C.-M. and Kao, Y.-J. 1994. *Reports of the Survey on Cultural Sites: The Site Selection of the Southern Cross-Island Highway*. Taipei: Ministry of Transportation and Communications Taiwan Area National Expressway Engineering Bureau.
- Lugay, J. B. 1974. Determination of the methods of manufacture of glass beads. In: *Proceedings of the First Regional Seminar on Southeast Asian Prehistory and Archaeology*, pp. 148-181. Manila: National Museum of the Philippines.
- McDonough, W. F. and Sun, S.-S. 1995. Composition of the Earth. *Chemical Geology*, 120: 223-253.
- Mielke, J. E. 1979. Composition of the Earth's crust and distribution of the elements. In: Siegel, 273

- F. R. (ed.) *Review of research on modern problems in geochemistry*, pp. 13-37. Paris: UNESCO Report.
- Mirti, P., Pace, M., Malandrino, M. and Ponzi, M. N. 2009. Sasanian glass from Veh Ardasir: new evidences by ICP-MS analysis. *Journal of Archaeological Science*, 36: 1061-1069.
- Mirti, P., Pace, M., Negro Ponzi, M. M. and Aceto, M. 2008. ICP-MS analysis of glass fragments of Parthian and Sasanian epoch from Seleucia and Veh Ardasir (central Iraq). *Archaeometry*, 50: 429-450.
- Munan, H. 2005. *Beads of Borneo*. Singapore: Editions Didier Millet Pte Ltd.
- Murillo-Barroso, M., Pryce, T. O., Bellina, B. and Martínón-Torres, M. 2010. Khao Sam Kaeo - an archaeometallurgical crossroads for trans-Asiatic technological traditions. *Journal of Archaeological Science*, 37: 1761-1772.
- Nanke Archaeological Team. 2005. Glass artefacts from the sites in Tainan Science Park. In: *Foreign Substances in Taiwan: Beads and Penannular Jade Ring*, pp. 194-201. Taipei: Institute of History and Philology, Academia Sinica.
- Paynter, S. 2008. Experiments in the reconstruction of Roman wood-fired glassworking furnaces: waste products and their formation processes. *Journal of Glass Studies*, 50: 271-290.
- Peake, J. R. N. and Freestone, I. C. 2012. Cross-craft interactions between metal and glass working: slag additions to early Anglo-Saxon red glass. *Proceedings of SPIE Integrated Approaches to the Study of Historical Glass*. Brussels, Belgium: SPIE.
- Peake, J. R. N. and Freestone, I. C. 2014. Opaque yellow glass production in the early medieval period: new evidence. In: Keller, D., Price, J. and Jackson, C. (eds.) *Neighbours and Successors of Rome: Traditions of Glass Production and Use in Europe and the Middle East in the Later 1st Millennium AD*, pp. 15-21. Oxford: Oxbow Books.
- Pearce, N. J. G., Perkins, W. T., Westgate, J. A., Gorton, M. P., Jackson, S. E., Neal, C. R. and Chenery, S. P. 1997. A compilation of new and published major and trace element data

- for NIST SRM 610 and NIST SRM 612 glass reference materials. *Geostandards Newsletter*, 21: 115-144.
- Pearson, M. P. 2003. *The Archaeology of Death and Burial*. College Station: Texas A&M University Press.
- Philippa-Touchais, A. 2010. Settlement planning and social organisation in Middle Helladic Greece. In: Philippa-Touchais, A., Touchais, G., Voustaki, S. and Wright, J. (eds.) *Mesohelladika: The Greek Mainland in the Middle Bronze Age. Proceedings of the International Conference Held in Athens [BCH Supplement 52]*, pp. 781-801. Paris: Ecole française d'Athènes.
- Price, J. 2005. Glass-working and glassworkers in cities and towns. In MacMahon, A. and Price, J. (eds.) *Roman working lives and urban living.*, pp. 167-190. Oxford: Oxbow Books.
- Pryce, T. O. 2009. *Prehistoric copper production and technological reproduction in the Khao Wong Prachan Valley of central Thailand*. PhD unpublished thesis, Institute of Archaeology, University College London.
- Pryce, T. O., Pigott, V. C., Martínón-Torres, M. and Rehren, Th. 2010. Prehistoric copper production and technological reproduction in the Khao Wong Prachan Valley of Central Thailand. *Archaeological and Anthropological Sciences*, 2: 237-264.
- Rehren, Th. 2000a. New aspects of ancient Egyptian glassmaking. *Journal of Glass Studies*, 42: 13-24.
- Rehren, Th. 2000b. Rationales in old world base glass compositions. *Journal of Archaeological Science*, 27: 1225-1234.
- Rehren, Th. 2014. Glass production and consumption between Egypt, Mesopotamia and the Aegean. In: Pfälzner, P., Niehr, H., Pernicka, E., Lange, S. and Köster, T. (eds.) *Contextualising Grave Inventories in the Ancient Near East*, pp. 217-223. Wiesbaden: Harrassowitz Verlag.
- Rehren, Th. and Pusch, E. B. 2005. Late Bronze Age glass production at Qantir-Piramesses,

- Egypt. *Science*, 308: 1756-1758.
- Rehren, Th., Pusch, E. and Herold, A. 1998. Glass coloring works within a copper-centered industrial complex in Late Bronze Age Egypt. In: Kingery, D. and McCray, P. (eds.) *The Prehistory and History of Glassmaking Technology*, pp. 227-250. Westerville, OH: American Ceramic Society.
- Renfrew, C. and Shennan, S. 1982. *Ranking, Resource, and Exchange: Aspects of the Archaeology of Early European Society*. Cambridge: Cambridge University Press.
- Robertshaw, P., Benco, N., Wood, M., Dussubieux, L., Melchiorre, E. and Ettahiri, A. 2010. Chemical analysis of glass beads from medieval Al-Basra (Morocco). *Archaeometry*, 52: 355-379.
- Saha, P. 1961. The system NaAlSiO₄ (nepheline)-NaAlSi₃O₈ (albite)-H₂O*. *The American Mineralogist*, 46: 859-884.
- Santiago, R. 1992. Techniques in classifying archaeological beads. *A Short Paper for SPFA Training Course in Archaeological Beads Analysis*. Bangi, Malaysia.
- Sato, B. 1988[1944]. *Studies on the Primitive Arts of Aborigines in Taiwan*. Taipei: SMC Publishing Inc.
- Sayre, E. V. 1963. The intentional use of antimony and manganese in ancient glasses. In: Matson, F. R. and Rindone, G. E. (eds.) *Advances in Glass Technology: Additional Papers from the 6th International Congress on Glass*, pp. 263-282. New York: Plenum Press.
- Sherratt, A. and Sherratt, S. 1991. From luxuries to commodities: the nature of Mediterranean Bronze Age trading systems. In: Gale, N. H. (ed.) *Bronze Age trade in the Mediterranean.*, pp. 351-386. Oxford: Jonsered Paul Astroms Forlag.
- Shi, M., He, O. and Zhou, F. 1986. Investigation on some Chinese potash glasses excavated from tombs of the Han dynasty *Journal of the Chinese Ceramic Society*, 14: 307-313.
- Shortland, A., Schachner, L., Freestone, I. and Tite, M. 2006. Natron as a flux in the early

- vitreous materials industry: sources, beginnings and reasons for decline. *Journal of Archaeological Science*, 33: 521-530.
- Sode, T. and Kock, J. 2001. Traditional raw glass production in northern India: the final stage of an ancient technology. *Journal of Glass Studies*, 43: 155-169.
- Solheim, W. 1964. Further relationships of the Sa-Huynh-Kalanay pottery tradition. *Asian Perspectives*, 8: 196-211.
- Solheim, W. 2006. *Archaeology and Culture in Southeast Asia: Unraveling the Nusantara*. Quezon City: The University of the Philippines Press.
- Stamps, R. B. 1980. Jar burial from the Lobusbussan Site, Orchid (Botel Tobago) Island. *Asian Perspectives*, 23: 181-192.
- Sung, W.-H. 1980. Understanding Taiwan by Archaeology. In: Chen, C.-L. (ed.) *The Chinese Taiwan*, pp. 93-220. Taipei: Zhong Yang Wen Wu Gong Ying She.
- Sung, W.-H., Yin, C.-C., Huang, S.-C., Lien, C.-M. and Liu, Y.-C. 1992. *Preliminary Evaluation of the Major Prehistoric Sites of Taiwan*. Taipei: Ethnological Society of China.
- Tan, L.-P., Lien, C.-M. and Yu, B.-C. 1997. The preliminary analysis on the origin of nephrites from the Peinan site of Taiwan. *Bulletin of the Department of Anthropology*, 52: 211-220.
- Tite, M., Pradell, T. and Shortland, A. 2008. Discovery, production and use of tin-based opacifiers in glasses, enamels and glazes from the late Iron Age onwards: a reassessment. *Archaeometry*, 50: 67-84.
- Tsang, C.-H. 1992. *The Archaeology of the P'eng-hu Islands*. Taipei: Institute of History and Philology, Academia Sinica.
- Tsang, C.-H. 1995. On the origin of the Yami people of Lanyu as viewed from archaeological data. *Journal of Austronesian Studies*, 1: 135-151.
- Tsang, C.-H. 2001. *The Prehistoric Residents in Shisanhang*. Taipei: Shi-San-Hang Museum of Archaeology.

- Tsang, C.-H. and Chang, K.-J. 1996. Excavation report of Yingiana site in Ali Mountain in Chiayi and the prehistoric remains from the upper Cengwen River valley. In: Chou, C.-H. (ed.) *The Study of Environmental Change and Resource Management: (1) Cengwen River valley*, pp. 373-397.
- Tsang, C.-H. and Li, K.-T. 2010. *The Report of the Archaeological Remains of the Salvage Excavation in the Tainan Science Park: Stage 1, Year 3*. Taipei: National Science Council.
- Tsang, C.-H. and Li, K.-T. 2013. *Archaeological Heritage in Tainan Science Park of Taiwan*. Taitung: National Museum of Prehistory.
- Tsang, C.-H., Li, K.-T. and Chu, C.-Y. 2009. *The Report of the Archaeological Remains of the Salvage Excavation in the Tainan Science Park: Stage 1, Year 2*. Taipei: National Science Council.
- Tsang, C.-H. and Liu, Y.-C. 2001. *The Salvage Excavation and Preliminary Research at Shihshanhang*. Taipei: Shihshanhang Museum of Archaeology.
- Turner, W. E. S. and Rooksby, H. P. 1959. A study of the opalising agents in ancient glasses throughout three thousand four hundred years. *Glastechnische Berichte*, 32K: 17-28.
- Umass, Z. 2005. Cultural atlas of Paiwan beads. In: *Foreign Substances in Taiwan: Beads and Penannular Jade Ring*, pp. 35-39. Taipei: Institute of History and Archaeology, Academia Sinica.
- van der Sleen, W. G. N. 1967. *A Handbook on Beads*. York, PA: George Shumway Publisher.
- Vicenzi, E. P., Eggins, S., Wysoczanski, R. and Logan, A. 2002. Microbeam characterization of corning archeological reference glasses: New additions to the Smithsonian Microbeam Standard collection. *Journal of Research of the National Institute of Standards and Technology*, 107: 719-727.
- Wang, K.-W. and Jackson, C. 2014. A review of glass compositions around the South China Sea region (the late 1st millennium BC to the 1st millennium AD): placing Iron Age

- glass beads from Taiwan in context. *Journal of Indo-Pacific Archaeology*, 34: 51-60.
- Wang, S.-C. 2013. *Non-destructive Testing Analysis the Ancient Glass Beads Unearthed from the Chungde Site, Hualien*. PhD unpublished thesis, Department of Resources Engineering, National Cheng Kung University.
- Wang, X., Griffin, W. L. and Chen, J. 2010. Hf contents and Zr/Hf ratios in granitic zircons. *Geochemical Journal*, 44: 65-72.
- Wagner, B., Nowak, A., Bulska, E., Hametner, K. and Günther, D. 2012. Critical assessment of the elemental composition of Corning archeological reference glasses by LA-ICP-MS. *Analytical and Bioanalytical Chemistry*, 402: 1667-1677.
- Wedepohl, K. H., Simon, K. and Kronz, A. 2011. Data on 61 chemical elements for the characterization of three major glass compositions in late antiquity and the middle ages. *Archaeometry*, 53: 81-102.
- Welter, N., Schüssler, U. and Kiefer, W. 2007. Characterisation of inorganic pigments in ancient glass beads by means of Raman microspectroscopy, microprobe analysis and X-ray diffractometry. *Journal of Raman Spectroscopy*, 38: 113-121.
- Weyl, W. 1976. *Coloured Glasses*. Sheffield: Society of Glass Technology.
- Wu, H.-C. The forming method of pottery from the Lower Cultural Layer of Kiwulan: a macroscopic analysis. In: Li, S.-Y. and Hsu, M.-C. (eds.) *The 9th International Symposium on Yilan Research: Tracing Kiwulan, 2012*, pp. 591-632. Yilan: Archives of Yilan History.
- Xiong, Z. and Li, Q. 2011. *Archaeology, Scientific and Technical Study on the Glass Artifacts of the Han Dynasty Unearthed from Guangxi, China*. Beijing: Cultural Relics Press.
- Yang, H., Lee, K. and Chen, W. 2012. The application of petrographic analysis to archaeological research: examples from the artifacts and sherds of Chiu Hsiang Lan site, Taitung, Taiwan. *Journal of Austronesian Studies*, 3: 71-88.
- Yeh, M.-C. 1993. Report of the trial excavation at Pasangan. *National Museum of Prehistory*,

1: 30-58.

Yeh, M.-C. 2001. *Research on the Hua-Kan-Shan Culture*. Taitung: National Museum of Prehistory.

Zhao, K. 1991. On the origin and development of traditional Chinese glass. *Studies in the History of Natural Sciences*, 10: 145-156.

Appendix 1: full sample list of each site.

Table A1. 1: A list of selected samples from Kiwulan.

Sample number	Original sample number	Artefact	Type	Location	Length (mm)	Diameter (mm)	Shape	End roundness	Colour	Diaphaneity	Manufacturing method
KWL001	KWL-GB-0047	Glass bead	LL02	P038	9.72	n/a	long tubular	tapered	orange	opaque	dipped or wound
KWL002	KWL-GB-0393	Glass bead	LL02	P250	12.28	9.84	long tubular	tapered	orange	opaque	dipped or wound
KWL003	KWL-GB-1462	Glass bead	LL03	M043	2.19	n/a	short tubular	tapered	orange	opaque	drawn
KWL004	KWL-GB-1462	Glass bead	LL03	M043	2.17	2.92	short tubular	tapered	orange	opaque	drawn
KWL005	KWL-GB-1462	Glass bead	LL03	M043	2.50	2.36	short tubular	tapered	orange	opaque	unidentifiable
KWL006	KWL-GB-0284	Glass bead	LL04	P187	2.99	2.85	long tubular	round	blue	translucent	unidentifiable
KWL007	KWL-GB-0284	Glass bead	LL04	P187	3.13	n/a	long tubular	n/a	blue	translucent	unidentifiable

Sample number	Original sample number	Artefact	Type	Location	Length (mm)	Diameter (mm)	Shape	End roundness	Colour	Diaphaneity	Manufacturing method
KWL008	KWL-GB-1459	Glass bead	LL05	M043	1.82	n/a	oblate	round	yellow	opaque	wound?
KWL009	KWL-GB-1459	Glass bead	LL05	M043	1.95	n/a	oblate	n/a	yellow	opaque	wound?
KWL010	KWL-GB-1459	Glass bead	LL05	M043	1.95	n/a	oblate	round	yellow	opaque	wound?
KWL011	KWL-GB-0285	Glass bead	LL05	P187	1.24	n/a	oblate	round	yellow	opaque	wound?
KWL012	KWL-GB-0285	Glass bead	LL05	P187	1.08	n/a	oblate	n/a	yellow	opaque	wound?
KWL013	KWL-GB-1464	Glass bead	LL10	M043	2.45	n/a	short tubular	tapered	yellow	opaque	drawn
KWL014	KWL-GB-1464	Glass bead	LL10	M043	3.42	n/a	oblate	tapered	yellow	opaque	drawn
KWL015	KWL-GB-1461	Glass bead	LL01	M043	1.55	3.12	short tubular	tapered	orange	opaque	drawn
KWL016	KWL-GB-0279	Glass bead	LL01	P187	5.33	5.72	short tubular	round	orange	opaque	drawn
KWL017	KWL-GB-0282	Glass	LL02	P187	8.64	7.47	long	tapered	orange	opaque	dipped or

Sample number	Original sample number	Artefact	Type	Location	Length (mm)	Diameter (mm)	Shape	End roundness	Colour	Diaphaneity	Manufacturing method
		bead					tubular				wound
KWL018	KWL-GB-0281	Glass bead	LL02	P187	8.56	6.22	long tubular	tapered	orange	opaque	dipped or wound
KWL019	KWL-GB-0294	Glass bead	LL03	P187	1.48	2.35	oblate	round	orange	opaque	drawn
KWL020	KWL-GB-0294	Glass bead	LL03	P187	1.33	2.26	oblate	round	orange	opaque	drawn
KWL021	KWL-GB-0283	Glass bead	LL03	P187	1.20	2.45	oblate	round	orange	opaque	drawn
KWL022	KWL-GB-0283	Glass bead	LL03	P187	1.41	2.07	oblate	round	orange	opaque	drawn
KWL023	KWL-GB-1456	Glass bead	LL04	M043	5.64	n/a	short tubular	tapered	dark blue	translucent	wound?
KWL024	KWL-GB-1456	Glass bead	LL04	M043	n/a	n/a	n/a	round	blue	translucent	unidentifiable
KWL025	KWL-GB-0284	Glass bead	LL04	P187	3.84	2.87	long tubular	tapered	black	translucent	drawn?
KWL026	KWL-GB-0284	Glass bead	LL04	P187	3.76	3.12	long tubular	round	dark blue	translucent	unidentifiable

Sample number	Original sample number	Artefact	Type	Location	Length (mm)	Diameter (mm)	Shape	End roundness	Colour	Diaphaneity	Manufacturing method
KWL027	KWL-GB-0284	Glass bead	LL04	P187	2.94	2.80	long tubular	round	blue	translucent	drawn?
KWL028	KWL-GB-0284	Glass bead	LL04	P187	3.46	3.15	long tubular	round	blue	translucent	drawn?
KWL029	KWL-GB-1459	Glass bead	LL05	M043	1.97	3.05	oblate	round	yellow	opaque	wound
KWL030	KWL-GB-1459	Glass bead	LL05	M043	2.31	3.13	oblate	round	yellow	opaque	wound
KWL031	KWL-GB-0285	Glass bead	LL05	P187	1.78	3.75	oblate	round	yellow	opaque	unidentifiable
KWL032	KWL-GB-0285	Glass bead	LL05	P187	1.58	2.73	oblate	round	yellow	opaque	wound
KWL033	KWL-GB-1458	Glass bead	LL06	M043	2.11	3.52	oblate	round	dark blue	translucent	unidentifiable
KWL034	KWL-GB-0287	Glass bead	LL06	P187	2.43	4.74	oblate	round	dark blue	translucent	wound
KWL035	KWL-GB-0287	Glass bead	LL06	P187	2.36	3.95	oblate	round	dark blue	translucent	wound
KWL036	KWL-GB-0287	Glass	LL06	P187	2.39	4.23	oblate	round	dark	translucent	wound

Sample number	Original sample number	Artefact	Type	Location	Length (mm)	Diameter (mm)	Shape	End roundness	Colour	Diaphaneity	Manufacturing method
		bead							blue		
KWL037	KWL-GB-0287	Glass bead	LL06	P187	2.36	4.74	oblate	round	dark blue	translucent	wound
KWL038	KWL-GB-1454	Glass bead	LL07	M043	2.81	3.49	short tubular	round	red	opaque	unidentifiable
KWL039	KWL-GB-1079	Glass bead	LL07	P260	3.31	4.06	short tubular	round	red	opaque	drawn
KWL040	KWL-GB-0650	Glass bead	LL08	P256	9.81	5.50	long tubular	tapered	blue	translucent	drawn
KWL041	KWL-GB-1455	Glass bead	LL09	M043	2.05	2.69	oblate	round	blue	opaque	drawn
KWL042	KWL-GB-1443	Glass bead	LL11	M038	1.55	3.45	oblate	round	blue	translucent	wound?
KWL043	KWL-GB-1457	Glass bead	LL12	M043	3.64	2.71	long tubular	round	blue	opaque	drawn
Previously analysed samples in Cheng 2007											
KWL-GB-295-1	KWL-GB-295	Glass bead	LL05	P187	n/a	n/a	oblate	n/a	yellow	opaque	n/a
KWL-GB-295-	KWL-GB-295	Glass	LL05	P187	n/a	n/a	oblate	n/a	yellow	opaque	n/a

Sample number	Original sample number	Artefact	Type	Location	Length (mm)	Diameter (mm)	Shape	End roundness	Colour	Diaphaneity	Manufacturing method
2		bead									
KWL-GB-303	KWL-GB-303	Glass bead	LL06	P187	n/a	n/a	oblate	n/a	dark blue	translucent	n/a
KWL-GB-305-1	KWL-GB-305	Glass bead	LL04	P187	n/a	n/a	long tubular	n/a	blue	translucent	n/a
KWL-GB-305-2	KWL-GB-305	Glass bead	LL04	P187	n/a	n/a	long tubular	n/a	blue	translucent	n/a
KWL-GB-306-1	KWL-GB-306	Glass bead	LL03	P187	n/a	n/a	n/a	n/a	orange	opaque	n/a
KWL-GB-306-2	KWL-GB-306	Glass bead	LL03	P187	n/a	n/a	n/a	n/a	orange	opaque	n/a
KWL-GB-569	KWL-GB-569	Glass bead	LL02	P256	n/a	n/a	long tubular	tapered	orange	opaque	n/a
KWL-GB-605	KWL-GB-605	Glass bead	LL02	P256	n/a	n/a	long tubular	n/a	orange	opaque	n/a
KWL-GB-606	KWL-GB-606	Glass bead	LL01	P256	n/a	n/a	n/a	n/a	orange	opaque	n/a
KWL-GB-759	KWL-GB-759	Glass bead	LL01	P258	n/a	n/a	n/a	n/a	orange	opaque	n/a

Sample number	Original sample number	Artefact	Type	Location	Length (mm)	Diameter (mm)	Shape	End roundness	Colour	Diaphaneity	Manufacturing method
KWL-GB-1468	KWL-GB-1468	Glass bead	LL10	M043	n/a	n/a	short tubular	n/a	yellow	opaque	n/a

Table A1. 2: A list of selected samples from Jiuxianglan.

	Original sample number	Artefact	Location	Length (mm)	Diameter (mm)	Shape	End roundness	Colour	Diaphaneity	Manufacturing method
JXL01	CHL-93-501-106	glass bead	T3P35-SE L3	2.80	4.45	oblate	round	red	opaque	drawn
JXL02	CHL-93-501-193	glass bead	T3P35-SW L4	2.75	4.21	short tubular	round	red	opaque	drawn
JXL03	CHL-93-501-143	glass bead	T3P35-NW L5	3.78	4.94	oblate	round	yellow	opaque	drawn
JXL04	CHL-93-501-206	glass bead	T3P35-SW L5	3.32	5.96	oblate	round	blue	opaque	drawn
JXL05	CHL-93-501-146	glass bead	T3P35-NW L6	2.38	4.64	oblate	round	yellow	opaque	drawn
JXL06	CHL-93-501-209	glass bead	T3P35-SW L6	n/a	n/a	n/a	n/a	blue	opaque	unidentifiable
JXL07	CHL-93-501-214	glass bead	T3P35-SW L6	3.52	4.03	oblate	round	yellow	opaque	drawn
JXL08	CHL-93-501-159	glass bead	T3P35-NW L7	3.32	6.56	oblate	round	green	opaque	drawn
JXL09	CHL-93-501-235	glass bead	T3P35-SW L7	3.61	5.84	oblate	round	green	opaque	drawn
JXL10	CHL-93-501-160	glass	T3P35-NW	4.96	5.12	oblate	round	red	opaque	drawn

	Original sample number	Artefact	Location	Length (mm)	Diameter (mm)	Shape	End roundness	Colour	Diaphaneity	Manufacturing method
		bead	L8							
JXL11	CHL-93-501-162	glass bead	T3P35-NW L8	4.19	6.65	oblate	round	green	opaque	drawn
JXL12	CHL-93-501-168	glass bead	T3P35-NW L9	2.62	4.37	n/a	round	yellow	opaque	drawn
JXL13	CHL-93-501-168	glass bead	T3P35-NW L9	4.74	4.64	long tubular	round	green	opaque	drawn
JXL14	CHL-93-501-168	glass bead	T3P35-NW L9	3.35	4.53	short tubular	round	green	opaque	drawn
JXL15	CHL-93-501-169	glass bead	T3P35-NW L9	3.50	4.80	oblate	round	yellow	opaque	drawn
JXL16	CHL-93-501-122	glass bead	T3P35-SE L12	4.05	3.73	short tubular	round	blue	opaque	drawn
JXL17	CHL-93-501-314	glass bead	T3P35-SE L13	3.62	4.67	oblate	round	blue	opaque	drawn
JXL18	CHL-93-501-315	glass bead	T3P35-SE L13	4.91	3.35	long tubular	round	blue	opaque	drawn
JXL19	CHL-93-501-124	glass bead	T3P35-SE L13	3.42	4.21	n/a	round	yellow	opaque	drawn
JXL20	CHL-93-501-316	glass	T3P35-SE	2.15	3.43	short	round	yellow	opaque	drawn

	Original sample number	Artefact	Location	Length (mm)	Diameter (mm)	Shape	End roundness	Colour	Diaphaneity	Manufacturing method
		bead	L13			tubular				
JXL21	CHL-93-501-186	glass bead	T3P35-NW L15	3.32	3.90	short tubular	round	blue	opaque	drawn
JXL22	CHL-93-501-288	glass bead	T3P35-SW L15	3.85	4.44	oblate	round	red	opaque	drawn
JXL23	CHL-93-501-515	glass bead	T3P37-NW L14	3.48	4.42	short tubular	round	green	opaque	drawn
JXL24	CHL-93-501-670	glass bead	T3P38-NW L6	4.06	5.26	oblate	round	orange	opaque	drawn
JXL25	CHL-93-501-634	glass bead	T3P38-NE L6	5.20	5.49	oblate	round	orange	opaque	drawn
JXL26	CHL-93-501-694	glass bead	T3P38-NW L6	3.39	n/a	n/a	round	green	opaque	wound?
JXL27	CHL-93-501-794	glass bead	T3P39-SW L3	2.40	2.63	oblate	round	orange	opaque	drawn
JXL28	CHL-93-501-2257	glass bead	surface	4.23	7.74	oblate	round	blue	opaque	drawn
JXL29	CHL-93-501-2257	glass bead	surface	3.62	5.94	oblate	round	blue	opaque	unidentifiable
JXL30	CHL-93-501-	glass	surface	4.18	5.19	short	round	green	opaque	drawn

	Original sample number	Artefact	Location	Length (mm)	Diameter (mm)	Shape	End roundness	Colour	Diaphaneity	Manufacturing method
	2258	bead				tubular				
JXL31	CHL-93-501-2258	glass bead	surface	3.72	4.85	oblate	round	green	opaque	drawn
JXL32	CHL-93-501-2260	glass bead	surface	4.75	4.52	long tubular	round	yellow	opaque	drawn
JXL33	CHL-93-501-2260	glass bead	surface	4.12	4.88	oblate	round	yellow	opaque	drawn
JXL34	CHL-93-501-2262	glass bead	surface	5.39	4.89	n/a	round	red	opaque	drawn
JXL35	CHL-93-501-2262	glass bead	surface	3.21	5.19	short tubular	round	red	opaque	drawn
JXL38	CHL-92-501-2238	glass bead	B2	3.83	n/a	short tubular	round	yellow	opaque	drawn
JXL39	CHL-93-504-29	glass waste	T3P38-SE L4	n/a	n/a	n/a	n/a	blue	translucent	n/a
JXL41	CHL-93-504-30	glass waste	T3P38-SE L5	n/a	n/a	n/a	n/a	turquoise	translucent	n/a
JXL43	CHL-93-504-65	glass waste	T3P39-SE L4	n/a	n/a	n/a	n/a	blue	opaque	n/a
JXL44	CHL-93-504-58	glass	T3P39-SW L4	n/a	n/a	n/a	n/a	blue	transparent	n/a

Original sample number	Artefact	Location	Length (mm)	Diameter (mm)	Shape	End roundness	Colour	Diaphaneity	Manufacturing method
	waste								
JXL46	glass waste	T2P39-NW L5	n/a	n/a	n/a	n/a	blue	opaque	n/a
JXL47	glass waste	T3P39-SE L5	n/a	n/a	n/a	n/a	red	opaque	n/a
JXL48	glass waste	T2P39-NW L7	n/a	n/a	n/a	n/a	yellow	opaque	n/a
JXL49	glass waste	T2P39-NW L8	n/a	n/a	n/a	n/a	turquoise	translucent	n/a

Table A1.3: A list of full samples from Guishan.

Sample number	Location	Length (mm)	Diameter (mm)	Shape	End roundness	Colour	Diaphaneity	Manufacturing method
GS001	DB2	3.31	3.22	short tubular	round	green	opaque	drawn
GS002	DB2	3.07	2.66	long tubular	round	blue	opaque	drawn
GS003	DB2	3.18	4.48	short tubular	tapered	yellow	opaque	drawn
GS004	DB2	6.32	3.28	long tubular	round	red	opaque	drawn
GS005	DB2	2.45	4.65	short tubular	tapered	yellow	opaque	drawn
GS006	DB2	3.06	4.21	oblate	round	green	opaque	drawn
GS007	DB2	1.71	2.90	oblate	round	red	opaque	drawn
GS008	DB2	1.96	3.59	short tubular	tapered	yellow	opaque	drawn
GS009	DB2	2.46	3.80	oblate	round	blue	opaque	drawn
GS010	DB2	3.76	3.81	short tubular	round	red	opaque	drawn
GS011	DB2	2.19	4.25	short tubular	tapered	yellow	opaque	drawn
GS012	DB2	2.87	3.75	short tubular	round	blue	opaque	drawn
GS013	DB2	2.91	4.21	oblate	round	blue	opaque	drawn
GS014	DB2	1.49	2.53	oblate	round	red	opaque	drawn
GS015	DB2	4.21	3.09	long tubular	round	orange	opaque	drawn
GS016	DB2	2.47	3.03	short tubular	round	green	opaque	drawn
GS017	DB2	2.15	4.25	short tubular	tapered	yellow	opaque	drawn
GS018	DB2	2.2	3.57	short tubular	round	red	opaque	drawn
GS019	DB2	6.02	3.90	long tubular	round	red	opaque	drawn

Sample number	Location	Length (mm)	Diameter (mm)	Shape	End roundness	Colour	Diaphaneity	Manufacturing method
GS020	DB2	2.25	4.03	short tubular	tapered	yellow	opaque	drawn
GS021	DB2	2.66	3.71	short tubular	round	green	opaque	drawn
GS022	DB2	3.19	4.89	oblate	round	yellow	opaque	drawn
GS023	DB2	7.72	4.89	long tubular	round	red	opaque	drawn
GS024	DB2	6.45	2.66	long tubular	round	red	opaque	drawn
GS025	DB3	4.06	4.71	short tubular	round	blue	opaque	drawn
GS026	DB3	1.74	3.81	oblate	round	green	opaque	drawn
GS027	DB3	1.61	2.00	short tubular	round	green	opaque	drawn
GS028	DB1	3.07	7.21	biconical	tapered	yellow	opaque	unidentifiable
GS029	DB1	2.40	5.91	biconical	tapered	yellow	opaque	unidentifiable
GS030	DB1	3.60	5.03	oblate	round	yellow	opaque	drawn
GS031	DB1	3.59	4.25	short tubular	round	green	opaque	drawn
GS032	DB1	2.54	4.14	short tubular	round	green	opaque	drawn
GS033	DB1	2.35	3.94	oblate	round	blue	opaque	drawn
GS034	DB1	2.52	2.88	short tubular	round	green	opaque	drawn
GS035	DB1	1.95	3.40	short tubular	round	green	opaque	drawn
GS036	DB1	2.74	2.95	short tubular	round	green	opaque	drawn
GS037	DB1	1.24	2.66	oblate	round	green	opaque	drawn
GS038	DB1	2.92	4.45	short tubular	tapered	red	opaque	drawn
GS039	DB1	3.34	3.97	oblate	round	blue	opaque	drawn

Sample number	Location	Length (mm)	Diameter (mm)	Shape	End roundness	Colour	Diaphaneity	Manufacturing method
GS040	DB1	3.34	6.22	biconical	round	yellow	opaque	unidentifiable
GS041	DB1	2.74	6.31	biconical	round	yellow	opaque	unidentifiable
GS042	DB1	3.05	5.09	short tubular	round	blue	opaque	drawn
GS043	DB1	3.98	5.17	oblate	round	blue	opaque	drawn
GS044	DB1	3.57	4.50	oblate	round	green	opaque	drawn
GS045	DB1	3.02	5.46	oblate	round	green	opaque	drawn
GS046	DB1	3.90	4.62	oblate	round	blue	opaque	drawn
GS047	DB1	2.53	3.26	short tubular	round	red	opaque	drawn
GS048	DB1	3.42	3.85	short tubular	round	blue	translucent	wound
GS049	DB1	4.67	3.75	long tubular	round	blue	opaque	drawn
GS050	DB1	3.13	4.23	short tubular	tapered	red	opaque	drawn
GS051	DB1	2.59	3.60	oblate	round	red	opaque	drawn
GS052	DB1	3.76	3.53	short tubular	tapered	green	opaque	drawn
GS053	DB1	4.96	4.49	long tubular	round	blue	opaque	drawn
GS054	DB1	3.83	4.12	short tubular	round	blue	opaque	drawn
GS055	DB1	2.38	4.17	oblate	round	red	opaque	drawn
GS056	DB1	6.58	6.30	oblate	round	dark blue	opaque	drawn
GS057	DB1	5.45	6.44	oblate	round	dark blue	opaque	drawn
GS058	DB1	5.58	6.61	oblate	round	dark blue	opaque	drawn
GS059	DB1	3.82	6.46	short tubular	round	dark blue	opaque	drawn

Sample number	Location	Length (mm)	Diameter (mm)	Shape	End roundness	Colour	Diaphaneity	Manufacturing method
GS060	DB1	3.82	6.46	oblate	round	dark blue	opaque	drawn
GS061	DB1	4.40	6.12	oblate	round	dark blue	opaque	drawn
GS062	DB1	2.86	2.50	long tubular	round	yellow	opaque	drawn
GS063	DB1	2.81	4.37	short tubular	round	red	opaque	drawn
GS064	DB1	2.41	3.17	oblate	round	yellow	opaque	drawn
GS065	DB1	1.26	2.50	oblate	round	green	opaque	unidentifiable
GS066	DB1	3.72	3.97	short tubular	round	blue	opaque	drawn
GS067	DB1	3.08	5.28	short tubular	tapered	yellow	opaque	drawn
GS068	DB1	4.75	7.03	oblate	round	dark blue	opaque	drawn
GS069	DB1	3.27	4.38	short tubular	tapered	yellow	opaque	drawn
GS070	DB2	2.51	3.98	oblate	round	red	opaque	drawn
GS071	DB2	3.48	4.32	short tubular	tapered	red	opaque	drawn
GS072	DB2	2.97	4.13	oblate	round	red	opaque	drawn
GS073	DB2	2.20	3.74	oblate	round	red	opaque	drawn
GS074	DB2	3.00	4.76	oblate	round	red	opaque	drawn
GS075	DB2	2.09	3.80	oblate	round	red	opaque	drawn
GS076	DB2	3.19	3.67	short tubular	round	blue	translucent	wound
GS077	DB2	2.71	3.67	short tubular	tapered	blue	translucent	wound
GS078	DB2	2.91	3.83	short tubular	tapered	red	opaque	drawn
GS079	DB2	2.72	3.19	oblate	round	red	opaque	drawn

Sample number	Location	Length (mm)	Diameter (mm)	Shape	End roundness	Colour	Diaphaneity	Manufacturing method
GS080	DB2	3.14	3.88	short tubular	round	blue	translucent	wound
GS081	DB2	1.67	2.74	oblate	round	yellow	opaque	drawn
GS082	DB2	1.72	3.73	short tubular	tapered	yellow	opaque	drawn
GS083	DB2	1.97	4.25	short tubular	round	yellow	opaque	drawn
GS084	DB2	2.13	3.65	oblate	round	red	opaque	drawn
GS085	DB2	2.42	3.85	short tubular	round	yellow	opaque	drawn
GS086	DB2	1.42	3.81	oblate	round	yellow	opaque	drawn
GS087	DB2	1.48	3.90	short tubular	tapered	yellow	opaque	drawn
GS088	DB2	2.92	3.65	short tubular	round	yellow	opaque	drawn
GS089	DB2	1.42	3.68	short tubular	tapered	yellow	opaque	drawn
GS090	DB2	1.68	3.68	short tubular	tapered	yellow	opaque	drawn
GS091	DB2	2.35	3.83	oblate	round	red	opaque	drawn
GS092	DB2	2.24	3.45	short tubular	tapered	yellow	opaque	drawn
GS093	DB2	2.47	4.10	oblate	round	yellow	opaque	drawn
GS094	DB2	1.63	4.25	short tubular	tapered	yellow	opaque	drawn
GS095	DB1	7.70	8.19	short tubular	tapered	yellow	opaque	unidentifiable
GS096	DB1	4.76	7.44	oblate	round	dark blue	opaque	drawn
GS097	DB1	5.44	7.33	oblate	round	dark blue	opaque	drawn
GS098	DB1	4.41	6.44	short tubular	round	dark blue	opaque	drawn
GS099	DB1	3.76	6.42	short tubular	round	dark blue	opaque	drawn

Sample number	Location	Length (mm)	Diameter (mm)	Shape	End roundness	Colour	Diaphaneity	Manufacturing method
GS100	DB1	4.57	7.20	oblate	round	dark blue	opaque	drawn
GS101	DB1	1.48	3.01	oblate	round	green	opaque	drawn
GS102	DB1	6.46	3.37	long tubular	round	red	opaque	drawn
GS103	DB1	2.44	4.18	oblate	round	green	opaque	drawn
GS104	DB1	2.29	4.68	short tubular	round	green	opaque	drawn
GS105	DB1	3.60	3.74	short tubular	round	blue	opaque	drawn
GS106	DB1	3.83	3.69	short tubular	round	green	opaque	drawn
GS107	DB1	3.38	3.99	short tubular	round	yellow	opaque	drawn
GS108	DB1	1.42	2.65	oblate	round	green	opaque	drawn
GS109	DB1	2.64	4.15	short tubular	round	green	opaque	drawn
GS110	DB1	2.40	4.28	short tubular	round	red	opaque	drawn
GS111	DB1	1.78	3.94	oblate	round	red	opaque	drawn
GS112	DB1	2.08	4.23	short tubular	tapered	yellow	opaque	drawn
GS113	DB1	2.20	5.97	biconical	tapered	yellow	opaque	unidentifiable
GS114	DB1	5.72	8.08	oblate	round	dark blue	opaque	drawn
GS115	DB1	2.21	3.23	short tubular	round	green	opaque	drawn
GS116	DB1	1.17	2.88	oblate	round	green	opaque	drawn
GS117	DB1	1.20	2.81	oblate	round	green	opaque	drawn
GS118	DB1	1.30	3.03	oblate	round	green	opaque	drawn
GS119	DB1	7.28	8.03	oblate	semi-round	dark blue	opaque	unidentifiable

Sample number	Location	Length (mm)	Diameter (mm)	Shape	End roundness	Colour	Diaphaneity	Manufacturing method
GS120	DB1	2.28	4.31	oblate	round	blue	opaque	drawn
GS121	DB1	3.46	4.16	oblate	round	blue	opaque	drawn
GS122	DB1	2.82	3.99	oblate	round	blue	translucent	drawn
GS123	DB1	2.29	4.32	oblate	round	green	opaque	drawn

Table A1.4: A list of full samples from Daoye.

Sample number	Original sample number	Artefact	Region	Trench	Burial	Length (mm)	Diameter (mm)	Shape	End roundness	Colour	Diaphaneity	Manufacturing method
DY01		glass bead	A2	T11P18F1		2.2	4.03	short tubular	round	blue	opaque	drawn
DY02		glass bead	A2	T11P18F1		3.3	3.08	short tubular	round	blue	opaque	drawn
DY03	GB008	glass bead	B2	T8P7L9	B4	1.74	3.08	oblate	round	blue	opaque	drawn
DY04	GB008	glass bead	B2	T8P7L9	B4	1.72	2.47	oblate	round	green	opaque	drawn
DY05	GB008	glass bead	B2	T8P7L9	B4	1.74	2.9	oblate	round	yellow	opaque	drawn
DY06	GB010	glass bead	B2	T13P6F1		2.8	4.02	short tubular	round	blue	opaque	drawn
DY07	GB013	glass bead	B2		B4	1.72	3.01	short tubular	round	blue	opaque	drawn
DY08	GB016	glass bead	B3	T9P3F1		11.47	5.34	long tubular	round	green	opaque	drawn
DY09	GB002	glass bead	C3		B5	3.09	4.01	short tubular	tapered	blue	opaque	drawn

Sample number	Original sample number	Artefact	Region	Trench	Burial	Length (mm)	Diameter (mm)	Shape	End roundness	Colour	Diaphaneity	Manufacturing method
DY10	GB009	glass bead	C3	T15P12F1		1.84	3.15	oblate	round	green	opaque	drawn
DY11		glass bead	C3	T10P9F3		1.5	3.52	short tubular	tapered	yellow	opaque	drawn
DY12	GB011	glass bead	C4	T11P8F1		2.32	3.95	oblate	round	blue	opaque	drawn
DY13	GB011	glass bead	C4	T11P8F1		2.32	4.18	oblate	round	yellow	opaque	drawn
DY14	GB011	glass bead	C4	T11P8F1		3.22	3.09	short tubular	round	yellow	opaque	drawn
DY15	GB003	glass bead	D6	T13P8F1		2.64	3.31	short tubular	tapered	blue	opaque	drawn
DY16	GB004	glass bead	D6	T10P7	B1	4.75	4.36	short tubular	round	blue	opaque	drawn
DY17	GB004	glass bead	D6	T10P7	B1	2.66	5.36	short tubular	round	blue	opaque	drawn
DY18	GB004	glass bead	D6	T10P7	B1	3.17	4.55	short tubular	round	blue	opaque	drawn
DY19	GB004	glass	D6	T10P7	B1	2.34	4.37	short	round	blue	opaque	drawn

Sample number	Original sample number	Artefact	Region	Trench	Burial	Length (mm)	Diameter (mm)	Shape	End roundness	Colour	Diaphaneity	Manufacturing method
		bead						tubular				
DY20	GB004	glass bead	D6	T10P7	B1	1.95	3.49	short tubular	round	blue	opaque	drawn
DY21	GB005	glass bead	D6	T8P3F1		2.98	4.41	short tubular	round	blue	opaque	drawn
DY22	GB005	glass bead	D6	T8P3F1		2.6	3.25	short tubular	round	blue	opaque	drawn
DY23	GB005	glass bead	D6	T8P3F1		1.8	3.31	short tubular	tapered	blue	opaque	drawn
DY24	GB006	glass bead	D6	T8P2F1		3.93	3.76	short tubular	round	blue	opaque	drawn
DY25	GB006	glass bead	D6	T8P2F1		3.52	3.99	short tubular	round	blue	opaque	drawn
DY26	GB006	glass bead	D6	T8P2F1		2.25	3.73	short tubular	round	blue	opaque	drawn
DY27	GB006	glass bead	D6	T8P2F1		2.49	4.08	short tubular	tapered	blue	opaque	drawn
DY28	GB006	glass bead	D6	T8P2F1		1.72	4.26	oblate	round	blue	opaque	drawn

Sample number	Original sample number	Artefact	Region	Trench	Burial	Length (mm)	Diameter (mm)	Shape	End roundness	Colour	Diaphaneity	Manufacturing method
DY29	GB006	glass bead	D6	T8P2F1		2.6	3.53	short tubular	tapered	yellow	opaque	drawn
DY30	GB006	glass bead	D6	T8P2F1		2.31	3.74	short tubular	tapered	yellow	opaque	drawn
DY31	GB007	glass bead	D6	T8P2L12F1		4.43	5.16	short tubular	round	blue	opaque	drawn
DY32	GB007	glass bead	D6	T8P2L12F1		2.91	3.51	short tubular	tapered	blue	opaque	drawn
DY33	GB007	glass bead	D6	T8P2L12F1		3.42	4.4	short tubular	round	green	opaque	drawn
DY34	GB007	glass bead	D6	T8P2L12F1		2.53	4.38	oblate	round	yellow	opaque	drawn
DY35	GB012	glass bead	D6	T13P8F1		2.89	5.22	short tubular	round	blue	opaque	drawn
DY36	GB014	glass bead	D6	T14P8F1		2.5	3.45	short tubular	round	blue	opaque	drawn
DY37	GB002	glass bead	A2	T18P19F1		1.82	3.29	short tubular	round	blue	opaque	drawn
DY38	GB002	glass	A2	T18P19F1		1.55	3.3	oblate	round	blue	opaque	drawn

Sample number	Original sample number	Artefact	Region	Trench	Burial	Length (mm)	Diameter (mm)	Shape	End roundness	Colour	Diaphaneity	Manufacturing method
		bead										
DY39	GB002	glass bead	A2	T18P19F1		2.49	4.11	oblate	round	blue	opaque	drawn
DY42-01	GB001	glass bead	C2		B5	1.78	3.48	short tubular	round	green	opaque	drawn
DY42-02	GB001	glass bead	C2		B5	1.84	2.87	oblate	round	green	opaque	drawn
DY42-03	GB001	glass bead	C2		B5	1.96	3.11	oblate	round	green	opaque	drawn
DY42-04	GB001	glass bead	C2		B5	1.81	2.76	oblate	round	green	opaque	drawn
DY42-05	GB001	glass bead	C2		B5	2.2	3	short tubular	round	green	opaque	drawn
DY42-06	GB001	glass bead	C2		B5	1.43	2.79	short tubular	round	green	opaque	drawn
DY42-07	GB001	glass bead	C2		B5	1.45	2.64	short tubular	round	green	opaque	drawn
DY42-08	GB001	glass bead	C2		B5	1.68	3	short tubular	round	green	opaque	drawn

Sample number	Original sample number	Artefact	Region	Trench	Burial	Length (mm)	Diameter (mm)	Shape	End roundness	Colour	Diaphaneity	Manufacturing method
DY42-09	GB001	glass bead	C2		B5	2.15	3.7	short tubular	round	green	opaque	drawn
DY42-10	GB001	glass bead	C2		B5	2.22	3.83	short tubular	round	green	opaque	drawn
DY42-11	GB001	glass bead	C2		B5	1.91	2.53	short tubular	round	green	opaque	drawn
DY42-12	GB001	glass bead	C2		B5	1.62	2.89	short tubular	tapered	green	opaque	drawn
DY42-13	GB001	glass bead	C2		B5	1.4	3.28	short tubular	tapered	green	opaque	drawn
DY42-14	GB001	glass bead	C2		B5	2.16	2.99	oblate	round	green	opaque	drawn
DY42-15	GB001	glass bead	C2		B5	1.24	2.73	short tubular	round	green	opaque	drawn
DY42-16	GB001	glass bead	C2		B5	1.3	2.66	oblate	round	green	opaque	drawn
DY42-17	GB001	glass bead	C2		B5	1.09	2.77	oblate	round	green	opaque	drawn
DY42-18	GB001	glass	C2		B5	1.23	3.32	short	tapered	green	opaque	drawn

Sample number	Original sample number	Artefact	Region	Trench	Burial	Length (mm)	Diameter (mm)	Shape	End roundness	Colour	Diaphaneity	Manufacturing method
		bead						tubular				
DY47	CB005	glass bead	B2		B4	2.18	3.06	short tubular	round	red	opaque	drawn
DY48	CB005	glass bead	B2		B4	1.83	3.57	oblate	round	red	opaque	drawn
DY49	CB008	glass bead	D6	T8P2F1		2.1	3.02	short tubular	tapered	red	opaque	drawn
DY50	CB015	glass bead	B3	T5P18F1		1.88	2.81	oblate	round	dark blue	opaque	drawn
DY51						1.85	3.04	oblate	round	red	opaque	drawn

Table A1.5: A list of full samples from Wujiancuo in Niaosong period.

Sample number	Original sample number	Region	Trench	Burial	Length (mm)	Diameter (mm)	Shape	End roundness	Colour	Diaphaneity	Manufacturing method
WJC012	2011.WCT000.06GB0.0009.000	KVII	T2P5F2		1.56	1.99	short tubular	tapered	blue	opaque	drawn
WJC013	2011.WCT000.06GB0.0010.000	KVIV	T0P6F3		1.27	2.38	short tubular	round	green	opaque	drawn
WJC014	2011.WCT000.06GB0.0011.000	KVIV	T3P24L9F1		0.91	1.53	short tubular	tapered	green	opaque	drawn
WJC015	WCT-GB-019	KVII	T2P6F2		3.64	3.61	short tubular	round	blue	opaque	drawn
WJC016	2011.WCT000.06GB0.0012.000	KVII	T2P22F2		1.44	1.73	short tubular	tapered	blue	opaque	drawn
WJC017	2011.WCT000.06GB0.0013.000	KVII	T2P22F2		2.14	2.86	short tubular	tapered	green	opaque	drawn
WJC018	2011.WCT000.06GB0.0014.000	KVI	T1P15F1		2.22	4.33	oblate	tapered	blue	opaque	drawn
WJC019	WCT-GB-023	KVII	T3P10F1		5.24	3.84	long tubular	tapered	blue	translucent	unidentifiable
WJC020	WCT-GB-024	KVI	T1P22F1		7.51	5.74	n/a	round	blue	translucent	unidentifiable
WJC021	2011.WCT000.06GB0.0015.000	KVI	T3P22F2		0.93	4.91	short tubular	round	blue	opaque	drawn

Sample number	Original sample number	Region	Trench	Burial	Length (mm)	Diameter (mm)	Shape	End roundness	Colour	Diaphaneity	Manufacturing method
WJC022	2011.WCT000.06GB0.0016.000	KVII	T3P19F1		2.28	2.88	long tubular	tapered	blue	opaque	drawn
WJC023	2011.WCT000.06GB0.0017.000	KVII	T3P24F1		1.71	3.36	short tubular	tapered	green	opaque	drawn
WJC024	WCT-GB-028	KVI	T0P15F1		5.18	4.18	short tubular	round	blue	opaque	drawn
WJC025	WCT-GB-029	KVI	T0P15F1		4.61	3.91	long tubular	tapered	blue	opaque	drawn
WJC026	WCT-GB-030	KVI	T3P24F1		3.37	4.23	oblate	round	blue	opaque	drawn
WJC027	WCT-GB-031	KVI	T3P24F1		3.63	4.25	short tubular	round	blue	opaque	drawn
WJC028	2011.WCT000.06GB0.0018.000	KVII	T2P4F1		1.65	2.19	short tubular	round	blue	opaque	unidentifiable
WJC038	2011.WCT000.06GB0.0031.000	TS1		B13	2.69	3.8	oblate	tapered	blue	translucent	drawn
WJC039	2011.WCT000.06GB0.0032.000	TS1		B13	2.01	3.12	short tubular	tapered	blue	translucent	wound?
WJC040	2011.WCT000.06GB0.0033.001	KVIII	T0P18F2	B12	2	2.37	short tubular	tapered	dark blue	opaque	drawn
WJC041	2011.WCT000.06GB0.0033.002	KVIII	T0P18F2	B12	1.95	2.45	short tubular	round	dark blue	opaque	drawn

Sample number	Original sample number	Region	Trench	Burial	Length (mm)	Diameter (mm)	Shape	End roundness	Colour	Diaphaneity	Manufacturing method
WJC042	2011.WCT000.06GB0.0033.003	KVIII	T0P18F2	B12	0.76	2.75	short tubular	tapered	dark blue	opaque	drawn
WJC043	2011.WCT000.06GB0.0033.004	KVIII	T0P18F2	B12	2.33	2.91	short tubular	tapered	dark blue	opaque	drawn
WJC044	2011.WCT000.06GB0.0033.005	KVIII	T0P18F2	B12	2	3.77	short tubular	tapered	green	opaque	drawn
WJC045	2011.WCT000.06GB0.0033.006	KVIII	T0P18F2	B12	2.36	4.03	short tubular	tapered	green	opaque	drawn
WJC046	2011.WCT000.06GB0.0033.007	KVIII	T0P18F2	B12	1.31	4.02	short tubular	tapered	green	opaque	drawn
WJC047	2011.WCT000.06GB0.0033.008	KVIII	T0P18F2	B12	1.79	3.58	short tubular	tapered	red	opaque	drawn
WJC048	2011.WCT000.06GB0.0034.001	TS1			1.48	2.39	short tubular	tapered	blue	translucent	wound?
WJC049	2011.WCT000.06GB0.0034.002	TS1			1.31	2.33	short tubular	tapered	blue	translucent	wound?
WJC050	2011.WCT000.06GB0.0034.003	TS1			1.05	2.54	short tubular	tapered	blue	translucent	wound?
WJC051	2011.WCT000.06GB0.0034.004	TS1			1.45	2.62	short tubular	tapered	blue	translucent	wound?

Sample number	Original sample number	Region	Trench	Burial	Length (mm)	Diameter (mm)	Shape	End roundness	Colour	Diaphaneity	Manufacturing method
WJC052	2011.WCT000.06GB0.0034.005	TS1			1.42	2.13	short tubular	tapered	blue	translucent	wound?
WJC053	2011.WCT000.06GB0.0034.006	TS1			2.1	3.09	short tubular	tapered	blue	translucent	wound?
WJC054	2011.WCT000.06GB0.0034.007	TS1			1.3	2.46	short tubular	tapered	blue	translucent	wound?
WJC055	2011.WCT000.06GB0.0034.008	TS1			1.44	2.42	short tubular	tapered	blue	translucent	wound?
WJC056	2011.WCT000.06GB0.0034.009	TS1			1.48	2.48	short tubular	tapered	blue	translucent	wound?
WJC057	2011.WCT000.06GB0.0035.000	TS2	T4P3F2		1.84	3.4	oblate	round	green	opaque	drawn
WJC058	2011.WCT000.06GB0.0036.000	TS1		B16	2.07	3.21	short tubular	tapered	blue	translucent	wound?
WJC059	2011.WCT000.06GB0.0037.000				2.19	3.43	short tubular	tapered	yellow	opaque	drawn

Table A1. 6: A list of analysed Shisanhang samples from Tsang and Liu (2001).

Sample number	Artefact	Type	Location	Shape	Colour	Diaphaneity
B001	glass bead	Type 13	BT7P0L4 BM17	short tubular	orange	opaque
B002	glass bead	Type 3	CT1P0CL4 CM29	short tubular	orange or red or yellow	opaque
B003	glass bead	Type 3	T2P2BL7 CM4	short tubular	orange or red or yellow	opaque
B004	glass bead	Type 3	CT2P2L7 CM4	short tubular	orange or red or yellow	opaque
B005	glass bead	Type 8	CT2P2BL7 CM4	short tubular	orange	opaque
B005	glass bead	Type 8	CT2P2BL7 CM4	short tubular	orange	opaque
B006	glass bead	Type 8	CT2P2BL7 CM4	short tubular	orange	opaque
B007	glass bead	Type 14	CT4P05AL8	short tubular	yellow	opaque
B008	glass bead	Type 8	CT2P2BL7 CM4	short tubular	orange	opaque
B008	glass bead	Type 8	CT2P2BL7 CM4	short tubular	orange	opaque
B011	glass bead	Type 17	HT12P03DL2 HM45	oblate	red	opaque
B012	glass bead	Type 3	CT2P3AL2	short tubular	orange or red or yellow	opaque
B013	glass bead	Type 14	HT9P02AL7 HM62	short tubular	yellow	opaque
B015	glass bead	Type 18	HT6P05BL7	oblate	red	opaque
B017	glass bead	Type 4	BT2P02AL3	short tubular	orange	opaque
B018	glass bead	Type 9	CT3P02DL7	oblate	yellow	opaque
B019	glass bead	Type 4	CT5P04D19d	short tubular	orange	opaque
B020	glass bead	Type 1	BT08P7CL9 BM62	oblate or long tube	dark blue	opaque or translucent
B021	glass bead	Type 15	HT12P03DL2 HM45	short tubular or oblate	blue	opaque

Sample number	Artefact	Type	Location	Shape	Colour	Diaphaneity
B024	glass bead	Type 2	BT6P0DL5	short tubular	blue	translucent
B026	glass bead	Type 15	HT8P07DL6	short tubular or oblate	blue	opaque
B027	glass bead	Type 15	HT14P13BL2	short tubular or oblate	blue	opaque
B028	glass bead	Type 18	HT6P05ALA HM5	oblate	red	opaque
B029	glass bead	Type 6	CT2P2BL7 CM4	long tubular	blue body	opaque
B029	glass bead	Type 6	CT2P2BL7 CM4	long tubular	orange surface	opaque
B032	glass bead	Type 1	CTP2BL7 CM4	oblate or long tube	dark blue	opaque or translucent
B033	glass bead	Type 1	CT2P2BL7 CM4	oblate or long tube	dark blue	opaque or translucent
B035	glass bead	Type 9	CT05P10BL5	oblate	yellow	opaque
B036	glass bead	Type 14	CT05P10BL5	short tubular	yellow	opaque
B037	glass bead	Type 1	BT2P02AL3	oblate or long tube	dark blue	opaque or translucent
B040	glass bead	Type 3	BT5P2DL2	short tubular	orange or red or yellow	opaque
B041	glass bead	Type 16	BT5P2DL3	short tubular	blue	opaque
B042	glass bead	Type 11	H6P05ALAHM5	long tubular	blue	opaque
B043	glass bead	Type 1	HT9P01CL3	oblate or long tube	dark blue	opaque or translucent
B045	glass bead	Type 12	HT8P07NEL6 HM62	short tubular	orange	opaque
B046	glass bead	Type 1	BT7P0L4 BM17	oblate or long tube	dark blue	opaque or translucent
B047	glass bead	Type 1	CT2P2BL7 CM4	oblate or long tube	dark blue	opaque or translucent
B048	glass bead	Type 1	CT4P05AL8	oblate or long tube	dark blue	opaque or translucent
B049	glass bead	Type 1	BT7P0L4 BM17	oblate or long tube	dark blue	opaque or translucent

Sample number	Artefact	Type	Location	Shape	Colour	Diaphaneity
B052	glass bead	Type 1	BT11P11CL10 BM68	oblate or long tube	dark blue	opaque or translucent
B054	glass bead	Type 11	HT9P01DL2	long tubular	blue	opaque
B055	glass bead	Type 15	HT8P07DL6	short tubular or oblate	blue	opaque
B057	glass bead	Type 10	ET3P7CL6 EM11	oblate	dark blue	n/a
B059	glass bead	Type 17	CT2P03BL8	oblate	red	opaque
B060	glass bead	Type 12	HT5P03DL2	short tubular	orange	opaque
B061	glass bead	Type 11	BT8P07NEL6	long tubular	blue	opaque
B062	glass bead	Type 1	HT9P01CL4	oblate or long tube	dark blue	opaque or translucent
B063	glass bead	Type 1	HT9P01CL4	oblate or long tube	dark blue	opaque or translucent
B064	glass bead	Type 1	HT9P01CL4	oblate or long tube	dark blue	opaque or translucent

Table A1.7: A list of analysed Xiliao samples from Chen and Cheng (2011).

Sample number	Artefact	Trench	Layer	Length (mm)	Diameter (mm)	Shape*	End roundness*	Colour	Diaphaneity
SL-GB001-1	glass bead	P14	L2d	2.42	3.60	short tubular	tapered	dark blue	translucent
SL-GB001-2	glass bead	P14	L2d	2.50	3.50	short tubular	tapered	dark blue	translucent
SL-GB001-3	glass bead	P14	L2d	3.51	3.46	short tubular	tapered	dark blue	translucent
SL-GB001-4	glass bead	P14	L2d	1.97	3.63	short tubular	tapered	dark blue	translucent
SL-GB002-1	glass bead	P14	L2d	2.97	3.66	short tubular	tapered	dark blue	translucent
SL-GB002-2	glass bead	P14	L2d	2.75	3.58	short tubular	tapered	dark blue	translucent
SL-GB002-3	glass bead	P14	L2d	2.17	3.69	short tubular	tapered	dark blue	translucent
SL-GB002-4	glass bead	P14	L2d	2.57	3.46	short tubular	tapered	dark blue	translucent
SL-GB002-5	glass bead	P14	L2d	1.82	4.22	short tubular	tapered	dark blue	translucent
SL-GB002-6	glass bead	P14	L2d	2.76	3.85	short tubular	tapered	dark blue	translucent
SL-GB004	glass bead	P90	L3a	1.13	3.28	short tubular	tapered	blue	translucent
SL-GB005-2	glass bead	P91	L2c	n/a	n/a	short tubular	tapered	blue	translucent

* Identification of shape and end roundness based on the colour plate in Chen and Cheng 2011.

Table A1.8: A full list of Xiliao samples in Niaosong period. Data collected from Liu (2011d).

Trench	Period	Location	Colour	Diaphaneity	shape
P74	Niaosong	L3b, F2	red	opaque	n/a
P74	Niaosong	L3b, F2	yellow	opaque	short tubular
P74	Niaosong	L3b, F2	yellow	translucent	n/a
P74	Niaosong	L3b, F2	blue	opaque	short tubular
P89	Niaosong	L2d, F2-L4	blue	opaque	short tubular
P90	Niaosong	L3a, M2-L2	blue	opaque	short tubular
P91	Niaosong	L3c	blue	translucent	short tubular
P91	Niaosong	L3c	blue	translucent	short tubular
P5	Niaosong	L3b, F1	yellow	translucent	n/a
P19	Niaosong	L2d, M1-L1	dark blue	translucent	n/a
P19	Niaosong	L2d, M1-L1	red	opaque	n/a
P19	Niaosong	L2d, M1-L1	red	opaque	n/a
P19	Niaosong	L2d, F6-L3	yellow	opaque	n/a
P19	Niaosong	L2d, F4-L1	green	opaque	n/a
P24UexTP2L	Niaosong	L2d, M1	red	opaque	short tubular
P24UexTP4L	Niaosong	L2c, M3	green	opaque	n/a
P24UexTP4L	Niaosong	L2c, M3	blue	opaque	short tubular
P24UexTP4L	Niaosong	L2b, M2	red	opaque	short tubular
P24UexTP4L	Niaosong	L2c, M3	red	opaque	short tubular

Trench	Period	Location	Colour	Diaphaneity	shape
P14	Niaosong	L2d	dark blue	translucent	short tubular
P14	Niaosong	L2d	dark blue	translucent	short tubular
P14	Niaosong	L2d	dark blue	translucent	short tubular
P14	Niaosong	L2d	dark blue	translucent	short tubular
P14	Niaosong	L2d	dark blue	translucent	short tubular
P14	Niaosong	L2d	dark blue	translucent	short tubular
P14	Niaosong	L2d	dark blue	translucent	short tubular
P14	Niaosong	L2d	dark blue	translucent	short tubular
P14	Niaosong	L2d	dark blue	translucent	short tubular
P15	Niaosong	L2b, F2-L3	blue	translucent	n/a
P16	Niaosong	L2a, F1	green	opaque	n/a
P16	Niaosong	L2a, F1	blue or green	n/a	n/a
P16	Niaosong	L2a, F1	blue or green	n/a	n/a
P16	Niaosong	L2a, F1	blue or green	n/a	n/a
P16	Niaosong	L2a, F1	blue or green	n/a	n/a
P16	Niaosong	L2a, F1	blue or green	n/a	n/a
P16	Niaosong	L2a, F1	blue or green	n/a	n/a
P16	Niaosong	L2a, F1	blue or green	n/a	n/a
P16	Niaosong	L2a, F1	blue or green	n/a	n/a
P16	Niaosong	L2a, F9	blue	opaque	n/a
P16	Niaosong	L2b, F3	green	opaque	n/a
P16	Niaosong	L2b, F7	blue	opaque	n/a

Trench	Period	Location	Colour	Diaphaneity	shape
P16	Niaosong	L2b, F7	green	opaque	n/a

Appendix 2: chemical composition of analysed samples.

Table A2.1: Chemical composition of samples from Kiwulan (major and minor elements analysed by EPMA, except for samples labelled with ‘*’, which are analysed by LA-ICP-MS.)

	colour	artefact type	n	compo	SiO ₂ (%)	Al ₂ O ₃ (%)	Na ₂ O (%)	K ₂ O (%)	MgO (%)	CaO (%)	FeO (%)	MnO (%)	CuO (%)	SnO ₂ (%)	PbO (%)	Cl (%)	SO ₃ (%)	Ti (%)	Ba (%)
KWL001_o	orange	bead	12	m-Na-Al	57.24	10.06	11.01	2.63	0.67	2.95	2.86	0.04	6.01	1.34	1.88	0.63	0.12	0.54	0.13
KWL001_i	dark blue	bead	30	v-Na-Ca	62.96	3.00	13.96	2.74	3.45	7.86	1.29	0.76	0.17	0.00	0.07	0.64	0.23	0.11	0.05
KWL002_o	orange	bead	5	m-Na-Al	56.76	10.72	11.34	1.91	0.79	2.96	2.84	0.07	7.81	0.35	1.96	0.41	0.18	0.29	0.16
KWL002_i	blue	bead	23	v-Na-Ca	62.23	1.89	14.00	2.73	5.61	5.43	0.96	1.23	0.18	0.13	2.02	0.58	0.29	0.10	0.04
KWL003*	orange	bead	4	m-Na-Al	61.60	12.35	15.21	1.39	0.84	2.68	1.22	0.03	3.13	0.02	0.02			0.16	0.04
KWL004	orange	bead	35	m-Na-Al	56.91	11.57	16.93	1.77	0.74	3.22	1.59	0.03	4.07	0.01	0.04	1.05	0.28	0.20	0.13
KWL005	orange	bead	28	m-Na-Al	54.93	9.28	19.22	1.38	0.78	3.03	1.61	0.05	4.95	0.71	0.69	1.33	0.37	0.21	0.09
KWL006	blue	bead	31	v-Na-Ca	64.17	1.93	15.92	2.82	3.46	6.55	1.20	0.03	0.11	0.01	0.04	0.82	0.33	0.08	0.05
KWL007	blue	bead	42	v-Na-Ca	65.36	1.88	16.02	2.81	3.38	6.56	1.23	0.06	0.08	0.01	0.05	0.80	0.32	0.07	0.05
KWL008	yellow	bead	21	v-Na-Ca	58.32	1.86	14.04	2.55	3.08	6.75	0.63	0.43	0.09	0.41	7.10	0.78	0.25	0.07	0.04
KWL009	yellow	bead	22	v-Na-Ca	56.50	1.81	13.86	2.23	2.56	4.63	0.58	0.47	0.10	0.47	12.02	0.98	0.22	0.06	0.05
KWL010	yellow	bead	23	v-Na-Ca	55.94	2.96	13.32	2.28	4.04	8.09	1.01	0.94	0.11	0.23	6.41	0.63	0.27	0.10	0.06
KWL011	yellow	bead	20	v-Na-Ca	55.44	1.96	13.27	2.82	2.86	5.99	0.57	0.35	0.09	0.51	11.37	0.79	0.24	0.06	0.04

	colour	artefact type	n	compo	SiO ₂ (%)	Al ₂ O ₃ (%)	Na ₂ O (%)	K ₂ O (%)	MgO (%)	CaO (%)	FeO (%)	MnO (%)	CuO (%)	SnO ₂ (%)	PbO (%)	Cl (%)	SO ₃ (%)	Ti (%)	Ba (%)
KWL012	yellow	bead	17	v-Na-Ca	54.57	2.22	12.85	2.88	3.34	7.95	0.72	0.63	0.10	0.41	9.61	0.87	0.16	0.09	0.04
KWL013	yellow	bead	24	v-Na-Ca	56.51	2.21	13.87	2.45	5.49	5.42	1.19	0.05	0.10	0.23	7.56	0.75	0.28	0.18	0.04
KWL014	yellow	bead	61	v-Na-Ca	58.08	2.36	12.45	2.48	3.52	6.75	0.68	1.06	0.07	0.23	7.95	0.73	0.18	0.07	0.04
KWL-GB295-1	yellow	bead	41	v-Na-Ca	57.50	1.98	12.27	2.47	3.43	6.08	0.59	0.99	0.11	0.49	9.56	0.65	0.23	0.07	0.06
KWL-GB295-2	yellow	bead	39	v-Na-Ca	58.78	2.30	13.82	1.73	2.97	5.79	0.55	0.39	0.07	0.25	8.81	1.01	0.16	0.06	0.04
KWL-GB-303	dark blue	bead	25	v-Na-Ca	62.34	2.43	14.31	2.58	4.33	7.58	1.08	1.37	0.17	0.00	0.69	0.04	0.25	0.10	0.05
KWL-GB305-1	blue	bead	40	v-Na-Ca	64.47	1.75	15.18	2.82	3.75	6.63	1.25	0.03	0.09	0.00	0.03	0.86	0.31	0.07	0.04
KWL-GB305-2	blue	bead	54	v-Na-Ca	64.53	1.66	14.18	3.05	3.78	6.73	1.27	0.05	0.08	0.00	0.03	0.84	0.26	0.07	0.02
KWL-GB306-1	orange	bead	40	m-Na-Al	56.22	11.55	15.85	1.72	0.86	3.66	1.59	0.04	5.09	0.03	0.10	1.08	0.32	0.20	0.10
KWL-GB306-2	orange	bead	38	m-Na-Al	57.90	12.19	14.05	1.91	0.79	3.39	1.70	0.04	4.66	0.04	0.16	0.88	0.24	0.23	0.09
KWL-GB-605	blue	bead	27	v-Na-Ca	64.37	2.84	12.92	3.17	4.16	5.58	1.37	1.29	0.17	0.02	0.47	0.65	0.18	0.09	0.06
KWL-GB-606	orange	bead	32	m-Na-Al	60.45	11.31	13.64	2.01	0.63	3.26	1.43	0.04	4.70	0.01	0.05	0.82	0.22	0.19	0.12
KWL-GB759	orange	bead	38	m-Na-Al	63.37	10.67	10.45	1.93	0.86	3.59	1.79	0.04	4.80	0.01	0.03	0.67	0.17	0.24	0.10
KWL-GB-1468	yellow	bead	30	v-Na-Ca	57.23	1.45	14.17	2.09	5.06	4.92	0.72	0.05	0.07	0.27	9.44	0.78	0.26	0.11	0.03

Table A2.2: Chemical composition of samples from Kiwulan (minor and trace elements analysed by LA-ICP-MS.)

	colour	artefact type	n	compo	P ₂ O ₅ (%)	Sc (ppm)	V (ppm)	Co (ppm)	Ni (ppm)	Zn (ppm)	As (ppm)	Rb (ppm)	Sr (ppm)	Y (ppm)	Zr (ppm)	Nb (ppm)	Ag (ppm)	Sb (ppm)	Cs (ppm)	La (ppm)
KWL001_o	orange	bead	4	m-Na-Al	0.15	5.6	47.7	55.47	277.2	553.5	178.7	33.4	196.6	8.1	294.0	4.7	20.8	65.3	0.4	26.8
KWL001_i	dark blue	bead	4	v-Na-Ca	0.40	4.5	21.4	5.87	32.0	29.9	7.3	10.4	276.9	3.8	42.7	1.5	2.6	3.6	0.4	6.3
KWL002_o	orange	bead	4	m-Na-Al	0.06	4.2	72.7	156.8 3	141.4	786.8	616.3	35.5	297.2	10.4	389.8	5.0	68.5	35.9	0.5	32.0
KWL002_i	blue	bead	4	v-Na-Ca	0.08	3.1	35.1	348.7 8	30.0	245.3	44.8	32.6	335.8	7.1	129.2	4.0	4.8	5.1	2.7	13.4
KWL003	orange	bead	4	m-Na-Al	0.08	5.9	95.9	5.01	32.3	29.6	22.1	25.8	313.2	7.3	133.7	2.0	20.3	7.0	0.4	19.4
KWL004	orange	bead	4	m-Na-Al	0.08	5.2	68.0	5.46	24.7	19.1	11.5	23.0	337.9	6.9	219.5	2.0	7.3	3.1	0.7	18.1
KWL005	orange	bead	4	m-Na-Al	0.12	6.1	107.6	15.69	76.6	75.3	132.9	24.7	274.4	8.6	251.4	2.1	43.0	49.4	0.4	23.4
KWL006	blue	bead	2	v-Na-Ca	0.00	648.4	84.9	11.52	0.0	2.1	9.3	331.9	2.7	68.9	1.1	<LLD	19.0	0.3	61.4	8.1
KWL007	blue	bead	4	v-Na-Ca	0.28	2.8	11.6	90.55	12.6	34.6	5.5	11.3	284.3	2.9	63.5	1.1	0.5	0.8	0.1	4.6
KWL008	yellow	bead	4	v-Na-Ca	0.24	<LLD	10.2	7.18	79.1	52.7	17.3	11.8	341.3	3.3	40.4	1.3	31.7	41.4	0.7	5.3
KWL009	yellow	bead	4	v-Na-Ca	0.22	<LLD	9.6	4.05	41.5	40.2	38.0	9.0	218.8	3.2	57.3	1.3	17.1	65.0	0.5	6.8
KWL010	yellow	bead	4	v-Na-Ca	0.29	<LLD	14.5	5.85	52.8	53.4	119.3	11.2	401.8	4.7	49.8	1.7	11.3	9.4	0.4	7.2
KWL011	yellow	bead	4	v-Na-Ca	0.30	<LLD	9.8	4.19	42.3	27.2	35.0	11.9	363.9	3.7	64.2	1.3	25.6	44.5	0.6	6.6
KWL012	yellow	bead	4	v-Na-Ca	0.25	<LLD	12.1	5.48	51.6	27.8	21.8	14.3	446.5	3.7	35.7	1.4	30.5	129.4	0.7	6.2
KWL013	yellow	bead	4	v-Na-Ca	0.38	<LLD	18.5	5.98	46.0	56.8	<LLD	22.0	356.8	6.9	80.1	4.4	15.9	3.5	0.4	9.4
KWL014	yellow	bead	4	v-Na-Ca	0.24	<LLD	12.0	5.26	50.7	37.3	6.5	11.9	418.6	4.1	59.7	1.6	13.8	20.2	0.4	7.3

	colour	artefact type	n	compo	P ₂ O ₅ (%)	Sc (ppm)	V (ppm)	Co (ppm)	Ni (ppm)	Zn (ppm)	As (ppm)	Rb (ppm)	Sr (ppm)	Y (ppm)	Zr (ppm)	Nb (ppm)	Ag (ppm)	Sb (ppm)	Cs (ppm)	La (ppm)
KWL-GB295-1	yellow	bead	4	v-Na-Ca	0.05	<LLD	11.3	3.98	17.5	39.5	22.5	12.5	325.9	3.9	57.7	1.6	19.6	22.3	<LLD	7.3
KWL-GB295-2	yellow	bead	4	v-Na-Ca	<LLD	<LLD	9.0	3.00	13.4	36.5	36.0	12.0	251.5	3.8	35.4	1.2	30.9	24.4	<LLD	6.9
KWL-GB-303	dark blue	bead	4	v-Na-Ca	0.44	4.1	20.1	537.4 8	32.7	1353. 3	14.7	12.0	459.5	4.6	91.9	1.8	0.8	3.4	0.7	8.6
KWL-GB305-1	blue	bead	4	v-Na-Ca	0.36	4.2	16.1	143.5 8	13.1	48.7	5.7	14.5	460.0	3.4	82.4	1.5	0.3	2.1	0.6	7.1
KWL-GB305-2	blue	bead																		
KWL-GB306-1	orange	bead	4	m-Na-Al	<LLD	3.2	116.3	19.46	52.6	48.6	48.9	34.1	467.0	10.8	315.5	2.9	21.1	28.1	0.6	30.3
KWL-GB306-2	orange	bead	4	m-Na-Al	<LLD	3.4	74.4	9.33	75.8	44.6	45.5	34.3	455.2	11.3	343.7	3.5	18.5	30.0	0.2	29.9
KWL-GB-605	blue	bead	4	v-Na-Ca	0.10	0.7	14.2	849.9 6	97.1	383.5	42.0	20.1	362.7	4.7	73.0	1.7	3.7	11.0	0.4	7.9
KWL-GB-606	orange	bead	4	m-Na-Al	<LLD	3.3	45.5	20.27	98.0	14.5	95.1	28.6	437.5	7.3	221.2	2.2	16.3	18.3	<LLD	19.9
KWL-GB759	orange	bead	4	m-Na-Al	0.18	8.0	62.3	25.84	118.7	202.3	116.2	41.8	446.5	10.6	273.3	2.9	22.2	36.7	1.7	26.9
KWL-GB-1468	yellow	bead	4	v-Na-Ca	0.44	1.5	14.0	3.77	13.7	52.8	11.8	20.8	372.3	5.7	67.3	3.4	14.5	1.0	0.4	7.3

	colour	artefact type	n	compo	Ce (ppm)	Pr (ppm)	Nd (ppm)	Sm (ppm)	Eu (ppm)	Gd (ppm)	Tb (ppm)	Dy (ppm)	Ho (ppm)	Er (ppm)	Tm (ppm)	Yb (ppm)	Lu (ppm)	Hf (ppm)	Th (ppm)	U (ppm)
KWL001_o	orange	bead	4	m-Na-Al	37.0	4.1	16.5	3.0	0.8	2.6	0.2	1.6	0.3	1.0	0.1	1.4	0.2	6.5	5.7	6.5
KWL001_i	dark blue	bead	4	v-Na-Ca	8.8	1.0	4.4	0.7	0.2	0.3	0.2	<LLD	0.2	0.5	0.1	<LLD	0.0	<LLD	1.2	0.3

	colour	artefact type	n	compo	Ce (ppm)	Pr (ppm)	Nd (ppm)	Sm (ppm)	Eu (ppm)	Gd (ppm)	Tb (ppm)	Dy (ppm)	Ho (ppm)	Er (ppm)	Tm (ppm)	Yb (ppm)	Lu (ppm)	Hf (ppm)	Th (ppm)	U (ppm)
KWL002_o	orange	bead	4	m-Na-Al	42.9	5.4	22.3	3.5	0.9	3.7	0.3	2.0	0.3	1.2	0.4	2.5	0.2	10.0	6.1	4.9
KWL002_i	blue	bead	4	v-Na-Ca	19.9	2.6	8.9	1.5	0.4	2.2	0.1	2.6	0.4	0.8	0.4	1.8	0.1	4.0	3.9	1.8
KWL004	orange	bead	4	m-Na-Al	26.9	3.0	11.2	1.5	0.6	2.1	0.1	<LLD	0.2	0.7	0.2	1.5	0.1	4.3	5.5	5.5
KWL005	orange	bead	4	m-Na-Al	20.5	2.7	13.4	2.1	0.6	1.6	0.2	1.6	0.2	0.8	0.2	1.2	0.1	5.8	9.3	9.7
KWL008	yellow	bead	4	m-Na-Al	31.5	3.8	5.5	<LLD	1.4	1.7	0.8	2.3	0.3	1.8	0.4	<LLD	0.3	2.1	1.4	1.5
KWL009	yellow	bead	4	v-Na-Ca	0.9	3.5	4.8	1.5	0.6	1.9	<LLD	1.8	0.4	1.1	0.2	<LLD	0.2	1.4	1.6	0.3
KWL010	yellow	bead	4	v-Na-Ca	6.9	0.8	6.3	2.2	0.2	1.4	0.3	1.6	0.5	1.4	0.4	<LLD	0.2	1.5	1.3	0.7
KWL011	yellow	bead	4	v-Na-Ca	7.9	0.9	3.4	0.9	0.4	0.5	0.3	1.8	0.2	1.1	0.2	<LLD	0.2	1.2	1.6	0.6
KWL012	yellow	bead	4	v-Na-Ca	8.2	0.7	2.7	<LLD	0.6	1.6	0.4	2.1	0.2	0.8	0.4	<LLD	0.2	1.3	1.6	0.4
KWL013	yellow	bead	4	v-Na-Ca	10.8	1.5	6.4	3.5	0.6	1.1	0.6	3.1	0.4	1.8	0.1	<LLD	0.2	1.8	1.9	0.7
KWL014	yellow	bead	4	v-Na-Ca	8.9	1.0	3.9	<LLD	0.3	1.2	0.6	2.8	0.2	0.4	0.3	<LLD	0.2	2.0	1.7	0.9
KWL-GB295-1	yellow	bead	4	v-Na-Ca	8.2	0.9	6.6	0.4	0.8	3.3	0.3	2.8	0.2	<LLD	<LLD	2.5	0.3	3.6	1.5	0.6
KWL-GB295-2	yellow	bead	4	v-Na-Ca	15.5	2.0	5.8	2.5	0.5	4.7	0.4	3.3	0.1	0.9	<LLD	2.1	0.3	2.3	1.1	0.7
KWL-GB-303	dark blue	bead	4	v-Na-Ca	10.4	1.2	6.7	1.7	0.4	3.1	0.3	1.2	0.2	0.8	0.2	0.9	0.2	1.8	1.5	0.8
KWL-GB305-1	blue	bead	4	v-Na-Ca	9.6	1.2	4.6	0.4	0.4	1.5	0.2	1.6	0.2	0.7	0.3	2.4	0.2	2.7	1.3	0.3
KWL-GB305-2	blue	bead	4	v-Na-Ca	8.9	1.1								0.0						
KWL-GB306-1	orange	bead	4	v-Na-Ca	13.4	1.5	21.9	2.3	0.8	4.1	0.4	2.2	0.3	1.2	0.4	1.5	0.3	8.3	10.0	7.8
KWL-GB306-2	orange	bead	4	v-Na-Ca	9.7	1.2	21.5	2.5	1.0	2.8	0.5	2.5	0.4	1.0	0.7	<LLD	0.3	9.0	9.3	10.4
KWL-GB-605	blue	bead	4	v-Na-Ca			5.4	2.0	<LLD	2.1	0.2	2.3	0.2	<LLD	0.6	1.3	0.2	2.6	2.1	0.4

	colour	artefact type	n	compo	Ce (ppm)	Pr (ppm)	Nd (ppm)	Sm (ppm)	Eu (ppm)	Gd (ppm)	Tb (ppm)	Dy (ppm)	Ho (ppm)	Er (ppm)	Tm (ppm)	Yb (ppm)	Lu (ppm)	Hf (ppm)	Th (ppm)	U (ppm)
KWL-GB-606	orange	bead	4	m-Na-Al	36.7	5.1	13.7	1.7	1.1	2.3	0.2	1.7	0.4	0.9	0.6	1.4	0.1	5.3	6.7	4.0
KWL-GB759	orange	bead	4	m-Na-Al	32.9	4.5	17.9	3.5	0.8	2.8	0.4	2.1	0.4	1.2	0.3	2.6	0.2	8.4	7.8	8.0
KWL-GB-1468	yellow	bead	4	v-Na-Ca	11.5	1.5	8.1	1.8	0.2	1.8	0.3	1.5	0.2	1.4	0.3	1.4	0.3	2.0	1.2	0.3
KWL003	orange	bead	4	m-Na-Al	24.5	3.0	13.3	2.1	0.6	2.0	0.2	1.2	0.3	0.7	0.1	1.2	0.1	3.0	5.8	6.0
KWL006	blue	bead	2	m-Na-Al	36.2	4.2	0.4	<LLD	0.7	0.1	<LLD	0.1	0.6	0.1	<LLD	<LLD	1.5	0.0	0.4	0.4
KWL007	blue	bead	4	v-Na-Ca	11.8	1.7	3.7	0.4	0.2	0.9	0.1	<LLD	0.1	0.6	0.1	<LLD	0.1	1.4	0.8	0.3

Table A2.3: Chemical composition of samples from Jiuxianglan (major and minor elements analysed by EPMA, except for samples labelled with ‘*’, which are analysed by LA-ICP-MS.)

	colour	artefact type	n	compo	SiO ₂ (%)	Al ₂ O ₃ (%)	Na ₂ O (%)	K ₂ O (%)	MgO (%)	CaO (%)	FeO (%)	MnO (%)	CuO (%)	SnO ₂ (%)	PbO (%)	Cl (%)	SO ₃ (%)	Ti (%)	Ba (%)
JXL01	red	bead	48	m-Na-Al	59.29	11.41	18.49	2.24	0.55	3.15	1.10	0.07	1.17	0.06	0.86	1.01	0.15	0.35	0.16
JXL02	red	bead	44	m-Na-Al	59.44	11.72	18.55	2.34	0.47	2.57	1.15	0.05	1.14	0.06	0.78	1.07	0.15	0.37	0.14
JXL03	yellow	bead	39	m-Na-Al	57.02	13.27	18.08	2.49	0.33	2.37	1.07	0.04	0.08	0.14	3.06	0.91	0.13	0.32	0.23
JXL04	blue	bead	29	m-Na-Al	61.83	10.65	18.38	3.29	0.11	1.19	0.62	0.05	1.05	0.00	0.30	0.86	0.18	0.28	0.12
JXL05	yellow	bead	35	m-Na-Al	55.65	13.23	21.19	2.58	0.42	2.58	1.12	0.04	0.09	0.04	1.22	1.12	0.24	0.40	0.24
JXL06	blue	bead	44	m-Na-Al	59.33	8.87	21.15	1.82	0.48	4.09	1.24	0.06	0.52	0.01	0.05	0.61	0.42	0.31	0.10
JXL07	yellow	bead	46	m-Na-Al	56.45	12.96	19.09	2.16	0.30	2.35	1.23	0.06	0.05	0.11	2.31	1.09	0.14	0.47	0.25
JXL08	green	bead	55	m-Na-Al	60.92	11.22	16.63	2.89	0.20	1.38	0.79	0.04	0.52	0.10	3.11	0.99	0.07	0.26	0.10
JXL09	green	bead	36	m-Na-Al	57.31	10.78	17.94	1.72	0.35	2.30	1.21	0.04	0.52	0.38	4.15	1.05	0.29	0.38	0.14
JXL10	red	bead	32	m-Na-Al	59.27	8.90	19.40	1.95	1.45	2.09	1.86	0.15	1.61	0.13	0.34	0.97	0.29	0.43	0.10
JXL11	green	bead	32	m-Na-Al	59.20	11.32	15.84	2.14	0.35	2.20	1.14	0.07	0.72	0.22	3.95	0.88	0.08	0.35	0.16
JXL12	yellow	bead	27	m-Na-Al	55.99	12.87	18.03	2.45	0.40	2.29	1.34	0.03	0.07	0.31	3.08	0.95	0.10	0.41	0.21
JXL13	green	bead	38	m-Na-Al	57.93	12.20	17.08	2.23	0.37	2.54	1.34	0.07	0.53	0.31	3.38	0.86	0.11	0.39	0.21
JXL14	green	bead	26	m-Na-Al	58.18	11.27	16.39	1.91	0.39	2.31	1.28	0.04	0.88	0.33	4.01	0.92	0.09	0.36	0.14
JXL15	yellow	bead	32	m-Na-Al	56.04	12.99	18.56	2.58	0.42	2.34	1.27	0.05	0.06	0.09	2.37	0.98	0.11	0.38	0.25
JXL16	blue	bead	39	m-Na-Al	62.28	10.46	16.33	2.30	0.30	1.91	0.95	0.05	1.16	0.11	1.35	0.97	0.08	0.27	0.12
JXL17	blue	bead	48	m-Na-Al	63.17	10.62	17.20	2.06	0.22	1.77	1.07	0.13	0.93	0.05	0.23	1.06	0.06	0.46	0.17

	colour	artefact type	n	compo	SiO ₂ (%)	Al ₂ O ₃ (%)	Na ₂ O (%)	K ₂ O (%)	MgO (%)	CaO (%)	FeO (%)	MnO (%)	CuO (%)	SnO ₂ (%)	PbO (%)	Cl (%)	SO ₃ (%)	Ti (%)	Ba (%)
JXL18	blue	bead	43	m-Na-Al	62.08	10.94	17.93	2.74	0.27	1.48	0.98	0.04	1.03	0.01	0.04	1.05	0.06	0.32	0.10
JXL19	yellow	bead	36	m-Na-Al	55.87	12.80	17.91	2.41	0.31	2.26	1.17	0.04	0.07	0.09	4.03	0.98	0.12	0.42	0.23
JXL20	yellow	bead	47	m-Na-Al	62.48	10.65	17.13	2.64	0.25	1.35	0.73	0.03	0.05	0.05	2.26	1.17	0.04	0.31	0.12
JXL21	blue	bead	32	m-Na-Al	60.39	11.86	19.54	2.55	0.22	1.61	0.84	0.03	1.33	0.15	0.19	1.22	0.08	0.28	0.14
JXL22	red	bead	45	m-Na-Al	58.59	12.07	17.49	2.59	0.59	2.58	1.27	0.06	1.23	0.06	0.61	0.97	0.12	0.41	0.17
JXL23	green	bead	33	m-Na-Al	57.18	12.01	15.86	2.43	0.28	2.15	1.10	0.03	1.36	0.43	5.62	0.96	0.08	0.34	0.20
JXL24	orange	bead	28	m-Na-Al	52.73	12.55	15.52	1.47	0.85	3.62	2.55	0.03	7.45	1.24	1.55	0.49	0.26	0.33	0.09
JXL25	orange	bead	34	m-Na-Al	57.38	9.63	16.62	1.50	0.87	3.05	1.94	0.05	4.75	0.47	1.43	0.95	0.21	0.25	0.09
JXL26	green	bead	42	m-Na-Al	60.31	10.70	17.07	1.92	0.30	2.16	1.14	0.04	1.08	0.13	2.70	1.04	0.10	0.38	0.15
JXL27	orange	bead	58	m-Na-Al	58.99	10.81	14.48	2.04	0.79	3.18	1.70	0.03	5.20	0.39	0.90	0.84	0.28	0.20	0.10
JXL28	blue	bead	53	m-Na-Al	63.45	11.28	17.52	2.48	0.23	1.69	0.83	0.05	0.86	0.03	0.26	1.07	0.09	0.25	0.11
JXL29	blue	bead	36	m-Na-Al	62.78	9.86	19.89	1.38	0.23	1.97	0.79	0.07	0.87	0.05	0.21	1.33	0.11	0.29	0.09
JXL30	green	bead	47	m-Na-Al	60.86	11.56	16.59	1.62	0.38	2.38	1.19	0.07	0.69	0.11	2.11	1.04	0.10	0.39	0.16
JXL31	green	bead	32	m-Na-Al	61.40	11.13	15.33	1.81	0.33	2.23	1.08	0.09	0.71	0.11	2.70	0.88	0.09	0.35	0.15
JXL32	yellow	bead	37	m-Na-Al	56.34	13.37	18.42	2.18	0.31	2.22	1.12	0.03	0.05	0.20	2.64	1.06	0.12	0.40	0.24
JXL33	yellow	bead	47	m-Na-Al	57.83	13.89	17.50	2.63	0.39	2.45	1.28	0.04	0.05	0.08	1.66	0.98	0.08	0.45	0.22
JXL34	red	bead	15	m-Na-Al	61.88	7.64	14.41	4.73	2.04	3.61	1.24	0.10	0.94	0.06	0.33	0.80	0.06	0.21	0.16
JXL35	red	bead	49	m-Na-Al	61.53	12.03	16.77	2.36	0.44	2.37	1.25	0.05	1.29	0.15	0.34	0.92	0.10	0.40	0.20
JXL38	yellow	bead	27	potash	73.43	1.72	0.40	13.64	0.16	0.90	0.41	0.20	1.85	0.10	3.55	0.13	0.06	0.03	0.07
JXL39	blue	residue	45	m-Na-Al	63.08	9.19	19.81	2.32	0.32	1.88	1.04	0.04	0.31	0.01	0.09	0.42	0.37	0.32	0.08

	colour	artefact type	n	compo	SiO ₂ (%)	Al ₂ O ₃ (%)	Na ₂ O (%)	K ₂ O (%)	MgO (%)	CaO (%)	FeO (%)	MnO (%)	CuO (%)	SnO ₂ (%)	PbO (%)	Cl (%)	SO ₃ (%)	Ti (%)	Ba (%)
JXL41	aqua	residue	39	m-Na-Al	67.60	6.45	18.06	1.78	0.39	1.83	1.21	0.05	0.21	0.01	0.03	0.46	0.38	0.29	0.11
JXL43	dark blue	residue	58	v-Na-Ca	64.03	1.40	15.84	2.79	5.80	5.29	1.19	1.57	0.24	0.00	0.02	0.59	0.28	0.06	0.04
JXL44	blue	residue	33	m-Na-Al	66.90	6.57	18.03	1.34	0.24	2.37	1.14	0.07	0.82	0.06	0.06	0.51	0.33	0.36	0.10
JXL46	blue	residue	48	v-Na-Ca	60.26	3.93	19.78	2.66	3.73	5.47	0.83	0.03	0.98	0.00	0.04	1.17	0.21	0.09	0.05
JXL47	red	residue	40	v-Na-Ca	59.33	3.28	16.46	2.50	3.89	8.52	1.65	0.48	1.26	0.06	0.34	0.59	0.33	0.11	0.06
JXL48	yellow	residue	36	m-Na-Al	54.27	12.62	19.51	1.94	0.12	1.75	0.67	0.03	0.06	0.62	5.83	0.88	0.30	0.27	0.13
JXL49	aqua	residue	40	m-Na-Al	62.26	10.53	19.49	2.70	0.28	1.91	0.73	0.04	0.20	0.00	0.02	0.40	0.22	0.30	0.13

Table A2.4: Chemical composition of samples from Jiuxianglan (minor and trace elements analysed by LA-ICP-MS.)

	colour	artefact type	n	compo	P ₂ O ₅ (%)	Sc (ppm)	V (ppm)	Co (ppm)	Ni (ppm)	Zn (ppm)	As (ppm)	Rb (ppm)	Sr (ppm)	Y (ppm)	Zr (ppm)	Nb (ppm)	Ag (ppm)	Sb (ppm)	Cs (ppm)	La (ppm)	
JXL01	red	bead	4	m-Na-Al																	
JXL02	red	bead	4	m-Na-Al	0.05	2.0	51.2	<LLD	<LLD	10.6	<LLD	27.0	511.8	6.7	390.9	5.0	21.7	13.3	<LLD	19.9	
JXL03	yellow	bead	4	m-Na-Al	0.00	2.2	52.5	<LLD	<LLD	<LLD	<LLD	31.3	664.6	6.1	267.0	3.7	6.4	1.6	<LLD	21.0	
JXL04	blue	bead	4	m-Na-Al	0.17	2.0	70.5	2.52	4.5	29.1	14.6	75.7	299.5	5.4	362.8	10.6	19.6	11.4	0.7	10.8	
JXL05	yellow	bead	4	m-Na-Al	0.05	<LLD	52.2	4.52	27.8	11.2	4.7	37.3	713.5	6.8	540.7	5.0	5.1	1.5	0.7	26.2	
JXL06	blue	bead	4	m-Na-Al	<LLD	2.5	77.4	<LLD	<LLD	<LLD	<LLD	36.2	335.5	12.8	390.7	3.4	0.7	3.5	<LLD	27.6	
JXL07	yellow	bead	4	m-Na-Al	0.02	2.8	58.8	<LLD	<LLD	<LLD	<LLD	29.8	734.0	7.0	388.7	5.4	5.0	5.5	<LLD	26.4	

	colour	artefact type	n	compo	P ₂ O ₅ (%)	Sc (ppm)	V (ppm)	Co (ppm)	Ni (ppm)	Zn (ppm)	As (ppm)	Rb (ppm)	Sr (ppm)	Y (ppm)	Zr (ppm)	Nb (ppm)	Ag (ppm)	Sb (ppm)	Cs (ppm)	La (ppm)
JXL08	green	bead	4	m-Na-Al	0.00	2.5	28.4	<LLD	<LLD	<LLD	<LLD	56.8	298.1	6.8	320.4	7.3	13.0	12.5	<LLD	11.7
JXL09	green	bead													0.0					
JXL10	red	bead	4	m-Na-Al	0.18	6.6	67.5	19.61	54.8	119.5	33.7	50.7	286.2	14.6	451.6	6.7	42.2	10.5	0.6	38.0
JXL11	green	bead	4	m-Na-Al	0.21	6.3	52.8	8.69	4.8	44.0	14.2	37.9	539.6	9.1	477.8	6.4	13.4	8.4	0.7	23.5
JXL12	yellow	bead	4	m-Na-Al	0.11	4.6	56.8	4.67	6.4	25.8	7.1	46.4	735.3	7.7	256.4	6.4	3.4	0.6	0.1	32.3
JXL13	green	bead	4	m-Na-Al	0.07	<LLD	53.4	11.36	40.3	61.6	13.7	34.5	629.0	8.8	514.6	5.4	8.4	4.5	0.7	27.4
JXL14	green	bead	4	m-Na-Al	0.12	2.8	52.5	6.84	12.4	40.8	17.4	34.7	649.1	10.6	501.7	6.8	22.2	11.3	0.2	27.0
JXL15	yellow	bead	4	m-Na-Al	0.11	3.5	58.1	3.24	6.8	18.3	8.2	44.5	765.2	6.9	303.2	6.2	4.6	0.4	0.6	29.2
JXL16	blue	bead	4	m-Na-Al	0.09	0.9	50.2	4.52	7.1	63.8	15.3	48.3	402.1	8.2	442.1	6.3	32.4	8.2	0.6	17.9
JXL17	blue	bead	4	m-Na-Al	0.16	5.6	39.0	12.42	4.4	49.8	14.0	34.0	403.3	10.5	653.8	8.1	5.8	8.1	0.4	19.2
JXL18	blue	bead	4	m-Na-Al	0.09	2.6	44.6	3.63	4.6	45.7	14.4	70.2	254.5	12.6	322.2	10.8	3.7	7.7	0.5	17.5
JXL19	yellow	bead	4	m-Na-Al	0.21	4.9	51.7	2.50	<LLD	21.2	9.7	39.2	731.8	5.9	273.8	5.8	2.1	2.4	0.9	24.9
JXL20	yellow	bead	4	m-Na-Al	0.06	<LLD	38.1	2.62	16.4	14.3	3.6	51.5	273.2	6.1	274.4	11.6	27.3	3.3	0.5	12.8
JXL21	blue	bead	4	m-Na-Al	<LLD	1.4	41.0	<LLD	<LLD	<LLD	<LLD	43.6	256.7	8.3	230.8	6.3	1.2	11.5	<LLD	12.3
JXL22	red	bead	4	m-Na-Al	0.32	6.4	57.2	4.30	3.8	61.7	13.0	46.3	654.3	9.9	529.3	6.6	17.3	15.1	0.9	27.6
JXL23	green	bead	4	m-Na-Al	0.03	2.6	31.4	<LLD	<LLD	<LLD	<LLD	37.1	502.5	6.2	165.7	4.5	74.4	3.7	<LLD	19.2
JXL24	orange	bead	4	m-Na-Al	0.14	5.3	71.0	21.69	13.6	1773.6	297.4	28.1	421.3	8.1	249.4	3.5	48.4	50.3	<LLD	28.1
JXL25	orange	bead	4	m-Na-Al	0.07	5.1	100.8	10.65	57.4	1103.3	92.6	36.1	352.5	12.0	156.2	3.3	44.9	91.6	0.5	25.5
JXL26	green	bead	4	m-Na-Al	0.08	<LLD	47.5	5.41	24.4	38.7	10.5	26.3	533.5	9.7	555.9	5.9	33.5	10.0	0.4	24.9

	colour	artefact type	n	compo	P ₂ O ₅ (%)	Sc (ppm)	V (ppm)	Co (ppm)	Ni (ppm)	Zn (ppm)	As (ppm)	Rb (ppm)	Sr (ppm)	Y (ppm)	Zr (ppm)	Nb (ppm)	Ag (ppm)	Sb (ppm)	Cs (ppm)	La (ppm)
JXL27	orange	bead	4	m-Na-Al	0.08	3.4	101.0	10.89	71.0	735.0	178.2	36.2	447.1	10.1	221.8	3.3	36.8	120.1	0.8	26.6
JXL28	blue	bead	4	m-Na-Al	0.06	<LLD	43.3	6.11	36.7	17.3	6.2	35.0	320.3	11.2	351.2	6.5	12.5	7.6	0.7	19.4
JXL29	blue	bead	4	m-Na-Al	0.05	<LLD	50.8	3.84	30.1	46.5	10.8	16.4	372.2	12.3	519.3	4.8	10.3	8.2	0.6	22.0
JXL30	green	bead	4	m-Na-Al	0.06	<LLD	49.8	10.87	35.4	113.4	11.0	26.7	521.8	11.2	393.2	6.5	15.2	5.2	0.8	26.1
JXL31	green	bead	4	m-Na-Al	0.12	2.9	49.1	12.80	10.4	18.8	12.8	32.3	523.9	10.8	388.9	5.6	8.8	7.8	1.4	25.4
JXL32	yellow	bead	4	m-Na-Al	0.16	4.8	56.3	2.78	8.7	22.7	8.1	34.0	801.3	7.6	297.3	6.0	3.8	1.2	0.4	26.7
JXL33	yellow	bead	4	m-Na-Al	0.05	<LLD	43.6	3.80	15.9	20.2	2.2	37.0	693.2	7.3	178.4	6.7	1.2	2.2	0.9	27.3
JXL34	red	bead	4	m-Na-Al	0.99	3.5	39.9	9.20	19.8	172.3	22.9	102.3	497.8	12.3	359.3	5.0	7.2	12.9	0.6	21.2
JXL35	red	bead	4	m-Na-Al	0.08	<LLD	52.6	10.92	70.5	68.2	27.1	36.7	640.5	8.1	593.0	5.8	14.6	18.5	1.0	30.4
JXL38	yellow	bead	4	potash	0.22	3.1	12.2	15.80	5.9	20.1	146.1	405.5	26.6	4.1	38.2	1.0	68.5	184.5	2.2	9.3
JXL39	blue	residue	4	m-Na-Al	0.06	0.6	64.6	4.15	15.7	13.8	4.3	64.3	261.6	7.9	517.8	6.6	3.6	4.0	0.6	64.2
JXL41	aqua	residue	4	m-Na-Al	0.13	4.2	93.1	3.52	3.5	13.6	9.4	44.0	231.1	7.2	685.8	6.0	1.3	2.3	0.4	38.7
JXL43	dark blue	residue	4	v-Na-Ca	0.14	<LLD	15.6	773.48	60.6	1161.4	11.3	12.2	466.8	4.6	133.6	1.3	0.9	2.7	0.4	8.3
JXL44	blue	residue												0.0						
JXL46	blue	residue	4	v-Na-Ca	0.48	4.6	10.6	6.22	15.2	32.1	22.3	23.3	417.2	8.8	58.7	3.5	1.0	8.6	0.9	29.2
JXL47	red	residue	4	v-Na-Ca	0.46	4.7	18.5	5.31	53.2	51.9	31.2	16.7	456.0	5.8	63.7	2.2	8.4	114.6	0.4	9.0
JXL48	yellow	residue	4	m-Na-Al	0.13	3.2	28.6	2.88	5.1	20.3	5.7	22.2	434.3	6.0	243.4	2.5	10.8	1.7	0.6	10.8
JXL49	aqua	residue	4	m-Na-Al	0.09	2.6	46.2	2.25	5.3	17.0	5.9	84.3	341.3	6.8	412.9	6.9	1.6	0.7	0.9	73.6

	colour	artefact type	n	compo	Ce (ppm)	Pr (ppm)	Nd (ppm)	Sm (ppm)	Eu (ppm)	Gd (ppm)	Tb (ppm)	Dy (ppm)	Ho (ppm)	Er (ppm)	Tm (ppm)	Yb (ppm)	Lu (ppm)	Hf (ppm)	Th (ppm)	U (ppm)
JXL01	red	bead																		
JXL02	red	bead	4	m-Na-Al	33.7	2.9	10.7	1.2	0.3	1.6	0.1	0.4	0.1	0.2	<LLD	<LLD	<LLD	6.6	4.9	8.0
JXL03	yellow	bead	4	m-Na-Al	32.7	2.8	10.2	0.2	0.4	1.4	0.1	0.5	<LLD	<LLD	<LLD	<LLD	<LLD	5.0	3.4	4.3
JXL04	blue	bead	4	m-Na-Al	20.6	1.8	5.4	1.1	0.5	1.6	0.2	<LLD	0.2	0.6	0.4	2.0	0.2	9.1	3.7	3.7
JXL05	yellow	bead	4	m-Na-Al	35.6	3.3	11.4	2.2	0.7	1.8	0.5	1.6	0.3	1.7	0.4	<LLD	0.4	12.7	6.8	3.4
JXL06	blue	bead	4	m-Na-Al	36.8	3.7	14.6	1.7	0.4	0.5	0.2	1.7	0.5	<LLD	0.3	<LLD	<LLD	6.8	4.6	4.3
JXL07	yellow	bead	4	m-Na-Al	45.7	3.6	11.0	1.0	0.1	1.3	0.1	<LLD	0.0	<LLD	<LLD	<LLD	<LLD	6.2	5.9	20.3
JXL08	green	bead	4	m-Na-Al	22.8	1.5	4.3	1.8	0.1	1.0	0.1	<LLD	0.0	<LLD	<LLD	<LLD	<LLD	4.9	2.9	16.1
JXL09	green	bead																		
JXL10	red	bead	4	m-Na-Al	48.7	6.0	25.5	3.6	0.8	4.7	0.5	2.5	0.4	1.0	0.4	1.7	0.6	9.9	6.9	5.0
JXL11	green	bead	4	m-Na-Al	38.1	3.3	14.5	2.6	1.2	3.0	0.3	2.1	0.3	0.8	0.1	<LLD	0.3	12.2	5.0	9.1
JXL12	yellow	bead	4	m-Na-Al	45.2	4.2	16.5	3.0	0.9	2.7	0.4	2.2	0.3	1.0	0.4	<LLD	0.2	7.0	6.6	4.0
JXL13	green	bead	4	m-Na-Al	44.7	3.7	17.3	3.5	1.1	3.5	0.7	2.9	0.6	1.6	0.2	<LLD	0.2	12.1	7.8	7.8
JXL14	green	bead	4	m-Na-Al	43.5	3.8	16.3	2.8	1.6	3.3	0.6	2.4	0.3	1.3	0.6	1.8	0.3	12.3	5.9	7.8
JXL15	yellow	bead	4	m-Na-Al	42.2	4.0	17.2	2.8	1.4	2.4	0.4	2.4	0.4	0.5	0.4	1.7	0.4	5.8	5.2	3.8
JXL16	blue	bead	4	m-Na-Al	32.6	3.0	12.0	1.3	0.8	2.8	0.3	1.0	0.3	1.1	<LLD	<LLD	0.3	11.2	5.0	9.4
JXL17	blue	bead	4	m-Na-Al	36.3	3.2	15.2	2.4	0.9	2.2	0.5	2.2	0.2	1.1	0.4	1.5	0.3	15.4	6.2	6.9
JXL18	blue	bead	4	m-Na-Al	38.3	3.0	12.2	1.6	0.8	3.0	0.5	2.6	0.5	1.6	<LLD	2.9	0.4	7.2	5.7	16.4
JXL19	yellow	bead	4	m-Na-Al	40.1	3.9	16.4	1.3	1.0	2.5	0.5	1.7	0.3	0.7	0.5	<LLD	0.2	7.6	6.1	11.0
JXL20	yellow	bead	4	m-Na-Al	30.6	1.7	8.9	2.9	0.4	2.1	0.4	3.3	<LLD	1.6	0.3	<LLD	0.3	8.5	5.4	12.2

	colour	artefact type	n	compo	Ce (ppm)	Pr (ppm)	Nd (ppm)	Sm (ppm)	Eu (ppm)	Gd (ppm)	Tb (ppm)	Dy (ppm)	Ho (ppm)	Er (ppm)	Tm (ppm)	Yb (ppm)	Lu (ppm)	Hf (ppm)	Th (ppm)	U (ppm)
JXL21	blue	bead	4	m-Na-Al	32.2	1.8	6.2	1.3	0.3	1.3	0.2	0.4	0.2	<LLD	<LLD	0.2	<LLD	3.9	4.7	32.9
JXL22	red	bead	4	m-Na-Al	42.9	4.3	16.4	2.6	1.3	3.1	0.3	1.7	0.2	1.1	0.3	2.0	0.3	13.0	6.4	7.8
JXL23	green	bead	4	m-Na-Al	32.6	2.5	8.2	1.3	0.1	1.6	0.1	0.7	<LLD	<LLD	<LLD	<LLD	<LLD	2.8	4.8	11.1
JXL24	orange	bead	4	m-Na-Al	43.4	4.1	13.9	1.8	0.3	1.2	0.1	0.6	0.0	<LLD	<LLD	<LLD	<LLD	4.0	3.8	7.0
JXL25	orange	bead	4	m-Na-Al	33.4	4.0	18.8	1.9	0.9	3.7	0.4	2.0	0.5	1.2	0.3	2.2	0.4	4.5	8.6	10.3
JXL26	green	bead	4	m-Na-Al	42.9	3.9	16.1	3.2	0.8	2.3	0.4	2.5	0.4	1.4	0.2	<LLD	0.4	13.6	7.5	13.5
JXL27	orange	bead	4	m-Na-Al	34.4	4.2	16.7	2.8	0.6	2.9	0.5	2.0	0.3	0.9	0.3	<LLD	0.2	5.8	10.9	8.2
JXL28	blue	bead	4	m-Na-Al	34.7	3.4	13.1	4.6	0.5	1.0	0.6	2.8	0.7	2.0	0.1	<LLD	0.5	7.3	6.4	18.7
JXL29	blue	bead	4	m-Na-Al	39.4	3.5	16.4	2.4	0.9	3.3	0.5	2.8	0.5	1.7	0.3	<LLD	0.3	12.2	7.2	9.0
JXL30	green	bead	4	m-Na-Al	45.6	4.4	19.0	4.0	1.2	2.8	0.8	2.9	0.6	1.6	0.3	<LLD	0.4	8.9	7.0	8.2
JXL31	green	bead	4	m-Na-Al	41.6	4.0	14.4	3.6	0.5	3.6	0.4	2.5	0.4	0.8	<LLD	2.3	0.2	9.7	4.8	6.0
JXL32	yellow	bead	4	m-Na-Al	46.1	3.8	16.5	2.6	1.3	2.5	0.3	1.3	0.3	1.5	0.4	2.3	0.2	6.1	5.3	14.9
JXL33	yellow	bead	4	m-Na-Al	37.7	3.8	13.7	2.9	0.6	1.1	0.6	2.1	0.3	1.2	0.1	<LLD	0.3	4.7	5.5	6.3
JXL34	red	bead	4	m-Na-Al	41.0	3.6	14.6	2.1	0.8	4.4	0.4	3.3	0.4	1.7	0.4	2.5	0.4	8.3	6.0	13.8
JXL35	red	bead	4	m-Na-Al	49.0	4.1	17.2	2.4	1.1	2.6	0.4	2.2	0.3	1.2	0.2	<LLD	0.6	12.5	9.0	10.7
JXL38	yellow	bead	4	potash	14.5	1.9	8.2	0.5	0.5	2.7	0.4	<LLD	0.2	1.4	<LLD	2.6	0.2	2.1	1.0	1.0
JXL39	blue	residue	4	m-Na-Al	89.1	7.0	26.2	3.0	0.8	2.4	0.5	2.4	0.2	1.2	0.3	<LLD	0.2	12.9	39.9	26.1
JXL41	aqua	residue	4	m-Na-Al	50.8	5.6	20.7	2.5	1.0	2.7	0.3	1.6	0.1	0.7	0.3	2.0	0.5	15.0	13.5	4.7
JXL43	dark blue	residue	4	v-Na-Ca	11.5	1.3	5.7	1.3	0.4	1.2	0.3	2.1	0.4	0.8	0.3	<LLD	<LLD	2.9	1.5	0.6

	colour	artefact type	n	compo	Ce (ppm)	Pr (ppm)	Nd (ppm)	Sm (ppm)	Eu (ppm)	Gd (ppm)	Tb (ppm)	Dy (ppm)	Ho (ppm)	Er (ppm)	Tm (ppm)	Yb (ppm)	Lu (ppm)	Hf (ppm)	Th (ppm)	U (ppm)
JXL44	blue	residue																		
JXL46	blue	residue	4	v-Na-Ca	42.5	4.4	18.5	4.0	0.3	4.4	0.5	2.3	0.3	0.7	0.3	<LLD	0.3	3.0	5.3	0.6
JXL47	red	residue	4	v-Na-Ca	13.2	1.5	6.9	0.4	0.4	0.9	0.1	1.2	0.2	0.2	<LLD	1.4	0.2	1.8	1.5	0.6
JXL48	yellow	residue	4	m-Na-Al	20.4	2.0	8.0	1.3	0.8	2.2	0.3	1.4	0.4	0.9	0.4	2.5	0.3	6.2	2.4	13.2
JXL49	aqua	residue	4	m-Na-Al	91.9	8.8	29.5	2.7	1.1	1.7	0.3	1.9	0.2	1.4	<LLD	1.4	0.2	11.3	37.8	18.8

Table A2.5: Chemical composition of samples from Guishan (major and minor elements analysed by EPMA, except for samples labelled with ‘*’, which are analysed by LA-ICP-MS.)

	colour	artefact type	n	compo	SiO ₂ (%)	Al ₂ O ₃ (%)	Na ₂ O (%)	K ₂ O (%)	MgO (%)	CaO (%)	FeO (%)	MnO (%)	CuO (%)	SnO ₂ (%)	PbO (%)	Cl (%)	SO ₃ (%)	Ti (%)	Ba (%)
GS001	green	bead	68	m-Na-Al	64.24	7.10	16.96	1.48	0.45	2.81	1.43	0.06	1.28	0.07	1.40	0.46	0.40	0.18	0.12
GS002*	blue	bead	4	m-Na-Al	66.51	9.93	16.72	2.11	0.45	2.91	1.37	0.05	0.33	0.01	0.04			0.29	0.08
GS003*	yellow	bead	4	m-Na-Al	61.25	6.45	13.84	1.49	0.33	1.83	1.16	0.03	0.00	2.15	11.53			0.40	0.08
GS004	red	bead	38	m-Na-Al	63.44	10.31	14.42	1.67	0.74	2.92	2.33	0.07	0.78	0.06	0.16	0.71	0.12	0.35	0.08
GS005	yellow	bead	40	m-Na-Al	60.88	8.58	15.68	2.03	0.35	2.69	1.82	0.08	0.09	0.38	4.76	0.56	0.33	0.34	0.11
GS006*	green	bead	4	m-Na-Al	61.86	11.91	17.44	1.66	0.28	2.51	1.01	0.04	0.41	0.45	2.81			0.34	0.08
GS009*	blue	bead	1	m-Na-Al	65.02	12.99	11.86	2.28	0.60	4.42	1.55	0.03	1.02	0.02	0.13			0.28	0.08
GS010*	red	bead	4	m-Na-Al	69.02	5.87	17.33	1.68	0.95	1.95	1.14	0.12	1.69	0.25	0.26			0.36	0.04
GS011*	yellow	bead	4	m-Na-Al	63.68	9.42	18.04	1.75	0.35	2.51	1.18	0.07	<LLD	0.48	3.02			0.33	0.07
GS012*	blue	bead	4	m-Na-Al	66.22	10.37	18.32	1.41	0.25	2.23	0.80	0.06	0.75	0.05	0.14			0.27	0.07
GS013*	blue	bead	4	m-Na-Al	61.99	12.05	20.82	2.41	0.19	1.61	0.59	0.02	1.06	0.10	0.14			0.18	0.09
GS015_1*	red	bead	4	m-Na-Al	63.56	12.43	14.91	1.75	0.84	3.05	2.26	0.05	1.27	0.01	0.06			0.30	0.06
GS015_2*	orange	bead	4	m-Na-Al	57.83	13.28	12.69	1.66	0.89	3.03	2.60	0.05	6.67	0.10	0.79			0.27	0.05
GS019*	red	bead	4	m-Na-Al	65.85	11.34	13.30	1.88	0.69	2.93	2.16	0.05	1.67	0.06	0.15			0.30	0.06
GS022	yellow	bead	57	m-Na-Al	66.51	6.32	15.21	0.82	0.26	2.42	1.70	0.06	0.16	0.14	3.44	1.03	0.11	0.20	0.07
GS023*	red	bead	4	m-Na-Al	60.98	15.35	12.76	1.85	1.03	3.34	3.24	0.06	1.11	0.01	0.05			0.34	0.06
GS025*	blue	bead	4	m-Na-Al	65.23	11.97	16.38	1.97	0.19	1.94	0.77	0.04	1.36	0.11	0.32			0.33	0.15

	colour	artefact type	n	compo	SiO ₂ (%)	Al ₂ O ₃ (%)	Na ₂ O (%)	K ₂ O (%)	MgO (%)	CaO (%)	FeO (%)	MnO (%)	CuO (%)	SnO ₂ (%)	PbO (%)	Cl (%)	SO ₃ (%)	Ti (%)	Ba (%)
GS026*	green	bead	4	m-Na-Al	66.78	9.98	14.58	2.04	0.48	2.28	1.47	0.06	0.67	0.32	1.65			0.30	0.07
GS028	yellow	bead	43	m-Na-Al	60.32	8.30	16.89	1.03	0.10	1.64	0.58	0.06	0.13	0.60	7.80	1.41	0.05	0.23	0.10
GS029	yellow	bead	60	m-Na-Al	55.27	11.96	17.83	1.95	0.09	1.81	0.59	0.03	0.10	0.31	6.73	0.95	0.25	0.28	0.12
GS030*	yellow	bead	4	m-Na-Al	58.56	13.12	19.91	2.13	0.26	2.20	0.80	0.03	<LLD	0.75	2.91			0.25	0.17
GS031*	green	bead	4	m-Na-Al	64.89	10.73	17.92	1.25	0.26	1.93	0.79	0.03	0.78	0.29	1.69			0.29	0.07
GS033*	blue	bead	3	m-Na-Al	68.43	8.66	15.79	1.99	0.44	3.30	1.00	0.05	0.65	0.02	0.17			0.25	0.06
GS034*	green	bead	4	m-Na-Al	60.08	11.72	22.02	1.24	0.52	2.33	1.10	0.04	0.49	0.17	1.25			0.25	0.04
GS037*	green	bead	4	m-Na-Al	65.79	10.42	20.83	1.47	0.69	2.18	1.64	0.04	1.33	0.15	0.89			0.24	0.05
GS038*	red	bead	3	m-Na-Al	65.69	8.01	12.16	3.05	2.37	3.78	2.32	0.20	1.57	0.00	0.02			0.22	0.02
GS040*	yellow	bead	4	m-Na-Al	65.66	5.00	18.78	2.11	1.27	2.37	1.02	0.05	0.00	0.73	3.63			0.10	0.01
GS041*	yellow	bead	4	m-Na-Al	59.05	9.81	20.74	1.59	0.12	1.58	0.62	0.08	0.00	1.63	5.76			0.20	0.05
GS043*	blue	bead	4	m-Na-Al	59.66	10.66	24.73	1.47	0.25	1.95	0.82	0.07	1.08	0.09	0.18			0.29	0.13
GS044*	green	bead	4	m-Na-Al	64.33	10.14	20.52	1.60	0.22	1.75	0.72	0.05	0.63	0.16	0.70			0.22	0.08
GS049*	blue	bead	4	m-Na-Al	65.83	10.26	19.62	2.83	0.08	1.18	0.42	0.02	0.50	0.03	0.10			0.20	0.08
GS050*	red	bead	4	m-Na-Al	63.82	10.23	14.71	3.74	1.48	3.04	1.15	0.11	1.35	0.12	0.20			0.24	0.09
GS052*	green	bead	4	m-Na-Al	63.93	8.90	19.52	2.04	0.28	1.53	0.82	0.02	0.85	0.35	2.47			0.23	0.12
GS053	blue	bead	20	m-Na-Al	64.31	9.32	17.71	1.48	0.19	1.95	0.72	0.10	0.85	0.06	0.20	0.97	0.21	0.21	0.14
GS055*	red	bead	4	m-Na-Al	65.14	10.76	15.22	1.97	0.54	3.22	1.90	0.06	1.13	0.20	0.05			0.33	0.06
GS056*	dark blue	bead	4	v-Na-Ca	68.65	2.75	18.89	1.59	2.20	5.00	1.30	0.10	0.16	0.00	0.09			0.20	0.01

	colour	artefact type	n	compo	SiO ₂ (%)	Al ₂ O ₃ (%)	Na ₂ O (%)	K ₂ O (%)	MgO (%)	CaO (%)	FeO (%)	MnO (%)	CuO (%)	SnO ₂ (%)	PbO (%)	Cl (%)	SO ₃ (%)	Ti (%)	Ba (%)
GS059	dark blue	bead	24	v-Na-Ca	65.31	3.00	14.59	1.74	3.71	7.40	1.57	0.30	0.11	0.00	0.08	0.83	0.24	0.12	0.06
GS060*	dark blue	bead	4	v-Na-Ca	68.17	2.94	18.00	2.31	2.95	4.91	1.20	0.06	0.08	0.00	0.05			0.12	0.01
GS064*	yellow	bead	4	m-Na-Al	62.78	9.00	21.70	1.04	0.36	2.46	0.39	0.05	0.01	0.34	1.89			0.12	0.05
GS065*	green	bead	4	m-Na-Al	67.18	9.39	17.07	0.81	0.59	2.68	0.55	0.04	0.54	0.19	0.89			0.10	0.05
GS068*	dark blue	bead	4	v-Na-Ca	67.85	3.02	19.13	1.20	2.98	5.22	0.46	0.13	0.03	0.00	0.05			0.01	0.01
GS070*	red	bead	4	m-Na-Al	67.87	9.96	15.63	1.51	0.38	2.67	0.74	0.06	0.99	0.14	0.08			0.17	0.05
GS073*	red	bead	4	m-Na-Al	61.76	11.40	20.69	1.07	0.45	2.17	0.27	0.04	1.56	0.11	0.31			0.14	0.07
GS074	red	bead	37	m-Na-Al	63.52	10.51	14.57	2.76	0.46	1.83	1.21	0.06	1.31	0.14	1.20	0.72	0.20	0.30	0.19
GS076*	blue	bead	4	v-Na-Ca	66.20	2.91	20.96	1.96	3.15	4.65	0.01	0.03	0.38	0.00	0.00			<LLD	0.01
GS077*	blue	bead	4	v-Na-Ca	64.72	3.39	21.87	2.23	3.55	4.09	0.09	0.03	0.38	0.00	0.00			<LLD	0.01
GS078*	red	bead	4	m-Na-Al	63.56	10.56	16.79	2.01	0.58	3.01	1.01	0.06	1.77	0.16	0.71			0.30	0.11
GS080*	blue	bead	4	v-Na-Ca	66.61	3.04	19.67	2.45	3.40	4.58	0.20	0.04	0.42	0.00	0.00			<LLD	0.01
GS085*	yellow	bead	4	m-Na-Al	51.76	8.46	19.85	0.96	0.34	2.91	0.52	0.06	<LLD	1.84	13.26			0.12	0.05
GS086*	yellow	bead	4	m-Na-Al	62.23	9.09	18.82	1.08	0.32	2.21	0.85	0.09	<LLD	0.68	4.60			0.16	0.05
GS087*	yellow	bead	4	m-Na-Al	59.50	9.30	19.60	1.04	0.27	2.90	0.62	0.05	<LLD	0.91	5.69			0.20	0.05
GS098*	dark blue	bead	4	v-Na-Ca	68.77	3.05	17.37	1.69	2.92	5.42	0.66	0.24	0.05	0.00	0.05			0.02	0.01

	colour	artefact type	n	compo	SiO ₂ (%)	Al ₂ O ₃ (%)	Na ₂ O (%)	K ₂ O (%)	MgO (%)	CaO (%)	FeO (%)	MnO (%)	CuO (%)	SnO ₂ (%)	PbO (%)	Cl (%)	SO ₃ (%)	Ti (%)	Ba (%)
GS099*	dark blue	bead	3	v-Na-Ca	67.46	3.13	18.45	<LLD	3.53	5.52	0.50	0.21	0.03	0.00	0.04			<LLD	0.01
GS101*	green	bead	4	m-Na-Al	63.21	10.37	20.68	0.57	0.55	2.16	0.64	0.03	1.01	0.12	0.60			0.08	0.04
GS102*	red	bead	4	m-Na-Al	65.25	12.41	15.79	1.00	0.72	2.47	1.09	0.04	0.98	0.02	0.06			0.14	0.04
GS103	green	bead	34	m-Na-Al	59.92	11.27	16.96	1.80	0.37	2.46	1.20	0.07	0.56	0.19	2.36	1.05	0.15	0.37	0.17
GS104*	green	bead	3	m-Na-Al	61.05	11.77	21.44	0.66	0.22	1.65	0.17	0.05	0.31	0.42	2.05			0.14	0.09
GS108*	green	bead	4	m-Na-Al	62.49	10.11	20.95	0.37	0.60	2.15	0.69	0.04	1.01	0.34	1.12			0.08	0.04
GS109*	red	bead	4	m-Na-Al	66.77	8.69	19.93	<LLD	0.16	1.64	0.04	0.03	0.45	0.28	1.65			0.13	0.04
GS111*	red	bead	4	m-Na-Al	60.06	10.95	23.55	1.70	0.50	2.20	0.19	0.04	0.96	0.10	0.28			0.08	0.07
GS114	dark blue	bead	20	v-Na-Ca	65.61	2.72	15.32	2.08	2.90	6.49	1.62	0.23	0.17	0.02	0.11	0.81	0.27	0.18	0.07
GS116*	green	bead	4	m-Na-Al	63.14	10.61	19.47	0.97	0.63	2.16	0.89	0.04	0.98	0.20	0.90			0.12	0.04
GS119*	dark blue	bead	4	SLS	69.25	1.82	21.52	<LLD	0.35	5.37	0.89	0.04	0.27	0.00	0.22			<LLD	0.01
GS120*	blue	bead	4	m-Na-Al	65.54	10.85	17.67	2.47	0.30	1.69	0.93	0.04	0.77	0.06	0.10			0.35	0.08
GS122	blue	bead	37	m-Na-Al	64.08	9.72	16.12	3.53	0.06	1.23	0.46	0.05	1.81	0.04	0.40	0.68	0.26	0.27	0.13

Table A2.6: Chemical composition of samples from Guishan (minor and trace elements analysed by LA-ICP-MS.)

	colour	artefact type	n	compo	P ₂ O ₅ (%)	Sc (ppm)	V (ppm)	Co (ppm)	Ni (ppm)	Zn (ppm)	As (ppm)	Rb (ppm)	Sr (ppm)	Y (ppm)	Zr (ppm)	Nb (ppm)	Ag (ppm)	Sb (ppm)	Cs (ppm)	La (ppm)
GS001*	green	bead	4	m-Na-Al	0.08	4.7	112.2	9.77	171.2	11.0	15.9	29.8	335.9	8.1	327.7	3.1	4.7	2.0	0.7	26.8
GS002*	blue	bead	4	m-Na-Al	0.08	5.3	101.5	3.22	42.9	26.1	15.5	60.6	356.6	10.6	253.2	4.2	3.6	3.5	0.9	35.4
GS003*	yellow	bead	4	m-Na-Al	0.06	3.8	56.7	4.43	8.5	18.3	9.1	41.0	192.6	8.6	426.2	7.1	10.7	4.5	0.9	42.6
GS004*	red	bead	4	m-Na-Al	0.15	7.0	82.1	15.53	61.9	151.5	30.4	48.0	376.2	10.9	410.9	4.8	48.7	7.8	0.4	32.5
GS005*	yellow	bead	4	m-Na-Al	0.07	4.6	53.3	4.02	5.0	25.3	3.5	49.0	285.5	13.5	439.0	4.2	1.1	3.0	1.1	30.7
GS006*	green	bead	4	m-Na-Al	0.07	4.5	51.5	5.98	6.4	29.7	2.8	32.7	448.0	9.5	493.1	6.8	10.3	6.1	0.4	34.2
GS009*	blue	bead	1	m-Na-Al	0.15	14.0	151.1	5.63	238.6	82.8	30.4	45.3	414.3	9.4	324.0	2.0	16.7	5.3	3.4	36.1
GS010*	red	bead	4	m-Na-Al	0.17	4.2	58.2	32.67	113.0	81.5	15.1	59.2	147.0	10.4	651.7	9.0	9.2	4.8	0.6	39.7
GS011*	yellow	bead	4	m-Na-Al	0.04	4.9	56.5	3.48	2.7	18.6	6.1	40.0	277.6	14.8	378.6	4.2	1.0	0.6	0.7	28.4
GS012*	blue	bead	4	m-Na-Al	0.07	3.5	53.3	5.16	6.1	12.7	15.7	22.0	396.0	9.1	248.2	4.5	73.3	7.0	0.5	23.3
GS013*	blue	bead	4	m-Na-Al	0.04	2.6	42.8	1.90	1.5	13.0	15.1	53.8	272.0	8.7	240.7	6.2	7.1	8.9	0.2	13.2
GS015_1*	red	bead	4	m-Na-Al	0.13	7.0	97.9	16.15	140.8	32.0	81.0	42.5	423.5	11.2	374.7	4.6	31.1	14.0	0.6	35.6
GS015_2*	orange	bead	4	m-Na-Al	0.32	5.9	109.5	81.66	1331. 4	69.3	1166. 2	36.3	404.1	10.7	306.5	3.6	21.1	261.6	0.9	32.4
GS019*	red	bead	4	m-Na-Al	0.13	6.1	75.5	14.01	291.2	102.8	24.4	40.6	382.2	9.4	328.4	4.9	19.8	11.1	0.3	30.2
GS022*	yellow	bead	3	m-Na-Al	0.01	14.0	72.6	3.22	<LLD	19.3	18.7	39.6	271.6	18.1	418.6	3.7	3.5	3.5	1.0	22.8
GS023*	red	bead	4	m-Na-Al	0.19	8.4	101.2	34.32	1106. 5	57.6	8.9	46.1	482.5	11.7	326.0	5.2	6.5	3.0	0.5	41.7
GS025*	blue	bead	4	m-Na-Al	0.04	2.8	27.6	3.65	8.3	25.6	13.3	33.5	407.6	7.5	467.2	6.6	21.5	11.8	0.6	17.2

	colour	artefact type	n	compo	P ₂ O ₅ (%)	Sc (ppm)	V (ppm)	Co (ppm)	Ni (ppm)	Zn (ppm)	As (ppm)	Rb (ppm)	Sr (ppm)	Y (ppm)	Zr (ppm)	Nb (ppm)	Ag (ppm)	Sb (ppm)	Cs (ppm)	La (ppm)
GS026*	green	bead	4	m-Na-Al	0.06	4.6	74.0	5.90	19.0	51.8	33.8	55.9	294.3	11.3	299.9	4.2	19.6	12.2	0.8	28.8
GS028*	yellow	bead	4	m-Na-Al	0.06	1.4	53.7	2.36	0.2	14.1	1.5	22.3	277.5	3.6	182.3	2.7	9.4	1.3	0.3	6.4
GS029*	yellow	bead	4	m-Na-Al	0.04	1.4	32.6	1.94	3.6	14.1	2.7	18.4	373.5	6.6	182.5	1.8	6.3	13.4	0.5	10.3
GS030*	yellow	bead	4	m-Na-Al	0.05	2.4	70.2	2.49	9.3	16.8	14.8	36.5	649.6	5.5	153.1	4.2	2.3	<LLD	0.4	20.6
GS031*	green	bead	4	m-Na-Al	0.04	1.7	57.6	3.18	9.7	45.1	8.1	18.7	494.9	6.4	299.5	4.5	11.5	10.7	0.5	14.5
GS033*	blue	bead	3	m-Na-Al	0.03	4.7	59.9	14.41	30.6	17.7	41.9	57.8	300.4	13.0	271.8	4.0	23.9	10.8	1.4	24.4
GS034*	green	bead	4	m-Na-Al	0.06	3.3	84.4	6.02	99.3	25.7	11.4	25.7	368.9	6.5	248.4	2.8	9.0	3.5	0.3	25.1
GS037*	green	bead	4	m-Na-Al	0.05	4.8	89.4	9.22	34.4	39.2	43.5	33.6	324.1	12.0	291.0	3.1	11.6	17.3	0.9	24.9
GS038*	red	bead	3	m-Na-Al	1.15	6.3	98.8	14.08	115.1	114.0	30.7	61.6	337.8	7.7	199.7	3.1	2.0	1.0	1.2	19.7
GS040*	yellow	bead	4	m-Na-Al	0.51	2.8	27.9	3.68	9.8	86.6	32.6	45.7	59.5	7.5	63.3	2.8	59.3	11.0	2.6	20.3
GS041*	yellow	bead	4	m-Na-Al	0.06	1.8	35.5	2.74	5.7	13.5	2.3	20.1	293.7	5.0	174.2	2.5	16.5	3.3	0.3	7.3
GS043*	blue	bead	4	m-Na-Al	0.06	3.3	49.7	6.47	10.9	32.7	22.6	22.0	534.4	6.4	393.3	5.0	6.3	13.5	0.5	20.5
GS044*	green	bead	4	m-Na-Al	0.09	2.7	60.5	5.70	22.4	90.4	17.8	29.9	383.1	8.1	290.0	3.9	8.9	6.1	0.4	18.5
GS049*	blue	bead	4	m-Na-Al	0.04	1.9	35.6	1.62	9.1	6.6	13.5	63.7	227.9	4.6	251.7	6.0	13.3	3.4	0.7	6.4
GS050*	red	bead	4	m-Na-Al	0.46	3.3	40.0	7.70	21.0	98.8	17.4	83.8	347.6	12.9	424.1	4.9	9.9	11.5	0.5	20.6
GS052*	green	bead	4	m-Na-Al	0.05	2.4	67.9	9.51	33.9	34.0	32.6	38.8	282.3	6.8	485.1	4.7	10.2	3.7	1.1	35.1
GS053*	blue	bead	4	m-Na-Al	0.07	2.0	61.0	5.48	10.1	129.4	7.1	23.2	329.3	7.9	186.6	3.3	13.7	8.2	1.5	16.4
GS055*	red	bead	4	m-Na-Al	0.13	3.6	73.9	10.88	30.7	58.4	86.3	48.7	323.6	13.9	370.0	4.6	6.3	23.9	1.2	31.9
GS056*	dark blue	bead	4	v-Na-Ca	0.16	3.2	27.1	399.4 3	31.4	31.6	4.2	14.3	321.4	6.7	150.4	3.1	0.8	2.0	1.1	7.0

	colour	artefact type	n	compo	P ₂ O ₅ (%)	Sc (ppm)	V (ppm)	Co (ppm)	Ni (ppm)	Zn (ppm)	As (ppm)	Rb (ppm)	Sr (ppm)	Y (ppm)	Zr (ppm)	Nb (ppm)	Ag (ppm)	Sb (ppm)	Cs (ppm)	La (ppm)
GS059*	dark blue	bead	4	v-Na-Ca	0.40	3.1	22.7	295.7 7	48.5	42.2	5.9	12.0	597.8	6.3	83.2	2.3	1.1	5.1	0.5	8.5
GS060*	dark blue	bead	4	v-Na-Ca	0.32	3.1	22.1	357.9 6	38.4	39.0	10.6	13.8	305.2	5.5	73.4	2.7	0.9	0.8	0.1	8.0
GS064*	yellow	bead	4	m-Na-Al	0.00	1.2	29.5	<LLD	<LLD	<LLD	<LLD	31.4	234.6	8.9	239.8	2.5	5.1	0.6	<LLD	18.9
GS065*	green	bead	4	m-Na-Al	0.01	4.1	182.6	<LLD	<LLD	<LLD	16.1	28.6	296.6	7.6	200.4	2.4	12.6	5.4	<LLD	15.7
GS068*	dark blue	bead	4	v-Na-Ca	0.24	1.2	10.3	280.8 9	<LLD	<LLD	<LLD	7.2	332.1	3.8	64.1	1.5	0.1	2.6	<LLD	5.4
GS070*	red	bead	4	m-Na-Al	0.07	2.7	48.0	0.87	<LLD	7.7	9.8	36.6	255.3	9.7	221.3	3.0	6.1	11.3	<LLD	22.1
GS073*	red	bead	4	m-Na-Al	0.09	0.6	41.4	<LLD	<LLD	8.2	2.8	20.2	418.0	5.2	280.6	3.0	23.0	10.8	<LLD	13.9
GS074*	red	bead	4	m-Na-Al	0.01	0.6	52.5	<LLD	<LLD	8.1	2.5	35.2	286.8	5.9	267.4	2.8	6.0	0.9	0.7	33.8
GS076*	blue	bead	4	v-Na-Ca	0.37	1.5	<LLD	<LLD	<LLD	<LLD	<LLD	21.1	240.1	4.1	33.2	0.8	0.8	3.2	<LLD	10.9
GS077*	blue	bead	4	v-Na-Ca	0.36	0.9	0.1	<LLD	<LLD	<LLD	4.7	16.8	263.1	5.4	33.5	1.7	0.8	12.4	<LLD	15.0
GS078*	red	bead	4	m-Na-Al	0.18	3.7	51.6	5.40	7.8	108.8	21.5	32.6	502.5	10.3	514.3	5.6	35.9	23.2	0.4	23.9
GS080*	blue	bead	4	v-Na-Ca	0.37	0.9	2.1	<LLD	<LLD	<LLD	<LLD	19.8	257.6	4.2	35.9	1.1	1.2	3.8	<LLD	11.6
GS085*	yellow	bead	4	m-Na-Al	0.02	1.8	46.3	<LLD	<LLD	<LLD	<LLD	24.7	233.9	8.9	229.0	2.3	1.4	0.7	<LLD	19.8
GS086*	yellow	bead	4	m-Na-Al	0.02	2.2	45.2	<LLD	<LLD	<LLD	<LLD	26.5	232.1	9.5	248.2	2.5	8.0	1.3	<LLD	20.7
GS087*	yellow	bead	4	m-Na-Al	0.01	2.7	36.0	<LLD	<LLD	<LLD	<LLD	22.5	213.1	10.4	342.0	2.8	7.1	4.7	<LLD	20.8
GS098*	dark blue	bead	4	v-Na-Ca	0.22	1.6	15.1	349.3 2	<LLD	8.2	<LLD	7.4	306.1	4.5	61.4	1.4	0.6	4.3	<LLD	5.7

	colour	artefact type	n	compo	P ₂ O ₅ (%)	Sc (ppm)	V (ppm)	Co (ppm)	Ni (ppm)	Zn (ppm)	As (ppm)	Rb (ppm)	Sr (ppm)	Y (ppm)	Zr (ppm)	Nb (ppm)	Ag (ppm)	Sb (ppm)	Cs (ppm)	La (ppm)
GS099*	dark blue	bead	3	v-Na-Ca	0.36	0.6	10.5	233.66	<LLD	11.0	<LLD	7.2	468.3	4.2	59.0	1.2	0.2	2.4	<LLD	5.9
GS101*	green	bead	4	m-Na-Al	0.01	3.3	62.2	<LLD	<LLD	<LLD	13.3	23.3	261.2	7.4	198.3	1.8	7.1	6.4	<LLD	17.0
GS102*	red	bead	4	m-Na-Al	0.12	2.6	52.0	<LLD	57.5	37.0	8.7	31.8	305.3	6.9	197.5	2.5	26.0	5.8	<LLD	22.2
GS103*	green	bead	4	m-Na-Al	0.07	5.2	83.5	7.82	136.9	31.6	16.8	35.6	454.2	9.0	264.3	3.7	10.3	7.3	0.6	30.6
GS104*	green	bead	3	m-Na-Al	0.01	<LLD	35.1	<LLD	<LLD	<LLD	<LLD	19.2	413.1	5.5	206.5	3.3	5.4	2.4	<LLD	16.5
GS108*	green	bead	4	m-Na-Al	0.03	2.6	62.1	<LLD	<LLD	<LLD	13.6	24.0	241.4	9.1	200.8	2.0	8.5	7.1	<LLD	17.9
GS109*	red	bead	4	m-Na-Al	0.01	0.3	26.1	<LLD	<LLD	<LLD	<LLD	17.4	221.4	6.6	335.3	4.4	5.0	3.9	<LLD	14.1
GS111*	red	bead	4	m-Na-Al	0.47	0.2	18.3	<LLD	<LLD	6.4	<LLD	43.9	270.8	5.5	278.3	4.9	15.0	10.4	<LLD	11.0
GS114	dark blue	bead	4	v-Na-Ca	0.36	2.1	21.0	308.00	<LLD	21.4	<LLD	16.2	341.5	5.3	74.9	1.8	0.1	3.5	1.3	7.5
GS116*	green	bead	4	m-Na-Al	0.02	3.9	67.6	1.48	<LLD	<LLD	20.2	24.2	261.4	8.8	203.0	2.0	7.2	6.3	<LLD	19.0
GS119*	dark blue	bead	4	SLS	0.03	0.4	2.9	1322.49	<LLD	25.0	5.7	3.3	337.8	3.7	38.8	0.5	<LLD	2.8	<LLD	4.4
GS120*	blue	bead	4	m-Na-Al	0.08	3.1	47.0	6.66	18.7	29.2	27.8	59.9	266.1	8.5	231.7	13.6	7.5	13.7	1.2	16.2
GS122*	blue	bead	4	m-Na-Al	0.07	2.8	56.8	7.50	16.5	23.8	31.8	88.5	275.7	4.9	351.1	8.8	34.7	8.7	0.8	8.3

	colour	artefact type	n	compo	Ce (ppm)	Pr (ppm)	Nd (ppm)	Sm (ppm)	Eu (ppm)	Gd (ppm)	Tb (ppm)	Dy (ppm)	Ho (ppm)	Er (ppm)	Tm (ppm)	Yb (ppm)	Lu (ppm)	Hf (ppm)	Th (ppm)	U (ppm)
GS001*	green	bead	4	m-Na-Al	39.7	3.4	11.6	2.9	0.8	2.5	0.3	1.8	0.5	1.1	0.1	0.9	0.5	6.8	11.0	7.5

	colour	artefact type	n	compo	Ce (ppm)	Pr (ppm)	Nd (ppm)	Sm (ppm)	Eu (ppm)	Gd (ppm)	Tb (ppm)	Dy (ppm)	Ho (ppm)	Er (ppm)	Tm (ppm)	Yb (ppm)	Lu (ppm)	Hf (ppm)	Th (ppm)	U (ppm)
GS002*	blue	bead	4	m-Na-Al	46.7	5.0	21.9	3.8	1.4	3.4	0.5	2.5	0.4	0.8	0.3	2.0	0.3	6.3	6.1	7.3
GS003*	yellow	bead	4	m-Na-Al	59.7	5.5	21.1	4.0	0.9	1.7	0.5	1.6	0.5	1.7	0.2	0.3	0.2	10.9	15.5	4.9
GS004*	red	bead	4	m-Na-Al	49.1	4.8	19.9	4.6	0.8	2.5	0.4	2.4	0.6	1.5	0.1	1.6	0.2	9.6	7.0	5.5
GS005*	yellow	bead	4	m-Na-Al	40.6	4.6	16.8	5.6	0.6	3.2	0.5	2.6	0.6	1.3	0.2	1.8	0.4	11.1	5.6	6.2
GS006*	green	bead	4	m-Na-Al	55.7	5.1	24.4	4.5	0.9	2.0	0.5	2.5	0.5	1.0	0.4	2.5	0.3	10.2	10.1	8.8
GS009*	blue	bead	1	m-Na-Al	39.7	3.2	25.0	7.3	2.5	1.8	<LLD	<LLD	<LLD	<LLD	<LLD	<LLD	1.9	<LLD	7.5	17.1
GS010*	red	bead	4	m-Na-Al	46.4	5.2	16.2	3.7	0.9	2.3	0.3	1.7	0.5	1.3	0.1	1.6	0.1	15.6	12.2	10.7
GS011*	yellow	bead	4	m-Na-Al	38.1	4.5	21.0	4.2	1.2	1.7	0.4	2.2	0.6	1.7	0.4	2.3	0.1	8.1	5.5	4.3
GS012*	blue	bead	4	m-Na-Al	41.0	3.7	16.3	2.9	1.1	2.7	0.3	2.4	0.5	1.5	0.3	0.9	0.2	4.4	4.8	7.8
GS013*	blue	bead	4	m-Na-Al	32.6	2.2	8.4	2.9	0.8	1.5	0.3	1.9	0.4	1.3	0.2	1.1	0.1	5.0	4.4	38.5
GS015_1*	red	bead	4	m-Na-Al	49.5	5.4	22.1	4.8	0.8	2.4	0.4	2.0	0.4	1.0	0.3	1.1	0.2	7.9	7.8	4.7
GS015_2*	orange	bead	4	m-Na-Al	47.4	4.7	20.7	4.7	1.2	3.6	0.8	3.2	0.8	1.5	0.4	2.0	0.4	6.5	7.0	4.4
GS019*	red	bead	4	m-Na-Al	45.6	4.4	20.1	2.0	1.0	2.2	0.4	2.1	0.5	1.3	0.2	1.5	0.3	7.3	6.7	3.3
GS022*	yellow	bead	3	m-Na-Al	35.6	3.0	18.7	10.0	1.6	1.1	0.9	<LLD	1.9	2.9	0.5	3.1	0.6	12.3	10.9	33.8
GS023*	red	bead	4	m-Na-Al	62.1	6.5	27.9	4.3	0.8	3.4	0.6	2.4	0.7	1.7	0.2	0.9	0.2	5.9	6.4	4.3
GS025*	blue	bead	4	m-Na-Al	29.8	3.2	11.9	5.7	1.2	1.5	0.4	2.7	<LLD	1.5	0.2	1.6	0.3	8.9	4.5	8.7
GS026*	green	bead	4	m-Na-Al	39.5	4.4	20.2	3.3	1.1	2.3	0.4	2.2	0.6	1.9	0.5	1.7	0.0	8.1	3.9	6.0
GS028*	yellow	bead	4	m-Na-Al	12.9	0.9	3.5	1.7	0.3	<LLD	0.2	1.6	0.3	0.6	0.2	1.0	0.2	4.6	1.1	3.9
GS029*	yellow	bead	4	m-Na-Al	23.3	2.0	7.7	2.8	0.4	2.0	0.2	1.1	0.5	0.9	0.2	0.9	0.2	4.5	2.0	15.8
GS030*	yellow	bead	4	m-Na-Al	34.9	3.5	15.4	5.4	1.0	0.4	0.6	2.8	0.6	2.5	0.2	0.2	0.4	3.2	3.2	6.3

	colour	artefact type	n	compo	Ce (ppm)	Pr (ppm)	Nd (ppm)	Sm (ppm)	Eu (ppm)	Gd (ppm)	Tb (ppm)	Dy (ppm)	Ho (ppm)	Er (ppm)	Tm (ppm)	Yb (ppm)	Lu (ppm)	Hf (ppm)	Th (ppm)	U (ppm)
GS031*	green	bead	4	m-Na-Al	32.0	2.4	11.1	2.9	1.0	1.9	0.4	4.7	<LLD	1.7	0.3	2.2	0.4	8.2	2.8	9.7
GS033*	blue	bead	3	m-Na-Al	32.1	3.8	14.8	5.8	<LLD	3.1	0.3	4.2	<LLD	1.9	0.4	4.1	0.8	6.6	3.0	5.2
GS034*	green	bead	4	m-Na-Al	31.2	3.2	14.8	1.8	0.5	1.1	0.4	1.4	0.5	1.0	0.3	0.8	0.3	5.1	3.6	5.0
GS037*	green	bead	4	m-Na-Al	36.5	3.9	16.8	5.1	0.8	2.9	0.7	2.4	0.7	1.8	0.1	1.2	0.1	7.6	8.9	9.4
GS038*	red	bead	3	m-Na-Al	36.1	3.1	16.3	5.8	1.1	1.2	0.4	1.8	0.5	0.6	<LLD	0.7	0.2	3.7	7.8	5.5
GS040*	yellow	bead	4	m-Na-Al	33.9	3.2	12.9	3.0	0.7	1.5	0.4	1.6	0.5	0.7	0.1	1.8	0.0	2.7	6.9	31.3
GS041*	yellow	bead	4	m-Na-Al	13.7	1.2	4.8	1.7	0.5	0.7	0.2	<LLD	0.4	0.8	0.3	0.4	0.3	4.4	1.3	13.8
GS043*	blue	bead	4	m-Na-Al	41.9	3.6	10.9	2.6	1.2	1.0	0.3	2.5	0.6	0.9	0.2	0.9	0.2	8.7	6.1	15.8
GS044*	green	bead	4	m-Na-Al	31.6	3.3	13.3	2.8	0.6	1.5	0.3	2.0	0.5	1.6	0.2	1.6	0.2	5.4	5.0	5.0
GS049*	blue	bead	4	m-Na-Al	21.0	1.0	5.7	4.2	1.3	0.6	<LLD	<LLD	<LLD	1.8	0.1	2.0	0.5	6.0	3.4	9.5
GS050*	red	bead	4	m-Na-Al	37.2	3.2	15.4	3.6	1.0	3.5	0.3	3.0	0.5	1.2	0.4	2.1	0.2	10.2	4.6	10.1
GS052*	green	bead	4	m-Na-Al	45.8	4.4	15.7	4.6	0.8	0.7	0.4	2.4	0.5	1.7	0.2	1.1	0.2	9.4	9.7	7.2
GS053*	blue	bead	4	m-Na-Al	29.5	3.3	12.7	3.5	0.5	0.7	0.6	2.1	0.6	1.6	0.1	0.7	0.2	5.8	2.0	2.8
GS055*	red	bead	4	m-Na-Al	41.2	5.4	18.3	4.2	1.3	2.8	0.4	3.7	1.0	1.8	0.3	2.4	0.2	8.1	5.2	5.5
GS056*	dark blue	bead	4	v-Na-Ca	13.3	1.2	7.0	2.4	1.1	1.9	0.3	1.5	0.3	1.3	<LLD	0.4	0.1	2.5	0.6	0.4
GS059*	dark blue	bead	4	v-Na-Ca	12.7	1.6	6.6	4.4	0.4	1.1	0.4	<LLD	0.5	1.1	0.4	1.6	0.1	2.2	0.9	0.5
GS060*	dark blue	bead	4	v-Na-Ca	10.2	1.6	4.3	1.9	<LLD	1.1	0.4	2.1	<LLD	0.8	0.3	0.5	0.4	2.1	0.8	0.3

	colour	artefact type	n	compo	Ce (ppm)	Pr (ppm)	Nd (ppm)	Sm (ppm)	Eu (ppm)	Gd (ppm)	Tb (ppm)	Dy (ppm)	Ho (ppm)	Er (ppm)	Tm (ppm)	Yb (ppm)	Lu (ppm)	Hf (ppm)	Th (ppm)	U (ppm)
GS064*	yellow	bead	4	m-Na-Al	25.7	2.7	9.4	0.2	0.1	1.5	0.1	1.0	0.1	<LLD	0.1	<LLD	<LLD	3.5	3.2	3.3
GS065*	green	bead	4	m-Na-Al	23.2	2.3	8.8	1.1	0.2	0.5	0.1	0.6	0.0	<LLD	0.1	0.2	<LLD	2.8	4.3	2.5
GS068*	dark blue	bead	4	v-Na-Ca	8.0	0.7	3.1	<LLD	<LLD	0.4	0.1	0.5	0.0	<LLD	0.1	<LLD	<LLD	0.4	0.6	0.2
GS070*	red	bead	4	m-Na-Al	27.3	2.7	11.0	0.7	0.2	0.9	0.1	1.5	0.1	0.4	0.1	0.7	<LLD	4.1	4.4	3.5
GS073*	red	bead	4	m-Na-Al	23.1	1.8	9.6	0.5	0.4	1.0	0.1	<LLD	0.0	<LLD	<LLD	<LLD	<LLD	4.3	3.6	6.3
GS074*	red	bead	4	m-Na-Al	39.5	3.7	12.7	3.5	0.2	1.3	0.2	0.8	<LLD	0.1	0.0	<LLD	<LLD	3.6	9.2	3.1
GS076*	blue	bead	4	v-Na-Ca	15.8	1.5	4.5	<LLD	<LLD	0.7	0.1	<LLD	1.5	0.1						
GS077*	blue	bead	4	v-Na-Ca	22.3	2.2	6.3	1.5	0.2	1.4	0.1	0.8	0.1	<LLD	<LLD	<LLD	<LLD	<LLD	1.9	0.0
GS078*	red	bead	4	m-Na-Al	43.3	4.1	16.1	2.2	0.9	3.2	0.4	1.7	0.7	0.7	0.2	1.2	0.2	13.2	5.7	8.6
GS080*	blue	bead	4	v-Na-Ca	17.0	1.7	6.5	0.5	0.1	1.0	0.1	0.6	<LLD	<LLD	0.1	<LLD	<LLD	<LLD	2.4	0.6
GS085*	yellow	bead	4	m-Na-Al	26.3	3.0	8.5	1.0	0.3	1.1	0.2	1.0	0.1	0.6	0.1	0.9	<LLD	4.5	2.8	7.9
GS086*	yellow	bead	4	m-Na-Al	25.7	2.9	11.0	0.5	0.4	0.7	0.3	0.9	0.2	0.3	0.0	0.4	<LLD	4.8	2.5	2.9
GS087*	yellow	bead	4	m-Na-Al	27.7	3.0	10.9	0.7	0.3	1.4	0.1	1.5	0.2	0.7	0.1	0.7	<LLD	7.1	3.2	4.4
GS098*	dark blue	bead	4	v-Na-Ca	8.3	0.9	2.9	0.2	0.1	0.3	0.0	0.5	0.1	<LLD	<LLD	<LLD	<LLD	0.7	0.4	0.0
GS099*	dark blue	bead	3	v-Na-Ca	7.8	0.8	3.3	<LLD	<LLD	0.9	0.0	0.2	<LLD	0.2	<LLD	<LLD	<LLD	0.5	0.4	<LLD
GS101*	green	bead	4	m-Na-Al	23.6	2.5	9.4	1.3	0.0	0.6	0.1	0.6	0.2	1.0	<LLD	0.4	<LLD	3.9	5.2	6.7
GS102*	red	bead	4	m-Na-Al	31.0	2.8	10.3	2.3	0.3	1.0	0.1	0.7	0.2	<LLD	0.1	0.4	<LLD	3.1	3.4	1.5

	colour	artefact type	n	compo	Ce (ppm)	Pr (ppm)	Nd (ppm)	Sm (ppm)	Eu (ppm)	Gd (ppm)	Tb (ppm)	Dy (ppm)	Ho (ppm)	Er (ppm)	Tm (ppm)	Yb (ppm)	Lu (ppm)	Hf (ppm)	Th (ppm)	U (ppm)
GS103*	green	bead	4	m-Na-Al	41.5	4.0	18.3	4.5	0.9	0.8	0.3	1.7	0.4	1.3	0.3	0.6	0.3	5.8	4.6	10.1
GS104*	green	bead	3	m-Na-Al	25.5	2.2	9.1	<LLD	0.3	1.2	0.1	0.6	0.1	<LLD	<LLD	<LLD	<LLD	3.9	2.7	2.9
GS108*	green	bead	4	m-Na-Al	26.0	2.5	10.4	1.5	0.3	1.3	0.1	1.6	<LLD	0.3	<LLD	0.2	<LLD	2.9	5.9	6.4
GS109*	red	bead	4	m-Na-Al	24.8	2.0	5.9	<LLD	0.1	0.9	0.1	0.5	0.0	<LLD	0.0	<LLD	<LLD	5.4	3.7	4.1
GS111*	red	bead	4	m-Na-Al	21.9	1.6	5.7	<LLD	0.0	<LLD	0.2	<LLD	<LLD	<LLD	<LLD	<LLD	<LLD	2.5	2.1	3.7
GS114	dark blue	bead	4	v-Na-Ca	9.7	1.0	3.1	0.2	0.2	1.0	0.1	0.9	0.0	<LLD	<LLD	<LLD	<LLD	0.8	1.2	0.1
GS116*	green	bead	4	m-Na-Al	25.2	2.7	10.0	1.3	0.5	1.1	0.2	1.4	0.1	0.4	0.1	0.9	<LLD	4.5	6.8	6.7
GS119*	dark blue	bead	4	SLS	5.3	0.6	2.4	0.9	<LLD	1.4	0.1	0.4	0.0	<LLD	<LLD	<LLD	<LLD	0.4	<LLD	0.3
GS120*	blue	bead	4	m-Na-Al	35.8	2.3	10.7	1.9	0.6	2.0	0.3	2.1	0.4	1.2	0.5	0.7	0.3	5.9	4.7	12.3
GS122*	blue	bead	4	m-Na-Al	17.8	1.3	5.7	3.1	0.7	1.2	0.1	1.7	0.4	1.5	0.2	1.4	0.2	8.5	4.4	8.4

Table A2.7: Chemical composition of samples from Daoye (major and minor elements analysed by EPMA.)

	colour	artefact type	n	compo	SiO ₂ (%)	Al ₂ O ₃ (%)	Na ₂ O (%)	K ₂ O (%)	MgO (%)	CaO (%)	FeO (%)	MnO (%)	CuO (%)	SnO ₂ (%)	PbO (%)	Cl (%)	SO ₃ (%)	P ₂ O ₅ (%)	Mn (%)	Ti (%)	Ba (%)
DY02	blue	bead	43	m-Na-Al	63.83	9.52	16.50	2.89	0.19	1.46	0.64	0.06	0.88	0.01	0.17	1.02	0.08	0.08	0.04	0.25	0.11
DY10	green	bead	45	m-Na-Al	67.86	7.64	12.73	1.78	0.40	2.33	1.20	0.05	0.68	0.09	1.57	0.53	0.15	0.07	0.04	0.29	0.12
DY14	yellow	bead	33	m-Na-Al	60.67	8.95	16.82	1.85	0.40	2.31	1.81	0.04	0.11	0.32	1.96	1.04	0.17	0.09	0.03	0.53	0.15
DY32	blue	bead	44	m-Na-Al	59.70	9.19	19.69	2.56	0.30	1.44	0.67	0.04	1.88	0.03	0.22	1.36	0.12	0.15	0.03	0.23	0.13
DY33	green	bead	34	m-Na-Al	61.07	10.47	15.39	3.04	0.20	1.61	0.91	0.06	0.64	0.14	2.51	0.96	0.10	0.10	0.05	0.30	0.13
DY39	blue	bead	45	m-Na-Al	62.39	9.16	17.78	2.80	0.16	1.39	0.69	0.06	1.29	0.03	0.31	1.16	0.12	0.11	0.04	0.30	0.12
DY42-1	green	bead	40	m-Na-Al	62.98	6.97	14.39	1.65	1.72	3.58	1.44	0.06	1.23	0.19	1.99	0.74	0.17	0.17	0.05	0.28	0.09
DY47	red	bead	54	m-Na-Al	62.04	7.26	16.82	1.33	0.82	4.25	2.10	0.09	0.92	0.04	0.21	0.90	0.33	0.21	0.07	0.34	0.08

Table A2.8: Chemical composition of samples from Wujiancuo (major and minor elements analysed by EPMA.)

	colour	artefact type	n	compo	SiO ₂ (%)	Al ₂ O ₃ (%)	Na ₂ O (%)	K ₂ O (%)	MgO (%)	CaO (%)	FeO (%)	MnO (%)	CuO (%)	SnO ₂ (%)	PbO (%)	Cl (%)	SO ₃ (%)	P ₂ O ₅ (%)	Mn (%)	Ti (%)	Ba (%)
WJC15	blue	bead	49	m-Na-Al	66.08	7.85	14.96	1.83	0.38	3.13	1.23	0.07	0.86	0.07	0.19	0.55	0.21	0.05	0.06	0.33	0.11
WJC19	blue	bead	37	m-Na-Al	67.96	5.82	15.79	1.58	0.21	2.08	1.51	0.08	1.14	0.09	0.09	0.45	0.28	0.07	0.06	0.59	0.11
WJC20	aqua	bead	46	v-Na-Ca	67.78	2.96	12.68	1.76	3.12	7.64	0.88	0.06	0.12	0.02	0.03	0.92	0.14	0.30	0.05	0.12	0.06
WJC24	blue	bead	45	m-Na-Al	62.89	9.94	17.03	3.36	0.11	1.26	0.62	0.05	0.99	0.04	0.27	0.83	0.21	0.10	0.03	0.30	0.12